NUCLEAR PHYSICS at GANIL - A COMPILATION 1983-1988

C. Detraz, S. Harar

NUCLEAR PHYSICS GANIL 1983 - 1988

a COMPILATION

NUCLEAR PHYSICS at GANIL

A COMPILATION

January 1983 - December 1988

GANIL

BP 5027 - 14021 CAEN Cedex (France)
Tél. 31 45 46 47 - Télex : 170 553 F
Fax 31 45 46 65

FALL 1989

CONTENTS

PREFACE

About 130 experiments have been carried out at GANIL since the beginning of the experimental program in January 1983. During these years, the accelerator ran continuously until december 1988, when it was decided to shut it down for a few months, in order to increase the energy of heavy ion beams. This was considered a good opportunity to collect and present the experimental results obtained so far. Since GANIL is a national facility, mainly used by outside physicists, this information is scattered among various laboratory annual reports.

The spokespersons of the GANIL experiments as well as theoreticians who contributed to the scientific life at GANIL through regular workshops were asked to present contributions of their results. In order to make this document as complete and homogeneous as possible, we suggested to the authors that they did not write a contribution per experiment but rather focus their presentation on the main goals and results even if they were achieved through several experiments. Furthermore, data for which the analysis is not completed are not presented here, but are rather mentioned in complement of a more complete work.

In summary this document is not a traditional progress report but rather a compilation of milestones concerning the topics studied at GANIL in the past few years. Over such a long period one can expect a strong evolution in the aim and complexity of both experimental approaches and theoretical studies. Indeed work performed at GANIL covers a wide variety of domains such as nuclear structure, reaction mechanisms, hot nuclear matter, production and properties of exotic nuclei, collective motions in nuclei, etc... Contributions have been tentatively ordered under several scientific topics. We are indebted to the authors for the quality of their contributions.

Claude DETRAZ
Director

Samuel HARAR
Vice-Director

I

COMPILATION

A. NUCLEAR STRUCTURE

A1 NUCLEAR SPECTROSCOPY

A2 EXOTIC NUCLEI AND DECAY MODES

B. NUCLEAR REACTIONS

B1 PERIPHERAL COLLISIONS - PROJECTILE-LIKE FRAGMENTS

B2 DISSIPATIVE COLLISIONS - HOT NUCLEI

B3 MULTI-FRAGMENT EMISSION

B4 PIONS AND PHOTONS

C. DEVELOPMENTS

– A –
NUCLEAR STRUCTURE

– A1 –
NUCLEAR SPECTROSCOPY

ELASTIC SCATTERING AT INTERMEDIATE ENERGY

N. Alamanos[1], F. Auger[1], J. Barrette[1], B. Berthier[1], D. Disdier[3], H. Doubre[4], B. Fernandez[1], J. Gastebois[1], A. Gillibert[1], D. Lott[3], W. Mittig[4], L. Papineau[1], V. Rauch[3], P. Roussel-Chomaz[1], F. Scheibling[3], C. Stephan[5], L. Tassan-Got[5]

1) DPhN, CEN Saclay, 91191 Gif-sur-Yvette Cedex, France. 2) Foster Radiation Lab, Mc Gill University, Montreal P.Q., Canada H3A 2B2. 3) CRN, 67037 Strasbourg, France. 4) GANIL, BP 5027 Caen Cedex, France. 5) IPN, 91406 Orsay, France.

The main purpose of elastic scattering studies is the determination of the nucleus-nucleus interaction. At low energy (E < 10 MeV/u), data have shown that due to strong absorption effects, the interaction potential can be probed only at the edge of the nuclear surface. Before 1984, few data existed on this subject at intermediate energies[1]. In order to study the sensitivity of elastic scattering to the nuclear potential in this energy range and to compare the energy dependence deduced from the data to that predicted by microscopic calculations[2,3,4], we have measured the elastic scattering of ^{16}O on ^{12}C, ^{28}Si, ^{40}Ca, ^{90}Zr and ^{208}Pb.

The elastic scattering studies reported here corresponds to two different experiments. Both used the ^{16}O beam at 94 MeV/u delivered by the GANIL accelerator. During the first one, which was performed in CYRANO with a position sensitive E-E solid state Si telescope, we measured the elastic scattering of ^{16}O on ^{12}C, ^{40}Ca, ^{90}Zr and ^{208}Pb. The energy resolution obtained in this experiment (2 MeV) did not allow a proper separation between the elastic and inelastic peaks in the case of ^{28}Si. We therefore performed another experiment, taking advantage of the achievement of SPEG, to measure the elastic angular distribution for $^{16}O + ^{28}Si$. The energy resolution obtained in this second experiment was less that 400 keV. In both experiments, the angular precision and resolution were less than 0.1°.

The angular distributions measured for the different systems are displayed on Fig. 1. For the system $^{16}O + ^{208}Pb$, the angular distribution presents a typical Fresnel type pattern associated with the Coulomb rainbow phenomenon. For lighter systems, strong oscillations appear, which correspond to the interference of the two scattering amplitudes from both sides of the nucleus. The negative angle amplitude increases as the mass of the target decreases and, in the case of ^{12}C, even dominates the angular distribution above 4°. The data have been analyzed in the optical model framework, using standard W-S potentials, but also squared W-S and double folded potentials[5]. The solid lines on Fig. 1 have been calculated with W-S potentials. They correspond to the best fit of the data, based on minimum χ^2.

To study which region of the potential is determined by the data, we proceeded in two steps. For each system, we performed first a notch test[6] to know the "sensitive region". Then, to evaluate with which precision the potential is fixed in the sensitive region, we compared the values taken in this region, by the different potentials which fit the data. The results are summarized on Fig. 2 in the case of $^{16}O + ^{28}Si$. For both the real and imaginary potentials the sensitive regions are 3 fm wide, that is much wider than at low energy, and the data seem to be much more sensitive to the real potential (factor 10 between the 2 curves in the insert). Indeed, all the real potentials wich fit

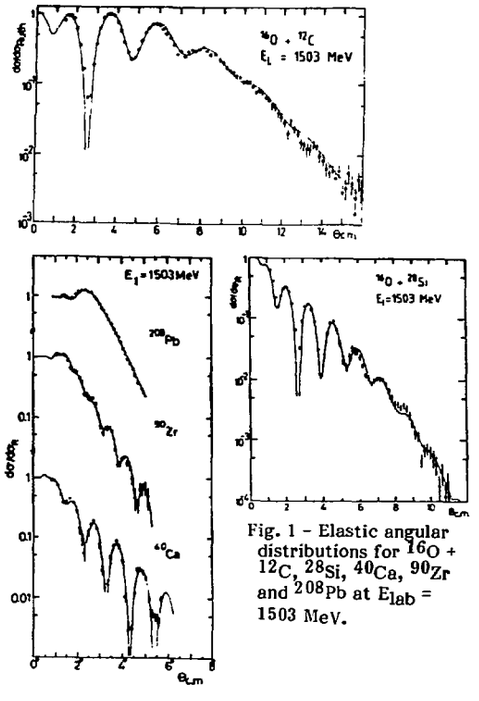

Fig. 1 - Elastic angular distributions for $^{16}O + ^{12}C$, ^{28}Si, ^{40}Ca, ^{90}Zr and ^{208}Pb at E_{lab} = 1503 MeV.

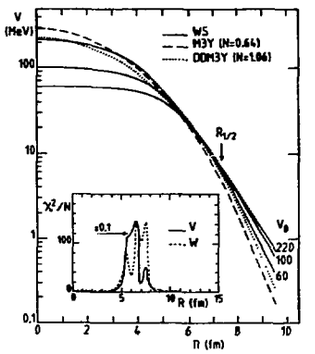

Fig. 2 - Radial dependence of real optical potentials which describe the $^{16}O + ^{28}Si$ angular distribution. The full lines are W-S potentials, whereas the dashed and dotted lines are double-folded potentials based on M3Y and DDM3Y interaction. The insert shows the results of a notch test on both parts of the potential.

the data take similar values, within 10 %, on the sensitive region. Concerning the imaginary potential, the picture is less clear and this potential is well determined only near the strong absorption radius. As a first conclusion, the striking feature of intermediate energy elastic scattering is that the data allow a precise determination of the real potential on a rather wide domain corresponding to a strong overlap of the two colliding nuclei.

Our data at 94 MeV/u completes the numerous data that exist at low energy for the same systems. Therefore they allow to study the energy dependence of the interaction potentials from the Coulomb barrier to 100 MeV/u. Fig. 3 displays for different systems the evolution of the normalization factor

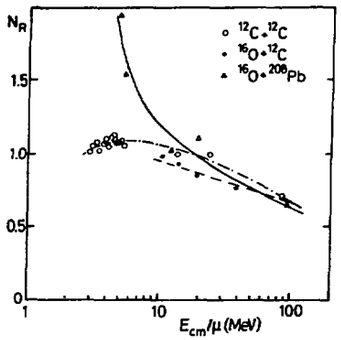

Fig. 3 - Energy dependence of the normalization factor of the M3Y double folded potentials for different systems. The lines are to guide the eye.

N which has to be applied to M3Y double folded potentials in order to fit the data. As these potentials have a very small intrinsic energy dependence, Fig. 3 reflects the evolution of the real potential. The increase observed for $^{16}O + ^{208}Pb$ near the Coulomb barrier is related, through the dispersion relation, to the rapid variation of W at the barrier[7]. Beyong this energy, a regular decrease of N is observed, of roughly 40 % from 10 to 100 MeV/u. This decrease is in good agreement with previous results obtained with heavier systems[8] (Ar + Ni, Sn, Pb). The variation of the imaginary potential with energy is less well known. At every energy it is determined only in a very small region near the strong absorption radius. As this radius decreases with increasing energy, it is difficult to disentangle the variation of the potential strength from that originating in the variation of $r_{1/2}$. However the general trend is also a smooth decrease of the imaginary potential in the region where it is determined. This decrease of both the real and imaginary potentials is in disagreement with the results of microscopic calculations[2,3,4] which predict a strong increase of nuclear strength in the considered energy range. The apparent failure of these models may be due to collective modes of excitation not included in the calculations and which can modify significantly not only the imaginary but also the real potential through coupled channel effects. Complete inelastic scattering data over a large range of bombarding energy could be essential to address this question and to assure a more detailed comparison between experiments and theory.

References

1) M. Buenerd et al., Nucl. Phys. **A424** (1984) 313.
2) A. Faessler et al., Nucl. Phys. **A428** (1984) 271c.
3) B. Bonin, J. Phys. **48** (1987) 1479.
4) R. Sartor and Fl. Stancu, Nucl. Phys. **A404**, (1983) 392.
5) G.R. Satchler and W.G. Love, Phys. Reports **55C** (1979) 183.
6) J.G. Cramer and R.M. DeVries, Phys. Rev. **C22** (1980) 91.
7) M.A. Nagarajan et al., Phys. Rev. Lett. 59 (1985) 1186.
8) N. Alamanos et al., Phys. Lett. **137B** (1984) 37.

References and contributions to Conferences related to these experiments

- N. Alamanos et al., Phys. Lett. **137B** (1984) 37.
- P. Roussel et al., Phys. Rev. Lett. **54** (1985) 1779.
- P. Roussel et al., Phys. Lett. **185B** (1987) 29.
- P. Roussel-Chomaz et al., Nucl. Phys. **A477** (1988) 345.
- N. Alamanos et al., BAPS 30 (1985).
- N. Alamanos et al. Proc. XXIII Intern. Winter Meeting on Nucl. Phys., Bormio (1985) 717.
- N. Alamanos et al., Proc. Second Intern. Conf. on Nucleus-Nucleus Collisions, Visby (1985) 36.
- P. Roussel et al., Proc. Intern. Conf. on Heavy Ion Nucl. Coll. in the Fermi Energy Domain, Caen (1986) 6.
- P. Roussel et al. Proc. Intern. Symp. on Magnetic Spectrograph, East Lansing (1989), to be published.

EXCITATION OF GIANT RESONANCES IN ^{90}Zr AND ^{208}Pb BY INELASTIC SCATTERING OF HEAVY IONS AT GANIL ENERGIES

D. Beaumel, Y. Blumenfeld, Ph. Chomaz*, N. Frascaria, J.P. Garron,
J.C. Roynette, J. A. Scarpaci, T. Suomijärvi
Institut de Physique Nucléaire, 91406 Orsay Cedex, France
J. Barrette, B. Fernandez, J. Gastebois, P. Roussel-Chomaz
DPh-N-BE, CEN Saclay, 91191 Gif-sur-Yvette Cedex, France
W. Mittig
GANIL, BP 5027, 14021 Caen Cedex, France

Giant resonances were observed for the first time about 40 years ago and since then they have been intensively investigated by the inelastic scattering of electrons, protons and alpha-particles. Since the advent of intermediate energy heavy ion beams the use of inelastic scattering of heavy projectiles to excite giant resonances has opened several new perspectives for these studies. First, the strong forward focusing of the reaction products leads to an increase of the inelastic scattering differential cross section. Moreover, the increase of the strength of the Coulomb interaction enhances the excitation of the isovector resonances like the GDR. Also high multipole resonances are expected to be strongly excited in heavy ion collisions.

In order to study the properties of giant resonances excited by inelastic scattering of heavy ions we have bombarded ^{90}Zr and ^{208}Pb targets with ^{20}Ne and ^{40}Ar projectiles at 40 MeV/u [1,2,3,4] and ^{208}Pb target with ^{86}Kr projectiles at the incident energy of 43 MeV/u [5,6]. These experiments were performed at Ganil using the magnetic spectrometer SPEG whose good energy and angular resolution has allowed an accurate analysis of the data.

An inelastic spectrum obtained for ^{20}Ne $+^{208}Pb$ is presented in fig. 1. The giant resonance bump can be seen at about 10 MeV of excitation energy with a peak-to-background ratio of 2:1. The main contribution to the physical background comes

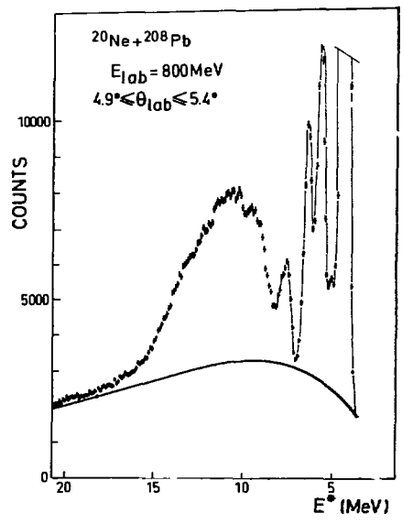

Figure 1: Inelastic spectrum from $^{20}Ne+^{208}Pb$ at 40 MeV/u.

*Division Physique Theorique, laboratoire associé au CNRS

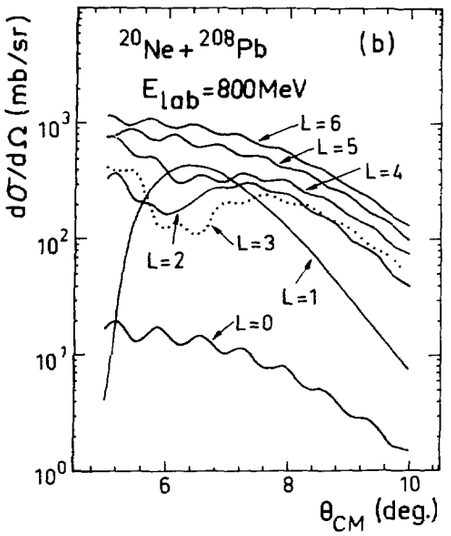

Figure 2: Theoretical angular distributions for ^{20}Ne+^{208}Pb at 40 MeV/u.

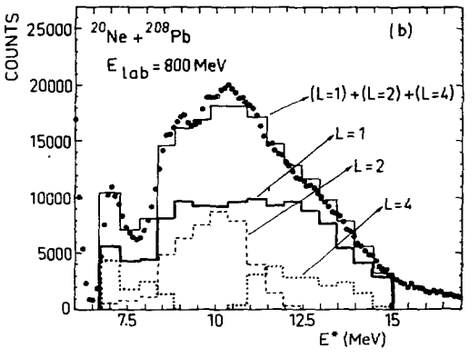

Figure 3: Multipole decomposition of the giant resonance bump in ^{208}Pb.

from the knock-out reactions which in the case of heavy projectiles decreases yielding good peak-to-background ratios.

The resonance bump generally contains several different multipolarity components which can be separated by their angular distributions. When the projectile size increases the multipole sensitivity of angular distributions decreases. Nevertheless, the interference between nuclear and Coulomb interaction yields angular distributions characteristic of the multipolarity. The angular distributions of different multipolarities for ^{20}Ne+^{208}Pb calculated with the code ECIS [7] can be seen in fig 2. A striking feature shown on this figure is the very high differential cross section (about 1 barn/sr). Note also the very strong excitation of the isovector GDR excited purely by the Coulomb interaction.

The multipole analysis for the ^{20}Ne and ^{40}Ar data was done by cutting the inelastic spectrum into small energy bins and fitting the angular distribution of each bin by a linear combination of theoretical angular distributions of different multipole transitions. The cross section distributions of different resonances extracted by this method for ^{20}Ne+^{208}Pb data are presented in fig. 3. Besides the GDR and GQR strength a small amount (20% of the EWSR) of L=4 strength was also extracted in ^{208}Pb. Another important feature to notice in this figure is the GDR cross section which is spread over a large excitation energy region. This shape is due to the Coulomb excitation probability which decreases exponentially as a function of excitation energy. In fig. 4. the cross section distributions of the GDR in ^{90}Zr and ^{208}Pb from photoabsorption [8] (Lorentz-curves, dashed lines) are compared to those obtained with inelastic scattering of ^{20}Ne and ^{40}Ar projectiles (histograms). When the photoabsorption strength is multiplied by the Coulomb excitation probability the cross section distributions obtained with heavy projectiles are well reproduced (full lines).

In the case of ^{40}Ar and ^{86}Kr data the deformation effect in the GDR cross section can also be seen. Furthermore, with all three projectiles the GDR dominates the GQR in ^{208}Pb. With ^{20}Ne projectiles the GQR cross section is still the largest component of the resonance bump in the ^{90}Zr spectrum but with ^{40}Ar the GDR becomes dominating also in zirconium.

The use of intermediate energy heavy ions yields good peak-to-background ratios and large cross sections for giant resonances which makes heavy ions an interesting probe for the study of the decay properties of these reso-

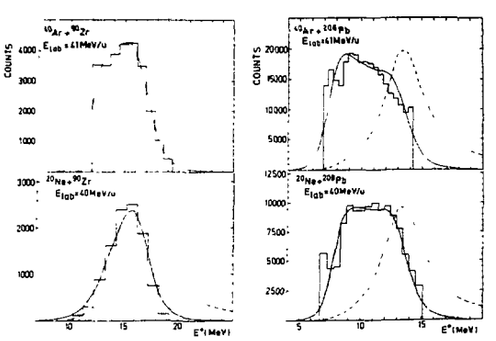

Figure 4: The experimental GDR cross section distributions in ^{90}Zr and ^{208}Pb obtained with ^{20}Ne and ^{40}Ar projectiles (histograms) compared to the photoabsorption data (dashed lines) and to the photoabsorption strength corrected for the excitation probability (full lines).

nances. Furthermore, we have shown that an accurate multipole decomposition is possible when very high resolution detection systems such as the SPEG spectrometer are used. In heavy ion collisions the Coulomb excitation is important favouring isovector resonances and the very strong excitation energy dependence of the Coulomb excitation can deform the cross section distribution of the GDR.

References

[1] T. Suomijärvi et al., Nucl.Phys, in press.

[2] Y. Blumenfeld et al., XXVI International Winter Meeting on Nuclear Physics, Bormio (Italy), 25-30 January 1988.

[3] T. Suomijärvi et al., XXVII International Winter Meeting on Nuclear Physics, Bormio (Italy), 23-27 January 1989.

[4] D. Beaumel, Thesis, Univ. Paris XI, Orsay.

[5] P. Roussel-Chomaz et al., Phys.Lett. B209(1988)187.

[6] P. Roussel-Chomaz et al., XXVI International Winter Meeting on Nuclear Physics, Bormio (Italy), 25-30 January 1988.

[7] J. Raynal, CEN de Saclay, Report DphT/7148, 1971.
J. Raynal, Phys. Rev. C23 (1981) 2571.

[8] B.L. Berman and S.C. Fultz, Rev. Mod. Phys. 77 (1975) 713.

INVESTIGATION OF THE SPIN-ISOSPIN-FLIP STRENGTH WITH THE (^{12}C, ^{12}N)-REACTION

W. von Oertzen

Hahn-Meitner-Institut, D-1000 Berlin 39, West Germany

(HMI, Berlin - GANIL, Caen - ISN, Grenoble - Univ. München - DPhBE, Saclay - INS, Tokyo - Collab. E85a)

1. Motivation

The charge exchange reaction (^{12}C, ^{12}N) has two characteristic features: (i) Isospin-flip $\Delta T=1$ with $T_f \approx T+1$ in the final nucleus (T isospin of the target). It corresponds to the (n,p)-reaction, but a much better resolution is achieved. (ii) Spin-flip $\Delta S= 1$, induced by the transition $^{12}C(0^+) \Rightarrow {}^{12}N(1^+)$ in the projectile. The sensitivity to spin-flip transitions has been already demonstrated [1]. The ^{12}C-nucleus is the lowest mass projectile to irduce a charge exchange reaction with the above characteristics, (except the (d,2p)-reaction). It is well suited to study the spin-isospin-flip strength in the $T_>$-channel, e.g. the spin-dipole resonance. The ^{12}N-ejectile is particle stable only in the ground state, and the transition strength in the projectile $^{12}C_{gs} \Rightarrow {}^{12}N_{gs}$ (B(GT) = 0.93) is quantitatively described by the wave function of ref. [2].

2. The reaction mechanism

The charge exchange reaction with a complex projectile such as ^{12}C can proceed via two different mechanisms: (i) the direct mechanism via the NN-interaction (meson exchange), and (ii) the two-step mechanism with the transfer of a proton from the target to the projectile and the transfer of a neutron in the opposite direction. We have studied the energy dependence of these two mechanisms on the ^{12}C-target with transitions to resolved states of ^{12}B. Angular distributions have been measured at Ganil/Caen for E/a = 70 MeV/u and at Vicksi/Berlin for 30 MeV/u. Calculations have been performed for both mechanisms and a quantitative description of the data could be achieved by the coherent sum (fig. 1). The NN-interaction of Anantaraman et al. [3] has been used for the direct mechanism for $E_{NN} \leq 10$ MeV and, at higher energies the interpolation between the interactions of [3] and of Franey and Love [4]. Tensor and exchange terms have been included. The two-step amplitudes are calculated in the exact-finite-range formalism with spectroscopic factors of the particle states (for the neutron) or hole states (for the proton) in the intermediate channels. Systematic calculations on this basis show that the two-step mechanism has a maximum at about 30 MeV/u and decreases for higher energies, while the direct mechanism rises further and dominates at 70 MeV/u [5]. The angular

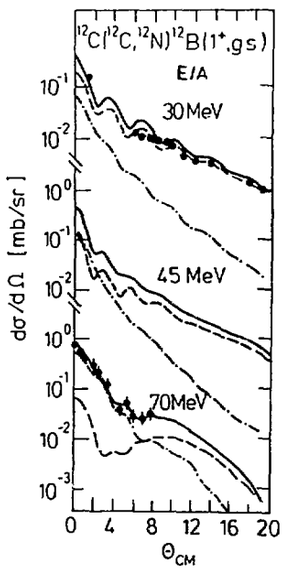

Fig. 1:
Angular distributions of the $^{12}C(^{12}C,^{12}N)^{12}B$ reaction to the ground state of ^{12}B at different incident energies. The lines represent calculations of the direct charge exchange (dashed-dotted lines), the proton-neutron exchange (two-step process, dashed lines) and the coherent sum of both (solid lines).

distributions of the direct process have a steeper slope at large angles than the two-step-process. Therefore it is important to extract the transition strength only at small angles.

3. The spin-isospin strength distribution

The (^{12}C, ^{12}N)-reaction has been measured at 70 MeV/u in a range of target masses between ^{12}C and ^{208}Pb. A typical spectrum is shown in fig. 2 (upper part) for the ^{40}Ca-target. The strong line at the ground state is due to the p(^{12}C, ^{12}N)n reaction on the hydrogen contaminant in the target. The pronounced structure between E_x = 7 and 13 MeV corresponds to the spin-dipole resonance. To obtain its strength we have assumed that the shape of the background corresponds to the shape of the spectrum at 2.5° (central part of fig.2), where the dipole angular distribution has a minimum. The difference is shown in the lower part of fig. 2. Targets with increasing mass number show a decreasing spin-dipole strength, as expected from the blocking of the β_+-strength due to the neutron excess [6]. The 'background' corresponds to the spin-isospin flip strength of higher multipolarities (L≥2). RPA-calculations are now performed up to $E_x \approx 50$ MeV for the strength distributions of L = 0 up to L = 5. They will be folded with DWBA-calculations and compared with the measured spectra and, for resolved states, with the angular distributions.

[1] H. G. Bohlen et al., Nucl. Phys. A488 (1988) 357c

[2] J. S. Winfield et al., Phys. Rev. C33 (1986) 1333

S. Cohen and D. Kurath, Nucl. Phys. 101 (1967) 1

[3] N. Anantaraman et al., Nucl. Phys. A398 (1982) 269

[4] M. A. Franey and W. G. Love, Phys. Rev. C31 (1985) 488

[5] H. Lenske et al., Phys. Rev. Lett. 62 (1989) 1457

[6] C. Gaarde et al., Nucl. Phys. A369 (1981) 258

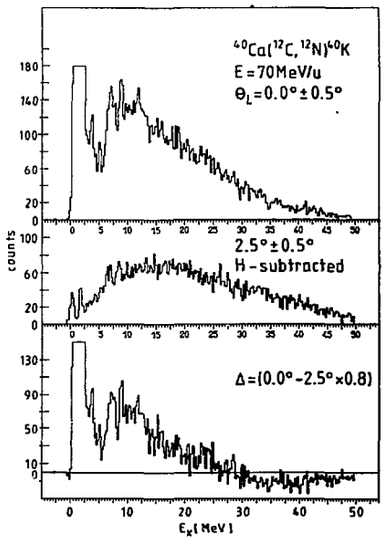

Fig. 2:
Spectra of the (^{12}C, ^{12}N)-reaction on ^{40}Ca at 0° (upper part) and 2.5° (central part) and their difference (lower part). The 2.5°-spectrum has been normalized by a factor of 0.8 to the high excitation energy region of the 0°-spectrum. The spin-dipole resonance is seen at about 10 MeV excitation energy.

CHARGE EXCHANGE REACTIONS TO PROBE THE ISOVECTOR ELECTRIC NUCLEAR RESPONSE

C. Bérat, M. Buénerd, P. Martin, J.Y. Hostachy, J. Chauvin, D. Lebrun, (ISN GRENOBLE),
J. Barrette, B. Berthier, B. Fernandez, A. Miczaika (CEN SACLAY), W. Mittig, A.Vilari (GANIL)
G. Bohlen, S. Stiliaris, and W.V. Oertzen (HMI BERLIN).

I - Motivations

Our present knowledge on the electric isovector nuclear response is limited mainly because of the lack of a suitable probe. The charge-exchange reactions, which have provided an impressive body of new data on the isovector spin modes by means of the outstanding selectivity of the (p,n) reaction, are also potentially good candidates for an exploration of the electric modes, provided one can find a reaction featuring the required selectivity.

The aim of the present programm was to test the (^{13}C,^{13}N) reaction at 50 MeV/u as a probe of the electric isovector response of nuclei, on its ability to excite the analog of the well known giant dipole resonance (IGDR), with the further purpose of investigating the isovector monopole mode (IGMR) of nuclei. This particular reaction was chosen because: 1) - the transition in the projectile is $(p^{1/2})_p \rightarrow (p^{1/2})_n$, allowing non spin-flip $\Delta S=0$ transitions in the target. In addition, the ratio of the Fermi to the Gamow-Teller matrix elements is about 5, ensuring a dominance of $\Delta S=0$ over $\Delta S=1$ (spin flip) transitions. 2) - the incident energy is low enough to ensure an acceptable magnitude of the electric isovector effective interaction which excite the transition.

II - Experiment

The measurements have been performed using the magnetic spectrometer SPEG equipped with its standard detection plus a plastic scintillator providing residual energy measurement and a fast timing signal for time of flight measurement. Data could be taken with the spectrometer set around zero degree. The beam entering the full ± 2° horizontal and vertical angular acceptance, was stopped on a faraday cup between the two dipoles.

III - Dipole excitation

Six targets have been studied in two runs: ^{12}C,^{40}Ca,^{58}Ni,^{60}Ni,^{90}Zr,^{120}Sn,^{208}Pb over an angular range Θ = 0-5°. Figure 1 shows the angle integrated spectra measured on the light targets[2]. Above small peaks corresponding to low excitation energy transitions, the spectra exhibit a common distinct feature : they are all dominated by a single, strongly excited peak, corresponding to the analog state of the IGDR. The excitation energy and width obtained for the IGDR are given in the table.

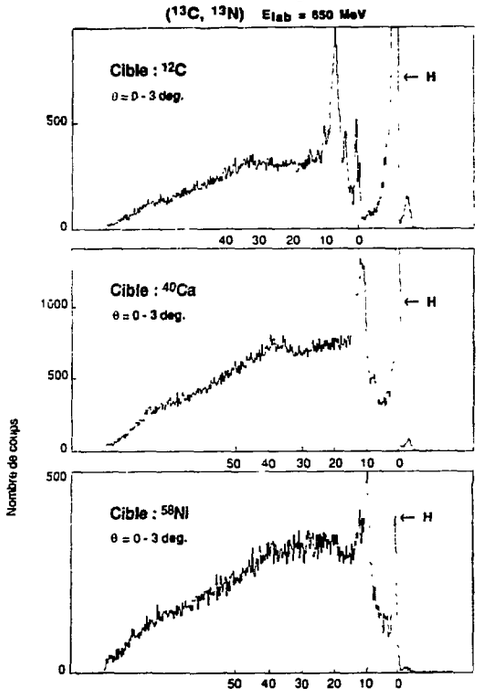

figure 1 - spectra on light nuclei

Note that in ^{40}K, the results are markedly below those measured in the (π^+,π°) reaction [1]. In ^{58}Co and in ^{60}Co the strength is splitted into two components. The dominance of the IGDR excitation establishes for this reaction the status of isovector electric probe of the nuclear response, and certainly opens the prospect of a possible future systematic study of this mode.

table 1-measured dipole excitations

Nucleus	E_x(MeV)	Γ(MeV)
^{12}B	7.7±0.1	1.9±0.1
^{40}K	11.5±0.3	3.1±0.2
^{58}Co	10.6±0.3	1.9±0.2
	12.8±0.3	1.5±0.3

IV - Monopole excitation

In heavier nuclei, the increasing nuclear asymmetry is expected to inhibit progressively the (1 hω) IGDR transition, whereas the (2 ħω) IGMR excitation is less

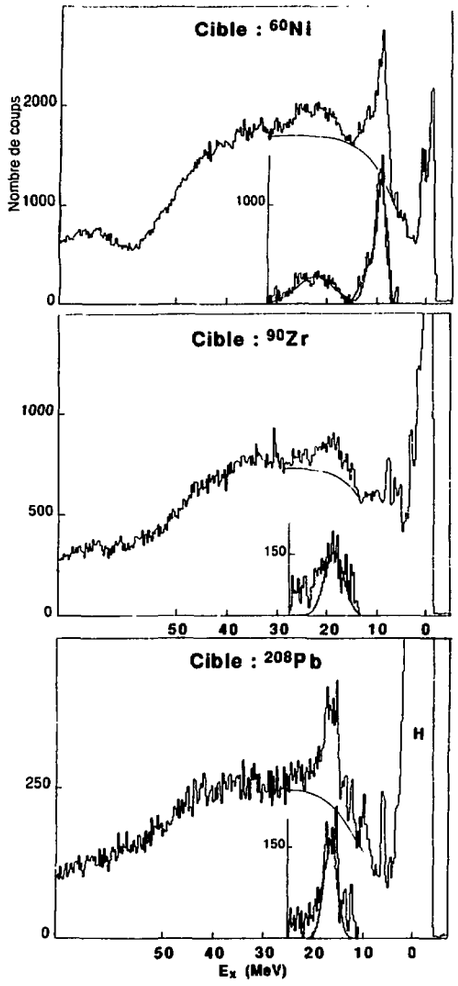

figure 2 - Spectra on medium mass and heavy nuclei

table 2 - monopole transitions (candidates)

Nucleus	E_x(MeV)	Γ(MeV)
^{60}Co	22.1±0.8	8.1±1
^{90}Y	18.7±1.6	4.6±0.8
^{120}In	14.7±0.9	4.1±0.8
^{208}Tl	16.5±0.6	3.1±0.5

rapidly inhibited. Figure 2 shows the spectra measured on the heavier nuclei studied[3]. In ^{60}Co, one observes above the IGDR, a wide peak sitting at the same E_x as the IGMR observed in ref.1. A similar situation is observed for ^{90}Zr and ^{120}Sn. In ^{208}Tl however, the structure observed is very different from that seen in ref. 1.

V - Angular distributions

The angular distributions measured for the various transitions observed reveal that an unexpectedly large component of two-step processes contributes to the cross-section and washes out the diffractive pattern of the single-step contribution[2,3]. This feature introduces serious complications for the quantitative analysis of the data.

VI - Symmetric reaction

The complementary reaction (^{13}C,^{13}B) which has also been studied does not show the same selectivity because the transition in the projectile $(p^{3/2})_p \rightarrow (p^{1/2})_n$, is dominated by ΔS=1. The measured spectra are correspondingly dominated by the excitation of the spin-isospin strength[3].

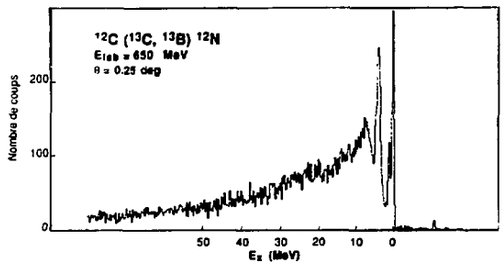

figure 3 - Spectrum of the symmetric reaction on ^{12}C.

1) A. Erell et al. Phys. Rev. C34 (1986) 1822

2) C.Bérat et al., to appear in Phys.Lett.

3) C.Bérat, thèse, Université de Grenoble, nov.1988. C.Bérat et al., in preparation for Nucl.Phys. A.

Isoscalar Giant resonances at finite temperature

E. Suraud[1], M. Barranco*,[2] and J. Treiner**

Institut des Sciences Nucléaires, 53 Avenue des Martyrs, F38026 Grenoble cedex, France
*) Departament d'Estructura i Constituents de la Materia, Facultat de Fisica, Universitat de Barcelona, Diagonal 64, SP-08028 Barcelona, Spain
**) Division de Physique Théorique, Institut de Physique Nucléaire, F91406 Orsay cedex, France

1) Present address : GANIL, BP5027, F14021 Caen cedex, France
2) Present address : Departament de Fisica, Universitat de les Illes Balears, E-07071 Palma de Mallorca, Spain

The study of nuclear collective motion built on excited states is presently of challenging interest both experimentally and theoretically [1].The proper description of such states is made delicate by the metastability of hot nuclei. However, at not too high temperatures it remains reasonable to picture a hot nucleus embedded in an external gas generated during the vibration. A physically sounded description has hence to properly take into account this gas contribution in order to prevent the excitation of spurious zero hω states, as was recently shown in the framework of Time Dependant Thomas-Fermi calculations [2]. By using a semi-classical version [3] of the Bonche, Levit and Vautherin prescription (BLV,[4]) for describing hot nuclei, we have hence developed a sum rule approach for isoscalar giant resonances at finite temperature [5]. The BLV prescription allows to handle properly with the continuum and sum rules give a nice description of the gross properties (centroids, widths) of resonances, even in the finite temperature case [6].

By using the semi-classical expressions for the moments m_{-1}, m_1 and m_3 of the strength function, one can define the two standart estimates of the resonance energy $E_1=\sqrt{m_1/m_{-1}}$ and $E_3=\sqrt{m_3/m_1}$. Our calculations have been performed with the Skyrme SKM* interaction, together with a phenomenological Extended Thomas Fermi approximation for the kinetic energy density. The latter functional gives results in very good agreement both with zero temperature RPA sum rules [6] and with the original BLV finite temperature Hartree-Fock results [4].

The importance of properly subtracting the continuum contribution is demonstrated in Figure 1 were the monopole E_1 and E_3 energies

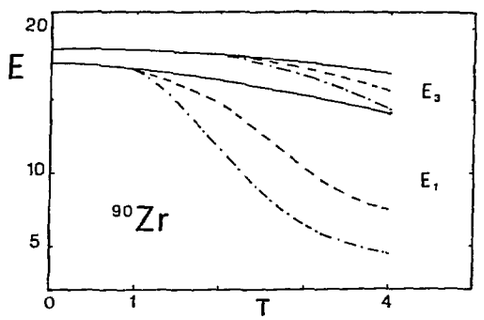

Figure 1
Values of non-subtracted (dashed line for box size R=14 fm and dashed-dotted line for R=12 fm) and subtracted (full line) monopole E_1 and E_3 energies (in MeV) as a function of the temperature T (in MeV) in the case of ^{90}Zr.

are plotted versus the temperature for a ^{90}Zr nucleus. One sees that even at low temperatures ($T \approx 1$ MeV) continuum may play a spurious role, with, in particular, a strong dependance on the size of the box in which calculations are performed. The same spurious effect is also found for higher multipolarities and disappears in the BLV formalism.

In figure 2 are shown the temperature evolution of the monopole E_1 and E_3 energies of various nuclei. Note the very smooth variation of these energies with the temperature. The same comment holds for Figure 3 in which the E_3 energy is plotted versus temperature for $l=2,3$ and 4 multipolarities. Note however that temperature effects are all the less important for low multipolarities and big nuclei. The first trend reflects the fact that it is easy to smooth the numerous wiggles present in large l deformed

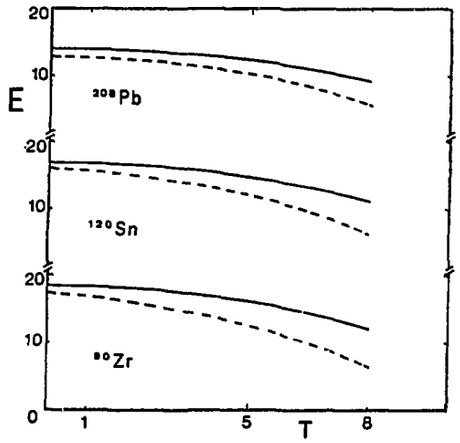

Figure 2
Variations of the E_1 (dashed line) and E_3 (full line) energies (in MeV) of the monopole resonance as a function of the temperature T (in MeV) for the 3 nuclei ^{90}Zr, ^{120}Sn and ^{208}Pb. Note that E_1 and E_3 stay very close together, which presumably indicates a small spreading of the mode.

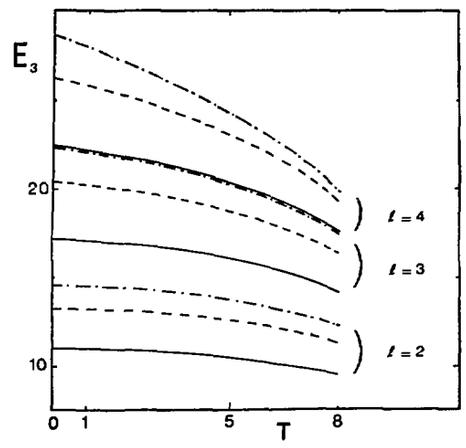

Figure 3
Variations of the E_3 energies (in MeV) of the $\ell = 2$, 3 and 4 giant resonances in ^{90}Zr (dashed-dotted line), ^{120}Sn (dashed line) and ^{208}Pb (full line) as a function of the temperature T (in MeV).

Fermi spheres. The second one is bound to the sensitivity of surface to temperature, surface playing a more important role in light nuclei, as compared to bigger ones.

In this work we have applied a semi-classical approximation of the BLV subtraction procedure to describe Giant Resonances at finite temperature. We have demonstrated that continuum effects play a very important role even at moderate temperatures and should hence be properly taken into account. The temperature dependance of the isoscalar collective modes we have studied is very smooth with small variations with the mass of the nucleus and the multipolarity of the mode.

References

[1] K.A. Snover, Ann. Rev. Nucl. Part. Sci.vol **36**, 1986 and references therein
[2] M. Barranco, J. Nemeth, Ch. Ngo and E. Tomasi, Nucl. Phys. **A464** (1987) 29
[3] E. Suraud, Nucl. Phys. **A462** (1987) 109
[4] P. Bonche, S. Levit and D. Vautherin, Nucl. Phys. **A427** (1984) 278
[5] E. Suraud, M. Barranco and J. Treiner, Nucl. Phys. **A 480** (1988) 29
[6] M. Barranco, A. Polls and J. Martorell, Nucl. Phys. **A444** (1985) 445

HIGH EXCITATION ENERGY STRUCTURES IN HEAVY ION COLLISIONS AT INTERMEDIATE ENERGY

D. Beaumel, Y. Blumenfeld, Ph. Chomaz,* N. Frascaria, J.P. Garron,
J.C. Jacmart, J.C. Roynette, J. A. Scarpaci, T. Suomijärvi
Institut de Physique Nucléaire, 91406 Orsay Cedex, France
J. Barrette, B. Berthier, B. Fernandez, J. Gastebois ,P. Roussel-Chomaz
DPh-N-BE, CEN Saclay, 91191 Gif-sur-Yvette Cedex, France
W. Mittig
GANIL, BP 5027, 14021 Caen Cedex, France

A few years ago , experimental evidence for the presence of simple structures at very high excitation energy in the inelastic and transfer channels of heavy ion reactions at 10 MeV/u was presented [1]. Since the data suggested that the structures were excited through a direct process, an interpretation in terms of collective modes was tentatively advanced. These results immediately prompted a large amount of theoretical work. A consistent representation of the data was given by the multiphonon calculation [2] which supposes the excitation of multiphonon states built mainly with the giant quadrupole resonance. One prediction of this model was that heavy projectiles with an incident energy lying around 30 to 50 MeV/u would be the optimal probes for the excitation of multiphonon states through the nuclear interaction.

In the light of these results we undertook at GANIL a new generation of experiments at intermediate energy. Because of the experimental difficulties connected with the observation of this low cross section phenomenon, a very careful study of these structures was carried out. To get a deeper insight into the mechanism responsible for the structures, systematic studies as a function of the target mass and of incident energy were undertaken using the Argon beam delivered by the GANIL facility [3].The $^{40}Ar + ^{208}Pb$, ^{120}Sn, ^{90}Zr and ^{40}Ca experiments were performed at 44 MeV/u and the $^{40}Ar + ^{90}Zr$ at 33 MeV/u for different angles close to the grazing . Special care was taken to obtain an unambiguous charge and mass identification. A time of flight spectrometer using a microchannel plates system without any grid on the trajectory of the ions was specially built for this purpose [4]. In this first set of experiments, high excitation energy structures were observed up to 70 MeV excitation energy in the inelastic channel of the four studied reactions. In order to quantify the conclusions concerning the existence, energies, widths and angular evolution of the structures double Fourier transform, autocorrelation and cross correlation analyses were carried out on the inelastic spectra.The comparison of the spectra from the four different targets shows that the excitation energies of the structures depend on target mass. The remarkable conclusion is that a coherent description of all the excitation energies can be obtained by supposing a target mass dependence of the form $E_x \sim A^{-1/3}$.

In the studied reactions, three body processes such as the decay of pick up channels ("pick up break up reactions") are expected to contribute strongly to the inelastic cross section in the region where the structures are observed. Thus, a complete knowledge of such a contribution is necessary. Extensive calculations [5] have been carried out for all the studied reactions The calculation reproduces very well the shape of the physical background but the cross section is difficult to evaluate because a precise knowledge of the transfer cross section to the continuum would be required. From this work, several conclusions were drawn:i)at GANIL energies the dominant pick up break up contribution to the inelastic channel is due to one nucleon transfer reactions ii)The contribution to the spectra of this pick up break up process can be very different for different projectiles. If many levels are populated in the ejectile, the pick up break up contribution will have the shape of a broad plateau. If one level is preferentially populated in the ejectile the pick up break up contribution from this level can be split into two nar-

*Division de Physique théorique, laboratoire associé au CNRS

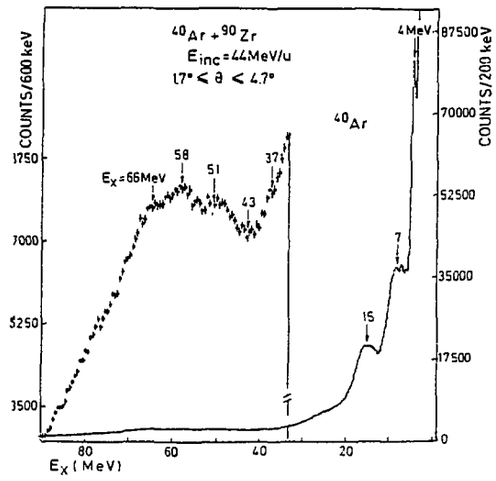

Figure 1: ^{40}Ar on ^{90}Zr inelastic spectrum. In full line the complete spectrum represented with 200 keV/channel bins. The high excitation energy part of the spectrum is also displayed with a 600 keV/channel binning and an expanded vertical scale.

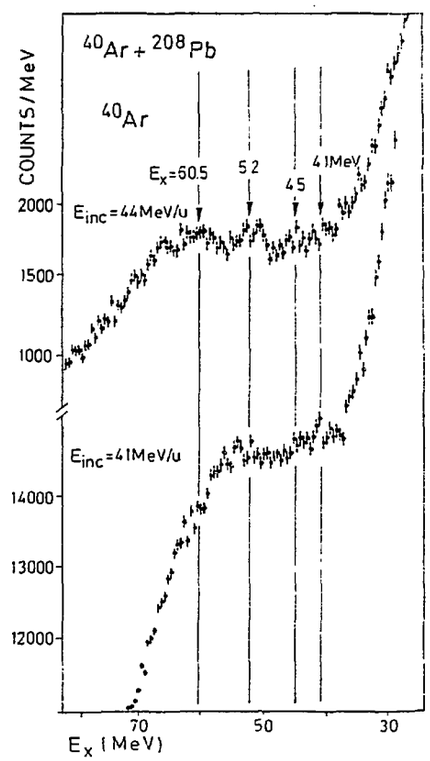

Figure 2: Comparison of the ^{40}Ar+^{208}Pb inelastic spectra at 41 MeV/u and 44 MeV/u.

row components superimposed on the plateau due to the other excited levels. Such a pattern is expected for certain light ejectiles where levels are very sparce above the emission threshold.In both cases the apparent excitation energy of the centroid of the pick up break up contribution depends linearly on the bombarding energy per nucleon. Consequently a clean method to conclude if the structures observed experimentally are due to target excitation or to pick up break up processes is to study a given system at two slightly different incident energies .

Since 1986 a new set of experiments has been performed at GANIL using the magnetic spectrometer SPEG. The aim of these experiments was to compare with high resolution and high statistics the inelastic spectra from the same reaction studied at two different energies and to compare these spectra with the one obtained on the same target using a different projectile. Therefore we studied the ^{40}Ar + ^{90}Zr and ^{40}Ar + ^{208}Pb reactions at 41 MeV/u and 44 MeV/u and the ^{20}Ne + ^{90}Zr and ^{20}Ne + ^{208}Pb reactions at 40 MeV/u (see for example fig.1).

In the first experiment [6], the bombarding energy was varied by 3 MeV/u which corresponds to an expected shift of the pick up break up component by 3 MeV which is approximately half of the mean interval between two observed bumps. Fig.2 displays the two inelastic spectra from the ^{40}Ar + ^{208}Pb reaction at 41 and 44 MeV/u.

Although the centroid of the broad plateau under the bumps is shifted by approximately 3 MeV as expected from a pick up break up calculation, the narrow structures show up at the same excitation energy in both spectra. In the case of the ^{40}Ar + ^{90}Zr experiment the bumps are clearly observed at 44 MeV/u but at 41 MeV/u important problems of linearity of the drift chambers were encountered and a correction function had to be applied to the inelastic spectra. Such a correction induces large error bars but nevertheless the results are incompatible with a 3 MeV shift of the bumps between 41 and 44 MeV/u.

As dicussed before the choice of the projectile in such studies is of great importance. To get more information on the influence of the projectile in these experiments the ^{20}Ne + ^{90}Zr and ^{208}Pb reactions have been stud-

ied at GANIL at 40 MeV/u. We have first compared the inelastic spectra from these reactions with those obtained at MSU at lower incident energies(25 MeV/u and 30 MeV/u) on the same systems [7]. At these lower energies the ^{208}Pb spectra exhibit two clear bumps superimposed on the pick up break up plateau which are shifted by 5 MeV between the two incident energies, as predicted from a pick up break up calculation for a light ejectile, while in the zirconium spectra, only very small oscillations are observed on the pick up break up plateau. The comparison of the 40 MeV/u inelastic spectra with those obtained at 25 and 30 MeV/u in ^{90}Zr and ^{208}Pb shows that the importance of the pick up break up plateau has diminished, thus reflecting the decrease of the transfer reaction probability with increasing bombarding energy. No clear double humped structure is visible in the $^{20}Ne + ^{208}Pb$ spectrum at 40 MeV/u but nevertheless no clear conclusions can be drawn from the comparison with the $^{40}Ar + ^{208}Pb$ spectra. This result suggests that in that case the contributions of target excitation and pick up break up process are strongly mixed. Conversely the $^{20}Ne + ^{90}Zr$ reaction inelastic spectrum presents clear bumps which are exactly at the same position as the ones observed in the $^{40}Ar + ^{90}Zr$ reaction studied at 33 MeV/u and 44 MeV/u. Fig 3 recapitulates all these inelastic spectra .The shape of the background is very different from one experiment to another.This evolution is well understood by the pick up break up calculation.Despite these widely different background shapes, structures appear at the same excitation energy in all spectra. This very complete set of data on the zirconium target allows to conclude to excitations of the target around 50 MeV excitation energy. More systematic work is needed on other targets to precise the position, width and angular evolution of the structures.

The study of inclusive inelastic spectra at two different energies allows to distinguish between the target excitation and pick up break up process for the interpretation of the structures but cannot yield the respective contribution of the two mechanisms to the total inelastic cross section. Very recently, we have studied the inelastically scattered ^{40}Ca on ^{40}Ca at 50 MeV/u in coincidence with light charged particles using CsI detectors at forward angles, a plastic wall and E.ΔE silicon detectors at backward angles. Preliminary results show that the pick up break up is clearly seen in the forward detectors and the detection of back-

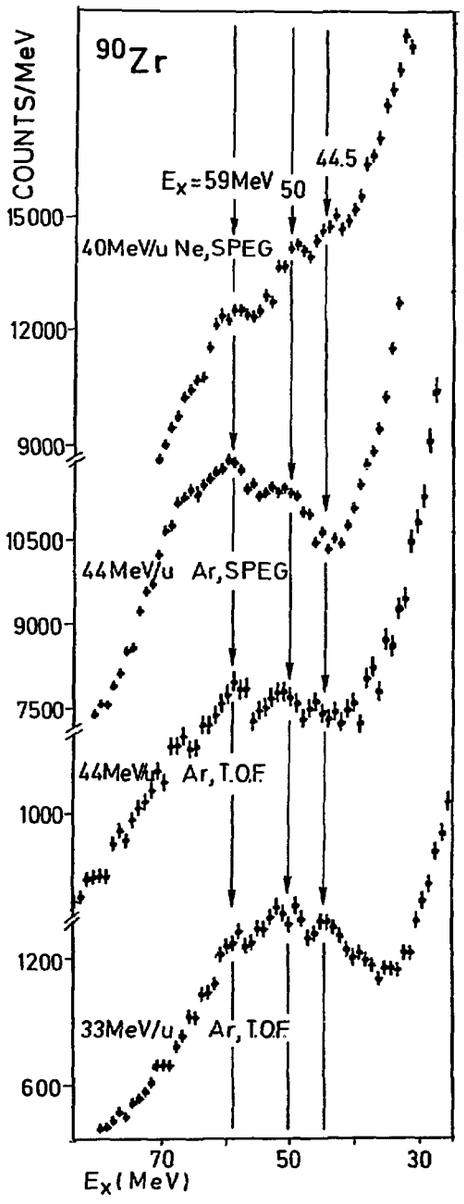

Figure 3: ^{90}Zr inelastic spectra obtained at different incident energies, with different experimental set ups and different projectiles.

ward emitted light particles allows to select target excitations.These first results are very promising and show that light particle heavy ion coincidence experiments should provide a unique tool to disentangle the target excitation and the pick up break up contributions and represent a further step towards the understanding of such complex reaction mechanisms.

References

[1] N.Frascaria et al. Z. Phys. A294 (1980) 167
Ph. Chomaz et al. Z. Phys. A318 (1984) 167

[2] Ph.Chomaz et al. Z. Phys. A319 (1984) 167

[3] N.Frascaria et al. Nucl. Phys. A474 (1987) 253
Y.Blumenfeld Thèse de Doctorat d'Etat, Orsay 1987
J.C.Roynette et al. HICOFED Caen 1986, p9
N.Frascaria XXIV Int. Winter Meet. Bormio, Italy 1986, p71

[4] E.C. Pollacco et al. Nucl.Inst. and Meth. 225 (1984) 41

[5] Y.Blumenfeld al. Nucl.Phys. A445 (1985) 151

[6] D.Beaumel These Orsay 1988
N.Frascaria First topic. Meet. on Giant Res. Excit. in Heavy Ion Collisions, Legnaro, Italy 1987, Nucl. Phys. A482 (1988) 245c
Y.Blumenfeld et al. XXVI Int. Winter Meet. Bormio, Italy 1988, p67
N.Frascaria RIKEN IN2P3 Symp.on Heavy Ion Collisions, Shimoda Japan 1987

[7] S.Fortier et al. Phys. Rev. C36 (1987) 183

MULTIPHONON EXCITATIONS IN HEAVY ION GRAZING COLLISIONS

Ph. CHOMAZ
Division de Recherche Expérimentale, Institut de Physique Nucléaire, 91406 Orsay Cédex, France

and

D. VAUTHERIN
Division de Physique Théorique [1], Institut de Physique Nucléaire, 91406 Orsay Cédex, France

Received 7 November 1983
Revised manuscript received 20 February 1984

A semiclassical model is used to study the excitation of giant resonances in heavy ion grazing collisions. The projectile is described as a moving Woods–Saxon potential with a fixed shape, and the evolution of the target state is calculated by time-dependent perturbation theory. Using random phase approximation wave functions, probabilities to excite various resonances are obtained. Multiple phonon excitations appear as the possible mechanism for the structures observed in heavy ion collisions.

CONTRIBUTION AS SENT BY THE AUTHOR

Nuclear Physics A476 (1988) 125–158
North-Holland, Amsterdam

COLLECTIVE EXCITATIONS OF CLOSED SHELL NUCLEI IN HEAVY ION GRAZING COLLISIONS*

Ph. CHOMAZ and NGUYEN VAN GIAI

*Institut de Physique Nucléaire, Division de Physique Théorique**, 91406 Orsay Cedex, France*

D. VAUTHERIN

Center for Theoretical Physics, Laboratory for Nuclear Science and Department of Physics, Massachusetts Institute of Technology, Cambridge, Massachusetts 02139, USA
*and Institut de Physique Nucléaire, Division de Physique Théorique**, 91406, Orsay, France*

Received 29 April 1987

Abstract: The single and multiple excitations of giant resonances in heavy ion reactions is investigated in the framework of a microscopic model. The scattering process is treated semi-classically as in the Copenhagen model but the target response is constructed from a microscopic RPA calculation using Skyrme forces. The importance of an accurate description of excitation operators and transition form factors is stressed. The connection with other approaches (time-dependent Hartree-Fock approximation, boson expansion method, second RPA) is discussed. The model is applied to reactions involving ^{208}Pb and ^{40}Ca nuclei. We conclude that, under near-grazing conditions, with medium or heavy projectiles and for incident energies around 30 MeV/nucleon, there is a substantial probability of observing multiphonon states built on $2\hbar\omega$ giant resonances.

CONTRIBUTION AS SENT BY THE AUTHOR

EXCITATIONS IN GRAZING HEAVY ION REACTIONS

K. Dietrich* and K. Werner

Physikdepartment of the TUM, Garching, FRG

* Guest at the GANIL, August 1984 - March 1985

Quite sometime ago, resonance-like structures were observed in peripheral reactions between composite nuclei[1]). Since then experiments were performed at various beam energies and for several projectile-target combinations, essentially supporting the original observations. It is a challenge to understand the origin of these structures, given the fact that simple explanations based on subsequent particle emission by the primary reaction products[2]) failed to explain the more comprehensive data[3]).

The first question is whether the observed bumps are due to the excitations of coherent states (giant resonances) or due to a concentration of strength of many incoherent excitations in the energy region of major shells. The majority of authors takes the first-mentioned stand-point i.e. interprets the observed structures as due to single[4]) or multiple[5]) excitation of giant resonances of different multipolarity. The 2nd possibility is investigated in refs. 6 and 7. Here it is assumed that independent and incoherent p-h excitations ("excitons") are generated during the collision either by tranfer of nucleons or by inelastic excitations. The important parameters of the model are the probability q that 1p-1h excitations are due to transfer rather than inelastic excitations, and the mean number z of excitons. Although the excitons are produced independently from each other, a concentration of strength in intervals of major shells is obtained due to the assumption that each exciton, irrespectively of whether it is produced by transfer of a nucleon or by inelastic excitation, corresponds to a mean excitation energy of one major shell distance. If one takes into account that the levels of a major shell are not exactly degenerate but distributed over an energy interval of a typical width Γ, and if one adopts a semiclassical description of the reaction, one obtains a closed expression for the cross-section[6,7]) depending on the 2 parameters q and z.

It turns out that a concentration of strength in certain energy regions is obtained for q-values close to 1, i.e. if transfer dominates over inelastic excitation. This is so since, for given net transfer of neutrons and of protons, the relative weight of transfer and of inelastic excitations is different for different exciton numbers. The data measured for ^{40}Ca on ^{40}Ca at a beam energy of 400 MeV[8] could be reasonably well reproduced by choosing the relative transfer probability q ≈ 1 and the mean exciton number Z=2.

The distinction between the two models is complicated by the fact that both yield Poisson distributions for the excitation probability of k modes and that the width of a major shell and a typical giant resonance like the quadrupole resonance are of the same order of magnitude[6]).

An important difference is that the model for incoherent exciton production would predict less pronounced bumps for reactions between two nuclei which are both far from shell closure compared to a scattering between two magic nuclei. On the other hand, giant resonances should be excited in both cases with comparable intensity.

1. N. Frascaria, C. Stéphan, P. Colombani, J.P. Garron, J.C. Jacmart, M. Riou, L. Tassan-Got, Phys. Rev. Lett. 39 (1977) 918
2. D. Hilscher, J.R. Birkelund, A.D. Hoover, W.V. Schröder, W.W. Wilcke, J.R. Huizenga, A.C. Mignerey, K.L. Wolf, H.F. Breuer, V.E. Viola, Phys. Rev. C20 (1979) 556
3. J.C. Roynette, N. Frascaria, Y. Blumenfeld, J.C. Jacmart, E. Plagnol, J.P. Garron, A. Gamp, H. Fuchs, Z. Phys. A299 (1981) 73
4. J. Dechargé, D. Cogny, B. Grammaticos, L. Sips, Phys. Rev. Lett. 49 (1982) 982 ; H. Flocard, M.S. Weiss, Phys. Lett. 105B (1981) 14 ; Nguyen Giai, Phys. Lett. 105B (1981) 11
5. Ph. Chomaz, D. Vautherin, Phys. Lett. 139B (1984) 244 ; Ph. Chomaz, Thèse 3è Cycle, Université de Paris Sud, IPNO-T-84-01, F-91406 Orsay
6. K. Dietrich, K. Werner, GANIL P.85-06
7. K. Werner, Nucl. Phys. A453 (1986) 486
8. N. Frascaria, P. Colombani, A. Gamp, J.P. Garron, M. Riou, J.C. Roynette, C. Stéphan, A. Ameaume, C. Bizard, J.L. Laville, M. Louvel, Z. Phys. A294 (1980) 167

– A2 –
EXOTIC NUCLEI AND DECAY MODES

PRODUCTION AND IDENTIFICATION OF NEW ISOTOPES AT THE PROTON AND THE NEUTRON DRIP-LINES

R. Anne[1], A.G. Artukh[2], D. Bazin[1], M. Bernas[3], V. Borrel[3], C. Détraz[1], J. Galin[3], D. Guerreau[1], B.A. Gvozdev[2], D. Guillemaud-Mueller[1], S.D. Hoath[3], J.C. Jacmart[3], D.X. Jiang[1], A.M. Kalinin[2], V.V. Kamanin[2], V.B. Kutner[2], M. Langevin[3]*, M. Lewitowicz[2], S.M. Lukyanov[2], A.C. Mueller[1], F. Naulin[3], Nguyen Hoai Chau[2], Yu. E. Penionzhkevich[2], E. Quiniou[3], A. Richard[3], E. Roeckl[1], M.G. Saint-Laurent[1], W.D. Schmidt-Ott[4]

1) *GANIL, BP 5027, Caen, France*
2) *Laboratory of Nuclear Reactions, Joint Institute for Nuclear Research, Dubna, USSR*
3) *Institut de Physique Nucléaire, Orsay, France*
4) *II Physikalisches Institut, Universität Göttingen, F.R.G.*

The search for new neutron-rich or proton-rich nuclei has much benefited from the effectiveness of heavy-ion projectile fragmentation at relativistic energies [1]. Therefore it was tempting to try similar experiments at Ganil. Establishing the limits of particle stability for nuclei has been the goal of a lot of experiments for many years. It is an important test of the validity of mass predictions based on the bulk properties of finite-charged nuclear matter or on the microscopic shell model.

The use of the fragmentation of different projectile has allowed us to map the drip-line on both sides of the valley of stability.

Mapping the neutron drip-line

Using the ^{40}Ar beam at 44 MeV/u on a tantalum target, selecting the projectile-like fragments with the doubly achromatic spectrometer LISE at zero degree [2] and identifying the nuclei through $\Delta E.E$, time-of-flight measurements, it was possible to produce for the first time the new isotopes ^{22}C ($T_Z = +5$), ^{23}N ($T_Z = 9/2$) and the two isotopes ^{20}Ne, ^{30}Ne [3,4].

It was also possible to prove the particle unstability of ^{18}B, ^{21}C, ^{25}O. Using the mass prediction formulae of Garvey Kelson [5] and Uno-Yamada [6] in the case of Boron isotopes, ^{19}B is predicted to be bound against neutron emission while ^{18}B and ^{20}B are unbound against one neutron emission ; all Boron isotopes with A≥21 unbound against two-neutron emission. The observed isotopes (fig. 1) are consistent with these predictions.

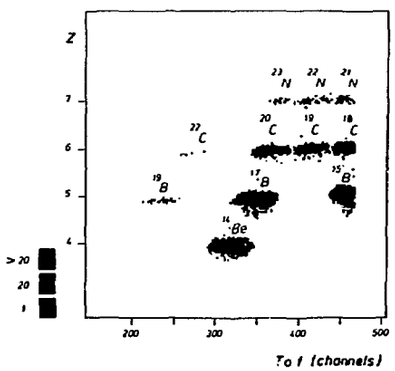

Fig. 1 : Two dimensional representation of events Z versus time of flight.

For the Carbon isotopes the same odd-even effect on the stability is predicted, ^{22}C being the last particle bound isotope while ^{21}C is particle unstable, again in agreement with our results. For the Nitrogen isotopes, ^{23}N is observed ; no counts of ^{24}N are present which is in accordance with its particle unstability prediction.

For Neon isotopes, ^{29}Ne was predicted particle unstable by the mass-formulae with the exception of the Uno-Yamada constant-shell term.

The next step of these experiments was made by fragmentating a ^{48}Ca beam at 55 MeV/u on a tantalum target [7]. In this experiment the new isotopes ^{29}F, $^{35,36}Mg$, $^{38,39}Al$, $^{40,41}Si$, $^{43,44}P$,

*deceased on April 11, 1985

$^{45,46,47}S$, $^{46,47,48,49}Cl$ and $^{49,50,51}Ar$ have been observed for the first time (fig. 2). The comparison of these results with the one obtained at Berkeley [8] at relativistic energy shows progress of typically two isotopes.

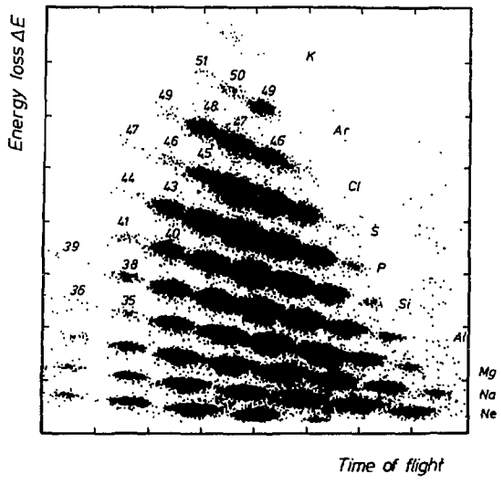

Fig. 2 : Two-dimensional representation ΔE versus time of flight ($\sim A/Z$). The new isotopes are indicated by their mass number.

Nevertheless one should note that we are still away from the neutron drip-line by about two to four masses.

Furthermore, from a reaction mechanism point of view, it is interesting to note the presence of strong transfer reaction channel at intermediate energy. Indeed, part of the new fragments contains more neutrons than the projectile did. The figure 3 shows the known isotopes of Nitrogen as well as ^{23}O, ^{24}O and the new isotope ^{29}F. The unstable isotope ^{25}O is obviously absent and no counts of ^{26}O are seen. Nevertheless taking into account the counting rate of the observed nuclei and using the fit of Sümmerer [9] for an estimate of production cross-section we should have observed only 2 or 3 counts. It was therefore impossible to conclude on the particle stability of ^{26}O (note however that we analyse presently an experiment with much improved statistics). ^{29}F is predicted to be bound by the mass formulae and observed. The odd-even effect on the stability of nuclei is clearly seen with ^{28}F and ^{30}F which are predicted unbound. Except for the constant-shell mass formula of Uno and Yamada ^{29}F is predicted to be the last stable isotope of Fluorine.

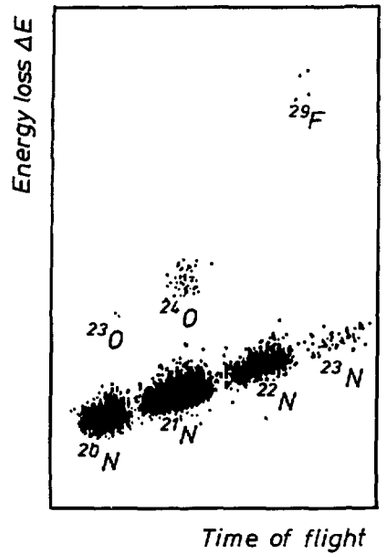

Fig. 3 : Two-dimensional representation ΔE versus absolute time of flight ($\sim A/Z$). The isotopes are labelled by their symbol. Four counts of the new isotope ^{29}F are observed.

In the fragmentation of the ^{86}Kr beam [10] it was possible to produce new isotopes in the $18 \leq Z \leq 27$ region such as ^{47}Ar, ^{57}Ti, $^{59,60}V$, $^{61,62}Cr$, $^{64,65}Mn$, $^{66,67,68}Fe$, $^{68,69,70}Co$. However in the range of mass, we are still very far away from the neutron-drip-line.

Mapping the proton drip-line

On the proton-rich side, two experiments [11,12] have been performed to produce new exotic nuclei. For the purpose the ^{40}Ca (77 MeV/u) and ^{58}Ni (55

MeV/u) have been used on a Ni target.

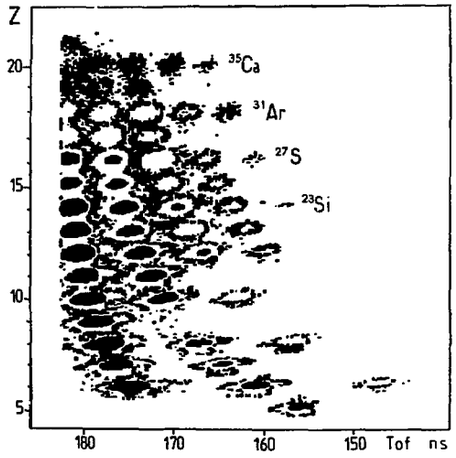

Fig. 4 : Two dimensional representation of events Z versus time of flight.

It has been possible for the first time to produce the whole series of light $T_Z = -5/2$ isotopes namely ^{23}Si, ^{27}S, ^{31}Ar, ^{35}Ca (fig. 4). The question of whether the drip line has been reached up to Z = 20 had to be handled with some caution due to the steepness of the valley of β stability. Nevertheless calculating the 1p and 2p separation energies by applying the charge symmetry formula of Kelson and Garvey [13] as done by Jänecke [5] but using the most recent experimental masses [14] all the nuclei beyond the ones seen in the experiment are largely unbound with the exception of ^{22}Si. This isotope has been identified in the fragmentation of an ^{36}Ar beam at 85 MeV/u on a Ni target[15].

With the ^{58}Ni beam the new isotopes ^{43}V, ^{44}Cr, $^{46,47}Mn$, ^{48}Fe, $^{50,51,52}Co$, $^{51,52}Ni$, $^{55,56}Cu$ have been identified (fig. 5).

All the new isotopes are predicted to be bound with the charge symmetry formula of Kelson-Garvey [13]. In this region two isotopes predicted bound remain unobserved namely ^{43}Cr and ^{47}Fe. The two unobserved isotopes ^{42}V and ^{54}Cu of the $T_Z = -2$ series are predicted unbound against one proton emission by about -400 keV.

The observation of the new proton-rich Vanadium to Copper isotopes seems to indicate that the proton drip-line has been reached for odd-Z elements Z = 23, 25, 29.

For the Cobalt isotopes Z = 27 a conclusion is premature at the present level of statistics (Two counts were seen for the isotope ^{49}Co, however predicted unbound by -940 keV).

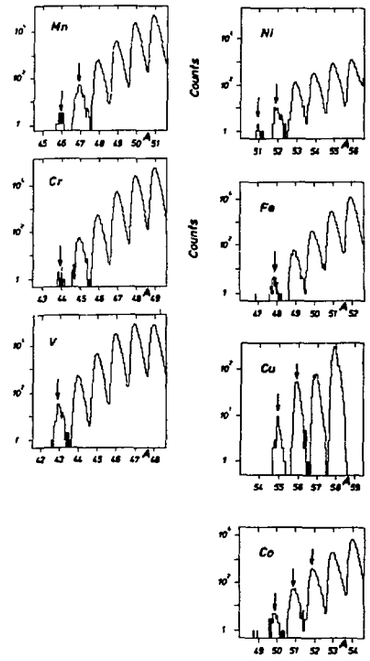

Fig. 5 : Mass spectra for the elements V, Cr, Mn, Fe, Co, Ni, Cu. Arrows mark new isotopes identified in this work.

As a conclusion

All these experiments have allowed to map the neutron-drip line up to Z = 7 and for Z = 9, the proton drip-line up to Z = 20 and for Z = 23,25,29.

These experiments have been very important for establishing the production conditions for subsequent study of the nuclear properties of exotic nuclei unknown before (see other contributions). They will continue with the availability of heavier beams of higher energy after the upgrading of the GANIL cyclotrons and the LISE spectrometer.

References

[1] T.J.M. Symons et al, Phys. Rev. Lett. 42

(1979) 40

[2] R. Anne et al, NIM A257 (1987) 215

[3] M. Langevin et al, Phys. Lett. 150B (1985) 71

[4] F. Pougheon et al, Europhys. Lett. 2 (1986) 505

[5] S. Maripuu, special editor, At. Data Nucl. Data Tables 17 (1976) 1

[6] M. Uno et al, INS Report NUMA 40 (1982)

[7] D. Guillemaud-Mueller et al, Zeit. Phys. A332 (1989)

[8] G.D. Westfall et al, Phys. Lett. 43 91979) 1859

[9] K. Sümmerer, GSI Scientific Report 87-1 (1986) 97

[10] D. Guillemaud-Mueller et al, Zeit. Phys. A322 (1985) 415

[11] M. Langevin et al, Nucl. Phys. A455 (1186) 149

[12] F. Pougheon et al, Zeit. Phys. A327 (1987) 17

[13] I. Kelson et al, Phys. Lett. 23 (1966) 689

[14] A.H. Wapstra et al, Nucl. Phys. A432 (1985) 1

[15] M.G. Saint-Laurent et al, Phys. Rev. Lett. 59 (1987) 33

MASS MEASUREMENTS OF NEUTRON RICH FRAGMENTATION PRODUCTS

G. Audi[1], L. Bianchi[2], A. Cunsolo[3], B. Fernandez[2], A. Foti[3], J. Gastebois[2], A. Gillibert[2], C. Grégoire[4], W. Mittig[4], M. Morjean[4], Y. Pranal[4], Y. Schutz[4], C. Stephan[6], L. Tassan-Got[6], A.C.C. Villari[7], Z. Wen Long[8].

1. C.S.N.S.M. Orsay, 2. D.Ph.N/BE C.E.N. Saclay, 3. I.N.F.N. Catania, 4. GANIL Caen, 5. C.E.N. Bruyères-le-Châtel, 6. I.P.N. Orsay. 7. I.F.U.S.P. Saô Paulo, 8. I.M.P. Lanzhou.

From the most fundamental models to very phenomenological ones, the calculations are expected to reproduce at least some static nuclear properties. Among them, the binding energy is of prime importance since it is the lowest energy eigenvalue of the nuclear Schrödinger equation. For the stablest nuclei, all calculations reproduce with more or less success the binding energy data. However such an agreement is ambiguous since a lack of physical description may be overcome by more unphysical free parameters. Thus, new data relative to β unstable nuclei very far from stability are very useful since they were not previously used to fit any parameter. The whole calculation may then be tested with the new initial conditions present in these nuclei, that is with a very different isospin. An other interest of these measurements is to lock at the behaviour of nuclei very far from β stability and especially the evolution of magic shell closures.

Projectile fragmentation at relativistic energy turned to be an efficient way to produce very neutron rich nuclei at Berkeley. A naive but rather successfull description of the results was obtained using a geometrical overlap model. At lower incident energy - the Ganil energy domain - the relevant mechanism is not yet well understood. Production of nuclei heaving more neutrons than the projectile shows clearly the importance of pick-up or diffusion processes. These diffusion processes may be partially responsible for the high production cross-sections of exotic nuclei observed at intermediate energies. This, together with the high beam intensity for light projectile (>10^{11} particles/s) like ^{40}Ar is the reason why Ganil is so attractive for production and study of light neutron rich nuclei. The primary neutron rich projectiles used so far were ^{40}Ar, ^{86}Kr and ^{48}Ca. Further, with that kind of reaction mechanism, not only a specified nucleus is produced and favoured, but all its neighbours in mass and atomic number. What would be a parasitic background for other studies is very useful here, since many calibration point - say nuclei with well-known mass-turned out to be measured (fig. 1).

According to the relativistic formulation between the magnetic rigidity B_ρ, the charge state q, the mass mc^2 and the velocity $\beta=v/c$,

$$qB_\rho = mc^2 \beta (1 - \beta^2)^{-\frac{1}{2}}$$

both the magnetic rigidity and the velocity are measured to deduce the mass value. Clearly the experimental resolutions have to be at least as good as the final mass resolution required to be in the 10^{-4} range. This goal is achieved with the help of the high resolution properties of the magnetic spectrometer SPEG and a time of flight measurement over a eighty meter long path. We measured fourty mass values, most of them being unknown so far. The mass resolution Δ m/m (full width at half maximum) is typically equal to 2-3 10^{-4}. The final accuracy of the binding energy is only ruled by the number of counts and the systematic error which was reduced to $\sim$ 5 10^{-6}. What should be kept in mind is that any measurement locses a large part of its interest when the error bar goes beyond 1 MeV.

As an exemple of results obtained with ^{40}Ar projectile, fig. 2 compares the experimental results with theoretical predictions for oxygen isotopes. The shell model calculation only has a good predictive power. It is a non trivial result that such a calculation is reliable far from stability.

Microscopic Hartree - Fock calculations performed by F. Naulin with a Skyrme SIII force on light even even nuclei reproduce nicely the two neutron separation energies, at least as well as other calculations where much more free parameters are included.

The ^{40}Ar beam is well-suited to study the shell closure N=20 far from stability. One sees on

fig. 3 the two neutrons separation energy S_{2n}. The sodium isotopes at CERN were found earlier to be much more bound than expected at this major shell closure. Instead of the classical behaviour seen with Ca isotopes, the isotopes ^{31}Na and ^{32}Na do not seem to be much less bound than the N<20 isotopes. This was interpreted in the shell model frame as the onset of a new deformation due to the energy lowering of the f7/2 orbital in a prolate configuration. Poves et al. have extended sd shell model calculations to the f7/2 p3/2 shells but fail to reproduce the binding energies in this region. They predict however strong contributions of 2p2h deformed configurations for N=20 and Z=11. A global theoretical description of this region is therefore still missing.

Data from ^{48}Ca and ^{86}Kr projectiles relative to shell closures *N=20* and *N=28* are presently analyzed. For more details, see references.

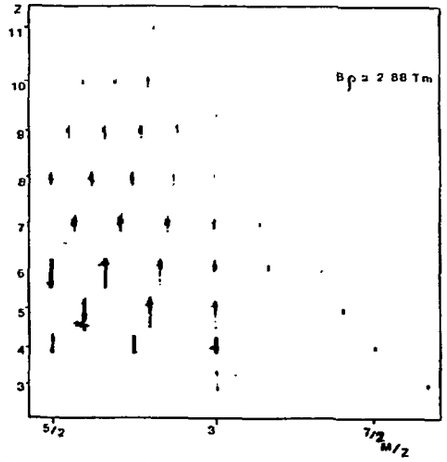

Fig. 1 : Matrice d'identification obtenue avec le projectile ^{40}Ar à 60 MeV/A et pour la valeur B_ρ = 2.88 Tm. L'abscisse correspond au rapport A/Z et l'ordonnée au numéro atomique Z.

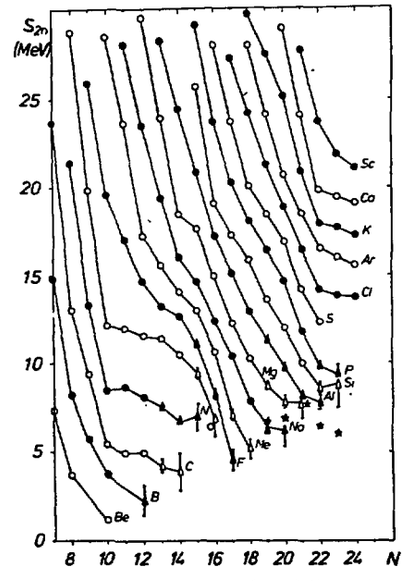

Fig. 3 : S_{2n} curves as a function of the neutron number. Open symbols stand for even-Z nuclei, circles for the values of tables and triangles for this work. The more neutron-rich sodium isotopes (N>19) measured at CERN are labelled by a star.

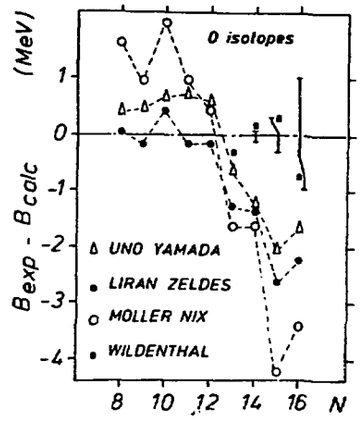

Fif. 2 :Difference between experimental mass excess and predictions from mass calculations for the oxygen isotopes. The error bars correspond to the experimental uncertainties.

- A. Gillibert et al., Phys. Lett. 176(1986)317 ; 192(1987)39.
- Y. Schutz et al., Preprint Ganil P 8717.
- Int. Winter Meetings on Nuclear Physics, Bormio (1986) ; (1987) 426.
- W. Mittig et al., 5th Int. Conf. on Nuclei far from Stability Roseau Lake (1987) 11 ; Riken, IN2P3 Symp. on Heavy Ion Collisions (1987) 70.

Study of β-Delayed Neutron Emission of Very Neutron-Rich Light Nuclei

R. Anne[1], A.G. Artukh[2], D. Bazin[1], V. Borrel[3], C. Détraz[1], D. Guerreau[1], D. Guillemaud-Mueller[1], J.C. Jacmart[3], A.M. Kalinin[2], V.V. Kamanin[2], M. Lewitowicz[2] S.M. Lukyanov[2], A.C. Mueller[1], *Nguyen Hoai Chau*[2], *Yu.E. Penionzhkevich*[2], F. Pougheon[3], A.Richard[3], M.G. Saint-Laurent[1], W.D. Schmidt-Ott[4]

1) GANIL, F-14021 CAEN. 2) Laboratory of Nuclear Reactions, JINR, PO-Box 79, DUBNA, USSR
3) IPN F-91406 ORSAY. 4) II. Physikalisches Institut der Universität, D-3400 Göttingen, FRG

The experiments on the production and identification of new nuclei far from stability which were performed at LISE (see elsewhere in this book) have stimulated us to undertake the next step in the study of these species. Their increasing distance to the valley of β-stability translates into increased values of the β-decay energy Q_β. Eventually, this opens up a window for decay into particle-unstable states in the daughter nuclei. The delayed neutrons which are observed for the decay of very neutron-rich nuclei being coincident to the β-rays provide a very valuable experimental tool for the measurement of β-decay half-lives $T_{1/2}$ at very low counting rate. The liquid-scintillator detector which we have developped for our experiments [1] also provides information on the delayed neutron emission probabilities P_n.

Systematic measurements of both quantities are important to test our knowledge of the nuclear weak interaction. Much theoretical progress has been made recently (see below), partly stimulated by our experiments. Furthermore, the information on basic decay properties of the very neutron-rich nuclei is needed in astrophysical scenarios [2].

So far, we have produced the neutron-rich nuclei by means of ^{86}Kr and ^{48}Ca beams from GANIL at 45 MeV/u and 55 MeV/u, respectively. The projectile-like fragments from the interaction with ^{181}Ta targets were analyzed by the doubly achromatic spectrometer LISE [3]. They were stopped, at the exit of LISE, in a semiconductor-detector telescope. The implanted nuclei were identified by their energy-loss and their time-of-flight through the spectrometer on an event-by-event basis. As soon as an isotope of interest was detected, the GANIL-beam was switched off for a period corresponding to the expected β-half-life in order to allow the registration of β-neutron coincidences at low background. For maximum efficiency, the β-rays and the neutrons were observed by a 4Π detector geometry (see fig.1): The semiconductor detector telescope was surrounded by a 3mm tumbler-shaped NE-102A plastic-scintillator for the β-rays, the whole being inside a NE-213 liquid-scintillator detector for the neutrons. The latter was chosen for its excellent neutron-γ separation properties.

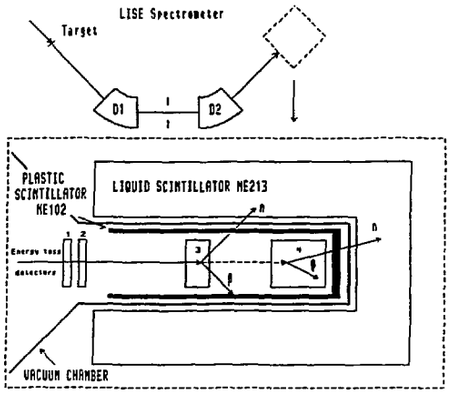

Fig.1 Schematical set-up of the experiment.

The quality of the observed signals may be seen in fig.2, which shows the decay of the isotope ^{15}B. The half-life of 10.3 ms is in perfect agreement with a previous result [4]. In this way we have obtained decay data for the first time for the following isotopes: ^{18,20}C, ^{20}N, ^{35}Al, ^{39,40,41,42}P, ^{43,44}S [5,6].

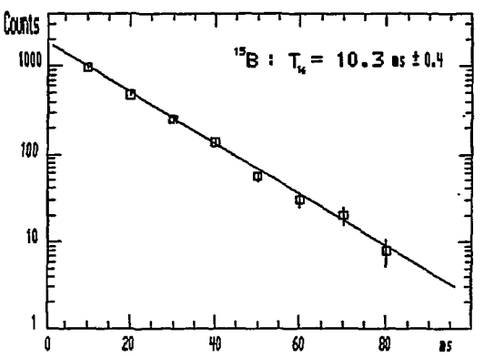

Fig.2 β-decay of the isotope ^{15}B.

We have compared, in fig.3, our experimental results to various theoretical predictions. They include the "old" gross theory by Takahashi [7], its recent refinement by Tachibana et al. [8] and the microscopic model of Klapdor et al. [9]. Furthermore, results are shown from the new calculation by Staudt and Klapdor [10] which is based on a proton-neutron quasi-particle random phase approximation.

Fig.3 Ratio of theoretical to experimental β half-lives versus the mass number A. The error bars correspond to (statistical) experimental errors. In the calculation by Staudt et al. experimental masses (Nucl. Phys. A432 (1985) 1) are used for ^{19}N and ^{34}Al; other masses are taken from v.Groote et al. (At. Data Nucl. Data Tables 17 (1976) 418). $\bar{x}$ denotes the mean value of the logarithm of the ratio between the experimental and the theoretical half-lives and σ the standard deviation.

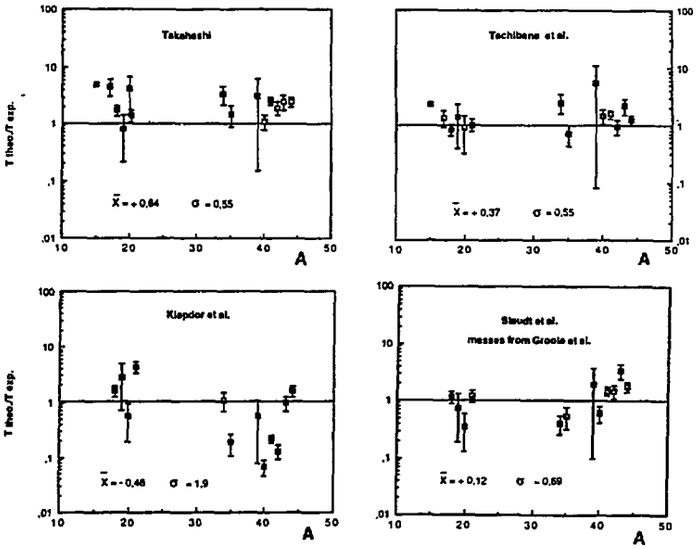

Several features are obvious from fig.3: The "old" gross theory substantially overestimates the experimental half-lives. This rather systematic deviation (see the small value of σ in fig.3) is clearly corrected for in the second-generation calculation by Tachibana et al. without deteriorating the scatter of the individual data points. The microscopic model by Klapdor et al. yield a rather good average of $\bar{x} = -0.46$. Here, however the standard deviation $\sigma = 1.9$ is indicating several large discrepancies to the experimental half-lives which makes the predictions from this model less reliable. On the other hand, the new microscopic model of Staudt and Klapdor seems to exhibit a remarkable predictive power far off stability. In the same experiments we could also measure the delayed neutron emission probabilities P_n, these results are also discussed in [5,6].

Concerning the astrophysical relevance of our data, one may mention, in addition to the global importance of decay data far off stability for network calculations of the nucleosynthesis, the particular case of $T_{1/2}$ of ^{44}S which is a key parameter for solar isotope abundances [11].

References

1) D. Bazin, thesis, Caen University 1987 and GANIL-report T.87-01
D. Bazin, A. C. Mueller and W.D. Schmidt-Ott submitted to Nucl. Inst. Meth. and GANIL-report P.89-01
2) H.V. Klapdor
Int. Symp. on Heavy Ion Physics and Nucl. Astrophysical Problems, Tokyo, 1988
3) R. Anne, D. Bazin, A. C. Mueller et al.
Nucl. Inst. Methods A257 (1987) 215
4) J.P. Dufour, S. Beraud-Sudreau et al.
Z. Phys. A319 (1984) 237
5) A.C. Mueller, D. Bazin et al.
Z. Phys. A330 (1988) 63
6) M. Lewitowicz, Yu. E. Penionzhkevitch et al.
Nucl.Phys.A in press and GANIL-report P89-02
7) K. Takahashi
Prog. Theo. Phys. 47 (1972) 1500
8) T. Tachibana, S. Ohsugi, M. Yamada
5th Int. Conf. on Nucl. far from Stability, Rosseau Lake, Canada 1987; to be published
9) H.V. Klapdor, J.Metzinger, T. Oda
At. Data Nucl. Data Tables 31 (1984) 81
10) A. Staudt and H.V.Klapdor
private communication and to be published
11) K.L. Kratz, P. Möller, W. Hillebrandt et al.
5th. Int. Conf. on Nucl. far from Stability, Rosseau Lake Canada 1987; to be published

β-DELAYED MULTI-NEUTRON RADIOACTIVITY OF ^{17}B, ^{19}C AND ^{14}Be

J.P. Dufour, M. Beau[4], R. Del Moral, A. Fleury, J. Frehaut[4],
G. Giraudet[4], E. Hanelt[3], F. Hubert, D. Jean, A.C. Mueller[1],
M.S. Pravikoff, K.-H. Schmidt[2], K. Sümmerer[2]

C.E.N. Bordeaux-Gradignan, [1]GANIL Caen, [2]GSI Darmstadt
[3]TH Darmstadt, [4]C.E.A. Centre d'Etudes de Bruyères-le-Châtel

Until recently, the experimental possibilities to investigate isotopes near the neutron drip line were almost restricted to the alkaline elements. Therefore, especially ^{11}Li was extensively studied and it has proven to be the precursor for the emission of up to three neutrons[1] and also tritons[2].

The nuclei ^{17}B, ^{19}C and ^{14}Be which have high Q_β-values up to 24 MeV should also be good candidates for β-delayed multi-neutron radioactivity. In our experiment these isotopes were produced at GANIL by the projectile fragmentation of a 60 MeV/u ^{22}Ne-beam impinging on a 1.2 g/cm^2 tantalum target. They were separated using the spectrometer LISE[3] operated as a momentum-loss achromat and implanted into a 7 mm thick plastic scintillator which was designed to detect both the implantation signal and the following beta decays. This method of Projectile-Fragments Isotopic Separation[4] has already successfully been applied to spectroscopic studies[5] and isotope search[6]. Additionnally, the nuclei at the exit of LISE could be electronically identified by a ΔE-time of flight measurement (fig. 1). This was done by means of a silicon transmission detector the signal of which was referenced to the accelerator rf. After the signal of a desired nucleus the beam was stopped for 100ms and the time between the implantation and the correlated β-decays during the beam pause was recorded. The neutrons occuring promptly after the β-decay were counted during a time window of 50μs triggered by the decay signal. They were detected with a mean delay of 11 μs and an efficiency of 70% by means of a 4π neutron ball[7] filled with 500l of liquid scintillator doped with Gadolinium. Since this detector is also sensitive to γ-rays with energies above 0.5 MeV, it was necessary to measure the number of background events. Therefore they were counted in a second 50μs window following the first one after a delay of 50μs.

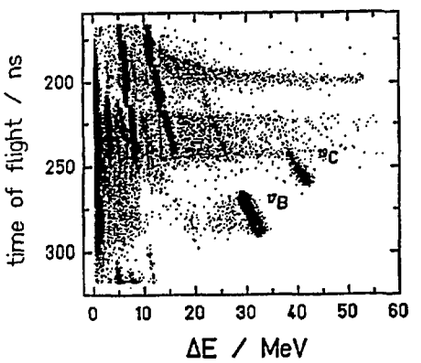

Fig. 1 : ΔE-TOF-spectrum (logorithmic intensity scale) measured at the exit of LISE which was optimized to separate ^{17}B

	^{17}B	^{19}C	^{14}Be
$t_{1/2}$/ms	5.08 (5)	49 (4)	4.35 (17)
p_{0n}/%	0.21 (2)	0.46 (3)	0.14 (3)
p_{1n}/%	0.63 (1)	0.47 (3)	0.81 (4)
p_{2n}/%	0.11 (7)	0.07 (3)	0.05 (2)
p_{3n}/%	0.035 (7)		
p_{4n}/%	0.004 (3)		

Table 1 : results (the error-bars correspond to one standard deviation)

The off-line analysis had to take into consideration three effects changing the measured neutron-multiplicity spectra : the daughter activities, the background pile-up and the finite neutron detection efficiency. Figure 2 shows the measured β-activities corresponding to different neutron multiplicities and their fits as a function of the time between the nucleus implantation and its β-decay.

The results for the normalized neutron multiplicity branchings p_{xn} and the half-lifes $t_{1/2}$ of the observed nuclei are summarized in table 1. All nuclei are precursors for the emission of at least two neutrons. In the case of ^{17}B a four neutron branch is reported for the first time. Thus, the β-delayed three neutron emission of ^{11}Li is not an outstanding case any more. The emission of several neutrons has proven to be a general decay mode of the light and extremely neutron-rich nuclei. This work has been published[8].

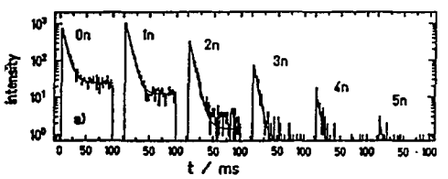

Fig. 2 : measured β-activities of ^{17}B and their fit (see text)

1 - R.E. Azuma et al., PL, 96B, 31 (1980)
2 - M. Langevin et al., PL, 146B, 176 (1984)
3 - R. Anne et al., NIM, A257, 215 (1987)
4 - J.P. Dufour et al., NIM, A248, 267 (1986)
5 - J.P. Dufour et al., Z. Phys. A-Atom. Nucl. 324, 487 (1986)
6 - M.G. Saint-Laurent et al., Phys. Rev. Lett. 59, 33 (1987)
7 - J. Frehaut, NIM, 135, 511 (1976)
8 - J.P. Dufour et al., PL, B206, 195 (1988)

BETA-DELAYED GAMMA SPECTROSCOPY ON LIGHT NEUTRON RICH NUCLEI

J.P. Dufour, R. Del Moral, A. Fleury, F. Hubert, D. Jean, M.S. Pravikoff
C.E.N. Bordeaux, IN2P3, Le Haut Vigneau, F-33170 Gradignan
H. Delagrange, GANIL, B.P. 5027, F-14021 Caen Cedex
H. Geissel and K.-H. Schmidt, GSI, D-6100 Darmstadt
E. Hanelt, TH, D-6100, Darmstadt

The GANIL intermediate energy heavy-ion beams have proved very efficient at producing exotic light nuclei. The application to the LISE spectrometer of the Projectile Fragments Isotope Separator[1], provided beta delayed gamma spectroscopic data on light neutron-rich nuclei (mass range 14-40). The production rates and the nature of the measurements are listed in table 1 for the 22 studied isotopes .

The bulk of information gathered on these decay is very large. A first list of gammas, intensities and half-lives has already been published[2,3]. The half-lives were all measured with beam pulsations uncorrelated to the nuclei implantation. The isotopes listed in table 1 lie in three different shells : p, sd and fp. The comparison of the experimental data with shell-model calculations is most complete in the sd shell where Wildenthal's predictions[4] are detailed and include the β decay. The accuracy of these predictions is very impressive.

Nuclei in the sd shell : an interesting property of the PFIS selection is a very good rejection rate of the daughter of the separated isotope. The beta branching of ^{23}F and ^{34}Si to the ground states of ^{23}Ne and ^{34}P have thus been obtained through the daughter's total activity determination. The experimental values (30 ± 8% and 65.5 ± 2.3% respectively) compare well with the theoretical predictions : 33.6% and 56%. Another specificity of the apparatus is its tuning versatility and very short transport time. Those properties were especially useful in the study of ^{26}Ne. When LISE was tuned on ^{26}Ne very little gamma activity was observed in a 600 μs beta-gamma coincidence window. The spectrometer was then tuned on ^{26}Na and it was possible to observe the direct decay of a 82.5 ± 0.5 keV excited state not in coincidence with betas. A multispectrum time-analysis starting after each implantation of a ^{26}Na isotope allowed the determination of the half-life, 9 ± 2 μs, of this excited state.

Nuclei in the fp shell : the extension of the shell-model description from the sd to the fp shell, further away from the ^{16}O inert core, has been recently improved by Warburton et al.[5] The comparison of the experimental data with the calculation is very encouraging. The *SDPF* interaction proves its predictive power for the N = 21 isotones from ^{38}Cl to ^{35}Si. Our data on ^{34}Al are still too scarce for a fruitful comparison. The experimental data need to be very extensive in this transition region where the decay from negative parity ground-states feeds very high energy excited states in the daughter. A good example is the 12% feeding from ^{36}P of the 7271 keV state in ^{36}S not seen in the first study of this nucleus. Extension of these calculations is in progress for ^{37}P and ^{36}Si for which good data are available.

1 - J.P. Dufour et al. Nucl. Inst. Meth. A248 (1986) 267
2 - J.P. Dufour et al. Z. Phys. A324 (1986) 487
3 - J.P. Dufour et al 5th Int. Conf. on Nuclei far from Stability, Canada (1987), 344
4 - B.H. Wildenthal et al. Phys. Rev. C28 (1983) 1343
5 - E.K. Warburton et al. Phys. Rev. C34 (1986) 1031 - Phys. Rev. C35 (1987) 1851

Table 1 : Summary of the spectroscopic data obtained by fragmentation of a ^{40}Ar beam at GANIL. A star notes a first study, open triangles and circles respectively note improvements and confirmations of previous measurements

ᴬZ	^{17}C	^{19}N	^{20}N	^{22}O	^{23}F	^{24}F	^{25}Ne	^{26}Ne	^{27}Na	^{30}Mg
$T_{1/2}$	○	☆	★	▲		☆	○	☆	○	▲
(s)	0,20(6)	0,30(8)	0,07(4)	2,25(15)		0,34(8)	0,62(3)	0,23(6)	0,295(20)	0,342(18)
Y	☆	☆	★	☆	▲	☆	○	☆	○	○
N/s	20	>40	8	23	>200	41	510	50	>10^3	860

^{32}Al	^{33}Al	^{34}Al	^{35}Al	^{34}Si	^{35}Si	^{36}Si	^{37}Si	^{35}P	^{37}P	^{38}P	^{40}S
▲		☆	☆	○	☆	☆	☆	○	☆	☆	☆
0,031(6)		0,05(2)	0,03(1)	3,9(11)	0,78(12)	0,45(6)		5,35(53)	2,31(12)	0,61(14)	8,6(21)
▲	☆	☆	☆	▲	☆	☆	☆	▲	☆	☆	☆
1700	260	40	5	>1600	430	100	6	22000	3300	225	58

BETA-DELAYED CHARGED PARTICLES SPECTROSCOPY OF LIGHT NEUTRON DEFICIENT NUCLEI

V. Borrel, J.C. Jacmart, F. Pougheon and A. Richard
INSTITUT DE PHYSIQUE NUCLEAIRE, BP n°1, 91406 ORSAY, FRANCE

R. Anne, D. Bazin, H. Delagrange, C. Détraz
D. Guillemaud-Mueller, A.C. Mueller, E. Roeckl*
and M.G. Saint-Laurent
GANIL, BP 5027, 14021 CAEN CEDEX, FRANCE

J.P. Dufour, F. Hubert and M.S. Pravikoff
CEN Bordeaux ,Le Haut Vigneau , 33170 GRADIGNAN, FRANCE

Light neutron-deficient nuclei exhibit several interesting decay modes. In this region, the rapid increase of mass differences leads, through β^+ decay, to a wide range of final states in the daughter nucleus, including in particular the super-allowed transition to the isobaric analog state. Due to the small proton binding energy, most of these states decay by proton emission, or in some cases by alpha emission. Thus, delayed emission of one, two or three protons and alphas are to be searched. In addition, for a few number of these nuclei, direct two-proton decay has been also predicted [1] .

In these experiments the decays of the T_z = -5/2 nuclei ^{31}Ar [2], ^{27}S and ^{23}Si and of the T_z = -2 nucleus ^{28}S[3] have been studied. The T_z = -3 nucleus ^{22}Si has been observed for the first time[4] and its decay has been measured.

1 THE EXPERIMENT

The GANIL facility, equipped with an ECR ion source operating with enriched ^{36}Ar provides a 85 MeV/u ^{36}Ar beam with an intensity of 4.10^{11} particles per second on the 385 mg/cm^2 natural Ni target. The nuclei under study are produced as projectile-like fragments and the LISE spectrometer is operated as an isotope separator [5,6]. This Projectile Fragment Isotope Separation method combines the magnetic analysis performed by the spectrometer itself with a momentum-loss selection of the ions which fly trough an energy degrader located in the dispersive intermediate focal plane of the spectrometer. In this region of light neutron-deficient nuclei, with carefull optimisation of the two dipoles magnetic rigidities, the PFIS method selects a series of isotones and the studied nucleus is collected at a rate going from 0.1 event per second (for the study of ^{22}Si) up to 5 events per second (for ^{31}Ar). The shape of the aluminium degraders has been designed in order to preserve the achromatism of the set-up. Thus, the transmitted nuclei are identified by deltaE and time of flight measurement between the target and the silicon-detectors telescope (fig.1) located at the final focal point. They are implanted in this telescope by slowing down in aluminium foils located in front of the detectors.

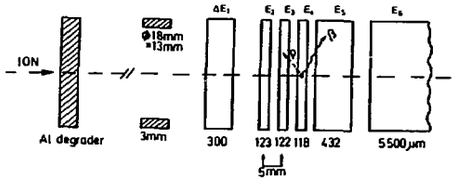

Fig. 1 : The solid-state telescope. The heavy ions are implanted in detectors E4 or E5 and the protons are detected in detectors ΔE1 to E5. The ions are identified on the two-dimensional plot ΔE1 versus time of flight (measured between the target and the ΔE1 detector). E6 is used as a veto to reject high-energy protons.

The radioactive decay of the nuclei of interest is studied on line: the charged particles emitted by the

*Permanent address G.S.I., Postfach 110552, 6100 DARMSTADT 11, Federal Republic of Germany

implanted ions are measured in the same telescope. Since there is no transport of the activity, it is easy to investigate very short half-lives. The detectors are equipped with two electronic chains which permit the detection of low energy protons a few microseconds after the arrival of a very energetic heavy ion. Two single channel analysers examine the ΔE and time of flight signals of each implanted ion and the beam is stopped each time that an interesting ion arrives. The length of the beam-off period can be chosen. The data-aquisition system consists in two systems working in flip-flop mode : the first one records the ions parameters and the second one works only during the beam-off periods and records the ligth particles energy deposits and the elapsed time between the particle emission and the last ion implantation.

2 RESULTS

2.1 ^{31}Ar

In the ^{31}Ar study, the only contaminant for proton detection is ^{29}S. Its beta-delayed protons, recorded during the experiment yield a precise proton energy calibration.

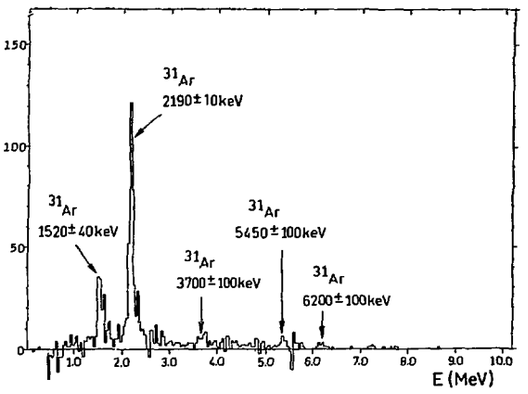

Fig. 2 : Energy spectra of the protons recorded in detector E4 during the 200 ms long beam-off periods. The preceeding ^{31}Ar nucleus is implanted into E4 and most of the emitted protons are stopped in this detector. This difference spectrum has been obtained after subtraction of the ^{29}S contribution estimated on the long-lived part of the spectrum.

In the long-lived part of the energy spectra of the protons emitted during the beam-off time by nuclei implanted, the strongest known [7] proton lines from the decay of ^{29}S are clearly seen. In the difference spectrum (fig. 2), obtained by subtracting the ^{29}S contribution, several peaks decay with the same short half-life and have been attributed to the decay of ^{31}Ar.

The half-life of the ^{31}Ar nucleus is found to be 15 ± 3 *ms* , from a two-component fit assuming the long-lived component to be entirely due to the 187 ms ^{29}S.

From these results a partial ^{31}Ar decay scheme is proposed (fig. 3).

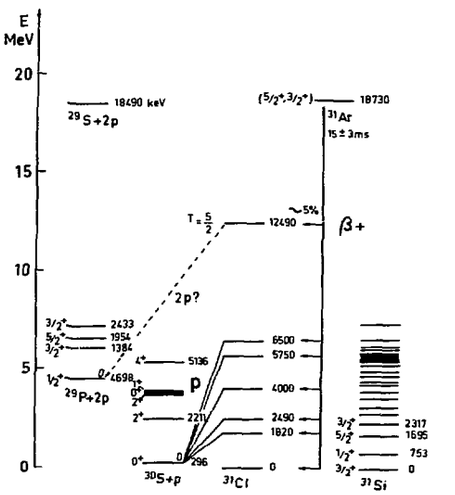

Fig. 3 : Partial decay scheme of ^{31}Ar. For the ^{31}Cl nucleus, the levels are deduced from the present expériment with the exception of the T=5/2 state, for which the energy has been calculated. The energy levels of its mirror nucleus ^{31}Si are also presented.

For the beta-decay of ^{31}Ar to the isobaric analog state in ^{31}Cl, under the assumption of a pure Fermi decay, the measured half-life (15 ms) yields a branching ratio equal to 5 %. These experimental results have been compared with the shell-model calculation of Brown and Wildenthal [8] : the five main predicted proton peaks are actually observed, the intensity ratios corresponding roughly to the calculated ones. The experimental determination of branching ratios is underway.

The isobaric analog state in ^{31}Cl is expected to decay both by one proton and two-proton emission. There is no evidence for any proton peak with energy around 12 MeV or 9.8 MeV. This absence may be due to the combined effects of a low branching ratio and of the strong decrease of the detection efficiency as protons become more energetic. On the contrary, a group of peaks, near 7.5 MeV, decaying with the ^{31}Ar half-life, appears on the sum spectrum (E_3 + E_4 + E_5). Coincidence rate measurements between detectors 3 and 4, 4 and 5 and 3, 4, 5 allow to conclude that one of them represents the summed energies of the two protons emitted by the T = 5/2 state in ^{31}Cl towards the ground-state in ^{29}P, with a calculated energy of 7.8 MeV [9].

The measured ^{31}Ar half-life of 15 ± 3 ms in good agreement with shell-model calculations shows that ^{31}Ar does not exhibit an important branching ratio for direct two-proton decay.

2.2 ^{28}S

With the same method, beta-delayed proton radioactivity has been studied for the ^{28}S isotope (T_z = -2) [3]. This experiment has lead to the location of the lowest T = 2, 0^+ state in the ^{28}P daughter nucleus, at 5900 ± 21 keV. This experimental value allows to complete the isospin quintet of mass 28. A comparison of the experimental data to the quadratic form of the isobaric multiplet mass equation shows that the energies of the five T = 2 states of the A = 28 quintet are well represented by that relation.

The measured half-life of 125 ± 10 ms and the proposed partial decay scheme show an excellent agreement with shell model calculations (fig. 4).

2.3 ^{27}S, ^{23}Si and ^{22}Si

The analysis of the data is underway.

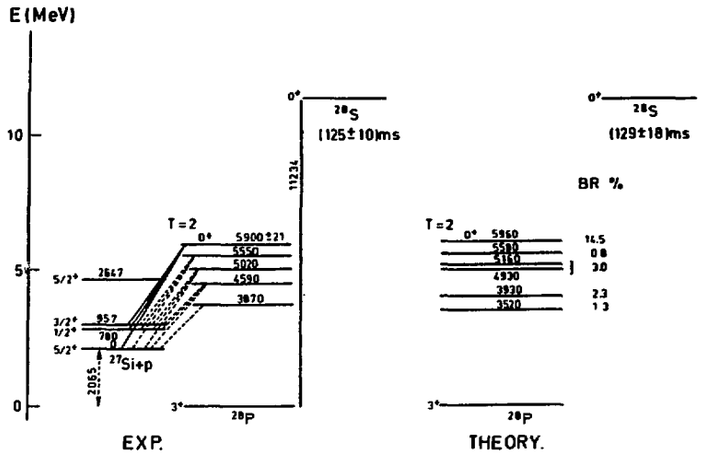

Fig. 4 : Partial decay scheme of ^{28}S. For the ^{28}P nucleus, the levels are taken from the $^{28}Si(p,n)^{28}P$ data [10] with the exception of the T = 2 state deduced from this work. Only the ^{28}P levels above 3 MeV have been indicated. Energies are in keV. The theoretical predictions are also presented.

References

[1] V.I. Goldansky, Nucl. Phys. **19** (1960) 482; Nucl. Phys. **27** (1961) 648; Phys. Lett. **B 212** (1988) 11

[2] V. Borrel et al, Nucl. Phys. **A 473** (1987) 331

[3] F. Pougheon et al, submitted to Nucl. Phys. A ; IPNO DRE 89-02

[4] M.G. Saint-Laurent et al, Phys. Rev. Lett. **59** (1987) 33

[5] R. Anne et al, Inst. Meth. **A 257** (1987) 215

[6] J.P. Dufour et al, Nucl. Inst. Methods **A 428** (1986) 267 and this book

[7] D.J. Vieira et al, Phys. Rev. C **19** (1979) 177

[8] B.A. Brown and B.H. Wildenthal, At. Data and Nucl. Data Tables **33** (1985) 347

[9] V. Borrel et al, to be published

[10] B.D. Anderson et al, Private Communication

Some Properties of β-delayed Charged Particle Emission of ^{39}Ti and ^{40}Ti.

R. Anne*, D. Bazin‡, P. Bricault*, C. Détraz*, J.P. Dufour‡, A. Fleury‡, D. Guillemaud-Mueller†, F. Hubert‡, J.C. Jacmart†, M. Lewitowicz*, A. Mueller†, F. Pougheon†, M.S. Pravikoff‡, A. Richard†, Y. H. Zhang*

1- Introduction

The study of nuclei far from stability has led to the discovery of new decays modes and new structures not seen in nuclei near stability. Work on nuclei near the proton drip-line, for example, has led to the discovery of proton radioactivity and beta-delayed one-proton, and two-proton decays.

Heavy ion fragmentation at intermediate energy has demonstrated its effectiveness in the production of many proton rich nuclei. In this region, the rapid increase of mass difference leads, though β^+-decay, to a wide range of final states in the daughter nucleus, including in particular the isobaric analog state, (IAS), through a super-allowed transition. Because of their small binding energy, most of the states decay by proton emission. The proton spectra are expected to give information on the position of the analog state and on the distribution of the Gamow-Teller strength.

In the case of ^{40}Ti, only β^+-delayed proton emission is energetically possible; but in the case of ^{38}Ti, β^+-delayed two-proton or alpha emission and direct two-proton emission may also occur. This nucleus, bound against one-proton emission, is indeed predicted to be slightly unbound against two-proton emission, with a two-proton separation energy, of $S_{2p} \simeq -740$ keV. Direct two-proton decay has been predicted long ago by Goldanskii[1], and discussed by Jänecke[2] and recently by Goldanskii[3]. But the search for this new radioactivity became possible only recently, with the new techniques used in heavy ion research. The half-life of this radioactive mode depends strongly on the barrier penetrability, thus on the decay energy and the angular momentum. The detection of a proton pair with a kinetic energy of few hundred keV is experimentally difficult. One may find evidence for direct two-proton emission by observing a half-life much shorter than one expected for beta decay.

2- The experimental method

Very proton-rich isotopes are produced through the fragmentation of heavy ions impinging on a target. The separation of the projectile-like fragments is performed using the 0° magnetic spectrometer, LISE[4], working in separation mode. The identification of the nuclei is done using a ΔE-time-of-flight technique. For this purpose the detection telescope consists of several surface-barrier Si-detectors. We used an energy degrader of variable thickness placed in front of the detectors tuned in such a way that the isotope of interest comes at rest in a very thin Si-detector located between two others detectors. On line, two single-analyzers examine the ΔE and the time-of-flight information. Each time that an isotope of interest is inside the corresponding window the beam is stopped during about 200 ms. During this time the heavy-ion data- acquisition system is set off-line and a clock and a second data-acquisition for registration of light particle emitted from this nucleus is started.

3- Experimental results and discussion

a) ^{40}Ti

The energy spectrum of the β-delayed protons emitted after the implantation of 190 nuclei of ^{40}Ti in the ΔE3 detector is shown in fig. 1. Total-decay energy spectrum is obtained, since both the proton and the recoil energies are recorded in the detectors. At least four peaks can be identified and assigned to β-delayed proton emission from ^{40}Ti. The partial decay scheme is presented in fig. 2. The time distribution for all β-delayed protons of ^{40}Ti is presented in fig. 3a. The β-decay half-life is found to be $T_{1/2} = 56^{+19}_{-12}$ ms. The measured half-life is close to the theoretical prediction of Tachibana et al[5], ($T_{1/2}$= 66.7 ms).

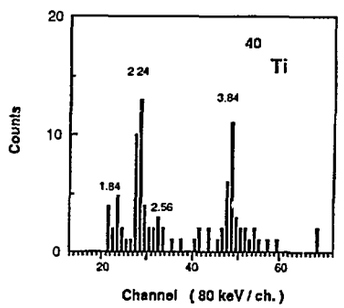

Fig. 1. Energy spectrum of β-delayed protons emitted from ^{40}Ti. Energies are given in MeV.

* GANIL, B.P. 5027, 14021 Caen, Cedex, France.
† Institut de Physique Nucléaire, B.P. N°1,91406 Orsay, France.
‡ C.E.N. Bordeaux, Le Haut Vigneau, 33170 Gradignan, France.

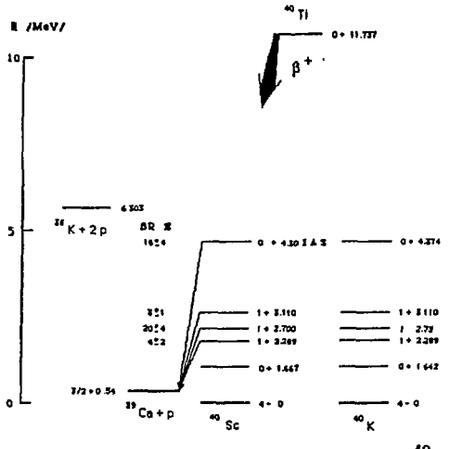

Fig. 2. Proposed partial decay scheme of ^{40}Ti. The corresponding levels of mirror nuclei, ^{40}K and measured BR values are shown. Energies are in MeV.

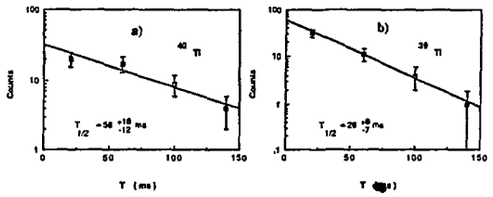

Fig. 3. Time spectra of charged particles from a) ^{40}Ti and b) ^{39}Ti. Error bars correspond to one standard deviation.

b) ^{39}Ti

In the present experiment the existence of ^{39}Ti is shown for the first time. However the collection of only 75 nuclei of ^{39}Ti leads to a charged-particle energy spectrum of rather low statistics. Only one peak at energy 3.52 ± 0.12 MeV is identified without any doubt. Possible contamination by β-delayed protons coming from ^{37}Ca can be excluded, since in the energy spectrum, fig. 4, the main peak of ^{37}Ca (BR = 46.74 %)[6], at 3.063 MeV is absent. Beta-delayed protons from ^{37}Ca produced as a daughter nucleus would also be observed in the case of direct two-proton emission of ^{39}Ti. The absence of protons from ^{37}Ca thus give a strong argument against the hypothesis that ^{39}Ti is a strong direct two-proton emitter.

From the time spectrum of charged- particle decay, shown in fig. 3b, a half-life of 26^{+8}_{-7} ms is deduced for ^{39}Ti, a value not far from theoretical expectation for β half-life of this isotope ($T_{1/2}$=36.3 ms[5]), providing a second argument against sizeable direct two-proton emission.

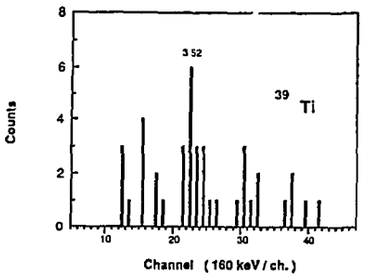

Fig. 4 Energy spectrum of β-delayed charged particles emitted from ^{39}Ti. Energy are in MeV.

4. Conclusions

The first observation of ^{40}Ti and ^{39}Ti decays are achieved with the very efficient selection of reaction products provided by the LISE spectrometer at GANIL. In the case of ^{39}Ti, it is the first successful attempt to produce and identify this isotope.

The measured charged particle energy shows evidence for β-delayed proton decay of ^{40}Ti. The experimental half-life (56^{+18}_{-12} ms) is in reasonable agreement with theoretical prediction (66.7 ms[5]).

In the charged-particle energy spectrum of ^{39}Ti, no evidence appears for β-delayed protons of ^{37}Ca. The measured half-life (26^{+8}_{-7} ms) is consistent with a β-decay mode for ^{39}Ti. Thus no evidence for direct two-proton decay of ^{39}Ti is found.

The new improvement of GANIL facility under realization will give us the opportunity to extend the range of the investigation to larger masses, with heavier projectiles available with a new ion source. Also, an electrostatic deflector will be placed just after the LISE spectrometer. This new device will permit higher beam intensity on the production target without any increase of the background in the detection area. This will allow us to search for very exotic nuclei, in particular exhibiting direct two-proton decay, without any contamination due to other isotopes transmitted by the spectrometer.

1. V.I. Goldanskii, Nucl. Phys. **19** (1960) 482 Nucl. Phys. 27 (1961) 648
2. J. Jänecke, Nucl. Phys. **61** (1965) 326
3. V.I. Goldanskii, Phys. Lett. B, **212**, N° 1 (1988) 11.
4. R. Anne, D. Bazin, A. C. Mueller, J. C. Jacmart, M. Langevin, Nucl. Inst. Meth. **A248** (1986) 267
5. T. Tachibana, S. Ohsugi, M. Yamada, Proceedings of the 5-th Int. Conf. on Nuclei far from Stability, Sept. 14-19, 1987, Rosseau Lake, Ontario, Canada
6. R. G. Sextro, R. A. Gough, J. Cerny, Nucl. Phys. **A234** (1974) 205

BETA DECAY OF ^{22}O

F. Hubert, J.P. Dufour, R. Del Moral, A. Fleury, D. Jean, M.S. Pravikoff,
C.E.N Bordeaux, IN2P3, Le Haut-Vigneau, F-33170 Gradignan
H. Delagrange, GANIL, B.P. 5027, F-14021 Caen Cedex
H. Geissel and K.-H. Schmidt, G.S.I. D-6100 Darmstadt
E. Hanelt, TH, D-6100 Darmstadt

As part of a program investigating the properties of exotic light nuclei produced at GANIL, we have studied the beta decay of the neutron rich nucleus ^{22}O. These nuclei were produced by a 60 MeV/n ^{40}Ar beam interacting with a thick Be target, and selected among all the produced nuclei with the LISE separator. Both β-γ and β-γ-γ coincidences could be measured using a Ge detector and a matched pair of NaI detectors. Five γ lines were attributed to the β decay of ^{22}O according to several criteria[1] (table 1). Coincidence data between the two NaI and the Ge detectors allow to established the partial decay scheme of fig. 1.

Values for the excitation energy of ^{22}F levels have been deduced that are consistent with previously published values[2-4] except for a ground-state and first excited state doublet hitherto unobserved. The relative β branchings represent only limits on the feeding of the involved levels.

Table 1

γ ray (keV)	Definite coincidence	Relative intensity (a)	Transition $E_i \rightarrow E_f$ (b)
71.6(2)	637, 918, 1862	100(32)	72→0
637.4(2)	72, 918, 1862	100(7)	710→72
709.6(3)			
918.0(2)	72, 637	34(4)	1627→710
1862.6(3)	72, 637	56(7)	2572→710
1874.2(10)		8(4)	

a) Intensities normalized to 100 for the 72keV and 637 keV γ lines and corrected for summing effects.

b) Proposed excited states in ^{22}F deduced from the present measurement. The uncertainty on the level value is ≈ 1keV.

Regarding the shell-model description of the β decay of ^{22}O the measured and predicted values for the half-life are in excellent agreement[5]. The theory successfully predicts the observed excited states in ^{22}F[6]. The calculation agrees well with the experimental limits set on the beta branching ratios. But the experimental γ ray results are only partially understood.

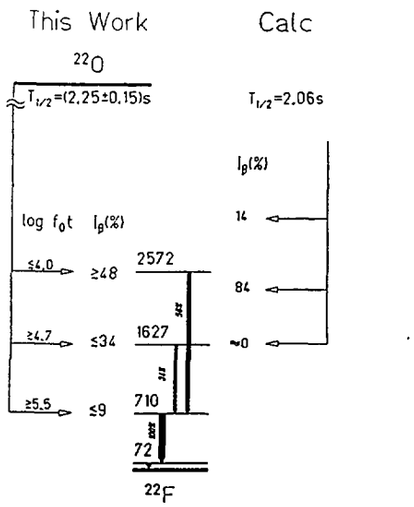

Fig. 1 :
Experimental and theoretical ^{22}O decay schemes.

1) F. Hubert et al., Beta decay of ^{22}O, Accepted for publi. in Z. Phys.
2) R. H. Stokes et al., Phys. Rev. 178 (1969) 1789
3) N. Orr - private communication
4) N.M. Clarke et al., J. Phys. G : Nucl. Phys. 14 (1988) 1399
5) B.H. Wildenthal et al., Phys. Rev. C28 (1983) 1343
6) B.A. Brown et al., Private communication

SPIN ALIGNMENT IN PROJECTILE FRAGMENTATION AT INTERMEDIATE ENERGIES

K. Asahi, M. Ishihara*, T. Ichihara, M. Fukuda**, T. Kubo, Y. Gono
RIKEN, Wako-shi, Saitama 351-01, Japan
A.C. Mueller+, R. Anne, D. Bazin++, D. Guillemaud-Mueller+
GANIL, B.P. 5027, 14021 Caen Cedex, France
R. Bimbot
IPN Orsay, B.P. 1, 91406 Orsay, France
W.-D. Schmidt-Ott
II. Physikalisches Institut, Univ. Goettingen, D-3400 Goettingen, FRG
J. Kasagi
Tokyo Institute of Technology, Oh-Okayama, Tokyo 152, Japan

1. Introduction

Recent studies of nuclei far from stability[1] using high- and intermediate-energy heavy-ion beams have proven that the projectile fragmentation process provides a powerful tool for production of unstable nuclei. Besides the advantage of high production rates available for wide ranges of unstable nuclei, the strong kinematical focusing of projectile fragments with respect to both the emission angle and velocity facilitates isotope separation with high collection efficiency by means of magnetic analysis during flight. The effectiveness of this method for isotope production arouses further interest in whether these product nuclei are spin-oriented. In fact, the presence of non-zero spin orientation in projectile fragments would enable more detailed spectroscopic investigations such as g-factor measurements on exotic nuclei. The measurement of the spin orientation in projectile fragmentation is also interesting as a source of unique information on reaction mechanisms. For example, a simple model of projectile fragmentation predicts a specific momentum. We thus performed a measurement of the dependence of the spin alignment on fragment spin alignment of projectile fragments.

2. Experimental Procedure

Spin alignment of ^{14}B nuclei produced in ^{18}O + ^{9}Be reaction at E(^{18}O)/A = 60 MeV/u was measured. Experimental setup used is shown in Fig. 1. Spectrometer LISE was used for the isotope separation of the reaction products. A wedge-shaped energy degrader for the momentum-loss technique[2] was placed in the momentum-dispersive focal plane between the two dipole magnets of LISE. Products ^{14}B were stopped in a stopper foil (Pt) placed at the achromatic focal point. Static magnetic field B_0 = 310 mT parallel to the two dipole fields of LISE was applied to the stopper. The 6.09-MeV γ rays emitted after the β decay of ^{14}B were detected by using two NaI(Tl) detectors placed at 0° and 90° to the direction of B_0. The ratio $R = N_\gamma(0°)/N_\gamma(90°)$ of the γ ray yield was measured both with B_0 on (i.e., with the alignment preserved) and off (with the alignment destroyed).

The spin alignment A produced by reaction in the beam axis is expressed as $A = (2a_{+2}-a_{+1}-2a_0-a_{-1}+2a_{-2})/2$ in terms of the population probability a_m for the magnetic sublevel m. As

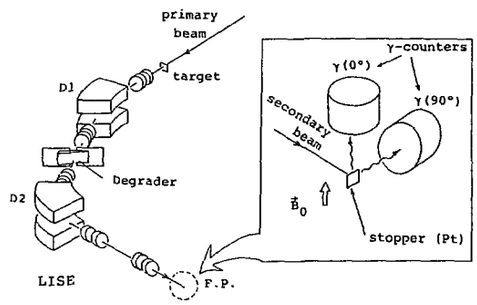

Fig. 1: Experimental setup.

---

* Also, Univ. of Tokyo, Tokyo 188, Japan.

** Present address: Osaka Univ., Toyonaka, Osaka 560, Japan.

\+ Present address: IPN Orsay, B.P. 1, 91406 Orsay, France.

++ Present address: CENBG Bordeaux, 33170 Gradignan, France.

a result of the spin precession in the dipole fields of LISE and in B_0, a new alignment $A' = -(1/2)A$ in the axis parallel to B_0 is established[3] after a short period of time characterized by the transverse relaxation time which is much shorter than the lifetime of ^{14}B. Thus the initial alignment A was deduced from the change in R between the two conditions, through $A = (-8/3)(R_{ON}/R_{OFF}-1)$ where ON and OFF refer to the measurements with B_0 on and off, respectively.

3. Results and Discusion

In Fig. 2 the result for the spin alignment is shown together with the measured momentum distribution of the ^{14}B particles. The ^{14}B yield exhibits a broad peak centered at a momentum p_c = 4.47 GeV/c which nearly corresponds to ^{14}B ions with the projectile velocity. Measurements of A were made for three different momentum windows. Around the peak momentum p_c, small values of A were observed both for a narrow ($\Delta p/p = \pm 1$ %) and a wide ($\Delta p/p = \pm 2$ %) momentum windows. An interesting feature appeared when the measurement was made for a window in the region of high-momentum tail: A negative value of A with a substantial size was observed for the window around a momentum 6.3 % higher than p_c. The negative sign of A in the high-momentum region conforms with the prediction from a simple projectile fragmentation model[4], as illustrated in Fig. 3.

The present result shows that the observation of the spin alignment in the projectile fragmentation brings an opportunity to test models for reaction mechanisms. It has also the important implication that projectile fragmentation provides a promising tool to produce spin-oriented unstable nuclei which must be extremely useful for detailed spectroscopic studies of nuclei far from stability and for other applications.

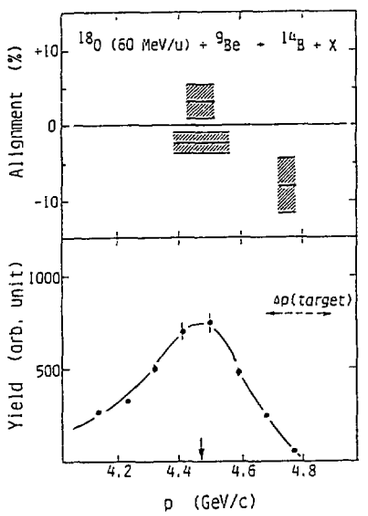

Fig. 2:
Experimental spin alignment A of ^{14}B produced in the reaction ^{18}O(60 MeV/u) + ^{9}Be; the observed momentum distribution for ^{14}B is also shown. The plotted value of A is averaged over the momentum bin indicated by horizontal bars. The vertical extension of the hatched zone corresponds to the uncertainty in A (one standard diviatioin).

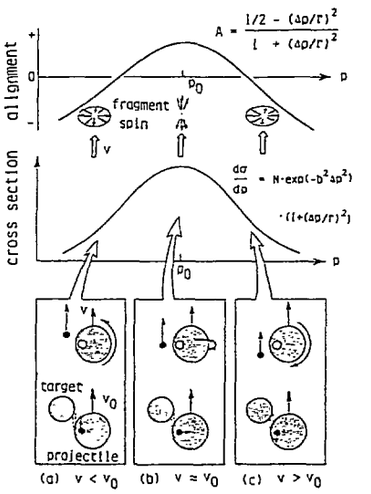

Fig. 3:
Predicted behavior of the fragment spin alignment based on a simple projectile fragmentation consideration. On the bottom, situations for the outgoing velocity (a) $v < v_0$, (b) $v \simeq v_0$, and (c) $v > v_0$ are intuitively illustrated, where v_0 denotes the projectile velocity.

1) D. Guillemaud-Mueller et al., Proc. of the 5th Int. Conf. on Nuclei Far From Stability (Rossau Lake, Canada, 1987) p. 757.
2) R. Bimbot et al., J. Phys. C4-8, 241 (1986).
3) H. Morinaga and T. Yamazaki, "In-Beam γ-Ray Spectroscopy" (North-Holland, 1976) Chap. 9.
4) K. Asahi et al., Nucl. Phys. A488, 83c (1988).

TOTAL REACTION CROSS SECTIONS AND LIGHT EXOTIC NUCLEUS RADII

M.G. Saint Laurent, R. Anne, D. Bazin, D. Guillemaud-Mueller,
U. Jahnke, Jin Gen Ming, A.C. Mueller (GANIL Caen)
J.F. Bruandet, F. Glasser, S. Kox, E. Liatard, Tsan Ung Chan (ISN Grenoble)
G.J. Costa et C. Heitz (CRN Strasbourg)
Y. El Masri (FNRS-UCL, Belgique), F. Hanappe (FNRS-ULB, Belgique)
R. Bimbot (IPN Orsay), E. Arnold and R. Neugart (Uni. of Mainz, RFA)

MOTIVATION

The strong absorption radius is determined by a measurement of the total cross sections in a nuclear reaction. Its dependence on the number of protons and neutrons in the interacting nuclei is the subject of two recent works :

- Using the transmission method, He, Li, Be unstable projectiles and Be, C and Al targets, Tanihata et al (1) found remarkably large values for ^{11}Li and ^{14}Be radii which were attributed to structure effects.

- In a thick Si target experiment in which the γ rays from the nuclear reactions were detected with a high efficiency, Mittig et al (2) measured the reaction cross-section integrated over the beam range, for a variety of unstable nuclei (Z = 5 - 12) ; their results show a surprising linear dependence of the reduced strong absorption radius on the neutron-excess.

The aim of this experiment is to verificate if exotic nuclei have an anomalous radius.

In the present experiment, we are using beams of nuclei which have a neutron-excess to N - Z = 7 in the range $2 \leq Z \leq 10$. The results thus overlop with those of ref (1) and (2).

EXPERIMENTAL PROCEDURE

The present work is a σ_R measurement using the 4 $\pi\gamma$ method ; this technique has already been used with success for stable nuclei (3,6) and is complementary to the transmission method used by Tanihata et al. Secondary beams of exotic nuclei are produced through ^{22}Ne fragmentation in Be target at 45 MeV/u incident energy and selected using the LISE spectrometer. The resulting 95 values of σ_R have thus been obtained for 49 isotopes : ^{4,6}He, $^{6-9,11}$Li, $^{7,9-12,14}$Be, $^{10-15,17}$B, $^{11-19}$C, $^{13-19}$N, $^{15-21}$O, $^{18-21}$F and ^{20,21}Ne. A convenient way of discussing the σ_R data and comparing them with the results of other experiments is to express them in terms of the reduced strong absorption radius R_o using the Kox parametrisation (4) :

$$\sigma_R = \pi R_o^2 \left[A_p^{1/3} + A_t^{1/3} + b \frac{A_p^{1/3} \cdot A_t^{1/3}}{A_p^{1/3} + A_t^{1/3}} - c + D \right]^2 \cdot \left[1 - \frac{B_c}{E_{cm}} \right]$$

with R_o = 1.1 fm, b = 1.85 and in which C is the only E dependent parameter accounting for the transparency effect C = 0.14 + 0.015 E/A and D is the neutron excess term $D = 5(A_t - 2Z_t)\, Z_p/(A_p A_t)$. The R_o^2 values extracted for each isotopes at different incident energies are in agreement with them, within uncertainties.

RESULTS AND DISCUSSION

The R_o^2 values deduced from these measurements and from Tanihata experiments, using eq. (1) are plotted in fig. 1 versus the neutron number N.

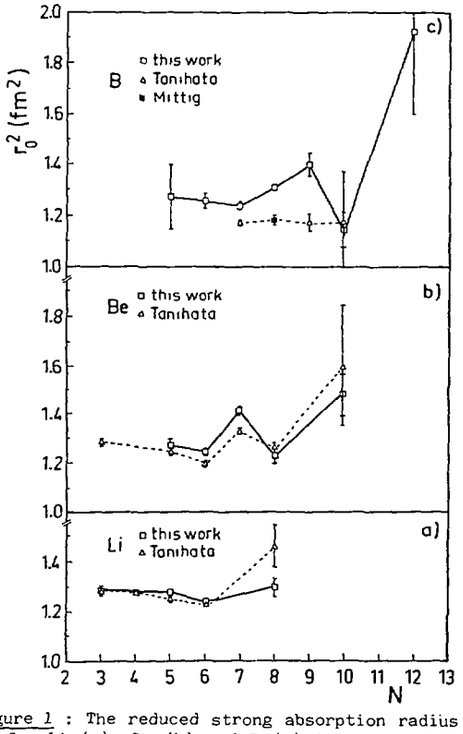

Figure 1 : The reduced strong absorption radius R_o^2 for Li (a), Be (b) and B (c) isotopes. Full black dots are data points obtained in this work, open circles are from Tanihata et al. (1) and the triangle from Mittig et al. (2).

The Tanihata R_o^2 values are in good agreement with the present ones within incertainties. For ^{14}Be, both results are consistent within the error bars and a large increase in R_o^2 for ^{17}B is observed here for the first time. The sharp increase in the matter radius for the weakly bound most neutron-rich isotopes has been associated with the occurence

of a spatially extended di-neutron halo (5). For ^{11}Li, we find a smaller value in R_o^2 radius than suggested by Tanihata. This discrepancy can be due to the electromagnetic dissociation of ^{11}Li into ^{9}Li + 2n, without γ emission, in the Coulomb field of the target as measured in ref 7. Neutrons, contrary to γ , are not very efficiently detected by our setup, leading to an underestimation of σ_R by our experiment.

Recent shell model calculations (8) of the radii of $^{6-11}$Li predict a much smoother dependence of $\langle R^2 \rangle$ on the neutron number than suggested by either experimental data set. In particular the increase of $\langle R^2 \rangle$ becomes smaller as one approaches the magic neutron number N = 8 for ^{11}Li. This is in agreement with the general expectation about shell effects, but it seems to be in contradiction to both experimental results.

In this context it is interesting to note that a recent measurement of the spin and the magnetic moment (9) has ruled out the suggestion of a deformed ground state of ^{11}Li (10) which would alternatively explain the increase in $\langle R^2 \rangle$.

The region of nuclides covered by our cross-section measurements includes the major shell closures at N = 8 and Z = 8. Here it is surprising to find no pronounced shell effects, i.e. relative minima in the radii, which are prominent in the N dependence of the mean square charge radii of heavier systems.

Looking at the more global trends, we find nearly constant values of R_o^2 as a function of N-Z as shown in fig 2. The mean value R_o^2 = 1.16 fm^2 is in agreement with the R_o^2 = 1.21 fm^2 value find by Kox for stable nuclei, within uncertainties. However, this is in contradiction to the linear increase with N - Z as reported in ref 2.

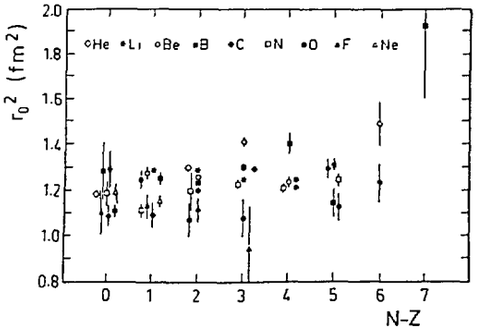

Figure 2 : The reduced strong absorption radius R_o^2 as a function of the neutron excess N - Z for all the isotopes measured in this work.

REFERENCES

(1) I. Tanihata et al. Phys Rev. Lett 55 (1985) 2676 - Preprint Riken AF-NP-60 (1987)

(2) W. Mittig et al. Phys Rev. Lett. 59 (1987) 1889

(3) J.F. Bruandet - J. Phys. (Paris) C4 (1986) 125
- present report

(4) S. Kox et al. Phys. Rev. C35 (1987) 1678

(5) P.G. Hansen and B. Jonson Europhys. Lett. 4 (1987) 409

(6) M.G. Saint Laurent et al. Third international conference on Nucleus Nucleus Collisions SAINT-MALO, France, June 6-11, 1988 ISBN2-905461-30-6
M.G. Saint Laurent et al. Z Phys. in press

(7) T. [illegible] et al. Phys. Rev. Lett. 60 (1[illegible]

(8) N.A.F.M. Poppelier et al. 5th Int. Conf. on Nuclei far from Stability, Rosseau Lake, Ontario, Canada, in AIP Conference proceedings Vol. 164, Ian S. Towner ed. New York 1988, p. 334

(9) E. Arnold et al. Phys. Lett. B 197 (1987) 311

(10) T. Björnstad et al. Nucl. Phys. A 359 (1981) 1

SEARCH FOR FAR FROM STABILITY NUCLEI WITH AN ON-LINE MASS-SPECTROMETER.

M. DE SAINT SIMON, A. COC, P. GUIMBAL, C. THIBAULT,F.TOUCHARD,
CSNSM Orsay
M. LANGEVIN, *IPN Orsay*
C. DETRAZ, D. GUILLEMAUD-MUELLER, A. C. MUELLER, *GANIL Caen*

1 - AIM OF EXPERIMENT.

At the start-up of the new beams of GANIL, it was tempting to gather most of the techniques devoted to collection and identification of nuclei in order to try to reach the nuclear stability limits, in the neutron rich heavy nuclei region particularly. Among these techniques, we can notice the He jet collection device, our mass-spectrometer with Z selection capability for alkali elements, well suited to collection at rest of target-like fragments, and afterwards, the electromagnetic separator LISE devoted to projectile-like fragment identification and in-flight collection, and the magnetic spectrometer SPEG. Our mass-spectrometer equipment had been successfully used in far from stability nuclei production and in nuclear structure measurements, and it had been set on-line to many acceleration facilities: U-300 Cyclotron (JINR - Dubna) [1],PS [2], SC [3], ISOLDE [4] (CERN - Geneva)... Results reported here have been measured at GANIL during the 1983-1984 period.

2 - EXPERIMENTAL SET-UP.

A conventional mass-spectrometer characterized by a resolving power $\frac{M}{\Delta M}$ of 300 and a good transmission is fitted with a surface ionization type ion source which is composed of 4 components: target, diffuser, ionizing device and focusing device. The target can be located outside or inside the diffuser, and in this last opportunity, it is made of 50 $1mg/cm^2$ foils mixed with the diffuser foils. The diffuser is an assembly of 100 $10mg/cm^2$ graphite foils located inside an oven heated at $1700°C$, convenient temperature to get a fast and selective thermal diffusion of alkali elements. The ionizing device is a Re or Ta tube according to the needed work function, heated at $1500°C$, convenient temperature to get good ionizing efficiency of alkali elements and to minimize ionizing efficiency for non-alkali elements. Both processes, thermal diffusion and surface ionization, are highly selective for alkali elements. The output of the equipment is fitted with a beam line in order to tranport identified nuclei across a concrete shielding into a low background area where detectors are located.

3 - EXPERIMENTAL RESULTS.

Three designs of the target-diffuser assembly fitted to 3 types of production mechanisms have been performed and a new device designed to get chemical selectivity with halogen elements has been tested.

3-1 Target-like fragments. The isotopic distributions of recoils measured with a ^{93}Nb (thickness $30mg/cm^2$) are fully independent of the projectile nuclei: ^{12}C, ^{18}O, ^{40}Ar and of energy in excess of 25 AMeV. The shape of the neutron deficient side of the isotopic distribution is governed by the ratio $\frac{\Gamma n}{\Gamma p}$ in the evaporative chain. As the target thickness is limited by the projectile range in target-diffuser assembly, the production rate of neutron deficient nuclei is determined by the beam intensity only, which has been always smaller than $5\times10^{11}ps^{-1}$ during the measurements. As a comparison the yield of ^{75}Rb is 100 atoms per second instead of 10^6 observed with ISOLDE and the 600 MeV proton beam of the SC (CERN). With a target exhibiting a different N/Z ratio (^{nat}Mo), the shape of the neutron deficient isotopic distribution remains completely unchanged, as attributed to a low collection efficiency for nuclei with very weak recoil energy (≤ 0.1 AMeV) which is expected for target-like fragments. Then the recoils cannot escape from the target thickness and reach the diffuser material.

3-2 Projectile-like fragments. Projectile fragmentation has been under study from the point of view of nuclear production using 44 AMeV Ar beam, the heaviest projectile accelerated with a large intensity at that time, bombarding a ^{181}Ta target and looking at Na fragments. The external target thickness has been made adjustable in order to set stopping location of recoils in the diffuser assembly; optimal target thickness has been determined to be $180mg/cm^2$. Yields are 100 times lower than those obtained with a $10g/cm^2$ Ir target bombarded by a 10 GeV proton beam of $5\times10^{12}ps^{-1}$.

3-3 Secondary reactions. A target-diffuser assembly has been designed for a 2 step process, but it could not be successful due to small yields in the primary step of projectile fragmentation (see 3-2).

3-4 Halogen selective ion source. A new ion source has been designed in order to get Z selectivity for halogen elements based on negative surface ionization of LaB_6 with the hope to get diffusion time as short as for alkali elements ($\sim 10ms$). Efficiency measured for Br and I is 10^{-3} and diffusion time is as long as 1 minute.

4- CONCLUSION.

Due to the lack of reaction mechanisms with good selectivity leading to large production cross-sections as at low energy for fusion-evaporation process, and due to the peculiar energy range of recoils, in the energy range of GANIL projectiles the dominant projectile fragmentation process has been shown less promising than foreseen at least for collection of fragments at rest. For projectile-like fragments the recoil energy is too large and most of the fragments are lost in slowing down process; for target-like fragments the recoil energy is too weak and most of the fragments cannot escape from the target material. Improvements of the geometry of target-diffuser assembly could be undertaken, but the beam current limitation, at least at that time, was not encouraging to hope to get better results than the existing facilities such as ISOLDE. Since that time, the LISE spectrometer has been shown to be better suited to the kinematics of recoils at GANIL.

References:

[1] M. de Saint Simon et al. Phys. Rev. C14 (1976) 2185.

[2] M. de Saint Simon et al. Nucl. Instr. Meth. 186 (1981) 193.

[3] M. de Saint Simon et al. Phys. Rev. C26 (1982) 2447.

[4] L. C. Carraz et al. Nucl. Instr. Meth. 158 (1979) 69.

— B —
NUCLEAR REACTIONS

– B1 –
PERIPHERAL COLLISIONS , PROJECTILE - LIKE FRAGMENTS

PROJECTILE-LIKE FRAGMENT PRODUCTION IN Ar INDUCED REACTIONS AROUND THE FERMI ENERGY

V. Borrel[1], J. Galin[2], B. Gatty[1], D. Guerreau[2] and X. Tarrago[1]

1) IPN, BP N° 1, 91406 Orsay, Cedex France. 2) GANIL, BP 5027, 14021 CAEN, Cedex France.

The primary aim of these experiments was to look for the transition from the one-body to the two-body dissipation through the study of the isospin degree of freedom (N/Z ratio) which is known to be, at low energy, the fastest mode to reach its relaxation (~2 10^{-22} sec). The N/Z ratio of the projectile-like fragments (PLF) was then supposed to provide relevant information concerning the disappearance (or the persistence) of a collective behaviour of nuclear matter.

The first run was the very first experiment performed at GANIL in January 1983. Isotopic distributions and energy spectra of PLF have been measured in the forward direction for 26.5 and 44 MeV/u Ar induced reaction on $^{58-64}$ Ni, ^{103} Rh and ^{197}Au (i.e. targets with significantly different N/Z ratios, from 1.07 up to 1.47)[1-4] . The most striking feature of these studies is the role still played by the target in the PLF production. This is stressed in fig.1 which shows the mean N/Z ratios of the PLF obtained with 26.5 MeV Ar projectile impinging on the four different targets. The more n-rich is the target, the more n-rich the PLF appear to be. At that time, this was already an indication for the mean field to play a significant role in this intermediate energy range. However, the effect is rather small on the mean values, and can also be explained as the result of a rather large energy dissipation leaving the primary PLF rather excited (30 to 50 MeV excitation energy according to recent exclusive experiments [5]). Furthermore, this target effect is strongly enhanced when looking at the production of the most n-rich fragments, as shown in fig.2 comparing the production rates for ^{58}Ni and ^{64}Ni targets. It should be stressed that this effect has been extensively exploited afterwards to produce isotopes near the n-drip line at these energies[6].

The second point worth to be stressed from these "first generation" of inclusive experiments is connected with the origin of PLF close to the projectile mass. The results show the coexistence of pure transfer reactions and break-up processes. For instance, ^{38}Ar, ^{39}Cl and ^{41}K have been clearly identified as preferentially produced through a transfer reaction. The maximum yields in the energy spectra for stripping reactions are observed at the expected optimum Q value whereas they are peaked at an energy close to the one corresponding to the Q_{gg} for pick-up products (fig.3). This can be explained as suggested by Siemens assuming that the transferred nucleons are at rest in the frame of the nucleus from which they originate. This hypothesis implies that most of the excitation energy is found in the recipient nucleus (and not in the donor). The energy spectra have been analysed successfully in terms of direct transfer reactions leading to continuum states. A good agreement is obtained with the prediction of the diffractionnal model [4].

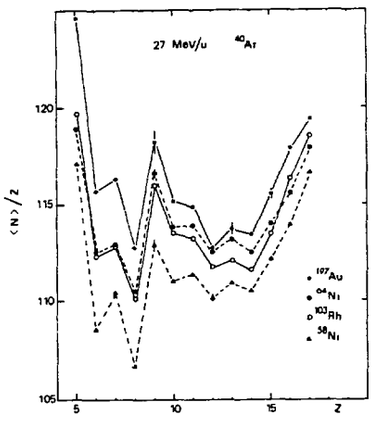

Fig.1. (N)/Z ratios for PLF from a 26.5 MeV/u Ar bombarding ^{58}Ni, ^{64}Ni, ^{103}Rh and ^{197}Au targets.

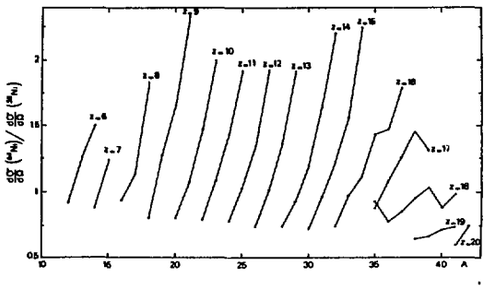

Fig.2. Evolution with PLF atomic number and mass of the ratio of differential cross sections obtained with ^{58}Ni and ^{64}Ni targets at 26.5 MeV/u.

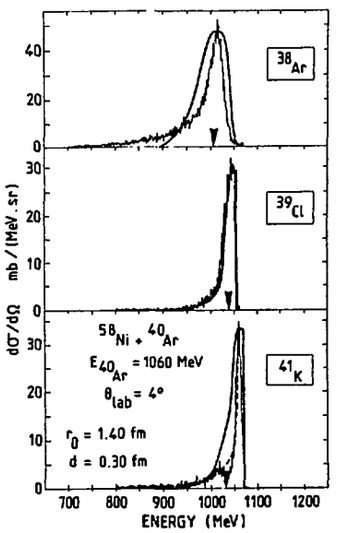

Fig.3. Energy spectra of one and two nucleon transfer reactions measured at the grazing angle. Solid curves are theoretical predictions using the diffractional model [4]. Arrows correspond to the optimum Q value for each channel.

1) D. Guerreau et al, Phys. Lett. 131B (1983) 293.
2) V. Borrel et al., Z. Phys. A314 (1983) 191.
3) V. Borrel et al., Z. Phys. A324 (1986) 205.
4) M.C. Mermaz et al., Z. Phys. A324 (1986) 217.
5) J.C. Steckmeyer et al., Internal Report LPCC 89-01.
6) D. Guerreau, J. Physique C4 (1986) 207.

Angular Evolution of the Production of Projectile like Fragments in Intermediate Energy Heavy Ion Collisions

D. Beaumel, Y. Blumenfeld, Ph. Chomaz*,
N. Frascaria, J.C.Jacmart J.P. Garron, J.C. Roynette,
J. A. Scarpaci and T. Suomijärvi
Institut de Physique Nucléaire, 91406 Orsay Cedex, France
J. Barrette, B.Berthier, B. Fernandez and J. Gastebois
DPhN/BE, CEN Saclay, 91191 Gif-sur-Yvette Cedex, France
D.Ardouin and W. Mittig
GANIL, BP 5027, 14021 Caen Cedex, France

1) Motivations

The abundant production of projectile like fragments (PLF) exhibiting velocities close to the beam velocity is a general feature of all intermediate energy heavy ion reactions. PLF's account for a large fraction of the total reaction cross section and their study is a necessary first step towards the understanding of the underlying reaction mechanisms. The scattering angles of the PLF's will be determined both by the interplay of the nuclear and coulomb deflections and by the reaction mechanism itself (nucleon transfer, abrasion, sticking....). The measurement of PLF angular distributions down to angles inside the grazing angle and the study of the properties of the PLF's (isotopic distributions, mean velocities, momentum widths...) as a function of angle should allow us to enhance our knowledge of peripheral reaction mechanisms.

2) Experiments

The mass, charge, energy, and angular distributions of the PLF from the $^{40}Ar + ^{208}Pb$ reactions at 44 [1,2] and 33 MeV/u [2] and the $^{40}Ar + ^{40}Ca$ [1,2] reaction at 44MeV/u were measured with a time of flight system [3] allowing to obtain simultaneously several points of the angular distribution. For the sake of comparison two short runs were performed at one angle for the $^{40}Ar + ^{40}Ca$ system at 27MeV/u and the $^{20}Ne + ^{208}Pb$ reaction at 44MeV/u. The elastic scattering counting rate limits the use of a time of flight system at very forward angles and hence to obtain data down to θ_{lab}=0.5° the $^{40}Ar + ^{208}Pb$ reaction at 60 MeV/u was studied [4] using the SPEG spectrometer.

3) Results

We will briefly review the features of the various quantities measured in these experiments and stress the analogies and differences with the behaviors observed at lower and higher incident energies.

Most probable PLF velocities : The PLF spectra are centered at velocities between 90 and 100 % of the beam velocity. The general trend is a decrease of the velocity with decreasing fragment mass. When one moves towards angles larger than the grazing the velocities tend to drop. These two last features are analogous to those observed at low bombarding energies when measurements are performed near the grazing angle (quasi-elastic reactions).

Momentum widths : The energy (or momentum) spectra of the PLF exhibit a gaussian shape prolonged by a low energy tail indicative of energy dissipation. In the framework of the fragmentation model [5] it has been claimed that the reaction mechanisms in various systems can be compared by fitting the high energy part of the spectra and extracting the reduced momentum width parameter σ_o. We have found that the σ_o values for the $^{40}Ar + ^{40}Ca$ reactions at 27MeV/u and $^{20}Ne + ^{208}Pb$ at 44Mev/u do not agree with the systematics compiled by Murphy and Stokstad [6]. This result seriously questions the relevance of the reduced momentum width to follow the evolution of reaction mechanisms at intermediate energies.

Isotopic distributions : In general for a given charge the PLF isotopic distribution is approximately Gaussian. Neutron rich isotopes are more strongly populated when neu-

*Division de Physique théorique, Laboratoire associé au CNRS

tron rich targets are used. However when fragments close to the projectile are considered the isotopic distribution presents two components, one of them extending over all angles and the other strongly focused at the grazing angle. This feature shows up spectacularly in the $^{40}Ar + ^{208}Pb$ reaction at 33MeV/u where the production of ^{39}Cl and ^{36}Ar (the p and α-particle transfer channels) is strongly enhanced around the grazing angle. This shows that simple direct transfer reactions subsist at intermediate energies.

Angular distributions : The striking evolution of the shape of the angular distributions with fragment mass is illustrated on fig.1 for the $^{40}Ar + ^{208}Pb$ reaction at 44MeV/u. For PLF close to the projectile a bell shaped distribution peaked slightly inside the grazing angle is observed while for lighter fragments the distributions decrease monotonously with angle. This pattern resembles the behavior observed at low incident energies. Classical trajectory calculations show that the bell shaped angular distributions are incompatible with an abrasion mechanism for which the density overlap required between the two nuclei induces forward peaked distributions. Thus the fragments close to the projectile must be produced by surface transfer reactions. At very forward angles the strong dependence of the angular distributions on fragment mass remains. A calculation supposing fragmentation accompanied by a deflection of the PLF by the mean field was performed. To reproduce the data for fragments with $M < 34$ a deflection angle between 1.5 and 2 degrees (much smaller than the grazing angle θ_g) was needed showing the importance of the attractive nuclear force. For heavier fragments the data could not be reproduced which points once again to the importance of surface transfer reactions.

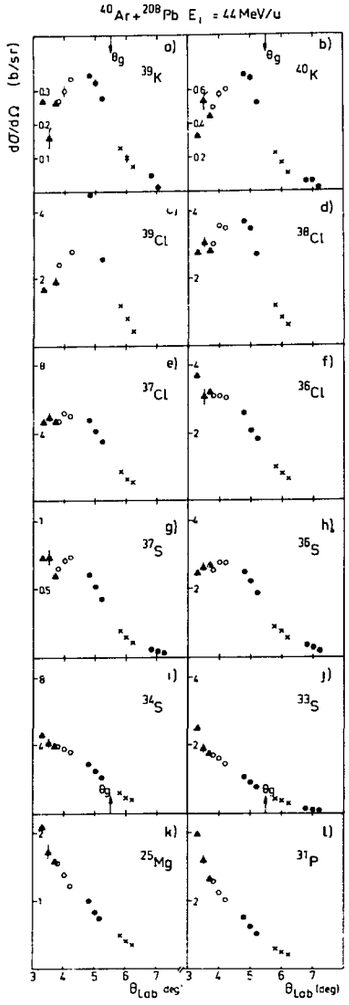

Figure 1: Angular distributions of PLF emitted in the $^{40}Ar+^{208}Pb$ reaction at 44 MeV/u.

4) Conclusions

We have shown that the measurement of the angular evolution of PLF production is crucial for the understanding of the reaction mechanisms responsible for their production. A surface transfer reaction component dominant at the grazing angle can be seperated from a second component which cannot be entirely accounted for by a simple fragmentation mechanism. Angular distribution studies yield important information on the deflection of the PLF's by the mean field potential.

References

[1] Y.Blumenfeld et al. Nucl.Phys. A455 (1986) 357

[2] Y.Blumenfeld These d'etat IPNO-T-87-07 (Orsay 1987)

[3] E.C.Pollacco et al. Nucl. Inst.Meth. 225 (1984) 51

[4] T Suomijärvi et al. Phys. Rev. C36 (1987) 2691

[5] A.S.Goldhaber Phys.Lett. 53B (1974) 306

[6] M.J.Murphy and R.G.Stokstad Phys.Rev. C28 (1983) 428

PERIPHERAL COLLISIONS IN THE $^{40}Ar + ^{68}Zn$ REACTION BETWEEN 15 AND 35 MeV/NUCLEON

J.P. COFFIN, A. FAHLI, P. FINTZ, G. GUILLAUME, B. HEUSCH, F. RAMI and P. WAGNER
Centre de Recherches Nucléaires and Université Louis Pasteur, 67037 Strasbourg Cedex (France)
Y. SCHUTZ
GANIL, B.P. 5027, 14021 Caen Cedex (France)
M. MERMAZ
C.E.N., Saclay, 91191 Gif sur Yvette Cedex (France)

1. Motivation

Below 10 MeV/nucleon, peripheral heavy ion collisions are associated with quasi-elastic and deep-inelastic transfer reactions, while at higher energy (≥ 100 MeV/nucleon), they are governed by a fragmentation process. The investigation of the intermediate energy region is essential to provide information about the nature of the transition from the mean field regime, characterizing the low energy reactions, to the nucleon-nucleon interaction regime governing the high energy collisions.

In order to shed some light on this question, we have investigated the competition between few nucleon transfer reactions and projectile fragmentation process in the $^{40}Ar + ^{68}Zn$ system, as a function of the bombarding energy.

2. Results and discussion

The experiments were conducted at ^{40}Ar incident energies of 14.6, 19.6, 27.6 and 35 MeV/nucleon.

Bidimensional spectra (A,E) and (ΔE,E) have been measured at several angles. Both projectile-like fragments and products resulting from low energy dissipative processes were identified. The momentum widths of the projectile-like fragments have been deduced from the analysis of their velocity spectra. The results indicate the presence of two reaction processes : transfer reactions and projectile fragmentation. The competition between these two mechanisms is clearly illustrated by the observation at 27.6 MeV/nucleon (Fig. 1) of two groups of fragments. For nuclides lighter than 36, the reduced momentum width σ_o is constant (σ_o = 84 MeV/c) and very close to the one observed in high energy experiments. Fragments close to the projectile (A ≥ 36) have a much smaller σ_o value (σ_o = 49 MeV/c). Other signatures of this competition between transfer and fragmentation processes were also obtained from the analysis of the average velocities of the projectile-like fragments.

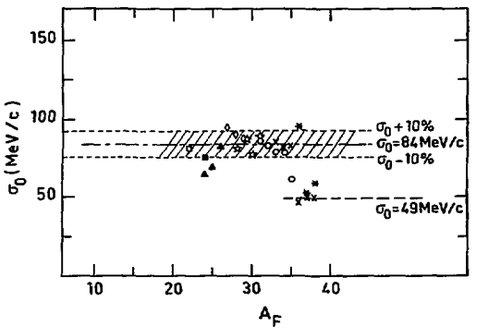

Fig. 1 : Reduced momentum widths σo plotted as a function of the ejectile mass for the $^{40}Ar + ^{68}Zn$ reaction performed at 27.5 MeV/nucleon.

Few nucleon pickup and stripping reactions were analysed (Fig. 2) in terms of direct surface transfer reactions leading to continuum states with a diffractional model. The data are consistent for stripping reactions with a direct transfer of nucleons and a target excitation yielding multiparticle - multihole configurations.

Fig. 3 shows the evolution with the bombarding energy of the reduced momentum widths of the projectile-like fragments. For

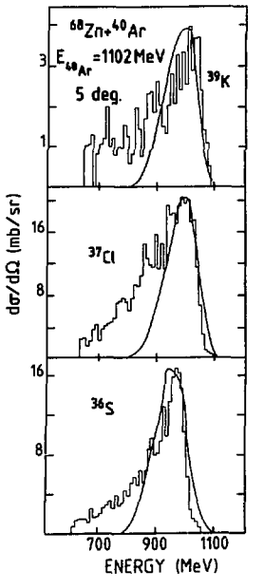

Fig. 2 :
Energy spectra of ^{39}K, ^{37}Cl and ^{36}S ejectiles measured at 5° laboratory angle. The solid curves are the result of calculations based on the diffractional model.

the projectile fragmentation processes the values of σ_0 at 27.6 and 35 MeV/nucleon are represented by solid points. Those corresponding to nucleon transfers are represented by open circles (the value at 35 MeV/nucleon corresponds to an upper limit).

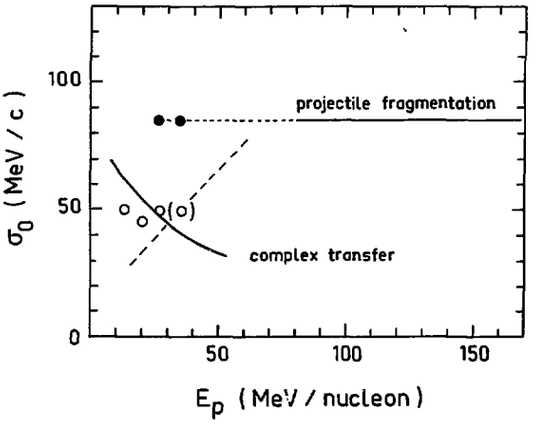

Fig. 3 :
Reduced widths σ_0 of the linear momentum distributions of projectile-like fragments as a function of projectile energy.

The solid curve is a diffractional model calculation for complex transfer of nucleons. The straight solid line corresponds to projectile fragmentation as found in the literature and extrapolated to lower incident energies. The slanted dashed line, indicating the tendency of the available experimental σ_0 values within the $10 \leq E_p/A \leq 50$ MeV/nucleon energy range, gives a wrong idea of the actual situation since it suggests that σ_0 increases with the bombarding energy. In fact, one has to distinguish the transfer component and the projectile fragmentation one, as it has been done in the present work.

In conclusion, two mechanisms have been identified : few nucleon direct transfer reactions and projectile fragmentation process which appears between 20 and 27 MeV/nucleon and competes strongly with transfer at 35 MeV/nucleon. The momentum width has been found to be the relevant parameter for distinguishing between transfer and fragmentation processes.

3. References

F. RAMI et al., XXIInd Int. Winter Meeting on Nuclear Physics, Bormio, Italy (1984)
F. RAMI et al., Z. für Physik A318 (1984) 239
M.C. MERMAZ et al., Phys. Rev. C31 (1985) 1972
F. RAMI et al., Nucl. Phys. A444 (1985) 325
F. RAMI, Thesis, Université de Strasbourg, France (1985)
F. RAMI et al., Z. für Physik A327 (1987) 207

EXCLUSIVE STUDY OF PERIPHERAL INTERACTIONS

G.Bizard,R.Brou,J.L.Laville,J.B.Natowitz,J.P.Patry,J.C.Steckmeyer,B.Tamain L P C , CAEN
H.Doubre,A.Péghaire,J.Péter,E.Rosato GANIL , CAEN
F.Guilbault,C.Lebrun L S N , NANTES
F.Hanappe U L B , BRUXELLES
J.C.Adloff,G.Rudolf,F.Scheibling C R N , STRASBOURG

1)Motivations and experimental set-up

When the first inclusive experiments were made on peripheral interactions in the GANIL energy range , the conclusion was that the high energy fragmentation regime , well understood by the Goldhaber theory , was already almost achieved with heavy ions beams of a few tens of MeV per nucleon. Later on , it was found that things were not so simple and that the so called fragmentation peak was in fact due to the superposition of different processes : direct break-up, transfer reactions , sequential break-up . The easiest way to disentangle all these contributions is to try to detect all the particles accompanying the remaining projectile like fragment . This is possible using the plastic wall in operation at GANIL . This multidetector covers the forward angular cone ($3° < \theta < 30°$) with 96 counters , allowing charge identification of the light nuclei up to Z=8 . The energy of the particles can be accessed throught the measurement of their velocity. To complete the experimental set up , a four elements solid state telescope was located near the grazing angle of the reactions, in order to detect and identify the projectile like fragments (figure 1). Two systems were studied : Ar+Ag and Ar+Au at four incident energies:35 , 39 , 50 , and 60 MeV per nucleon , in two separate experiments .

2)Transfer reactions

Among the various classes of experimental events , the simplest one is constituted of projectile like fragments which are not accompanied by any charged particle in the wall . Apart from small corrections due to rapid particles not detected in the wall ($\theta < 3°$ or $\theta > 30°$) , these events are associated with charge transfer reactions mainly from the projectile to the target. In figure 2 the charge transfer probabilities are displayed for Ar+Au and Ar+Ag at 60 MeV/A and for Ar+Ag at 35 MeV/A as a function of the projectile like fragment atomic number . We can see that these probabilities are independent of the target and that they decrease quite slowly with increasing energy , indicating that mean field effects are still important at 60 MeV/A .

3)Sequential break up

Let us consider now the events for which at least one rapid charged particle is found in coincidence with the projectile like fragment . If we restrict the detection zone of the wall to the few counters which are located nearly in the direction of the telescope (those counters which are hatched in figure 1) , the correlation plot between the energy of the light charged particle (LCP) and that of the projectile like fragment (PLF) exhibits two distinct regions (fig 3) . This observation is a clear signature of a sequential binary decay mechanism of a primary excited PLF ,the two regions of the correlation plot corresponding to the forward and backward emission of the LCP in the center of mass system of the primary PLF. It can be shown that a large number of the rapid light particles detected in the whole plastic wall (around 75% of the alpha particles and at least one third of the protons) originate from such a sequential decay of an excited projectile like fragment for a bombarding energy of 60 MeV/A.

4)Excitation energies

Taking into account the sequentially emitted particles (and correcting for the unseen neutrons and gamma rays) , the excitation energy of the primary projectile like fragments can be evaluated .The results are displayed in figure 4 for the 60 MeV/A Ar+Ag system and compared with different models : abrasion model , equal temperature in quasi projectile and quasi target fragments , equipartition of the excitation energy ...They show that none of these models are able to describe the data.

5)Conclusion

Peripheral interactions at incident energies as high as 60 MeV/A cannot be described by high energy models (participant spectator) .To account for transfer reactions and sequential decays of the projectile, low energy concepts implying inelastic interactions between projectile and target have also to be considered.

6)References

Fragmentation and/or transfer reactions in the 35 MeV/A Ar+Ag system
G. Bizard et al
Phys. Lett. B172(1986) 301

Transfer reactions and sequential decay of the quasi projectile in the 60 MeV/A Ar+Ag and Ar+Au reactions
Proceedings of the 25th winter meeting on nuclear physics -Bormio-(italy) 19-24 january 1987 , P 229

Transfer reactions and sequential decays of the projectile like fragments in the 60 MeV/nucleon Ar+Ag,Au reactions
J. C. Steckmeyer et al
Submitted to Nuclear Physics

Etude semi exclusive de la réaction Ar+Ag à 35 MeV/nucleon
G. Ployart
Thèse de 3ème cycle. Caen 1985

Etude de l 'émission des fragments quasi projectiles produits dans des réactions induites par ions Ar à 60 MeV/nucléon
A. Thiphagne
Thèse de l 'université de Caen *1987*

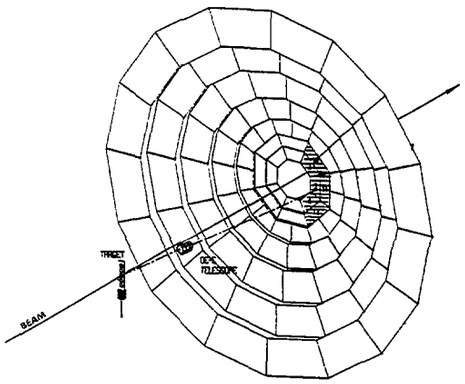

Figure 1

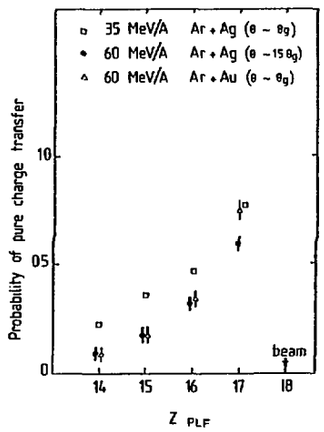

Figure 2

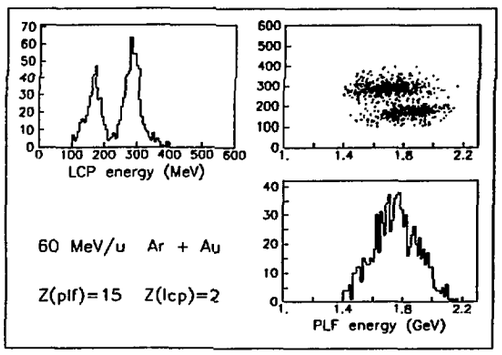

Figure 3

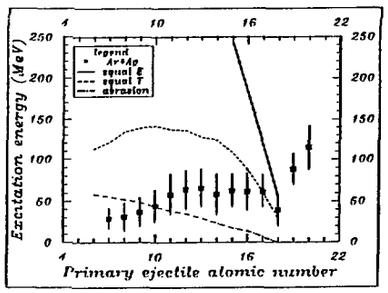

Figure 4

STUDYING PERIPHERAL COLLISIONS IN THE REACTION Ar + Au AT 27.2, 35 AND 44 MeV/u BY THE ASSOCIATED NEUTRON MULTIPLICITIES

M. MORJEAN[a,b], J. FREHAUT[a], D. GUERREAU[b], J.L. CHARVET[a], G. DUCHENE[a,1], H. DOUBRE[b], J. GALIN[b], G. INGOLD[c], D. JACQUET[d], U. JANHKE[b,c], D.X. JIANG[b,2], B. LOTT[a], C. MAGNAGO[a], Y. PATIN[a], J. POUTHAS[b], Y. PRANAL[a] and J.L. UZUREAU[a]

[a] CEA Bruyères-le-Châtel, BP.12, F-91680 Bruyères-le-Châtel, France.
[b] GANIL, BP.5027, F-14021 Caen Cedex, France.
[c] Hahn-Meitner Institut, Berlin 39, Germany.
[d] IPN, BP. N°1, F-91406 Orsay Cedex, France.

When considering peripheral collisions, the knowledge of the amount of thermalized energy shared by the partners is very important to help distinguish between transfer and break-up types of reactions. The neutron detection is well suited for collisions involving heavy targets as they will cool down essentially by neutron evaporation. In that case, measuring the multiplicity of evaporated neutrons provides the information on the excitation energy deposited in the target-like fragment (TLF).

The system $^{40}Ar + ^{197}Au$ has been studied at three bombarding energies 27.2, 35 and 44 MeV/u[1,2]. Peripheral collisions were selected by detecting the projectile-like fragments (PLF) near the grazing angle and at the same time, the multiplicity of slow neutrons (originating from the TLF) was deduced by means of a 4Π neutron detector (500 liters Gd loaded liquid scintillator). The efficiency of such a detector was found to be 74% for Cf neutrons.

Fig. 1 shows, for the three bombarding energies, the correlation between the most probable average neutron multiplicity $\langle M_n \rangle$ and the PLF mass. It clearly stresses that, for PLF's with masses between 40 and about 25, the lighter the detected PLF, the more excited the undetected TLF is. This is a clear indication for $\langle M_n \rangle$ to characterize the degree of violence of the collision and, the impact parameter. However, no significant change of $\langle M_n \rangle$ for a given PLF is observed when increasing the incident energy. This definitely rules out the idea of a dominant massive transfer process for peripheral collisions, as it was observed at lower energies. These results have been compared with a phenomenological model developped by Bonasera et al. [3] consisting of a two step process (a standard one body dissipation taking into account the Pauli blocking effects possibly followed by an abrasion step). The agreement is quite satisfactory and shows clearly that mean field effects still play a significant role at these energies.

However, the size of the detected fragment is no longer characteristic of a given impact parameter for PLF's with mass lower than about 25. This feature can also be seen for very large kinetic energy losses of the PLF (fig.2) for which the associated $\langle M_n \rangle$ becomes rather high and independent of the detected PLF. This could correspond to a process rather similar to deep inelastic collisions as observed at lower energies.

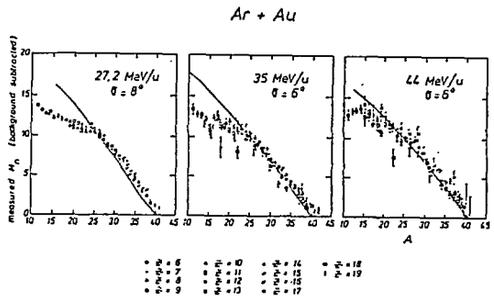

Fig.1. Evolution with incident energy of the correlation between $\langle M_n \rangle$ (not corrected for efficiency) and the mass of the PLF. Solid curves result from a calculation according to Bonasera et al.[3].

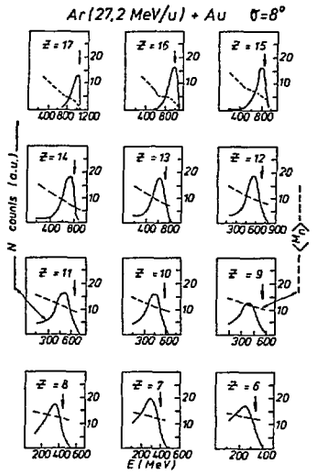

Fig.2. Energy spectra of PLF observed at 8° (solid lines). Dashed lines show the evolution of $\langle M_n \rangle$ (not corrected for efficiency) as a function of the PLF kinetic energy. Arrows indicate the beam velocity.

1) M. Morjean et al., Phys.Lett. 203B (1988) 215.
2) D. Guerreau et al., Proceedings of the RIKEN-IN$_2$P$_3$ Symposium of heavy ion collisions, Shimoda (Japan), October 1987, p.391.
3) Bonasera et al., Nucl. Phys. A463 (1987) 653.

DISSIPATIVE FRAGMENTATION IN MEDIUM ENERGY HEAVY ION COLLISIONS

A.Adorno[1], A.Bonasera[1-2], M.Di Toro[1], Ch.Grégoire[3], F.Gulminelli[4]

[1] Dipartimento di Fisica and I.N.F.N., Catania, Italy
[2] Sektion Physik der L.M.U., Garching b.München, W.Germany
[3] GANIL, Caen, France
[4] Dipartimento di Fisica and I.N.F.N., Milano, Italy

Heavy ion reactions at the GANIL energies raise very difficult problems in nuclear dynamics. Pauli blocking is less and less effective and we expect to see a quite strong competition between mean field and collisional dynamics. Microscopic treatments require large numerical efforts with some fundamental problems of difficult solution, e.g. variations in the mean field and effective forces, medium effects on the collision term, accurate description of phase space distributions. The aim of this project is to develop a relatively transparent model in phase space, based on safe physical grounds, able to quantitative reproduce a large volume of data and to make reliable predictions (1,2,3). We introduce a two stage mechanism (see Fig.1).

In the first stage we have a one-body dissipation process (incoherent nucleon exchange through a neck) quite well described within the window formula, suitably corrected due to the partial overlap of momentum distributions. We can evaluate energy and angular momentum losses, orbiting and prompt particle emissions. Coherent one-body dissipation is also included in the approaching phase through the excitation of high frequency collective motions, giant resonances, expected to play an important rôle just on the basis of time matching conditions ($\Omega_{coll} * \tau_{cross} \approx 1$). The second stage is an abrasion mechanism with formation of an highly excited intermediate source, whose properties (mass, energetics) are substantially affected by a still active Pauli blocching and one-body corrections. Compression effects can be also included with a possible test on the nuclear equation of state. Three primary bodies are formed in the exit channell with well defined properties: excitation and kinetic energies, spins, masses, deflection angles. All possible correlations can be worked out, and sequential statistical emissions of particles can be evaluated. Since the classical impact parameter analysis of different reactions, the model is particulary suitable to study exclusive measurements, using as a trigger fragments of different mass bins in forward direction. Applications are discussed on: i) transtion from deep inelastic processes to peripheral fragmentation (1); ii) exotic isotope production (5); iii) formation and decay of fragments with high excitation energy and angular momentum (4); iv) energetic particle (pions, hard photons, h.e,protons), emission from a hot intermediate source (2,6); v) dynamical polarization of nucleon momentum distributions and effects on fragment momentum widths (7).

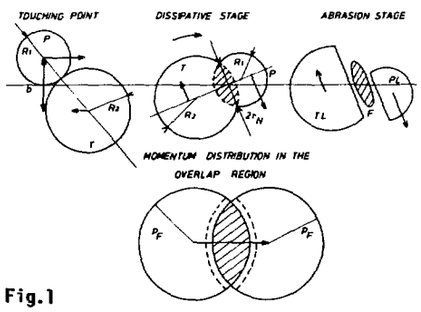

Fig.1

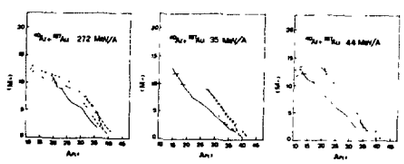

Fig.2

Due to the persistence of mean field effects, a large amount of energy is dissipated in the "spectator" fragments. This has been observed in the neutron emission from target-like fragments (Fig.2) and it has noticeable effects on isotopic production. Fig.3 shows the primary projectile fragment production cross section and excitation energy for 35 and 100 MeV/A ^{48}Ca beams on ^{232}Th. At 35 MeV/A we have much less fragmentation, only with PLF masses larger than 30 units and more neutron rich.

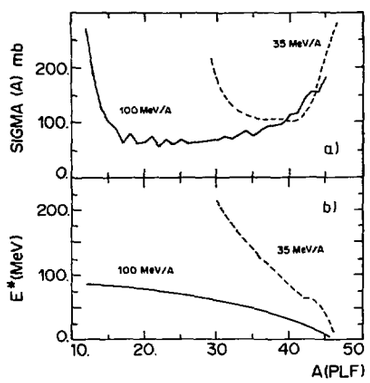

Fig.3

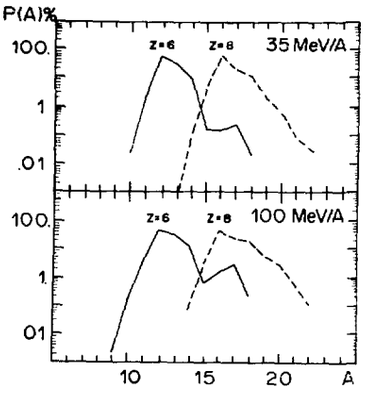

Fig.4

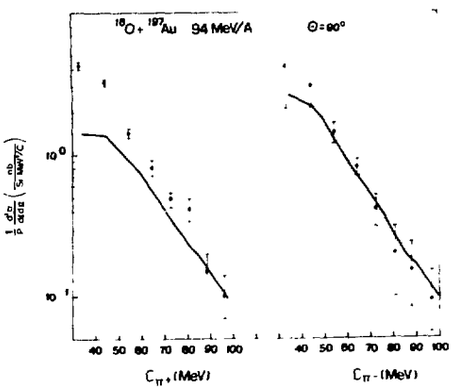

Fig.5

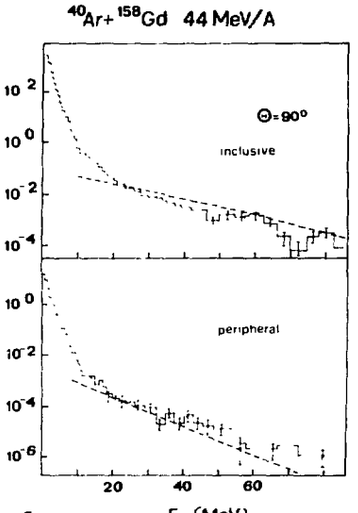

Fig.6

However (Fig.3b) we have also much larger excitation energies which finally will compensate the different initial conditions with a longer ablation chain. The final production yield will be essentially the same (Fig.4): probably for this projectile-target system some intermediate energy (∿ 60 MeV/A) will optimize the production of neutron rich isotopes.
Intermediate mass fragments (IMF) can be produced by direct break up of projectile and/or target. Moreover the primary PLF and TLF can have a relatively large excitation energy and angular momentum. In this view it would be important to look carefully at sequential decays before discussing direct multifragmentation.
The fireball-like source can emit energetic particles. Some inclusive pion spectra are presented in Fig.5. Since we have an impact parameter-PLF correspondence, our results are suitable for exclusive measurements. An example is shown in Fig.6 for hard photon production in inclusive measurements and in coincidences which select peripheral processes.
We reproduce not only the absolute values but also the slope variation of the spectra.
In conclusion we have developped a quite nice model, easy to work with, which reproduces, without free parameters, the main features of dissipative medium energy collisions and can be used to plan new, more exclusive, experiments.

---

1. A.Bonasera, M.Di Toro and Ch.Grégoire:
   Nucl.Phys. A**463**, 653, 1987
2. A.Bonasera, M.Di Toro and Ch.Grégoire:
   Nucl.Phys. A**483**, 738, 1989
3. M.Di Toro:
   in "Trends in Nuclear Physics", E.Fermi School, Varenna 1987, Ed. P.Kienle
4. A.Adorno, F.Gulminelli, A.Bonasera, M.Di Toro and Ch.Grégoire:
   Int. Winter Meeting on Nuclear Physics, Bormio 1988, p. 491
5. A.Adorno, A.Bonasera, M.Di Toro, Ch.Grégoire and F.Gulminelli:
   Int. Conf. on Nuclear Reaction Mechanisms, Varenna 1988, p. 231
6. A.Adorno, A.Bonasera, M.Di Toro, Ch.Grégoire and F.Gulminelli:
   St. Malo 1988, Nucl.Phys. A**488**, 451c, 1988
7. M.Di Toro, G.Lanzanò and A.Pagano:
   Phys.Rev. C**37**, 1485, 1988

FORMATION OF HIGHLY EXCITED QUASI-PROJECTILE FRAGMENTS IN THE ^{84}Kr + ^{93}Nb REACTION AT 35 MeV/u

J.L. Charvet[1a], R. Billerey[2], B. Chambon[2], A. Chbihi[2], A. Chevarier[2], N. Chevarier[2], D. Drain[2], G. Duchene[1], S. Joly[1], C. Magnago[1a], M. Morjean[1b], C. Pastor[2], Y. Patin[1], A. Peghaire[3], Y. Pranal[1], L. Sinopoli[1], M. Stern[2], and J.L. Uzureau[1].

(1) CEA, Bruyères-le-Châtel, Service PTN, BP 12, F-91680 Bruyères-le-Châtel
(2) IPN, Université Claude Bernard, Lyon 1, F-69622 Villeurbanne Cedex
(3) GANIL, BP 5027, F-14021 Caen Cedex.

a) present address: CEA Saclay, DPhN/BE, F-91191 Gif-sur-Yvette
b) present address: GANIL, BP 5027, F-14021 Caen Cedex

1. Introduction

In heavy ion induced reaction at intermediate energies, the production of fragments having a velocity close to the projectile one has been generally interpreted in terms of a projectile fragmentation process (1). The abrasion model including dissipation seems to reproduce the essential features of argon induced reaction data (2), although recent calculations based on a primary two-body process, similar to a deep inelastic collision, give also a good understanding of the data (3, 4). Nevertheless, when using projectiles heavier than argon, the situation seems much more complex (5, 6) and we have chosen to study the properties of the projectile-like fragments issued from the ^{84} Kr + ^{93} Nb reaction at 34.5 MeV/u. In addition to the inclusive measurements we tried to determine the excitation energy of the primary fragments by measuring the fragment-fragment and fragment-light particle correlations in the forward direction.

2. Inclusive measurements

On one side of the beam direction the experimental set-up was constituted of a large gas ionization chamber and located between 3.5° and 15.5°, which measured the nuclear charge (Z=38 down to 10) and the energy of the projectile-like fragments. The main properties observed for these fragments can be summarized as follows (7): i) all of the fragment energy distributions exhibit a relative broad peak at an energy corresponding to a velocity about 80-90% of the beam velocity; ii) the production of light fragments (Z=<20) become predominant beyond the grazing angle. These results cannot be understood in a pure geometrical abrasion-ablation model.

3. Fragment-fragment correlation measurements

On the other side, with respect to the beam axis, we placed at 7° a three-stage telescope and measured the fragments (Z2) in coincidence with those detected in the chamber (Z1). The average of the sum Z1+Z2 of all fragments in coincidence is about 28-30, lower than the projectile charge (Z=36). The relative velocityV1-V2 between two fragments in coincidence has been calculated event by event and a typical distribution is shown in fig.1 for an angle in the chamber selected at 8°. The most probable value of about 2cm/ns agrees with the expectation of Coulomb repulsion between two fragments both having a charge of the order Z=15. The broadening of the distribution can be explained by the nucleon evaporation effect from the fragments (5). We concluded that our data are compatible with a binary break-up of a source having a velocity around 90% of the beam velocity and a mass close to the projectile one, which are the characteristics of a quasi-projectile fragment (8).

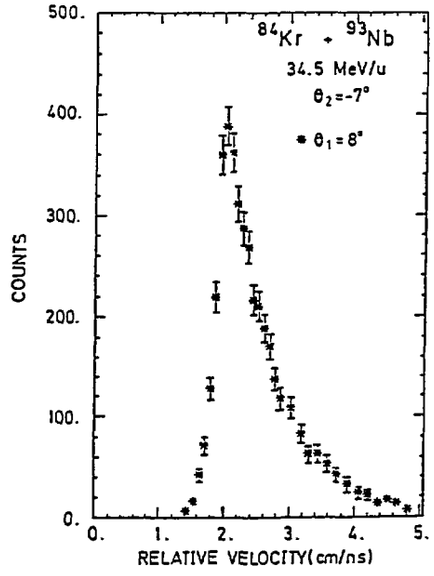

Fig.1. Spectrum of relative velocity of two fragments measured in coincidence between the chamber at 8° and the telescope at -7°.

4. Fragment-light charged particle correlation measurements

The back of the ionization chamber was covered with a thick titanium foil in order to place six light charged particle detectors, each one constituted of a 1mm thick NE102 scintillator followed by a photomultiplier and located at 4.3°, 7.6°, 10.5°, 12.1°, 13.6° and 15.3°. In fig.2 we have reported typical energy spectra for Z=1 and Z=2 in coincidence with fragments having a charge 10<Z1<20 and integrated over the entire angular range of the chamber. The correlated fragment energy

spectra exhibit approximately the same shapes as measured in the single spectra. The solid curves shown in fig.2 result from a fit using the expression of the moving source model (9). The extracted velocities of the sources corresponding to emission of particles with Z=1 and Z=2 are almost equal (94% and 93% of the beam velocity respectively) and close to the one obtained from the correlated fragment measurements. The T parameters are indicative of the source temperature and we deduced the values of 5.1 MeV and 6.4 MeV showing a highly excited source. It should be noted that the discrepancy at high energies can be connected to the presence of direct particle emission.

We clearly showed that the intense production of fragments with charge Z<=20 are originated from a source with a high excitation energy and velocity close to the beam one (8). Such data could be consistent with the early stage of deep inelastic collisions in which the quasi-projectile arised with strong excitation energy and decayed by break-up associated with both pre- and post- break-up evaporation.

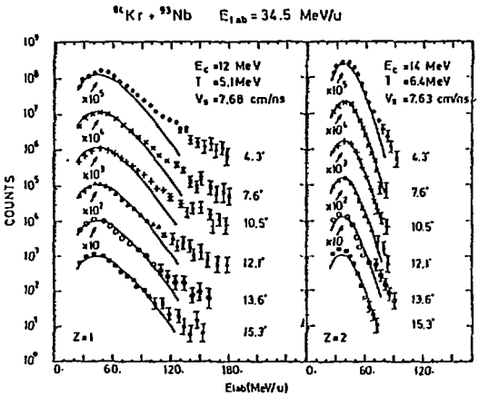

Fig.2. Energy spectra of Z=1 and Z=2 particles detected at various angles in coincidence with the 10<Z<20 fragments measured between 3.5° and 15.5°

References

(1) D. Guerreau, Nucl.Phys. A447 (1985) 37c.
(2) R.A. Dayras et al., Nucl.Phys. A460 (1986) 299.
(3) R.A. Dayras et al., Phys.Rev.Lett. 62 (1989) 1017.
(4) L. Tassan-Got, Ph.D. Thesis, Orsay, 1988.
(5) M.J. Murphy et al., Phys.Rev.Lett. 53 (1984) 1543; Phys.Rev. C33 (1986) 165.
(6) G. Rudolf et al., Phys.Rev.Lett. 57 (1986) 2905.
(7) J.L. Charvet et al., Z.Phys. A321 (1985) 701.
(8) J.L. Charvet et al., Phys.Lett. B189 (1987) 388.
(9) T.Awes et al., Phys.Rev. C25 (1982) 2361.

PROJECTILE FRAGMENTATION IN HEAVY-ION REACTIONS AT INTERMEDIATE ENERGIES

G. ROYER, B. REMAUD, C. GREGOIRE+, C. LEBRUN, A. OUBAHADOU and F. SEBILLE
Laboratoire de Physique Nucléaire (UA CNRS N°57) 44072 NANTES Cedex 03-FRANCE
+GANIL, BP 5027, 14021 CAEN Cedex-FRANCE

1. Motivation

At intermediate energies (10-100 MeV/A) the peripheral collisions lead to three distinct emitting sources : a target-like source, a projectile source and an intermediate source. The mere abrasion-ablation model developped to describe these sources at relativistic energies is expected to lose gradually its validity with decreasing energies since collective effects play a larger role. We study[1,2] how far the binary fragmentation of a projectile can be describe macroscopically within a rapid fission process induced by the target field.

2. Three-body macroscopic model of the projectile fission

The projectile is considered as the combination of two nuclei 1 and 2 while the third particle is the target. The potential energy is the sum of three contributions : $V = V_{12} + V_{13} + V_{23}$. The potential V_{12} which governs the projectile fission is the liquid-drop model energy including the nuclear proximity energy. The shape sequence describes the path leading from a sphere to two unequal spheres. The potential V_{13} and V_{23} are calculated in the sudden approximation. Friction forces between the part 2 of the projectile and the target have been added to take into account the dissipation energy.

3. One and two peak energy spectra

Besides the fusion and elastic or inelastic reactions the projectile breaking occurs naturally. For small impact parameters, the projectile part which is in contact with the target is strongly slowed down by the nuclear and frictional forces and is trapped by the target. The remainder part (the quasi-projectile) tends to escape almost freely. The kinetic energies are well reproduced (Fig.1). For medium impact parameters the two fragments are emitted and the part 2 which has grazed the target has a velocity of about 0.6V beam (Fig.2). It might be a contribution to the relaxed fragment events detected at intermediate angles (Fig.3). The sequential fission of the projectile far from the target is also reproduced.

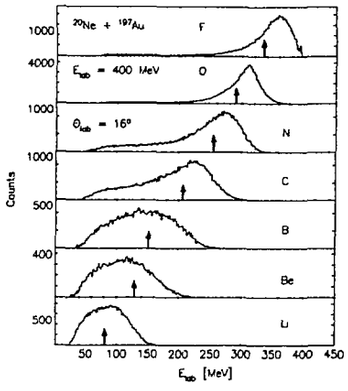

Fig.1: Theoretical value of mean energies of the quasi-projectiles and one-peak spectra.

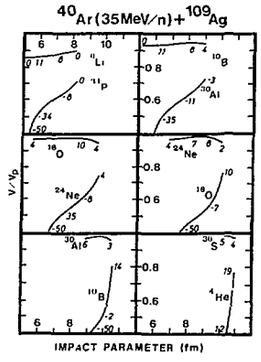

Fig.2: Relative velocity of the two emitted fragments.

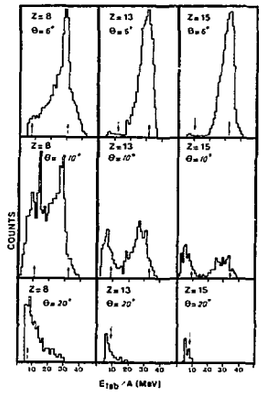

Fig.3: Theoretical value of the mean energy of the two emitted fragments in the 40Ar(35 MeV/A) + 197Au reaction and experimental data.

4. Conclusion

In heavy-ion reactions at intermediate energies, the ion-ion potential between the projectile and the target induces strong stress between the projectile parts and leads to the fission projectile. The description of this asymmetric fission process within the liquid drop model including the proximity energy allows to reproduce semi-quantitatively the mass distribution of the quasi-projectiles and the position of the maxima in the one and-two peak energy spectra. The target is supposed unaltered and such a model cannot describe the frontal collisions and the competition between fission and evaporation.

1) G. ROYER, Y. RAFFRAY, A. OUBAHADOU and B. REMAUD, Nucl. Phys. A466(1987)139
2) C. GREGOIRE and B. REMAUD, Phys. Lett. 127B(1983)308

PE54. MEASUREMENTS OF TIME DELAYS FOR PROJECTILE-LIKE FRAGMENTS IN THE REACTION ^{40}Ar + Ge AT 44 MeV/NUCLEON

J. Gomez del Campo
Oak Ridge National Laboratory,* Oak Ridge, Tennessee 37831
R. A. Dayras, J. P. Wieleczko, and E. C. Pollacco
Servicie de Physique Nucleaire-Basse Energie, CEN Saclay, 91191 Gif-sur-Yvette, Cedex, France
J. Barrette
McGill University, Foster Radiation Laboratory, 3610 University Street
Montreal PQH3A2B2, Canada
F. Saint-Laurent
GANIL, B.P. 5027, 14021 Caen, Cedex, France
M. Toulemonde
CIRIL, B.P. 5133, 14040 Caen, Cedex, France
and
N. Neškovič and R. Ostojič
Boris Kidrič Institute of Nuclear Sciences, Belgrade, Yugoslavia

To achieve a better understanding of the reaction mechanisms in peripheral collisions between heavy ions in the intermediate energy domain of 20-1000 MeV/nucleon, it is important to know the mass and energy transfer to primary fragments during the collision. These quantities can be obtained through detailed exclusive measurements of all particles emitted in coincidence with the fragments. In the work reported here an approach, sensitive to the primary fragment excitation energies, is taken. The formation times of the secondary fragments produced in the reaction are measured by the crystal blocking technique.[1]

In a recent review of the crystal blocking method[1] preliminary accounts of this work were reported and now a more detailed description of the results will be given. Particular attention is placed in the extraction of the decay times which for fragmentation reactions is ambiguous due to the uncertainty on the angular distribution of the primary fragments. Basically, the blocking technique provides an experimental determination of the perpendicular displacement, measured with respect to the nuclei arranged in a row of one of the crystal channels, of the reaction products. This displacement is equal to the product of the reaction time and the velocity of the recoiling nuclei and therefore, only for cases where the velocity is known, like in light ion resonance reactions, heavy ion fission or fusion reactions, the decay time can be uniquely extracted.

In the present experiment, models have to be used to predict the experimental displacements, and the resulting time distributions will depend mainly on the modeling of the angular distributions and excitation energies of the primary fragments.

The experiment was performed by bombarding a 10 μm crystal with a 1.76 GeV ^{40}Ar beam extracted from the GANIL cyclotron facility. The reaction products were detected using a two-dimensional position sensitive gas proportional detector system placed at 1.85 m from the target and equipped with a solid-state telescope to identify the nuclear charge (Z) of the fragments. The first stage of the telescope consisted in a 300 μm thick, 600 mm^2 solid state detector followed by another 5000 μm thick and 600 mm^2. A beam spot of 2 mm was used and the measured intrinsic position resolution of the detector was .8 mm. These values combined gave an overall position resolution σ = 0.04°.

The basic ingredient of the crystal blocking experiments consist of the measurement of the two-dimensional blocking patterns. In the present experiments these patterns were obtain at four laboratory angles: 3.5°, 5.3°, 8°, and 11.8°.

Fragments of Z>9 were analyzed and showed the typical kinematic characteristics of projectile fragmentation products. The resulting two dimensional blocking pattern obtained for all reaction products of Z>9 emitted at a laboratory angle of 5.3° and along the <110> axial direction is shown in Figure 1, where the typical <110> axial structure can be seen. This pattern was obtained after the <110> axis of Ge was aligned to the beam direction by observing the typical "star" channeling patterns on a zinc sulfide screen placed at zero degree. Rotating the <110> axis to an angle θ_{lab} = 5.3°, where the detector was located the two dimensional pattern of Figure 1 was obtained. To observe the axial and planar patterns a very small beam divergence < 0.02° was necessary.

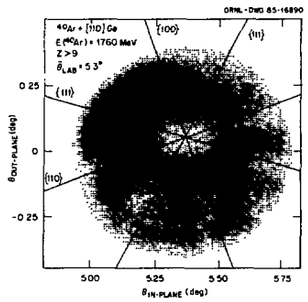

Fig. 1: Two-dimensional blocking pattern of all the projectile-like fragments of Z>9 produced at θ_{lab} = 5.3°.

Integrating the two dimensional patterns in the azimuthal direction of the axis a blocking angular distribution is obtained, and by analyzing these blocking angular distributions the decay time information can be extracted. The reduction of the yield (blocking dip) seen towards zero degree (<110> direction) is directly proportional to the decay time of the primary fragment. For very short decay times, the primary fragments deexcite on a lattice site; hence, the secondary fragments are blocked by the lattice atoms, yielding a *minimum*. For longer decay times, the deexcitation point is displaced towards the center of the channel thus increasing the yield along the channel direction.

From the analysis of the blocking angular distribution we conclude that for all fragments, a significant filling in of the blocking dip is observed, indicating sizable time delay effects. These delays show that emission of light particles is an important process to be considered in the description of projectile fragments produced in intermediate-energy heavy-ion reactions. The extracted decay times are consistent either with a broad primary distribution of fragments with relatively low excitation energies (<50 MeV), of the type given by the abrasion model, or with a deep-inelastic like process in which the primary fragments have a narrow mass distribution with high (~150 MeV) excitation energy. This ambiguity results from the fact that the blocking technique is sensitive to the product of the recoil velocity and the decay time, rather than to the time alone. Removal of these ambiguities can be accomplished by improving the measurements incorporating Z, and M identification and some angular correlation measurements between the PLF and the emitted light particles.

*Oak Ridge National Laboratory (ORNL) is operated by Martin Marietta Energy Systems, Inc., under Contract No. DE-AC05-84OR21400 with the U.S. Department of Energy.

1). J. Gomez del Campo, Nucl. Instrum. Meth. Phys. Res. B24, 447 (1987).

NUCLEAR CALEFACTION

M. Berlanger[1], S. Chiodelli[2], D. Dalili[1], A. Demeyer[2], D. Guinet[2], R. Lucas[1], C. Ngô[1], C. Cerruti[3], S. Leray[1], C. Mazur[1], M. Ribrag[1], T. Suomijarvi[1]

[1] DPhN/MF Saclay, [2] IPN Lyon, [3] Laboratoire National Saturne

At low bombarding energy the fusion of two very heavy ions is impossible due to their too large Coulomb repulsion. Instead of that, one observes a large deep inelastic cross section. As the bombarding energy goes above about 10 MeV/u one start to observe some products coming from three body processes [1]. The probability of the three body process increases with the bombarding energy [1]. The question is : what happens at larger bombarding energies with very heavy projectiles?

An inclusive experiment performed on the Kr+Mo, Ag and Au systems at 22 MeV/u [2] has shown the existence of events which might come from a three body mechanism. Basically, if one detects the products emitted between 6° and 12° in the laboratory system, one observes a correlation between their mass and kinetic energy which is displayed in fig. 1. Here only the most probable values of the two dimensional plot are shown (points). The horizontal bars correspond to the standard deviation of the kinetic energy distribution. One observes two components : the first one with a ridge extending from A=84, E=1800 MeV down to A=50, E=600 MeV. A second one where the ridge is practically at constant kinetic energy (E≅500 MeV). Similar results have been observed with Xe projectiles at 23 MeV/u [3].

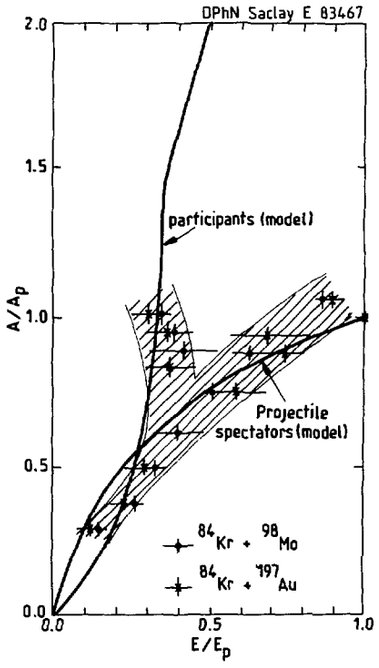

Fig. 1

At very high bombarding energies one knows that nucleon nucleon collisions dominate. As a consequence one has, to a first approximation, the participant spectator of ref. [4]. One gets three kinds of subsystems which have quite different velocities : the fireball and the spectators of the projectile and target.

If one applies this picture to our data one cannot reproduce the mass-energy correlation shown in fig. 1. This is not be too surprising since we are at a bombarding energy where mean field effects are still important.

One can reproduce the mass-energy correlation of fig. 1 if one modifies the participant picture. Let us start, in the interaction region, with the three zones of the participant spectator picture. Then, because of the mean field, which is still important at this energy, there are interactions between the pieces. For projectiles like Ar or smaller, there will be a fusion of the three pieces after

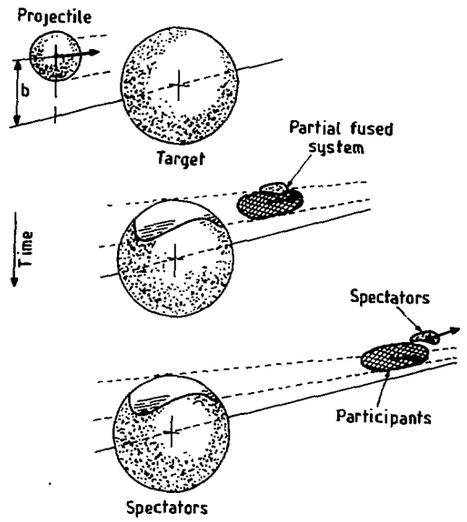

Fig. 2

the hot zone has emitted some preequilibrium particles. This would correspond to incomplete fusion. Such a process is not possible when the projectile and target are too heavy. Indeed, we know that two very heavy ions cannot fuse. However, nothing prevent that two, among the three parts, fuse together. Let us for instance consider the fusion of the participant zone with the spectators of the projectile. One gets a partial fused system moving with a velocity which depends on the number of participants of the target. We could imagine that, after some time, this partial fused system reseparates into the projectile spectators and the participants, before thermalization occurs (fig.2). This could be understood in analogy with *calefaction phenamenon*, an effect observed in macroscopic physics when one pours a drop of water on an overheated plate.

The above simple picture can be compared with the experimental data. This gives the two lines in fig.1. One observes a surprisingly good agreement between the assumptions and the data. Why is it so is still an open problem which deserves further attention.

[1] A.Gobbi, Topical Meeting on phase space dynamics, triestre (1985)
S.Gralla et al, Phys. Rev. Lett. 54 (1985) 1899
[2] D.Dalili et al, Nucl. Phys. A454 (1986) 163
C.Ngô et al, Prog. Part. Nucl. Phys. 15 (1985) 171
[3] O.Granier et al, Nucl. Phys A481 (1988) 109
[4] J.D.Bowan et al, LBL report n°29098 (1975)
G.D.Westfall et al, Phys.Rev. Lett. 37 (1976) 1202
[5] M.Lefort et al, Nucl. Phys. A216 (1973) 166

PROJECTILE FRAGMENTATION NEAR THE FERMI ENERGY

R. Dayras[1], J. Barrette[1], B. Berthier[1], D.M. de Castro-Rizzo[1], E. Chavez[1], O. Cisse [1], R. Coniglione[1], H. Delagrange[3], F. Gadi[1], B. Heusch[4], G. Lanzano[2], R. Legrain[1], M.C. Mermaz[1], W. Mittig[3], A. Pagano[2], A. Palmeri[2] and E. Pollacco[1].

1 D.Ph.N/BE, C.E.N. Saclay, 91191 Gif-sur-Yvette. 2 I.N.F.N. Catania, Corso Italia 57, I-95129 Catania.
3 GANIL Caen, BP. 5027, 14021 Caen Cedex. 4 C.R.N. Strasbourg, 67037 Strasbourg Cedex.

1. Motivations.

In peripheral heavy ion induced reactions, production of fragments in the beam direction with velocities close to the projectile velocity is a very common process at all projectile energies[1]. For projectile energies smaller than ∿ 20 MeV/u, these fragments are clustered around the projectile mass and are produced either by a transfer of few nucleons (stripping or pick-up) or by an incomplete fusion process in which only part of the projectile fuses with the target. On the other hand, for projectile energies greater than 200 MeV/u, these fragments are thought to be produced by a fast removal (abrasion) of the nucleons in the region of overlap between projectile and target. Then the questions arise to when and over which energy range does the transition between those two processes occur. In order to answer those questions, we have undertaken two kinds of experiments : i) inclusive measurements (isotopic yields, energy spectra, angular distributions) of the fragments from an ^{40}Ar projectile bombarding Al and Ti Targets at 44 MeV/u and Ag targets at 30 and 60 MeV/u. The purpose of these experiments was to determine the general properties of the projectile-like fragments (PLF). ii) measurements of the correlations between projectile-like and target-like (TLF) fragments in the reactions $^{40}Ar + ^{27}Al$ at 44 MeV/u and $^{40}Ar + ^{nat}Ag$ at 30 and 60 MeV/u in order to characterize the mechanisms responsible for the fragmentation process.

2. Properties of the projectile-like fragments.

As in high energies (E/A > 200 MeV) collisions, the mass spectrum of the fragments with approximately the beam velocity extends from the projectile mass down to the lightest elements[2-6]. The production rate is large and exhausts about two thirds of the reaction cross section and is well reproduced by the geometrical abrasion model[7]. However some marked differences can be noted with the high energy data. The presence of fragments heavier than the projectile clearly indicates that direct surface transfer reactions may still play an important role in the fragment production at least in the vicinity of the projectile[8,9]. Further evidence of nucleon exchange between projectile and target is provided by the slight dependence of the neutron to proton ratio of the fragments upon the target[5,10].

Although the widths $\sigma_{//}$ of the fragment momentum distributions in the beam direction are well reproduced by Goldhaber's relation[11] with a value of σ_0=85 MeV/c in agreement with high energy data, these momentum distributions are asymmetrical with a low momentum tail indicating dissipative processes. Thus, although the essential features of the data may be reproduced by abrasion models including dissipation[5,12], the features described above cast some doubts on the validity of such models in the intermediate energy domain.

3. Correlations between projectile-like and target-like fragments.

Fig. 1 shows the PLF-TLF mass correlation in the reaction $^{40}Ar + ^{27}Al$ where the PLF's were detected at 3.1° relative to the beam direction whereas the TLF's were detected on the other side of the beam between 15° and 85° (refs. 8,13, 14). The data points represent the ridge of the correlation whereas the horizontal (vertical) bars indicate the full width at half-maximum of the PLF's (TLF's) mass distributions for a given mass of the TLF's (PLF's). On average, the mass lost by the target is equal to the mass lost by the projectile which is consistent with an abrasion process as indicated by the full line in fig.1. However, the dependence of the TLF recoil angle upon the TLF mass is reminiscent of a more simple two-body mechanism were only two excited primary fragments emerge from the collision, which then decay by particle emission. Assuming just such a process,

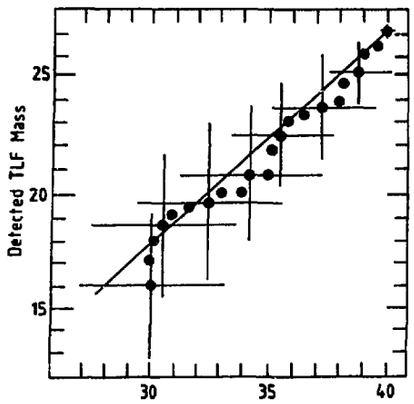

Fig. 1

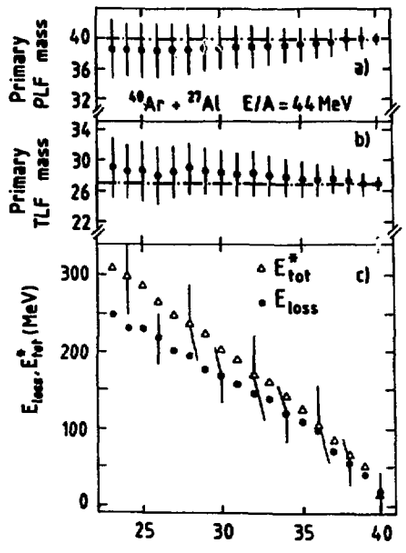

Fig.2

we have use momentum conservation for a full kinematic reconstruction of the binary events, which yields primary quantities like fragment masses, excitation and kinetic energies. The average primary masses of the PLF's and of the TLF's, independently reconstructed are shown in fig.2 a-b as a function of the detected PLF mass. The total kinetic energy loss E_{loss} of the primary fragments, derived from energy conservation is compared in fig.2c to the total excitation energy E^*_{tot} deduced from the mass difference between the primary and detected fragments. As the mass of the detected PLF's decreases, E^*_{tot} increases more rapidly than E_{loss}. This behaviour is consistent with an emission of less than five fast nucleons prior to the separation of the fragments.

Thus the data are consistent with a two-body process reminiscent of the early stage of deeply inelastic collisions in which projectile and target share an approximately equal amount of excitation energy. Recent calculations[15], assuming a stochastic exchange of nucleons between projectile and target give a good description of the $^{40}Ar + ^{nat}Ag$ data at 30 MeV/u. However, in order to solve the ambiguities between the two processes just discussed (abrasion vs. two-body) it would be necessary to accede directly to the excitation energy of the primary fragments for which the two approaches give very different predictions. We have just undertaken such measurements by looking at the spectra of the light particles emitted by the fragments.

1) R. Dayras, J. Phys. (Paris) C4(1986)13.
2) J. Barrette et al., Proc. 22nd Int. Meeting on Nuclear Physics, Bormio (Italy), Jan. 1984.
3) R. Dayras, Proc. 8thOaxtepec Simposium on Nuclear Physics (Mexico), Jan. 1985.
4) R. Coniglione, Tesi di Laurea, Universita Degli Studi di Catania, 1984.
5) R. Dayras et al., Nucl. Phys. A460(1986)299.
6) F. Gadi-Dayras, Thèse, Université de Paris Sud (Orsay), Juin 1988.
7) J.D. Bowman, W.J. Swiatecki and C.F. Tsang, LBL report n° LBL-2908, 1973 unpublished.
8) O. Cisse, Thèse, Université de Paris Sud (Orsay), Sept. 1985.
9) M.C. Mermaz et al., Nucl. Phys. A441(1985)129.
10) D. Guerreau et al., Phys. Lett. 131B(1983)293.
11) A.S. Goldhaber, Phys. Lett. 53B(1974)306.
12) A. Bonasera, Nucl. Phys. A463(1987)653.
13) R. Coniglione et al., Nucl. Phys. A447(1986)95c.
14) R. Dayras et al., Phys. Rev. Lett.(1989) in print.
15) L. Tassan-Got, Thèse, Université de Paris Sud (Orsay), 1988.

– B2 –
DISSIPATIVE COLLISIONS, HOT NUCLEI

DYNAMICAL ASPECTS OF VIOLENT COLLISIONS IN Ar + Ag REACTIONS AT E/A = 27 MeV. PERSISTENCE OF DEEPLY INELASTIC PROCESSES

B.BORDERIE, C.CABOT, H.FUCHS, D.GARDES, H.GAUVIN, F.HANAPPE*, D.JACQUET, D.JOUAN, F.MONNET, M.MONTOYA, M.F.RIVET

Institut de Physique Nucléaire, F-91406 ORSAY
*FNRS and U.L. Bruxelles, B-1050 Bruxelles

1. Motivation

The observation of intermediate-mass fragment (IMF) emission in heavy-ion collisions at intermediate energies has appeared, in the last few years, as a puzzling question giving birth to many theoretical speculations. Experimentally, using a three-source parametrization, it was possible to successfully reproduce the measured inclusive energy spectra [1]. To better understand the origin of the intermediate-velocity source and to have an overview on violent collisions involving IMF emission, coincidence measurements between IMF or light particles and heavy residues (HR) were performed bombarding a ^{nat}Ag target by 1090 MeV ^{40}Ar ions.

2. Experimental results

The in-plane data were analyzed assuming two body kinematics after preequilibrium particle emission [2]. The mean relative velocities V_{rel} between the IMF and HR were calculated as well as the mean velocities of the center of mass of the binary system $V_{c.m.}$ (IMF-HR) ; this last quantity was derived assuming that the particles emitted prior to separation of the two partners, which are essentially preequilibrium particles, do not carry a sizeable mean transverse momentum. The figure summarizes the results. The evolution of V_{rel} between 7 and 30° is similar to what was observed in incompletely damped deeply inelastic collisions at low energies. For $\theta_{IMF} > 40°$ a complete damping seems to be observed ; from an experimental point of view, IMF can be regarded as emitted from a fused system as well as the light partner of a completely damped deeply inelastic collision.

The bottom part of the figure shows the evolution of $V_{c.m.}$ (IMF-HR) which can be compared with the c.m. velocity of the total system (V_{FMT}) ; the deviations observed from this value clearly reveal the appearance and the increase of preequilibrium particle emission with the degree of dissipation of the collision.

3. Semi-classical calculations

It was very tempting to quantitatively compare our experimental observations with a semi-classical approach based on the Landau-Vlasov equation [3]. For central collisions (0 to 5 fm) an incomplete fusion occurs for which only one HR and nucleons are found in the exit channel (no complex particles or IMF can be evaporated in such a calculation). At t = 4.10^{-22} s the momentum distribution of emitted nucleons becomes isotropic and one can then define this instant as the end of the preequilibrium phase for collisions (b_{red} = 0-8 fm). The recoil velocity of the fused system can then be compared

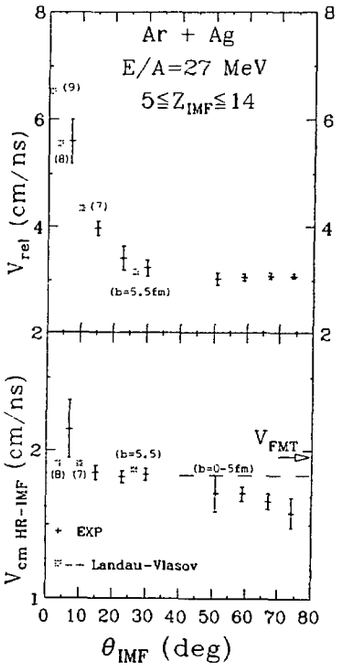

Fig. 1 :Comparison between Landau-Vlasov calculations (see text) and experimental results.

with $V_{c.m.}$ (IMF-HR) (see figure 1). Experiment and calculation agree on one point : the amount of preequilibrium emission increases with the violence of the collision. However, for the more central collisions the experimental values are lower than the calculated ones ; experimental results on protons emitted in coincidence with heavy residues after subtraction of an isotropic component attributed to heavy-residue evaporation also show a disagreement with some of the characteristics of the preequilibrium protons given by the calculation [4]. This discrepancy may have its origin in either the approximate character of the nucleon-nucleon effective interaction used in the calculations or in some underestimation of the nucleon mean free path.

Beyond b = 5 fm two main products are found in the exit channel (one HR and one IMF with average primary Z = 15). The relative velocity between the two partners is found larger than a pure Coulomb repulsion and depends on θ_{IMF} which is a negative angle. The correlated values V_{rel} and θ_{IMF} can thus be compared with experimental ones (see figure 1). A good agreement is observed which is confirmed by the measured cross-sections.

4. Excitation-energies involved

From the knowledge of the two main partners, A_{HR} and Z_{IMF} ($A_{IMF} \simeq 2\ Z_{IMF}+0.5$), and by incorporating results from Landau-Vlasov calculations for preequilibrium emission, it was possible to deduce the missing mass ΔA which is associated to evaporated particles. Figure 2 shows the strong difference between incompletely damped DIC (θ_{IMF} = 15°) and statistical emission from incomplete fusion process (θ_{IMF} = 67°) ; in this latter case, as expected the missing mass or the calculated excitation energy is found rather constant whatever Z_{IMF} [5].

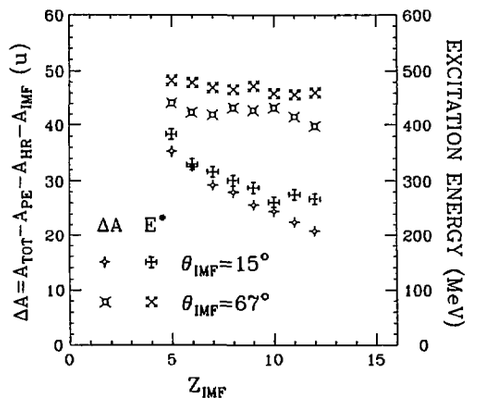

Fig. 2 : see text.

4. Conclusions

Through experimental and theoretical studies dynamical aspects of heavy-ion collisions around E/A = 30 MeV have been investigated. After a preequilibrium emission depending on the violence of the collision it was shown that highly dissipative processes are present namely incompletely damped deeply inelastic collisions at intermediate impact parameters and incomplete fusion for central collisions.

As a consequence, intermediate-mass fragments detected at intermediate angles ("intermediate velocity source") are for a large part the final light partners of deeply inelastic collisions.

[1] B.Borderie et al, Z. Phys. A318 (1984) 315.
[2] M.F. Rivet et al, Proc. of the Texas A&M Symposium on Hot Nuclei, College Station (USA), p. 400 World Scientific (1988).
B.Borderie et al, Proc. XXVI Int. Winter Meeting on Nuclear Physics, Bormio (Italy) p. 84 (1988).
B.Borderie et al, Phys. Lett. B205 (1988) 26.
[3] B.Borderie et al, Third Int. Conf. on Nucleus-Nucleus Collisions, Saint Malo (France), contribution p. 125 (1988).
M.F.Rivet et al. Phys. Lett. B215 (1988) 55.
[4] D.Jouan et al, Proc. XXV Int. Winter Meeting on Nuclear Physics, Bormio (Italy), p. 135 (1987).
[5] B.Borderie et al, to be published.

CHARACTERISTICS OF THE MANY-BODY EXIT-CHANNELS IN HIGHLY DISSIPATIVE COLLISIONS

A. Olmi*, G. Casini*, P.R. Maurenzig*, A.A. Stefanini*, R.J. Charity‡, R. Freifelder‡, A. Gobbi‡, N. Herrmann‡, K.D. Hildenbrand‡, F. Rami‡, H. Stelzer‡, J. Wessels‡, M. Petrovici†, J. Galin•, D. Guerreau°, U. Jahnke•, M. Gnirs°, D. Pelte°, D. Raimold°, J.C. Adloff', B. Bilwes', R. Bilwes' and G. Rudolf'.

‡GSI, Darmstadt, W. Germany;*INFN and Univ. of Florence, Italy;†INPE, Bucharest, Romania;•GANIL, Caen, France;°Univ. of Heidelberg, W. Germany;'CRN, Strasbourg, France.

At incident energies from 12 to 24 MeV/nucleon, the excitation energy of the primary fragments formed in a deeply inelastic reaction spans a very broad range (0 to ~1 GeV) and leeds to the observation of processes involving three, four or even more heavy fragments in the exit channel. These processes have been systematically investigated in the reaction of ^{100}Mo + ^{100}Mo using incident energies of 23.7 MeV/nucleon at GANIL and of 12.0, 14.7 and 18.7 MeV/nucleon at the UNILAC. The heavy fragments (A$\geq$ 20) were detected with high efficiency employing a set-up of 12 parallel plate avalanche counters arranged to cover ~ 80% of the forward hemisphere.

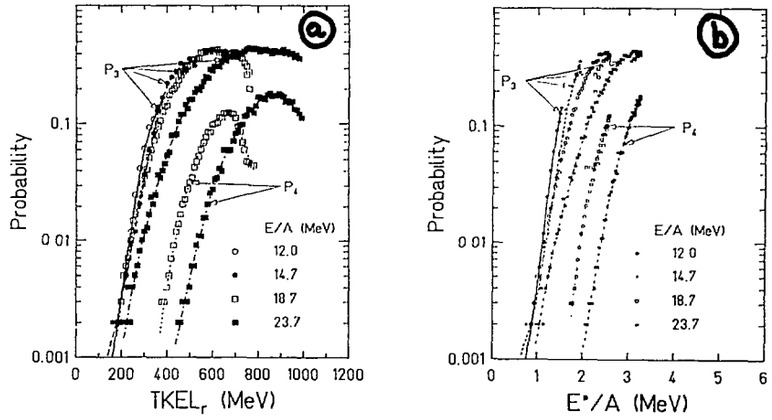

Fig.: 1. Ratios (P_3 and P_4) of 3- and 4-body cross sections to the total cross section for 2-, 3- and 4-body events measured at four bombarding energies.

As a result of these measurements, it has been possible to extend the observation of ternary processes[1] to a broad range of incident energies and to the observation of 4-body decay channels. Figure 1a summarizes all the data concerning the probability of these processes obtained between 12 and 24 MeV/nucleon. Detailed studies of the 3-body process using a refined kinematical coincidence method[2] show that these events are associated with the fission-like decay of a highly excited deep-inelastic product; P_4 seems to scale

approximately quadratically with P_3, as would be expected for independent decay probabilities of the two deep-inelastic products. Beside the high values of the fission probability and the similarity of P_3 at different bombarding energies[1], one has to note: (i) the shift of the curves at 23.7 MeV/nucleon with respect to those at lower bombarding energies, and (ii) the decrease of P_3 and P_4 with increasing TKEL for fully damped interactions. The second feature seems to be a consequence of an equilibrium particle emission during the first step deep-inelastic collision. The strength of such an emission has been estimated using as ingredients: the interaction times derived from a phenomenological model[3] and the particle emission time calculated with the statistical model. One effect of equilibrium emission during the collision is to lower the excitation energy per nucleon E^*/A of the emerging primary fragments, thus explaining the decrease of P_3 and P_4 at high TKEL, as shown in Fig. 1b.

The equilibrium emission can however not explain the shift seen between the 23.7 and the 12 MeV/nucleon excitation functions. One possibility is, that the shift arises from pre-equilibrium particle emission (PEPE) during the early collision stage. This effect is expected to be more important at the higher bombarding energies. The magnitude of such pre-equilibrium effects can be estimated if P_3 is assumed to be predominantly dependent on the thermalized excitation energy of the primary fragments. P_3 is thus used as a "thermometer" to deduce the "temperature" (or excitation energy) of the fragments. It was calibrated at 12 MeV/nucleon where no pre-equilibrium particle emission is expected. Having inferred the thermalized excitation energy of the primary fragments, it is possible by applying the energy balance to estimate the amount of energy lost due to PEPE.

This can then be directly compared to calculations of the Qunatum Mechanical Phase Space Model[4]. In figure 2 the ranges of pre-equilibrium energy losses consistent with the data are shown. (The impact parameter was derived from the measured differential cross-section $d\sigma/dTKEL$).

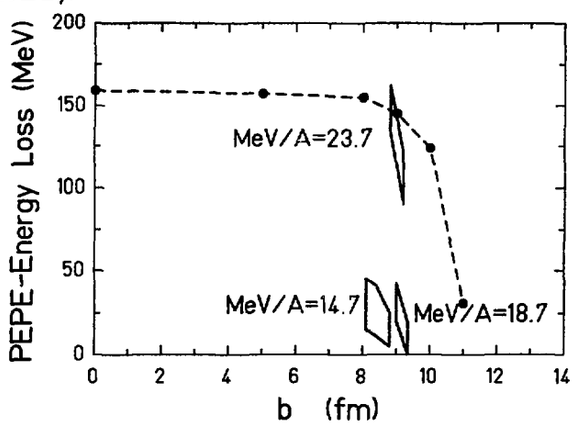

Fig.: 2. The range of pre-equilibrium energy losses consistent with the data are indicated

by the bands. The dashed lines shows the predictions of the Quantum Mechanical Phase Space Model at 19 MeV/nucleon. According to the experiment for the 23.7 MeV/nucleon reaction as much as 100 - 150 MeV are removed by PEPE.

The statistical equlibrium decay model appears to be important in characterizing the heavy fragment exit channel probabilities. The measured angular distribution of the fission-like second step process seems however to contradict the equilibrium hypothesis and is indicative of the role played by dynamical properties. This conclusion can be drawn from the experimental finding of a strong alignment of the fission separation axis with the initial direction of flight of the fissioning nucleus in the 3-body exit channel. Figure 3 shows the in-plane angular distribution of the heavier fission fragments for two different bins in mass-asymmetry $\eta = |(m_1 - m_2)|/(m_1 + m_2)$. $\phi = 0°$ refers to the emission in the direction of flight of the fissioning nucleus; the window in TKEL was chosen such that it was possible to clearly identify the fissioning system by gating on the relative velocity between the fragments. It can be seen that for asymmetric fission in the second step, there is a high probability for collinear emission of the three fragments suggesting that the decision for fission may already be taken during the first step of the reaction.

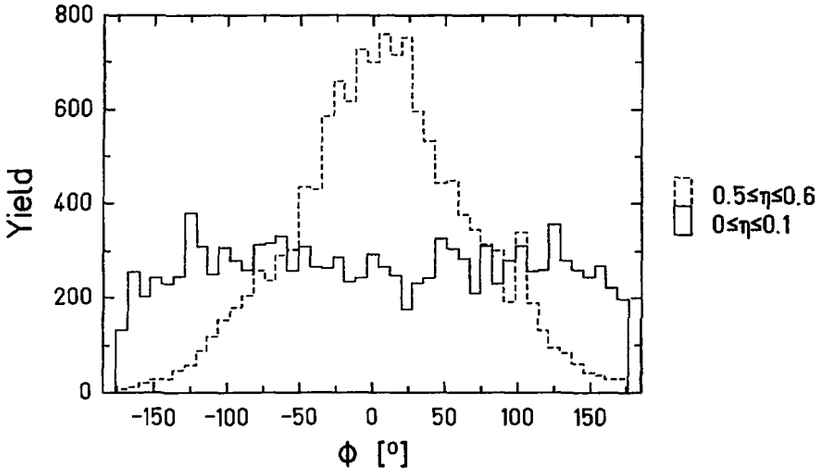

Fig.: 3. In-plane angular distribution for the heavier fragment resulting from the scission of one of the primary products in the collision ^{100}Mo + ^{100}Mo at 18.7 MeV/nucleon ($350 \leq TKEL \leq 550 MeV$).

[1] A. Olmi et al., Europhys. Lett. **4** (1987) 1221.; [2] G. Casini et al., NIM **A227** (1989) 445.;[3]G. Wolschin and W. Nörenberg, Z. Phys. **A284** (1978) 209.;[4]W. Cassing et al., Phys. Lett. **B181** (1986) 217.

COEXISTENCE OF COLLECTIVE AND PARTICIPANT-SPECTATOR MECHANISMS IN THE INTERACTION BETWEEN KRYPTON AND GOLD NUCLEI AT 44 MeV/u.

J.C.Adloff, B.Bilwes, R.Bilwes, M.Glaser, G.Rudolf, F.Scheibling, L.Stuttge, C.R.N.Strasbourg
G.Bizard, R.Bougault, R.Brou, F.Delaunay, A.Genoux-Lubain, C.Lebrun, J.F.Lecolley, F.Lefebvres,
M. Louvel, J.C.Steckmeyer, L.P.C. Caen
J.L. Ferrero, IFIC Valencia (Spain)
Y. Cassagnou, R. Legrain, DPhN/BE Saclay
F. Guilbault, C. Lebrun, B. Rastegar L.S.N Nantes
G.M.Jin, A. Peghaire, J. Peter, E. Rosato GANIL Caen

1.Motivation

At low bombarding energy, the interaction between two nuclei is of collective nature, i.e. all nucleons participate to it. At high bombarding energy, only some of them participate, the others being spectators. The transition between one mode and the other is expected to occur in the Fermi energy domain, i.e. for relative velocities close to the velocity of the nucleons inside the two nuclei. This domain is precisely that covered by Ganil. First experiments, based on inclusive measurements, have generally indicated that the high energy regime starts very early. More recent experiments based on coincidence measurements have reached the opposite conclusion.

Because in this domain collisions are quite violent, many fragments are expected to be produced. A special set of multidetectors has been developped to allow measurements as exclusive as possible: XYZt and DELF detect fragments at forward angles and around the target, respectively, while the MUR and the TONNEAU measure light particles in the same angular ranges.

The present results have been obtained in two experiments. They show that both types of mechanisms coexist in the interaction of Kr with Au at 44 MeV/u.

2. Velocity correlations between fragments

In Fig.1 we show the correlation between the velocities of two fragments detected in XYZt. All these fragments have intermediate mass (A ≈ 16-50). Grossly speaking, we can distinguish three kinds of fragments: i) fast ones ($V/V_p>0.75$), ii) slow ones ($V/V_p<0.25$) and iii) intermediate velocity fragments (IVF) with a velocity close to half of that

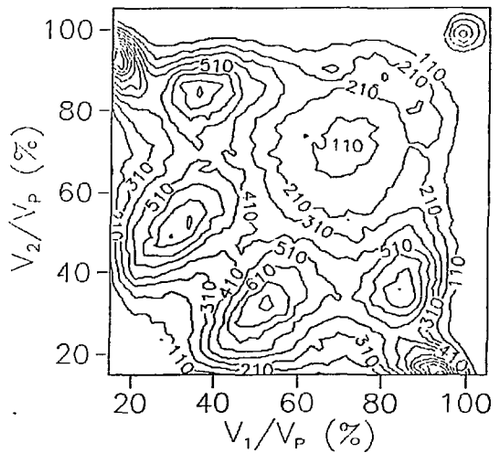

Fig.1

of the beam (V_p). These latter ones are of particular interest: they may be produced either by the decay of a participant zone, by the fission of the projectile or by evaporation from the target. The origin of these fragments is therefore a signature of the mechanism.

3. Deep-inelastic collisions.

We shall first investigate the origin of the fast-intermediate coincidences in Fig.1. Light particle multiplicities show that this component corresponds to intermediate impact parameters. More precisely, we shall select events in which one single IVF is detected in coincidence with one fast and two slow fragments (4-fold coincidences). These slow ones (measured by DELF) have typical properties of fission fragments from a heavy and slowly moving nucleus. The relationship between the charge of the fast fragment and that of the sum of the two slow ones (full dots in Fig.2) seems fairly well reproduced supposing that

the fast fragment is the spectator of the projectile and the slow fragments are produced by the fission of the spectator of the target. The calculation is based on a model [1]) in which the mechanism has first a collective step and then a participant-spectator one (dotted curve). However, this agreement is misleading. Indeed, the relative velocity between the IVF and the center of mass of the two slow fragments demonstrates that this IVF has been evaporated by a target-like nucleus before it fissioned. The charge of the IVF must be added to the sum of the two slow fragments. We obtain thus the charge of the target-like nucleus minus the evaporation of light particles (open dots). The relationship between this charge and that of the fast fragment agrees well with a calculation based on a deep-inelastic model in which the fast fragment is the projectile-like nucleus and the excitation energy is shared equally between the two partners (full curve).

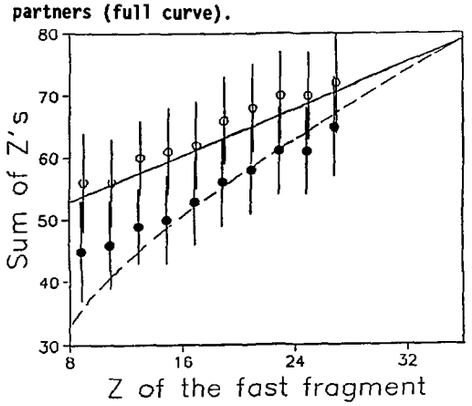

Fig.2

4. Fragments emitted by a participant zone.

Coincidences between two IVF's correspond to the most central collisions observed in this experiment. They are observed in double (Fig.1) and triple coincidences in XYZt: in this case, the third fragment is sometimes a fast one, which excludes that this component is due to the fission of a very slowed-down projectile. Shown in Fig.3 is the relationship between the difference in velocity and the relative angle between the two IVF's. The

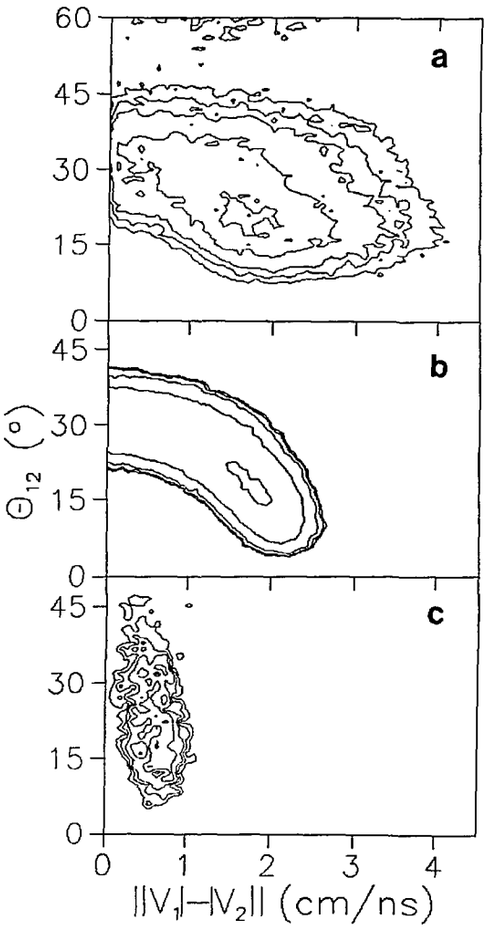

Fig.3

experimental data are reported in Fig.3a, a simulation based on the decay of a source with mass ≈ 120 and velocity ≈ $0.4V_p$ in Fig.3b and another one based on a deep-inelastic reaction followed by a double evaporation from the target in Fig.3c. The calculation lends definitely support for the existence of a separate participant zone.

A close inspection of the characteristics of the fast fragment in the triple coincidences shows that the system evolves from the mechanism described in section 3. to that of section 4. when about 1 GeV kinetic energy is dissipated.

1) A.Bonasera et al., Nucl.Phys A463 (1987)653

INCOMPLETE LINEAR MOMENTUM TRANSFER

C. Cerruti[1], J. L. Charvet[2], S. Chiodelli[1], A. Demeyer[1], O. Granier[3], C. Grégoire[3], D. Guinet[1], G. La Rana[3], C. Lebrun[4], S. Leray[3], P. Lhènoret[3], J. P. Lochard[2], R. Lucas[3], C. Mazur[3], M. Morjean[2], G. Nebbia[3], C. Ngô[3], Y. Patin[2], A. Péghaire[2], M. Ribrag[3], L. Sinopoli[2], T. Suomijarvi[3], E. Tomasi[3], J. Uzureau[2], L. Vagneron[1]

[1] IPN Lyon, [2] CEN Bruyères le Chatel, [3] DphN/MF Saclay, [4] LPC Caen

At low bombarding energies central collisions between heavy ions lead to the fusion of the projectile and target into a compound nucleus. When the energy increases fusion becomes incomplete, that is, only part of the incident nuclei fuses together to form a quasi compound nucleus. When beams at intermediate energies became available the questions were : what is the mecanism for incomplete fusion ? how does the rate of linear momentum transfer, LMT, vary with energy and with the mass of the two ions ? Is there a limitation to this process and in particular to the energy deposit into the quasi compound system ?

In order to answer these questions we have performed a serie of experiments with ^{40}Ar projectile on ^{197}Au and ^{238}U targets[1-3] at different bombarding energies. Because we were dealing with heavy targets the main decay channel of the compound system was expected to be fission. Thus, information about the percentage of linear momentum transferred to the quasi compound nucleus was obtained through the measurement of the folding angle, θ_{fold}, between the two fission fragments, since θ_{fold} increases with decreasing LMT. In the last experiment[3] light particles were also detected in coincidence with the fission fragments.

Fig. 1 shows the folding angle distributions for the system Ar + U that we obtained at SARA[3] (a) and at GANIL[1-3] (c,d) as well as results of Jacquet et al[4] (b). At 20 and 27 MeV/u two peaks can be seen : the first one at low θ_{fold} values can be ascribed to incomplete fusion while the one with θ_{fold} around 170° is due to sequential fission following peripheral collisions. The arrow labelled FMT indicates to which value of θ_{fold} full momentum transfer would correspond. The position of the peak is in good agreement with an empirical law established on lighter systems (the Viola systematics[5]) as shown by the arrow labelled

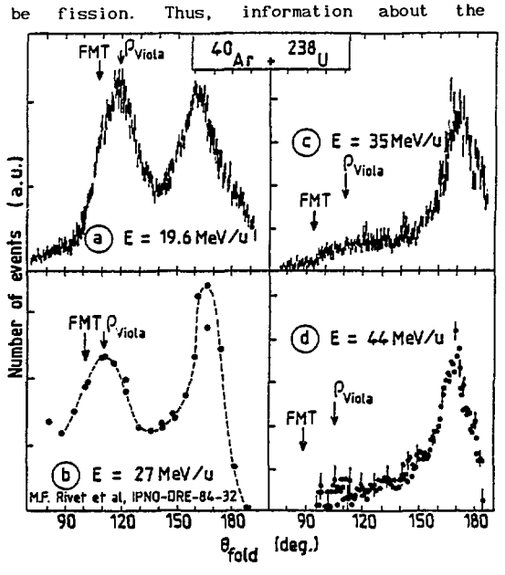

Fig. 1. Folding angle distributions for the Ar + U system at different bombarding energies (from ref.[3,4,2,1]).

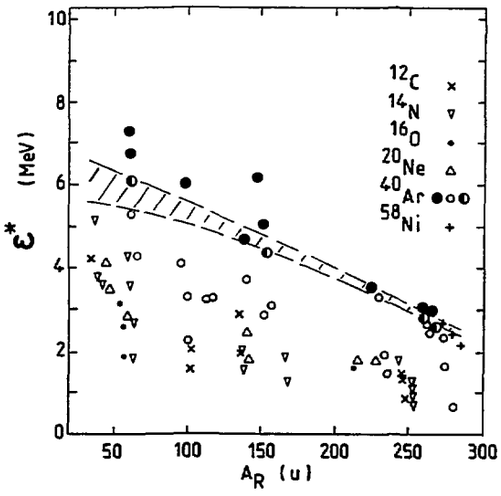

Fig. 2. Excitation energy per nucleon deposited in a quasi compound nucleus versus its mass. The filled and half filled circles correspond to systems for which no fusion products were observed (from ref.[5]).

ρ_{Viola} on the figure. The situation is quite different at 35 and 44 MeV/u since no peak can be seen where one would expect it. This suggests that the quasi compound nucleus does not decay any longer via usual ways or that incomplete fusion becomes impossible above 35 MeV/u. The same conclusions can be drawn from results obtained by other authors with different targets : it appears that one no longer observes evaporation residues[6,7] or fisson fragments[8] in central collisions above 35 MeV/u.

One possible explaination is that the disappearance of these products of fusion could be due to the reaching of the limit of the excitation energy which can be deposited in a compound system. In fig.2 the excitation energy per nucleon, ε^*, in the quasi compound nucleus is plotted versus its mass, A_R, for different systems[9]. Systems for which the usual decay products of a quasi compound nucleus were not observed are represented by filled or half filled circles. It appears that all the systems for which products of fission were not observed are above the dashed region in fig.2.

In a simple model[10] we have evaluated the maximum excitation energy, ε^*_{max}, that a nucleus can sustain before boiling off into nucleons and clusters from the binding energies of nucleons and clusters in nuclei and the probability of cluster emission supposed to be proportional to $A^{-\tau}$. As it can be seen in fig.3 where ε^*_{max} is plotted, for different values of τ, versus the mass of the nucleus this model is in good agreement with what can be deduced from the experimental data in fig.2.

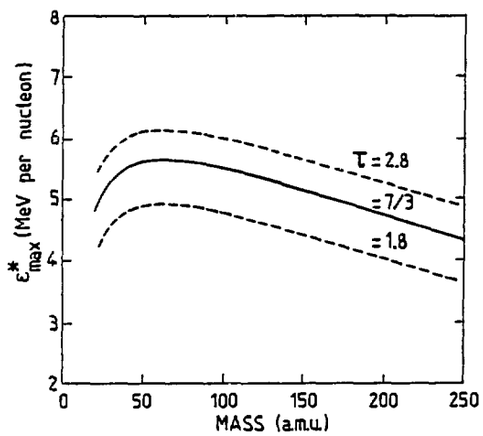

Fig.3. Maximum excitation energy that can be deposited in a nucleus versus its mass calculated assuming that clusters of A are formed with a probability $A^{-\tau}$ for different values of τ (from ref.[10]).

We have also developped a theoretical model for promptly emitted particles[11] based on the coupling between the intrinsic motion of the nucleons in a nucleus and the relative motion of the two ions. This model fits rather well the experimental data concerning fast protons detected in coincidence with fission fragments[3] and neutrons measured by Holub et al[12] but cannot explain the measured amount of transferred linear momentum. This indicates that a large part of the missing mass is carried away by alphas or even heavier fragments.

1) S. Leray et al, Nucl. Phys. A425 (1984) 345
2) S. Leray et al, Z. Phys. A320 (1985) 533
3) Y. Patin et al, Nucl. Phys. A457 (1986) 146
4) D. Jacquet et al, Phys. Rev. Lett. 53 (1985) 140
5) V.E. Viola Jr et al, Phys. Rev. C26 (1982) 178
6) G. Auger et al, Phys. Lett. 169B (1986) 161
7) A. Lleres et al, J. Phys. 47 (1986) 365c
8) E.C. Pollaco et al, Phys. Lett. 146B(1984) 29
9) S. Leray, J. Phys. 47 (1986) 275c
10) C. Ngô et al, Z. Phys. A322 (1985) 419
11) S. Leray et al, Z. Phys. A320 (1985)383
12) E. Holub et al, Phys. Rev. C28 (1983) 252

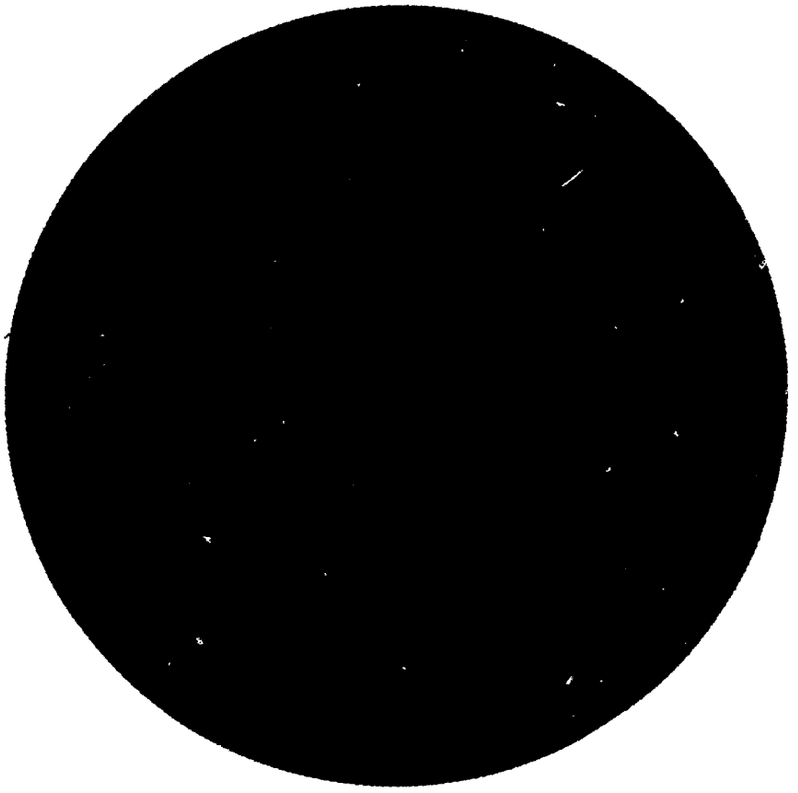

Formation and decay of hot nuclei in the Ar, Ni and Kr + Th systems

Y. Cassagnou, M. Conjeaud, R. Dayras, S. Harar, R. Legrain, M. Mostefaï,
E.C. Pollacco, J.E. Sauvestre, C. Volant
DPhN/BE, CEN Saclay, 91191 Gif-sur-Yvette Cedex, France

G. Klotz-Engmann, V. Lips, H. Oeschler
Institut für Kernphysik, Technische Hochschule Darmstadt, Germany

In compressing and heating nuclear matter via nucleus-nucleus collisions our ultimate objective is to draw information on the Nuclear Matter Equation of State (NMES). Our work at GANIL has focussed on a particular aspect, namely : what are the limits *in thermalised excitation energy* E^* can a nucleus contain ? An answer is very pertinent since NMES is very sensitive to this limit[1]. Thus, experimentally we have considered different systems with varying available energy and looked for the conditions whereby the evaporation residue ceases to exists. To date no limit can be given however a number of key results have been obtained which open very interesting prospects.

The main results are shown in fig. 1. The experimental technique employed is the angular correlation method where the recoil velocity of the fissioning nucleus as well as the mass of both fragments are measured[2]. Of interest are the peaks at small θ_{ff} (large linear momentum transfer (LMT)) which correspond to events of almost complete fusion or otherwise called, central collisions (CC). By performing kinematic balance calculations we obtain an estimate of E^* which in turn is compared with the final measured mass. *From the ensemble of measurements we draw* a number of salient results :

- the attained energy E^* is high of the order of 1 GeV and correspond to 60 % of the total binding energy[3,4]. For the Kr + Th system, values are even higher and lead to values well above the expected theoretical and extrapolated experimental values[5].

- Heavy projectiles yield a higher cross section for the formation of very hot nuclei.

- By using heavy projectiles we conclude that the fall in the yield of the CC peak is not as a result of limiting E^* values but rather due to dynamic effects. Therefore,

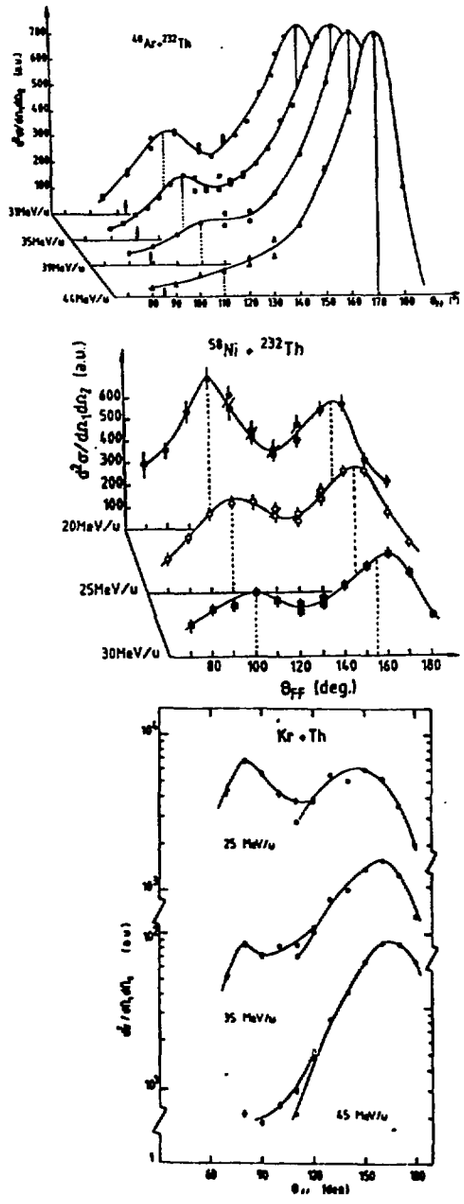

- Dynamic effects are present. From fig. 1. it is clearly seen that the CC position is independent of incident energy. In fact a scaling of linear momentum transfer with mass of the projectile is clearly shown by our work. This suggests that in heavy ion reactions around the Fermi energy, one can only deposit a limited amount of energy.

A problem which we have also addressed is whether the hot nuclei being formed are indeed thermalised and how do very hot nuclei desexcite. This work is in its infancy.however the preliminary results[6] are most encouraging. In fig. 2 are shown data of angular correlations with and without coincident intermediate mass fragments (IMF). The fact that the condition filters out the most violent collisions is of primary importance since it allows an additional method to scrutinize these events. Further, analysis of the spectra from the detected IMF's show fall off's which are coherent with the LMT measurements.

It is clear from our work and others that dynamics play an important role. In particular it is not yet clear how the heating up of nucleon matter is achieved and how compression, for example, affects the limits.

The second generation of experiment will seek to establish a 4π coverage. This will yield a greater selectivity for the events, and permit to obtain information on the production mechanisms and hence allow the establishing of limits in excitation energy and their interplay with other parameters.

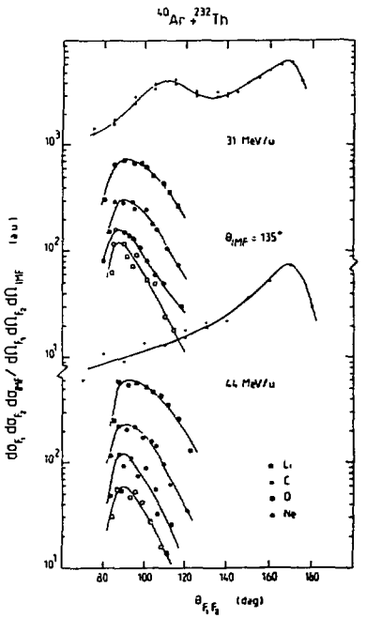

Fig. 2

1) S. Levit and P. Bonche, Nucl. Phys. **A437** (1985)426.

2) E.C. Pollacco et al., Phys. Lett. **146B** (1984) 29.

3) M. Conjeaud et al., Phys. Lett. **159B** (1985) 244.

4) C. Volant et al., Phys. Lett. **195B** (1987) 22.

5) E.C. Pollacco et al., Nucl. Phys. **A488** (1988) 319c.

6) C. Volant et al., Third International Conference on nucleus-nucleus collisions, Sain-Malo June 6-11, 1988, contributed papers p. 100.

SATURATION OF THE THERMAL ENERGY DEPOSITED IN Th NUCLEI BY Ar PROJECTILES BETWEEN 35 AND 77 MeV/u

D.X.Jiang*[1], H. Doubre[1], J. Galin[1], D. Guerreau[1], E. Piasecki**[1], J. Pouthas[1], A. Sokolov[1], B. Cramer[2], G. Ingold+[2], U. Jahnke[2], E. Schwinn[2] J.L. Charvet++[3], J. Fréhaut[3], B. LottΔ[3], C. Magnago[3], M. Morjean○[3], Y. Patin[3], Y. Pranal[3], J.L. Uzureau[3] B. Gatty[4], D. Jacquet[4]

1) GANIL, BP. 5027, 14021 Caen-Cedex, France
2) Hahn Meitner Institut Berlin -D-1000Berlin 39, Germany FRG
3) CE Bruyères le Châtel, BP 12 91680 Bruyères-le-Châtel, France.
4) IPN BP 1, 91406 Orsay-Cedex, France
Present address : Dept. of Physical Technics, Univ. of Beijing, China
* Present address : Inst. Of Exp. Phys. Warsaw University, Hoza 69, Warszawa
+ Present address : Phys. Dept., State Univ. of New York, Stony-Brook, NY 11794
++ Present address : DPhN/BE, CEN Saclay, 91191 Gif-sur-Yvette Cedex
Δ Present address : CRN Strasbourg, BP 20 CRO, 67037 Strasbourg cedex
○ Present address : GANIL, BP 5027, 14021 Caen-cedex.

1 Motivations

The fate of nuclei heated-up to high temperatures (T≥5 MeV) has been a hotly debated question for several years. In order to progress in this domain, one needs to know how to prepare these hot nuclei, and how to control the amount of energy which is eventually stored as randomized energy (heat) in them.

The influence of the projectile velocity on the amount of dissipated energy is still under debate ; saturation of the momentum transfer has been documented for projectile energies larger than 30 MeV/u. However, these observations rely mainly on the binary fission channel, and one cannot preclude the existence of other important exit channels at higher bombarding energies. In order to investigate this question, we believe on the one hand, that it is necessary to probe the energy dissipation by way of all exit channels as opposed to just one. On the other hand, all exit channels are not a priori known. Thus, it follows that one has to find a suitable observable which can be expected to introduce the minimum possible bias to the measurements.

We have chosen the multiplicity of evaporation - like light particles (n, H, He) as our minimum bias probe. This choice was motivated by one simple fact: irrespective of the decay process - standard fission, intermediate mass fragment emission or multi - fragmentation - all massive fragments finally "cool" by emitting light particles.

2 Experiment

We present data for the reactions Ar + Th for three different projectile energies (35, 44 and 77 MeV/u)[1].

The neutron multiplicity data have been collected using a 4π, Gd loaded liquid scintillator detector. The detection efficiency of such an apparatus depends primarily on the kinetic energy of the neutrons, and on the amount of liquid surrounding the target. Two detectors have been used in successive experiments : the first one from CE Bruyères le Châtel of 500 liters at 35 and 44 MeV/u, the second one from HMI Berlin of 1500 liters at 44 and 77 MeV/u. As checked in Monte Carlo detection simulations, the growth in detector size results in a spectacular gain in the efficiency from about 60% to about 80% for evaporative neutrons. However, the efficiency remains small for high energy preequilibrium neutrons.. Light charged particles were detected close to 160° by standard Si telescopes.

3 Saturation of the thermal energy

A glance at the inclusive neutron multiplicity distributions fig. 1 for the three bombarding energies gives already an interesting information : no sizeable shift is observed in the location of the high multiplicity bump, associated to the most dissipative collisions. The most spectacular effect is related to a change in detection efficiency when the 44 MeV/u experiment is performed, first with a 500 l detector and, then with a 1500 l detector. Apart this experimental effect, no important change can be seen from 35 MeV/u up to 77 MeV/u. Triggering the neutron detection by backward emitted light charged particles (l.c.p.) leads also to similar neutron multiplicity distributions whatever the bombarding energy. Moreover, the evaporation like l.c.p. have been detected at 160° with similar multiplicities. Thus, the extra energies of 307 MeV and 1433 MeV brought by the projectile, in the center of mass Ar + Th system as compared to the initial 1194 available bombarding energy at 35 MeV/u have hardly any effect on the neutron multiplicity data as well as on evaporative l.c.p. emitted backwards.

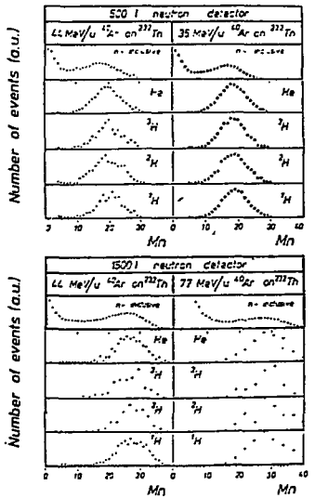

Figure 1: Inclusive and exclusive (triggered by light charged particles emitted at 160°) neutron multiplicity distributions as measured with two detectors.

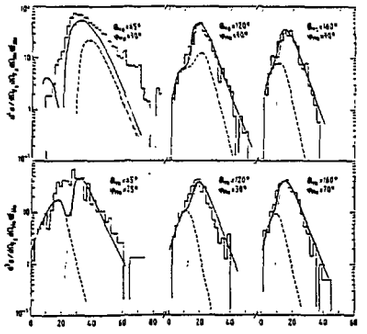

Fig.3. Calculated spectra for alpha particles emitted by the composite nucleus (CE: dotted lines) by the fission fragments (FE:dashed lines) and their sum (full lines) compared to the experimental spectra (histograms).

data [3]. It is a rather cold nucleus which undergoes scission irrespective of its initial temperature. Due to their origin the light charged particles constitute a good probe of the hot nuclei. The slope temperature which is deduced from the energy spectra indicates that α-particles are emitted rather early by strongly deformed and spinning nuclei. These strong deformations are also found in a Landau-Ulasov simulation of the collision for different impact parameters. The shape degree of freedom are shown to slowly relax in the course of the cooling of the nuclei. Thus it is quite consistent to observe a signature of the deformation in the evaporated particles.

To summarize, light charged particle evaporation becomes increasingly important when the temperature of heavy nuclei is raised, as confirmed by additional data on similar systems [4]. These charged particles constitute a good probe for investigating the average properties (temperature, spin, deformation) of very excited nuclei (T ≃ 5 MeV) formed after violent nucleus-nucleus collisions.

1) D. Jacquet et al. Phys. Rev. Lett. 53 (1984) 2226.
D. Jacquet et al. Phys. Rev. 32 (1985) 1594.
D. Jacquet et al. Submitted for publication.
2) D.X. Jiang et al. Contribution to the III Conference on Nucleus-Nucleus Collisions, St.Malo (1988).
3) D. Hilscher et al. Phys. Rev. Lett. 62 (1989) 1099.
4) D.X. Jiang et al. Submitted for publication.

MOMENTUM TRANSFER LIMITATION IN ^{20}Ne AND ^{40}Ar INDUCED REACTIONS ON ^{124}Sn

A. Lleres[+], J. Blachot[*], J. Crançon[*], A. Gizon[+] and H. Nifenecker[*]

[+] Institut des Sciences Nucléaires, 53 Avenue des Martyrs, F-38041 Grenoble, France
[*] Centre d'Etudes Nucléaires, DRF/Ph.N, BP 85 X, F-38041 Grenoble Cedex, France

A limitation of the linear momentum transfer in central heavy ion collisions has been observed in a lot of various experiments performed at intermediate incident energy on heavy and light targets (Ref. 1,2,3). It was shown that, as the incident energy increases, the complete fusion process becomes less and less probable and gives place to increasingly incomplete fusion. To follow the evolution of fusion processes in central collisions on medium mass targets, we have focused our effort on a series of systematic velocity measurements of heavy residues recoiling at forward angles in ^{12}C to ^{40}Ar induced reactions on ^{124}Sn.

In this paper, we report a set of results on ^{20}Ne and ^{40}Ar induced reactions at energy from 20 to 60 MeV/nucleon. Simple incomplete fusion calculations are applied to estimate the amount of linear momentum transferred to the fusion-like systems in the most violent collisions. Estimated momentum transfers are compared to predictions of a pre-equilibrium emission model and a simple Fermi jet model.

The experiments were performed with ^{20}Ne ions of 20, 30, 40 and 49 MeV/nucleon and ^{40}Ar of 24, 27, 30, 35, 44 and 60 MeV/nucleon. The highest energy beams were delivered by the accelerators GANIL (27 - 60 MeV/nucleon) and SC at CERN (49 MeV/nucleon) and the lowest ones by the SARA facility (20 - 30 MeV/nucleon).

The experimental technique is based upon off-line gamma-activity measurements following target irradiations associated with on-line collection of reaction products (Ref. 4). Heavy products emitted around the beam axis were collected by a stack of thin aluminium foils (1 or 2 μm) set behind a thin target (400 μg/cm^2), perpendicularly to the beam axis. A collimator set between the target and catchers defined a solid angle with an angular aperture of 10°. Identification and production cross sections of heavy reaction residues ($70 < A < 130$) were established from the analysis of gamma-activities measured on the catchers. Velocity distributions were extracted by use of range-energy conversion tables.

Typical residue velocity-mass spectra obtained for the $^{20}Ne + ^{124}Sn$ and $^{40}Ar + ^{124}Sn$ reactions are shown in figures 1 and 2, respectively. On these figures, the dashed lines represent the evolution of the most probable velocity as a function of mass ; the highest values are associated to the most violent collisions. V_{cm} is the center of mass velocity.

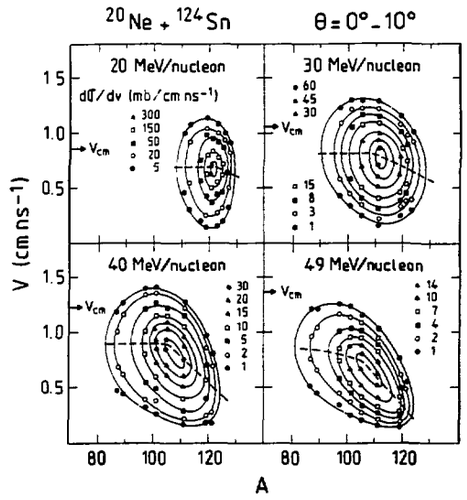

Fig. 1 : Velocity-mass spectra of forward emitted heavy residues from the $^{20}Ne + ^{124}Sn$ reaction at 20, 30, 40 and 49 MeV/nucleon (see text).

One observes clearly that, at each bombarding energy, the most probable velocities of the residues, although relatively high, are lower than the center of mass velocity. This indicates that, for all incident energies, the final products correspond to evaporation residues coming from incomplete fusion mechanisms. Moreover, with increasing incident energy, the difference between the measured most probable velocities and the center of mass velocity increases, indicating that the involved momentum transfer is more and more incomplete.

To estimate the amount of linear momentum transferred from the projectile to the fusion-like system, several assumptions can be done to describe the formation and the de-excitation of the fusion-like nucleus (Ref. 4,5,6). We assume that a part α of the projectile fuses with the totality of the target, the spectator nucleons being emitted (as nucleons, clusters or a quasi-projectile fragment) along the beam axis with a part β of their initial velocity. We suppose that the composite nucleus de-excites by isotropic nucleon evaporation. Linear momentum tranfers were estimated by fitting α and β to reproduce the measured residual most probable velocities and masses. Calculated β values show that non-absorbed projectile nucleons keep around 75 to 100 % of their initial velocity.

It is far too early to conclude unambiguously on this point. Nevertheless, Landau-Vlasov calculations strongly suggest that compression energy could represent a sizeable part of the total excitation energy for bombarding energies of about 50 MeV/u . Our aim in the future will be to find signatures of these features. One way for that is to study fusion nuclei of comparable total excitation energies but with different values of the compression energy involved in the collisions.

4) References

A Semi-Exclusive Study of Heavy-Residue Production in the $^{40}Ar+Ag$ Reaction at 35 MeV/u Incident Energy
Z. Phys. A - Atomic Nuclei 323, 459-464 (1986)

Evolution of fusion reaction with Ar projectiles from 30 to 60 Mev/u
Invited talk Texas A and M Symposium on Hot Nuclei. College Station USA Dec 1987

Evolution de la fusion pour les systèmes $^{40}Ar+^{108}Ag$ et $^{40}Ar+^{197}Au$ entre 39 et 60 MeV/A
P. Eudes - Thèse de l'Université de Caen, 1988.

E MeV/A	T_{BV} MeV	T_{MV} MeV	T_{HV} MeV
39	4.2±0.4	3.8±0,4	4.0±0.2
50	4.2±0.2	4.5±0.5	5.1±0.9
60	5.5±0.1	5.4±0.2	6.9±1.0

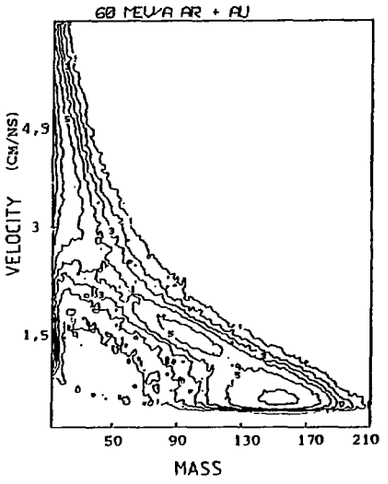

Figure 1

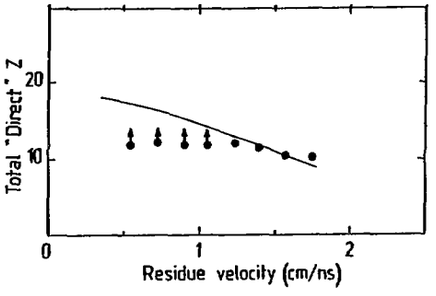

Figure 3

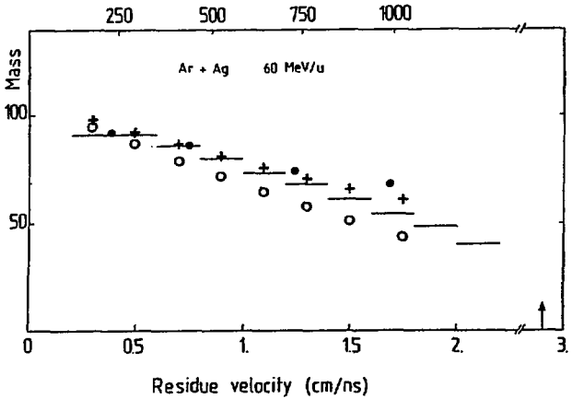

Figure 2

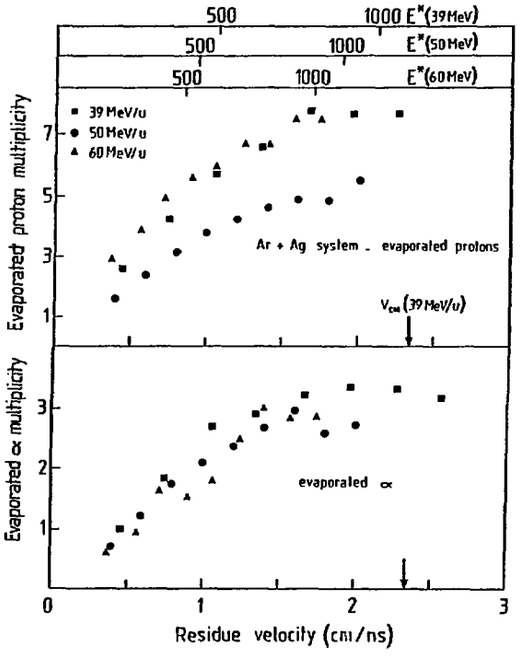

Figure 4

FUSION RESIDUES BETWEEN 35 AND 60 MeV/A

G.Bizard,R.Brou,J.L.Laville,J.B.Natowitz,J.P.Patry,J.C.Steckmeyer,B.Tamain L P C, CAEN
H.Doubre,A.Péghaire,J.Péter,E.Rosato GANIL, CAEN
F.Guilbault,C.Lebrun L S N, NANTES
F.Hanappe U L B, BRUXELLES
J.C.Adloff,G.Rudolf,F.Scheibling C R N, STRASBOURG

1) Motivations

The purpose of our experimental program is to study the evolution of the fusion process for Ar projectiles up to 60 MeV/A .At low bombarding energies, fusion nuclei may be recognized in detecting either fission fragments or evaporation residues. Our experiment considered the latest ones. Two targets have been used : silver and gold. A specificity of our measurements lies in the use of multidetectors. The triggering signal is given by a telescope which identify the evaporation residue. In coincidence with this residue, we are looking at light charged particles emitted either in the forward direction (detected in the plastic wall) or at larger angles (detection in the barrel). The experiment performed up to now has been achieved by using the whole plastic wall but only few pieces of the barrel covering a large polar angular range but a limited azimuthal one. The results may be analysed in two sections : results concerning the inclusive detection of the residue ; and results obtained by analysing the coincident light charged particles.

2) Inclusive measurements

The fusion nuclei have been identified by the detection of evaporation residues at forward angle in a time of flight silicon telescope. The energy threshold was set low enough to enable detection of very slow heavy residues ($v > 0,3$ cm/ns). As shown in Fig.1, which is an example of experimental data of correlations between mass and velocity residues from Ar+Au system at 60 MeV/A , the classes of events appear clearly : quasi-projectile, fission and evaporation residue contributions. In the case of Ar+Ag system there is no evidence for fission contribution. It appears that the evaporation residue velocity distributions do not exhibit any peak above the velocity threshold, where as it exists at 27 MeV/A. However evaporation residues are observed with recoil velocities which can represent a significant fraction of the center of mass velocity (arrows of Fig 2&4), which decrease with bombarding energy. The analysis of coincident light charged particles will show that the events correspond really to very hot fusion nuclei formation. The existence of such events for bombarding energies reaching 60 MeV/A is a first qualitative result of our experiment. In Fig.2 experimental results (horizontal lines) are the most probable evaporation residue masses for each recoil velocity bin. The points have been calculated in the framework of an incomplete fusion model. The projectile is assumed to partially fuse with the target, its remaining part flying away at zero degree with the beam velocity. This model is able to nicely reproduce the most probable masses of the detected residues. The agreement is a first indication that excitation energies as high as 700-1000 MeV could be reached in fusion nuclei. For Ar+Au system at 60 MeV/u there is a sizable evaporation cross section which have a recoil velocity exceeding half the center of mass velocity. The above simple incomplete fusion model indicates that in this case, the fusion nucleus would have a mass of at least 220 amu and an excitation energy of about 1 GeV . The fact that such a nucleus does not undergo fission with a stronger probability cannot be understood in the static statistical model but only in a dynamical statistical model where evaporation takes place before fission.

3) Coincident measurements : semi exclusive analysis

Velocities of light particles detected in coincidence with evaporation residues at 39, 50 and 60 MeV/A, have been measured. The backward spectra (90-150°) exhibit a maxwell shape and have been fitted by standart evaporation code (Lilita) in which it was assumed that all the backward detected particles were evaporated from the fusion nucleus. It has then been possible to calculate the corresponding forward contribution and, to subtract it from the forward detected spectra. The corresponding spectra account for particles which are not evaporated from the fusion nucleus. These particles may be due to direct processes or to preequilibrium emission or to sequential decay of a projectile like fragment. We will call it fast component. By integration of this component it has been possible to estimate the percentage of the initial beam energy which has not been dissipated in the target nucleus.

In Fig.3 the corresponding charge multiplicity is compared with the prediction of the massive transfer model for various velocities of the fusion nucleus (V_R). In the case of small V_R values (peripheral collisions) the disagreement between the curve and the experimental points, is due to the undetected very forward projectile like fragments ; for large V_R (central collisions) the agreement is very nice which shows that the massive transfer model is able to predict the excitation energy dissipated in the fusion nucleus. This excitation energy is plotted on the upper axis of Fig.4. These figures are related to the fusion nucleus decay particles multiplicities. Both p and α multiplicities increase and saturate for an excitation energy of about 750 MeV whatever incident energy. Such result is surprising when considering temperatures extracted from backward proton kinetic energy spectra slopes (silicon telescope at 150°) which are tabulated . The three columns low (LV) , medium (MV) and high velocity (HV) correspond, to more and more violent (or central) collision. The absolute values of T increase with bombarding energy. How do we can reconcile these results with the multiplicity evolution noted above ? One explanation may be found in the excitation of collective (compression) modes. In such a framework, the fusion nucleus excitation energy would be divided in two parts (thermal+Collective) and the collective part could affect significantly both the slopes of the particle kinetic energy spectra and the relative multiplicity of clusters.

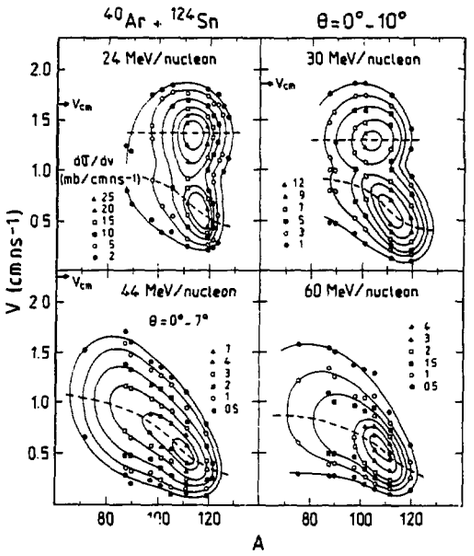

Fig. 2 : Velocity-mass spectra of forward emitted heavy residues from the $^{40}Ar + ^{124}Sn$ reaction at 24, 30, 44 and 60 MeV/nucleon (see text).

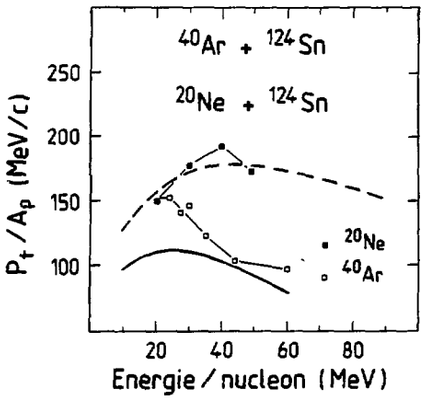

Fig. 3 : Linear momentum transfers per incident nucleon estimated for the $^{20}Ne + ^{124}Sn$ and $^{40}Ar + ^{124}Sn$ reactions. Comparison with pre-equilibrium emission calculations (dashed line) and Fermi jet calculations (solid line).

The linear momentum transfers estimated for the most central collisions are displayed in figure 3. We clearly see a limitation in the linear momentum transfer which occurs at an incident energy around 40 MeV/nucleon for neon induced reactions and 20 MeV/nucleon for argon. The maximum value of the transfer is 190 MeV/c per incident nucleon for neon (the total transfer is 3.8 GeV/c) and 150 MeV/c per incident nucleon for argon (6.0 GeV/c). Estimated momentum transfers per incident nucleon exhibit a clear dependence upon projectile mass : heavier is the projectile, less efficient is the transfer to the target nucleus.

Linear momentum transfers calculated in the framework of a pre-equilibrium emission model and a simple Fermi jet model are plotted in figure 3. In the pre-equilibrium model (Ref. 7), one supposes that all the projectile and target nucleons form a composite system which equilibrates by internal nucleon-nucleon scatterings and emissions into the continuum (two-body process). In the Fermi jet model (Ref. 8), which is based on momentum space considerations, one assumes that nucleons are ejected from the projectile due to the target mean field (one-body process). These two models qualitatively reproduce the observed momentum transfer limitation, indicating that it could be due to fast particle emission. For neon, momentum transfers extracted from experimental data are quantitatively in good agreement with pre-equilibrium calculations, suggesting that nucleon-nucleon collisions contribute strongly to the incident energy dissipation. For argon, the disagreement observed with pre-equilibrium calculations could be correlated with (static) limitations of hot nuclei stability or (dynamic) compression effects.

References :

1) *H. Morgenstern et al., Phys. Rev. Lett. 52 (1984) 1104.*
2) *A. Fahli et al., Phys. Rev. C34 (1986) 161.*
3) *S. Leray, J. Phys. 47 (1986) C4-275.*
4) *A. Lleres, Thèse d'Etat, Université de Grenoble (1988).*
5) *H. Nifenecker et al., Nucl. Phys. A447 (1985) 533c.*
6) *A. Lleres et al., J. Phys. 47 (1986) C4-365.*
7) *M. Blann, Phys. Rev. C31 (1985) 1245.*
8) *C. Grégoire and F. Scheuter, Phys. Lett. 146B (1984) 21.*

PRODUCTION AND DEEXCITATION OF HOT NUCLEI IN 27MeV/u ^{40}Ar + ^{238}U COLLISIONS

D. JACQUET[a], G. PEASLEE[b], J.-M. ALEXANDER[b], B. BORDERIE[a], E. DUEK[b], J. GALIN[c], D. GARDES[a], D. GUERREAU[c], G. GREGOIRE[c], H. FUCHS[d], M. LEFORT[a], M.-F. RIVET[a] and X. TARRAGO[a]

a) Institut de Physique Nucléaire, Orsay, France.b) State University of New York, Stony Brook, USA. c) GANIL, Caen, France. d) Hahn-Meitner Institut, Berlin, Germany.

The aim of the present study was to infer the properties (temperature deformation and spin) of hot nuclei formed in the Ar + U collisions from the characteristics of the charged particles they evaporate. A selection of the hottest nuclei which are formed exploits the recoil properties of the fused nuclei, assuming that the greater the linear momentum transfer from the projectile nucleus to the target nucleus, the larger the energy deposit must be. With a highly fissile target, like uranium, the momentum transfer can be deduced from the folding angle of coincident fision fragments. Three-fold coincidences were thus measured between two fision fragments and light charged particles, the latter being detected at several angles with respect to the fission plane or in a plane containing the beam axis but perpendicular to the fission plane. Such an arrangement was chosen in order to increase the sensitivity to spin effects. Special emphasis has been put on a precise measurement of all light particles, particularly those of low velocity which are stopped in the first silicon member of each telescope. Fission fragments were detected, on one hand, by small areas standard silicon counters and, on the other hand, by position sensitive counters to precisely record the relative emission angle of the fragments.

The usual folding angle picture (fig.1) shows that the events are roughly evenly divided between fission following fusion with about 80% momentum transfer and sequential fission of weakly excited target-like nuclei[1]

Such results were confirmed lately by detecting the evaporated neutrons in coincidence with the fission fragments[2].

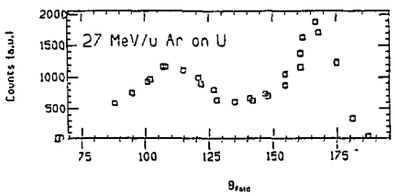

Fig.1. Folding angle distribution of the fission fragments.

Correlated charged particles exhibit quite different behaviors depending on whether they are emitted forward or backward (fig.2). The differential multiplicity of those emitted forward and thus of both equilibrium and pre-equilibrium origin does not show a very strong sensitivity on the folding angle of the fission fragments, thus indicating that a forward hodoscope cannot be used as a very sensitive filter on the violence of the collision. On the contrary the multiplicity of backward emitted particles, all of evaporative origin, is extremely sensitive to the folding angle and thus can be efficiently used to select the most dissipative collisions.

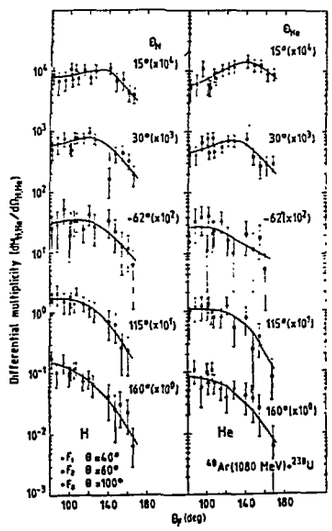

Fig.2. Differential multiplicity for H/He for various angles $\theta_{H/He}$ as a function of the folding angle of the fission fragments.

A kinematical analysis of the charged particles was then performed to infer their origin: either the hot nucleus prior to fission, or the accelerated fission fragments (fig.3). Eighty percent of the α-particles could be unambiguously attributed to emission prior to scission, in good agreement with what has been observed more recently from neutron

A crude estimate of the excitation energies at saturation can be performed by adding up the energies carried away by all the neutral and charged evaporation-like particles. The measured neutron multiplicity needs to be corrected for detector efficiencies. As for the l.c.p.

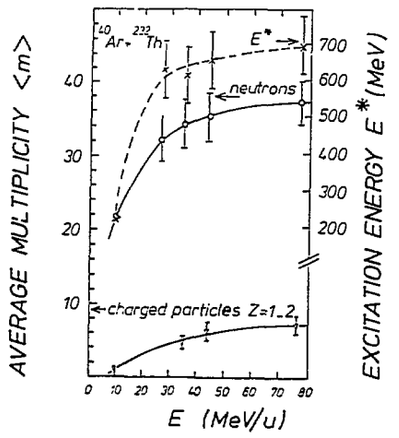

Figure 2: Evolution with bombarding energy of the total number of neutron (0) corrected for detector efficiency and evaporated charged particles (∇) summed over Z=1,2, released from the most dissipative collisions. The excitation energies are given by the right hand scale.Data at 10 MeV/u and 27 MeV/u are published elsewhere[1]

one has to extrapolate from the single recording angle, assuming an isotropic angular distribution in the reference system of the emitter and carrying out the jacobian transformation. Since the solid angle transformation depends only weakly on the recoil velocity, the result is not too sensitive to the integration procedure. The recoil velocity V_R has been taken independent of the bombarding energy as suggested by both the fission data and by the behaviour of the energy spectra of the particles observed backwards.

The result of this evaluation does not show any significant increase in the excitation energy from 35 up to 77 MeV/u within the experimental uncertainty(fig. 2) The value of 650 ± 100 MeV, or $T = 4.5 \pm 0.4$ MeV (with $a \sim \frac{A}{8}$), matches very nicely the temperature extracted from the slope of the α-particle energy spectra recorded backward.

4 Conclusions

Clearly, in these Ar induced reactions one witnesses the effects of the dynamics, but by no means the manifestation of a limiting temperature that the composite nucleus could sustain. Indeed, recent experimental data obtained with Kr beams around 30 MeV bombarding energy clearly show that the linear momentum transfer is roughly twice as large as the one observed with Ar and that the excitation energy, as simply deduced from inclusive neutron multiplicity measurements, exceeds by about 50% the one deduced with the Ar beam.

References

[1] D.X. Jiang et al. accepted for publication in Nucl. Phys. A.
See also J. Galin et al. proceeding of the Symposium on Nuclear Dynamics and Nuclear Disassembly (Dallas April 1989) published in World Scientific.

DYNAMICS OF HEAVY-ION COLLISIONS AT GANIL ENERGIES

C. GREGOIRE*, B. REMAUD+°, F. SEBILLE+, L. VINET*, Y. RAFFRAY+

*GANIL BP 5027, 14021 CAEN Cedex
+LPN - UA 57, Université de Nantes, 44072 NANTES Cedex 03
°IRESTE, La Chantrerie, Université de Nantes, 44087 NANTES Cedex 03

1. Motivation

In the energy range of GANIL facility, pure mean-field theories fail in describing the stopping power of nuclei, which prevents them to cross each other with relatively small perturbations. The Vlasov equation completed with the Uehling-Uhlenbeck collision term provides a semi-classical framework[1] which treats dynamically the balance between the mean-field effects and the two-body collisions. A serie of studies within this theory has been undertaken to analyze the regimes of heavy ion reactions that could be expected in the energy range of 30 Mev/u to 100 Mev/u.

2. Regimes of heavy-ion reactions

At these energies, the Pauli blocking is strong enough to forbid most nucleon-nucleon collisions, the nucleon mean free path (5-10 fm) is still of the order of the nucleus diameter. However, the collision rates are sufficient to destroy the nuclear transparency predicted by pure mean field theories. Below 30/40 Mev/u in symmetric reactions (and higher for asymmetric ones), the Landau-Vlasov approach describes reaction regimes inherited from lower energies : fusion at central impact parameters and formation of quasi-projectile/quasi-target fragments for peripheral collisions. However, these processes are incomplete since preequilibrium emissions (see fig. 1) - in increasing multiplicities with increasing energies - indicate that some nucleons do not participate to the equilibration process. The preequilibrium processes last less than 60 fm/c (2 10^{-22} sec) and are progressively replaced by isotopic emissions; apparent thermalizations of the initial kinetic energies may then occur in time ranges of few 10^{-22} sec, for central collisions.

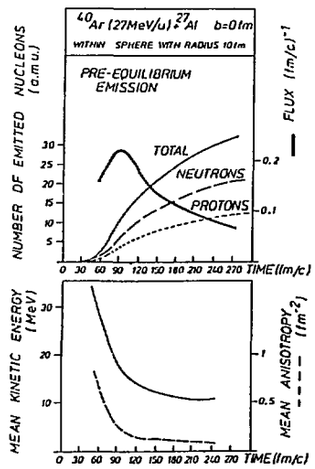

Fig. 1:
Characteristics of nucleon emission in the entrance channel of H-I reactions.

In more peripheral collisions, a participant zone is formed in the region of the overlapping densities ; this participant zone evaporates quickly and two fragments emerge with reduced relative velocities. Although the correlation between the masses of quasi-projectile and quasi-target are close to a pure geometrical abrasion , the process is similar to deep inelastic reactions if one considers the strong deviation of the fragments trajectories induced by the mean-field. When the initial kinetic energies increase, peripheral collisions come closer to abrasion limit. However a relatively quick transition occurs in central collisions where the disassembly of the fused system is observed at 40/50 Mev/u in symmetric systems.

3. Excitation mechanisms

As a transport equation, the Landau-Vlasov

equation can go beyond the description of bulk observables as linear momenta, angular distributions, etc...; it allows the microscopic and local analysis[2] of the various mechanisms for the dispersion of the coherent initial kinetic energy.

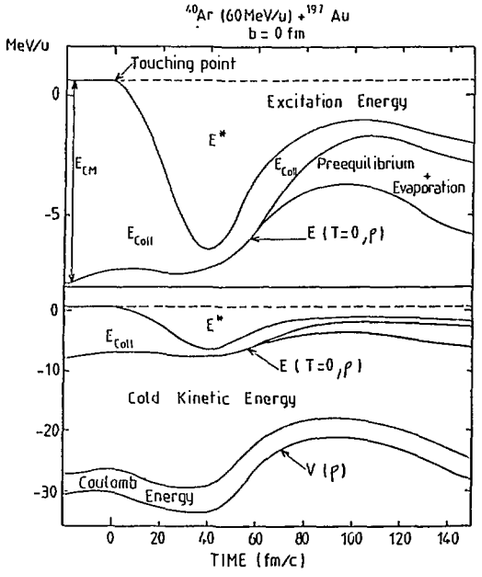

Fig. 2

Analysis of the contributions to the total energy. Top figure enlarges the upper part of bottom figure.

The lower part of fig.2 shows that the initial kinetic energy (E_{coll} at t = 0) is a small part of the total kinetic energy; due to the mutual stopping power of the nuclei, this collective energy could be progressively transformed in excitation energy. However after a compression phase at t = 40 fm/c, the system expands very quickly, which very efficiently removes excitation energy, while preequilibrium nucleons and first evaporative ones start leaving the system.

Such calculations emphasize the role of the collective resonance (mainly monopole) in the limitation of the excitation energy immediately available to the system; it provides a clue for the interpretation of the experimentally observed limitation of "nuclear temperature".

4. Conclusions and outlooks

The Landau-Vlasov approach provides a natural link between the mean-field models (as TDHF) at low-energy and pure cascade models which apply at very high energy. It meets success in the description of bulk one-body observables ; however, it presents limitations both on theoretical and technical sides.

As a mainly one-body approach, it is not fitted to systems with large fluctuations. In that sense, it is an entrance channel model which needs to be completed to describe exit channels, particularly when fragments are formed.

On the technical side, its numerical solution with Monte-Carlo methods is very demanding to to-day computers. Studies of phenomenas like induced fission, competition between fission and particle evaporation, excitation energy share between nuclear fragments, etc..., seem at the limit of actual possibilities for systems with more than 100 nucleons. However the above list constitutes the open field of studies for the Landau-Vlasov equation in the near future.

5. Main references

1) C. Gregoire et al., Nucl. Phys. A465 (1987) 317.

2) B. Remaud et al., Nucl. Phys. A488(1988) 423c.

A NEW THEORY OF COLLISIONS

B. G. Giraud
Service de Physique Théorique, IRF, CEA, CEN-Saclay, F-1191-Gif-sur-Yvette
and
M. A. Nagarajan
Daresbury Laboratory, Warrington, WA4-4AD, UK

Abstract: We introduce a time-independent generalization of the static Hartree-Fock equations, which become inhomogeneous.

There is a large domain of heavy ion physics where the only degrees of freedom to be considered are just nucleons, while pions, exchange currents, nucleon isobars, etc. are neglected. This purely nucleonic domain, however, subdivides into a "high energy" domain (HEND), where all nucleons are active and a "low energy" domain (LEND), where the dynamics reduces to fewer degrees, usually of a collective nature: deformations, rotation velocities, etc. From DWBA to hydrodynamics, many ad hoc theories provide elegant, but restricted descriptions of some aspect of these domains.

It would be desirable, however, to use a fully quantal and microscopic theory, as a reasonable approximation of the Schroedinger equation, in order to interpolate beween all these domains. As a matter of fact, the GANIL energy range, 10-100 MeV/nucleon, demands such a theory valid for transitions between LEND and HEND.

For several years, there was a hope that TDHF would provide the answer. It turned out, unfortunately, that TDHF could not account for large fluctuations in the observables of heavy ion physics. The reasons for this failure are unclear: maybe the mean field approximation is not justified, or maybe the boundary conditions of TDHF are not correct. We have now a new microscopic theory, which takes care of the boundary conditions.

Our idea is very simple: instead of approximating the time-dependent Schroedinger equation (TDSE) by a mean-field approximation (MFA) such as TDHF, let us approximate the time-independent Schroedinger equation (TISE) by another MFA. This is not just an academic trick, for the Fourier tranform which connects TDSE to TISE does not commute with a MFA. In other words, there is no Fourier transform equivalence between TDHF and a MFA performed on TISE.

We describe the initial channel by a Slater determinant $|\chi\rangle$, with boosted orbitals, like TDHF. What is new is that we describe also the final channel by an explicit, time-independent determinant $\langle\chi'|$, while in TDHF the final channel was a black box, often time dependent. We know the prior and post potentials V and V', respectively, and now calculate the (multistep) T-matrix element $D=\langle\chi'|V'(E-H)^{-1}V|\chi\rangle$, via a MFA.

The details of the formalism have been published[1-2]. The amplitude D is calculated from an EXACT Breit-Wigner formalism, $D=\Gamma'\Gamma/(E-E')$, with transitions via two "doorway" states Φ', Φ, and $\Gamma=\langle\Phi'|V|\chi\rangle$, $\Gamma'=\langle\chi'|V'|\Phi\rangle$, $E'=\langle\Phi'|H|\Phi\rangle$. The MFA consists in taking Slater determinants for Φ and Φ'.

A variational principle[3] defines the orbitals φ_i, φ'_i of Φ, Φ', respectively, via generalizations of the static Hartree-Fock equations,

$$(\eta_i - h_i)\,|\varphi_i\rangle = |\sigma_i\rangle, \quad \langle\sigma'_i| = \langle\varphi'_i|\,(\eta_i - h_i), \tag{1}$$

where the source terms σ_i, σ'_i are due to the initial and final channels[1,2]. Like in static Hartree-Fock, one finds mean-field Hamiltonians h_i and self energies η_i.

This theory has been successfully tested on exactly soluble models for

two-body problems[4,5] and three-body problems[6]. The cases of four[7,8,9] and five[10] bodies are also investigated, with very positive results. At present we are investigating a realistic proton-triton collision, with a Gaussian two-body force. It turns out that the mean-field equations, Eq.(1), are technically more difficult to solve than static Hartree-Fock equations, but still manageable. We show on the Figure the momentum density plots of several "transition orbitals" φ_i, φ'_i, taken out of a whole atlas generated by our computer.

We have thus reached a first, and important conclusion: this new theory of collisions, based on non-linear equations with yet poorly known properties, does have solutions. Moreover, as shown by the Figure, the "transition orbitals" seem to be smooth, like extensions of shell-model states. We are able to calculate quantal transition amplitudes.

Besides comparison of our transition amplitudes with experimental data, our atlas of orbitals raises, and probably partially answers, several interesting questions. Among them, is there a systematic zoology of such orbitals, similar to the classification provided by the static shell model? What are the criteria for the identification of a modification of reaction mechanisms? Last but not least, the self-consistent mean-field potentials contained in the single particle hamiltonians h_i define a new optical theory, whose interpretation and zoology is just beginning.

References:
1)B.Giraud, M.Nagarajan and I.Thompson, Ann.Phys.152,475(1984)
2)B.Giraud, M.Nagarajan and C.Noble, Phys.Rev.A34,1034 (1986)
3)B.Giraud and M.Nagarajan, J.Phys.G4,1739(1978)
4)M.Nagarajan and B.Giraud, Phys.Rev.C27,232(1983)
5)B.Giraud, Physical9D,112 (1986)
6)Y.Abe and B.Giraud, Nucl.Phys.A440,311(1985)
7)B.Giraud and M.Nagarajan, Phys.Rev.C28,1918(1983)
8)B.Giraud, S.Kessal and A.Weiguny, J.Math.Phys.29,2084(1988)
9)J.Lemm and A. Weiguny, private communication
10)B.Giraud, S.Kessal and L.C.Liu, Phys.Rev.C35,1844 (1987)

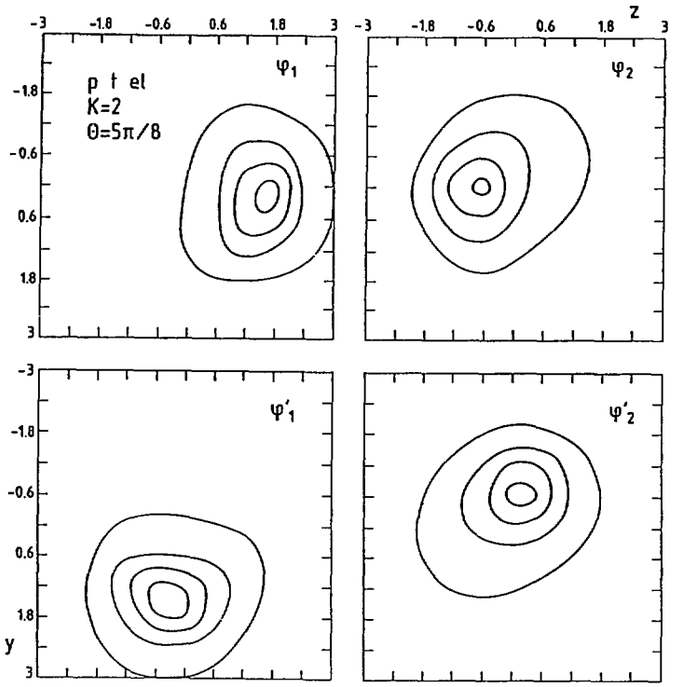

MEDIUM CORRECTION OF TRANSPORT EQUATION

J. Cugnon*, P. Grangé** and A. Lejeune*

*Université de Liège, Physique Nucléaire Théorique, Institut de Physique au Sart Tilman, B.5, B-4000 LIEGE 1, Belgium

**CRN, B.P. 20, CRO, F-67037 STRASBOURG Cédex, France

A large consensus has emerged on the fact that a transport equation suitable to describe heavy ion collisions at intermediate energy has a Landau-Vlassov (LV) form :

$$\left(\frac{\partial}{\partial t} + \frac{\vec{p}}{m}.\vec{\nabla} - (\vec{\nabla}U).\vec{\nabla}_{\vec{p}} - (\vec{\nabla}_{\vec{p}}U).\vec{\nabla}\right) f(\vec{r},\vec{p},t)$$

$$= \int \frac{d^3p_2}{(2\pi)^3}\frac{d^3p_3}{(2\pi)^3}\frac{d^3p_4}{(2\pi)^3}\,\delta^3(\vec{p}+\vec{p}_2-\vec{p}_3-\vec{p}_4)\delta(e(p)+e(p_2)-e(p_3)-e(p_4))$$

$$\{\omega(pp_2 \leftarrow p_3p_4)f_3f_4(1-f)(1-f_2)-\omega(pp_2 \rightarrow p_3p_4)ff_2(1-f_3)(1-f_4)\}. \qquad (1)$$

In this equation, $f(\vec{r},\vec{p},t)$ can be considered as the usual Wigner transform of the one-body density, U is the average single-particle field, e(p) is the single-particle energy, ω is the transition probability and f_1 stands symbolically for $f(\vec{r},\vec{p}_1,t)$. The situation is still confuse on knowing whether equation (1) retains the right physics. For instance, it does not retain retardation effects in the collision term[1], which could be important[2]. Moreover, even if eq. (1) is considered as a good starting point, the question arises to know what are the "best" input data (U,e,ω) for this equation. The point is that the LV equation can be obtained as a truncation of the density matrices (BBGKY) hierarchy. In the simplest case (the weak coupling limit), the LV equation is obtained in second order in the interacting potential v [1]. Of course, in the nuclear case, the relevant physics cannot be described at this order, unless resummation and medium renormalization of the successive interactions are introduced. This is shown in refs. [3,4], which establish the connection with the Brueckner theory of nuclear matter, where the same concepts are used. It is then natural to identify the input data with the corresponding quantities in Brueckner theory (in the local density approximation)

$$U = U_B(\rho,T,p) \qquad (2)$$

$$e(p) = \frac{\hbar^2k^2}{2m} + U_B(\rho,T,p) \qquad (3)$$

$$\omega(pp_2 \rightarrow p_3p_4) = \langle\vec{p}\vec{p}_2|g(\rho,T)|\vec{p}_3\vec{p}_4\rangle \quad , \qquad (4)$$

where $g(\rho,T)$ is the Brueckner g-matrix at density ρ and temperature T, U_B is the single-particle field in the Brueckner-Hartree-Fock approximation. In ref. [5], we give this quantity for some range of density and temperature. The input e and ω can be introduced in a very tractable manner. For e(p), one can replace them in eq. (1) by kinetic energies, provided the collision term is multiplied by the effective mass m*, which is given in refs. [5,6]. For the medium correction of the transition matrix, we presented our results in the following form

$$\omega(\vec{p}\vec{p}_2 \rightarrow \vec{p}_3\vec{p}_4) \approx \alpha(\rho)\,\langle\vec{p}\vec{p}_2|T|\vec{p}_3\vec{p}_4\rangle \quad , \qquad (5)$$

where T is the free transition matrix. The value of the coefficient α is given in fig. 1, for various temperatures and densities. Convenient parametrizations can be found in ref. [6]. Further refinements including the angular distribution

for scattering inside nuclear medium are in progress.

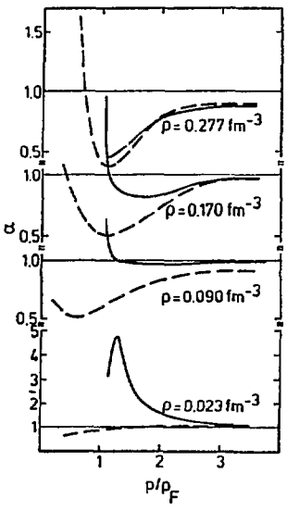

Fig. 1. The ratio α eq. (5), as a function of the relative momentum p/p_F and for various densities. Full curve : T = 0 MeV ; dashed curves : T = 10 MeV.

1) L.P. Kadanoff and G. Baym, Quantum Statistical Mechanism (Benjamin, New York, 1962).
2) P. Danielewicz, Ann.Phys. 152 (1984) 305.
3) R.F. Snider, J.Chem.Phys. 32 (1960) 1051.
4) W. Botermans and R. Malfliet, Phys.Lett. 171B (1986) 22.
5) A. Lejeune, P. Grangé, M. Martzolff and J. Cugnon, Nucl.Phys. A453 (1986) 189.
6) J. Cugnon, A. Lejeune and P. Grangé, Phys.Rev. C35 (1987) 861.

NON LOCALITY EFFECTS IN NUCLEAR DYNAMICS

F. Sebille, G. Royer, C. Gregoire*, B. Remaud**, P. Schuck***, V. De la Mota, Y. Raffray.
Laboratoire de Physique Nucléaire. UA 57, 44072 NANTES Cedex 03 France
* GANIL BP 5027 F-14021 CAEN Cedex France
** IRESTE route de la Chantrerie F-44003 NANTES Cedex France
*** ISN, F-38026, GRENOBLE Cedex, France

1. Motivation

Current theoretical investigations on heavy ion collisions in the GANIL energy range, widely use kinetic approaches based on a self-consistent microscopic framework [1]. Generally, in these semiclassical descriptions of nuclear dynamics, the effective nuclear interaction is taken as a simplified Skyrme force, local and density dependent. Their main drawback is to neglect the momentum dependence of the nuclear force and the resulting effective mass, important effects which stem from the Brueckner theory. Then works [2] have been undertaken in order to study signatures of non locality effects on sensitive observables in phenomena ranging from induced fission to collective transverse matter flow observed in heavy ions reactions near 100 MeV per nucleon

2. Description of non locality effects.

Description of non locality effects and nuclear dynamics have been made starting from a semi classical approximation of the time dependent Hartree Fock equation (the Vlasov equation), where the residual interactions are introduced with the Uehling-Uhlenbeck term, taking into account in medium effects. Even if the final aim is to derive the mean field and collision terms from a bare interaction, a first attempt to cure the drawbacks of local forces consist in improving the functional from of the effective interaction. The effective interaction proposed by Gogny allows to reach this goal, this force relies upon finite range exchange terms and provides a successful description of many nuclear properties in the phase space representation the Gogny force generates a momentum dependence of the mean field through its finite range exchange terms In fig 1 the energy dependence of the potential depth gives some clear insights in the physical mechanisms introduced by the non locality. A salient feature is the momentum dependence of the attractive potential which weakens with increasing momenta, leading to a less attractive global potential. Another important consequence is the influence of the momentum dependence on the nucleon motion inside the nucleus, the resulting effective mass implies a faster motion of the nucleons inside the nuclear matter than in free space.

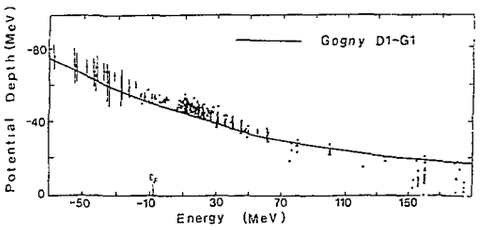

Fig. 1. Real nuclear optical potential for the Gogny D1-G1 interaction, compared with experimental results.

3. Signatures on collective observables.

The field of application of our model implemented with the Gogny force is essentially the low and medium energy range of heavy ion collisions. Nevertheless, as underlined by several recent works, the Gogny interaction contains highly interesting properties which motivate to explore the energy range around 100-400 Mev per nucleon. In addition, this is supported by promising experimental and theoretical works which aim at extracting informations on the Equation of State (E.O.S), especially from the experimental evidence of a nuclear matter collective flow near 100 MeV/u

Thus, the non locality effects on nuclear dynamics can be illustrated with an observable called flow and defined within the transverse momentum analysis of the

sideward collective matter flow. In Fig. 2. results are displayed for three effective forces, namely, the finite range Gogny force, the soft and stiff local Zamick forces. Their incompressibility modulus are respectively 228 MeV, 200 MeV and 380 MeV. This figure reveals that the momentum dependence of the Gogny force is able to reproduce flows only obtained with a high incompressibility modulus when local forces are considered.

This can be explained by the momentum dependence of the mean field. In the overlap region of two colliding nuclei. a nucleon feels not only the field of his initial nucleus. but also the one due to the other nucleus whose nucleons are moving fast with respect to it Considering Fig. 1, we observe that high relative kinetic energies weaken considerably the field experienced by the incoming nucleon It provides a more repulsive character to the momentum dependent forces compared to the local ones with the same compressibility

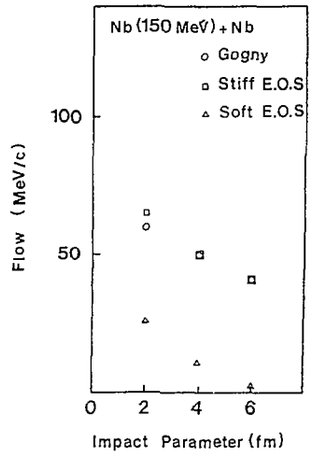

Fig. 2 Dependence of the flow on the impact parameter for various nuclear interactions with the Nb (150 MeV/nucleon) - Nb system.

4. Conclusions.

We have introduced for the first time the effective finite range interaction of Gogny in the semi-classical description of heavy ion reactions based on the Landau Vlasov equation. This has been worked out in order to take properly into account the non local character of the effective nuclear mean-field and to track down the non locality effects on observables at medium energies Studies of phenomena like induced fission competition between fission and evaporation collective matter flow ..... are actually concerned. The previously mentionned results related to the transverse matter flow near 100 MeV per nucleon. underlines that the momentum dependence of the nuclear force have to be properly described if one wants to extract informations on the Nuclear Equation of State. either at high energies or at medium energies

[1] C. Gregoire et al., Nucl. Phys. A465 (1987) 317
B. Remaud et al., Nucl. Phys A488 (1988) 423C.
[2] F. Sébille et al., XXVII International winter meeting on nuclear physics (Bormio) 1989, and to be published.

THE PSEUDO PARTICLE METHOD FOR THE SOLUTION OF THE LANDAU-VLASOV EQUATION

P. SCHUCK, Institut des Sciences Nucleaires, 53 Avenue des Martyrs, 38026 Grenoble-Cédex, France

GREGOIRE C, VINET L.[a], PI M[b], REMAUD M., SEBILLE F[c], SCHUCK P., SURAUD E.[d]

a) GANIL - Caen
b) Dept. de Estructura i constituentes de la Materia - Barcelona
c) LSN - Nantes
d) ISN - Grenoble

The solution of the Landau-Vlasov alias Vlasov-Uehling-Uhlenbeck (LVUU) equation represents a formidable numerical challenge. It is a non linear integro-differential equation in seven (!) variables (six phase space and one time variable) and it is clear that such an equation can not be solved "exactly". Nevertheless the pseudoparticle method which we want to explain here has proven to be a very powerful tool and it has turned out that certain average quantities like e.g. the "nuclear flow" are well converged as a function of a manageable number of pseudoparticles per nucleon.

In order to keep the discussion as transparent as possible we will neglect the Pauli principle which is not essential for the explanation of the pseudoparticle method and the assessment of its validity. The two basic equations are the (coupled) quantal equation of motion for the one body density matrix $\rho_{11'}$ and the correlated part of the two body density matrix $g^{(2)}{}_{12\ 1'2'}$:

$$i\hbar\,\dot{\rho}_{11'}(t) - [h^{H.F.},\rho]_{11'} = \frac{1}{2}\ \Sigma\ (\bar{v}_{1234}\ g^{(2)}{}_{341'2} - g^{(2)}{}_{1234}\ \bar{v}_{341'2}) \qquad (1)$$

$$i\hbar\ \dot{g}^{(2)}{}_{12\ 1'2'} - [h^{HF}(1) + h^{HF}(2),\ g^{(2)}]_{12\ 1'2'} = \Sigma\ (\bar{v}_{1234}\ \rho_{31'}\ \rho_{41'} - \rho_{13}\ \rho_{24}\ \bar{v}_{34\ 1'2'}) \quad (2)$$

where $h^{H.F.}$ is the meanfield hamiltonian and $\bar{v}$.... the antisymmetrized matrix element of the (effective) nucleon-nucleon interaction. It is evident from eq. (2) that the rhs has been approximated by its first order Born term what makes (1,2) a closed system of equations.

In order to arrive from (1,2) at the classical Boltzmann equation, one approximates the r h s of (1) by its classical limit, i.e. one transforms it into phase space and replaces the commutator by the classical Poisson bracket. The r h s of eq. (1) as well as of eq. (2) are evaluated in local density approximation, that is one calculates everything like in nuclear matter and gives ρ and $g^{(2)}$ a parametrical dependence on the position **R**. This then leads to the Boltzmann equation in replacing v^2 by the differential cross section $d\sigma/dE$. However even in nuclear matter the r h s of (1) and eq. (2) are still <u>quantal</u> expressions. In order to arrive at the pseudoparticle method we have to recognize that the rh sides of (1,2) have a commutator structure. These commutators then have to be replaced by their corresponding classical Poisson brackets. Solving then (2) for $g^{(2)}$ in terms of ρ and inserting into (1) yields a completely classical equation for ρ alone. With the pseudoparticle ansatz

$$f(\mathbf{R}, \mathbf{p}, t) = \frac{1}{n} \sum_{i=1}^{n\cdot A} \delta(\mathbf{R} - \mathbf{R}_c(t))\ \delta(\mathbf{p} - \mathbf{p}_{ic}(t))$$

where n is the number of pseudoparticles per nucleon and A the nucleon number, we obtain the following set of classical equations for $\mathbf{R}_{ic}(t)$ and $\mathbf{p}_{ic}(t)$ (in practice we use Gaussians instead of δ-functions in (3) but this should not be the point here).

$$\mathbf{R}_{ic} = \frac{\mathbf{p}_{ic}}{m} + \frac{\partial V^{HF}}{\partial \mathbf{p}_{ic}} \tag{4}$$

$$\mathbf{p}_{ic} = -\frac{\partial V^{HF}}{\partial \mathbf{R}_{ic}} - \frac{1}{n} \sum_{k=1}^{n\cdot A} \frac{\partial v(\mathbf{R}_{ic} - \mathbf{R}_{kc})}{\partial \mathbf{R}_{ic}} \tag{5}$$

However, in order to arrive at equation (5) an additional approximation has been applied, i.e. when there is a collision it should occur as if the meanfield were absent. This condition can only be fullfilled if the meanfield varies little within the range of the two body force. For a step function like two body potential, the force would be δ-function like and then this condition would be fullfilled exactly. In fact for consistency eq. (5) should also be treated in this spirit. Indeed if the scattering process is almost instantaneous, all what counts is the deflection angle or equivalently the differential cross section. One therefore follows all pseudoparticles pairwise in time and whenever a pair at closest approach is within the nucleon-nucleon cross section reduced by a factor of n we redistribute the momenta of the pair according to the differential cross section. As a matter of fact only s-wave scattering has been considered so far and thus the relative momenta of the pairs are redistributed with equal probability whereas total momentum and individual energies are conserved in each scattering event.Under the condition that the differential cross section is isotropic (this condition could be released) and for the case that results are converged with the number of pseudoparticles this should then come quite close to an exact solution of the Boltzmann equation (see below).

So far we have not spoken about the Pauli principle which has to be incorporated when dealing with fermions. This, however, is easily done in evaluating the phase space occupancies $f(\mathbf{R}, \mathbf{p}_1)$ and $f(\mathbf{R}, \mathbf{p}_2)$ of the two scattered pseudo particles ($\mathbf{R}$ is the localisation of the scattering event) and in multiplying the cross sections with $\bar{f}(\mathbf{R}, \mathbf{p}_1) \cdot \bar{f}(\mathbf{R}, \mathbf{p}_2)$ where $\bar{f} = 1 - f$. Only if the distance of closest approach is within this reduced cross section, the scattering event is effective.

Fortunately certain quantities like e.g. the nuclear flow converge relatively fast with the number of pseudoparticles. With n = 30 the flow of Nb + Nb at b = 4 fm is converged for E/A = 150 and 250 MeV. Also the relaxation of the momentum tensor of two interpenetrating pieces of nuclear mater compares well with n = 30 with an "exact" numerical integration of the LVUU equation. For the Boltzmann equation exist certain analytically solvable models. Again the exact solution is well reproduced in the case studied with the pseudoparticle method.

In conclusion the pseudoparticle method seems to work very well at least for inclusive quantities. The main open question remains in the calculation of the effective medium modified cross section entering the collision integral. In principle this should be calculated self consistently as the reaction between the heavy ion goes on. This task goes beyond our present facilities and we have to rely on G-matrices in local density approximation which are calculated at equilibrium. This implies uncertainties coming from the initial phase of the reaction where non equilibirum processes are important.

FORMATION AND DEEXCITATION OF HOT MEDIUM MASS NUCLEI AROUND 30 A.MeV

B. BORDERIE, C.CABOT, D.GARDES, H.GAUVIN, F.HANAPPE*, J.PETER**, M.F.RIVET

Institut de Physique Nucléaire, F-91406 Orsay
*FNRS and U.L. Bruxelles, B-1050 Bruxelles
**G.A.N.I.L., F 14021 Caen

1. Motivation

When increasing the bombarding energy, *incomplete fusion become* more and more domimant with rather light projectiles (A < 20). The present study was a first step to explore the mechanisms involved in central collisions with Ar projectiles and medium mass targets (Ar and Ho).

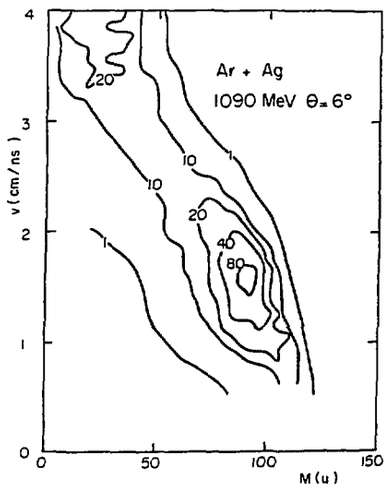

Fig. 1 : Typical mass-velocity diagram.

Inclusive (heavy residues - Fig. 1) [1] and exclusive (fission fragments) measurements were performed to carefully study the competition between fission and evaporation during the deexcitation of fused *nuclei*.

2. Incomplete fusion characteristics

From direct (heavy residues) or deduced recoil velocities from angular correlations (fission fragments), average linear momenta transferred to fusion-like nuclei were derived [2]. The measured ΔP/P *values around* 70 % *indicate* a strong persistence of collective effects which was not so evident in view of the large energy deposit ; such collisions account for about 15 % of the reaction cross-section [2]. Moreover, the characteristics of invariant energy spectra (width and variation of their maximum versus θ) and angular distributions (Fig. 2) of heavy residues were found in complete agreement with what is expected for *evaporation residues*.

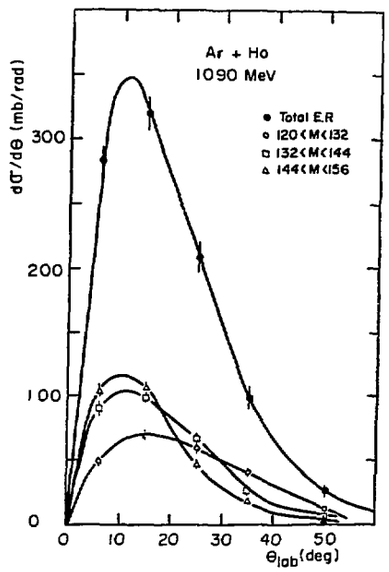

Fig. 2 : Angular distributions of evaporation residues.

3. Deexcitation

Competition fission-evaporation

Evaporation residue and fission characteristics (final masses, out-of-plane distributions) indicate that one can have some confidence in the simple reaction scheme used (part of the projectile which fuses with the target) to derive excitation energies. The most probable

excitation energy of fusion-like nuclei is about 500-600 MeV for both systems and the distribution extends up to more than 700 MeV [2]. This indicates that nuclei have been formed in rather extreme conditions, close to the limit of instability (static calculation).

The evolution of the ratio $\sigma_{ER}/(\sigma_{ER} + \sigma_{FIS})$ with incident energy is displayed in Fig. 3. For both systems, a change of

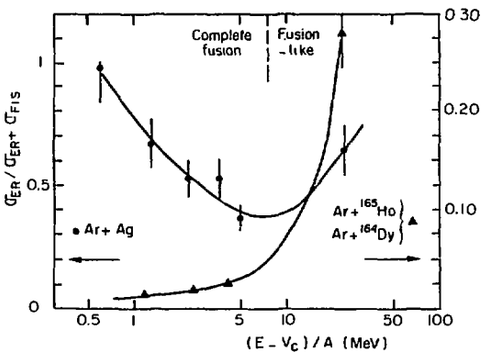

Fig. 3 : Evolution of residue over fusion cross-sections with incident energy.

the slope is observed when the bombarding energy reaches 8-9 MeV per nucleon, indicating inhibition of the fission path in favor of the evaporation path. Two reasons can be found to explain this evolution of the competition between fission and evaporation. Firstly, the onset of incomplete fusion occurs in this energy region, lowering masses and atomic numbers of fusion-like nuclei and therefore their fission probability. The second reason can be found in the deexcitation process itself. We know that prefission evaporation occurs when temperatures larger than about 3 MeV are reached. This evaporation is now well understood, at least qualitatively, in terms of particle emission time and fission time.

4. Conclusions

Through measurements of nuclei formed in 27 MeV/nucleon Ar induced reactions in Ag and Ho, it was shown that fusion-like reactions still occur at this intermediate energy ; they account for 15 % of the reaction cross-section. Fusion-like nuclei have been characterized through the properties of their cold remnants, either evaporation residues or fission fragments. All these properties show that fusion-like nuclei were formed with a very high excitation energy, close to the limits predicted by different theoretical models. Cross-section fractionation between ER and fission shows that fission barriers still play an important role, even at high excitation energy, due to the very short particle emission time as compared to fission time.

[1] B.Borderie et al, Z. Phys. A316 (1984) 243.
M.F.Rivet et al, Proc. of the Tsukuba Int. Symposium on Heavy Ion Fusion Reactions, Tsukuba (Japan), p. 311 World Scientific (1985).
[2] B.Borderie et al, Proc. XXIII Int. Winter Meeting on Nuclear Physics, Bormio (Italy), p. 445 (1985).
M.F.Rivet et al, Phys. Rev. C34 (1986) 1282.
M.F.Rivet et al, HICOFED, Caen (France), Contributed papers p. 39 (1986).

PRODUCTION AND DECAY OF HIGHLY EXCITED NUCLEI BETWEEN 26 AND 45 MeV/NUCLEON

F. Auger[a], B. Berthier[a], A. Cunsolo[b], B. Faure[a], A. Foti[b], W. Mittig[c], J.M. Pascaud[d], E. Plagnol[e], J. Québert[d], and J.P. Wieleczko[a]

[a]DPhN/BE, CEN Saclay, 91191 Gif-sur-Yvette Cedex, France. [b]Dipartimento di Fisica and Istituto Nazionale di Fisica Nucleare, I-95129 Catania, Italy. [c]GANIL, 14021 Caen Cedex, France. [d]CEN Le Haut Vigneau, 33170 Gradignan, France. [e]IPN Orsay, 91406 Orsay Cedex, France.

Motivations

Two fundamental questions of Nuclear Physics are : what is the limiting excitation energy of the nuclei ? How do the deexcitation modes of these nuclei evolve with increasing excitation energy ?

The Ganil facility allowed to investigate those questions. In 1983, it was well known that all central heavy ions collisions lead to the fusion of the whole system for beam energies below 10 MeV/nucleon. It was also known that above this value the incomplete fusion mechanism (composite system doesn't contain any more all the mass of the system) plays an increasing role as the beam energy increases[1]. However, one expected to produce hotter and hotter nuclei as the available energy would increase. Concerning the underlying mechanism, experiments using light beams around 10 MeV/nucleon had shown that the nucleons of the projectile which don't fuse with the target act as spectators of the reaction (massive transfer)[2].

Experimental choices

We have chosen to study A ∿100 nuclei who mainly deexcite by light particles evaporation. The mean recoil velocity of the residues (cold nuclei at the end of the deexcitation chain) gives the source velocity. Mass and excitation energy of the source are generally deduced from the recoil velocity in the framework of the massive transfer.

Statistical model predicts that the probability for complex fragments emission (Li..., C, O, ...) increases with the excitation energy. These fragments should thus sign the hottest nuclei produced in the reactions. If the projectile is heavier than the target, the inclusive spectra of the complex fragments present two branches (forward and backward emission with respect to the velocity of the source) whose positions provide both the source velocity and the emission velocity in the reference frame of the source.

According to these points, and in order to study the influence of the asymmetry of the system and of the incident energy on the incomplete fusion mechanism, we have bombarded ^{12}C, ^{27}Al, ^{48}Ti targets with a ^{84}Kr beam of 26, 34 and 45 MeV/nucleon.

Inclusive velocity spectra, atomic number and mass of nuclei from A = 10 to A = 90 have been measured with time of flight telescopes consisting of three solid state detectors. Mass and velocity correlations were also measured between a telescope kept at 3° on one side of the beam and another one which was moved on the other side of the beam. Integrated cross sections were obtained with a good precision (∿10 %) for most of the fragment.

Highly excited nuclei production

Kinematical simulations of the spectra show that for a given system :

- the major part of the complex fragments cross section (A < 40) can be attributed to the asymmetric fission of the same equilibrated source S. The mass and excitation energy of the source are consistent with the massive transfer hypothesis.
- A > 60 fragments result both from central and peripheral collisions. Residues from central collisions come from the same mean source S'. The mass distributions of these residues are consistent with the massive transfer hypothesis except for Kr + Ti at 34 MeV/nucleon.
- fusion becomes more incomplete as the incident energy increases.

In addition the simulations show that for a given incident energy the fusion is the more incomplete as the colliding system becomes more symmetrical.

The excitation energies per nucleon ε^* of the sources S and S' are plotted on figure 1 as a function of the available energy per nucleon $\varepsilon_{av} = E_{cm}/(A_{proj.} + A_{target})$.

One observes that :

- although fusion is more and more incomplete, ε^* increases regularly with ε_{av}.
- the source associated with the complex fragments is always hotter than the one associated with residues. As expected complex fragments are a good tool to probe the hottest nuclei.
- for 8 MeV/nucleon available energy the largest excitation energy is 5.8 MeV/nucleon. This value agrees with the theoretical limit of ref. 3.

Beyond ε_{av} = 8 MeV/nucleon we encountered difficulties to analyse the data (Kr + Al and Ti at 45 MeV/nucleon). This may indicate the opening of another reaction channel such as prompt or sequential multifragmentation. More exclusive experiments are needed to precise this point.

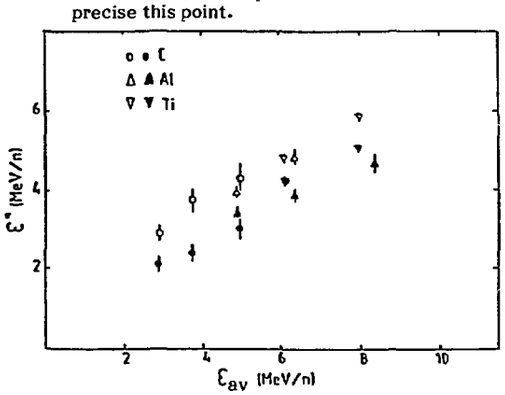

Fig. 1 : Evolution of the excitation energy of the source of the complex fragments (open symbols) and of the source of the residues (full symbols) with the available energy per nucleon.

Deexcitation

Mass distributions corresponding to the deexcitation of the source of complex fragments are presented on figure 2. A qualitative analysis of the distributions in terms of statistical and sequential deexcitation of a nucleus gives excitation energies compatible with those obtained with the kinematical analysis except for the hottest nucleus (Kr + Ti 34 MeV/nucleon). In this case the statistical analysis attributes about 4.5 MeV/nucleon to the source instead of 5.8 MeV/nucleon. This difference can be taken as the error in the determination of the excitation energy, and we may write $\varepsilon^* = (5. \pm 0.8)$ MeV/nucleon.

A quantitative analysis of the mass distributions would require sophisticated entrance channel model for the incomplete fusion mechanism.

One observes that the residues bump ($A \sim 60$-80) progressively flattens as the excitation energy increases. Finally the complex fragments cross section dominates the mass distribution.

Conclusion

Nuclei of $A \sim 100$ can be heated up to $(5. \pm 0.8)$ MeV/nucleon by an incomplete fusion mechanism with 8 MeV/nucleon available energy. Beyond this value, the experimental results can no longer be analysed with the simple models used, and one needs more exclusive experiments to draw conclusions.

The underlying entrance channel mechanism is not really understood although the massive transfer hypothesis agrees reasonably well with most of the data.

Experimental yields are consistent with a statistical and sequential decay of the composite system after incomplete fusion. The discrepancies can be due both to the uncertainties of the entrance channel model and of the statistical model in this energy domain.

We have shown for the first time that at high excitation energy the emission of complex fragments becomes and important or even dominating process.

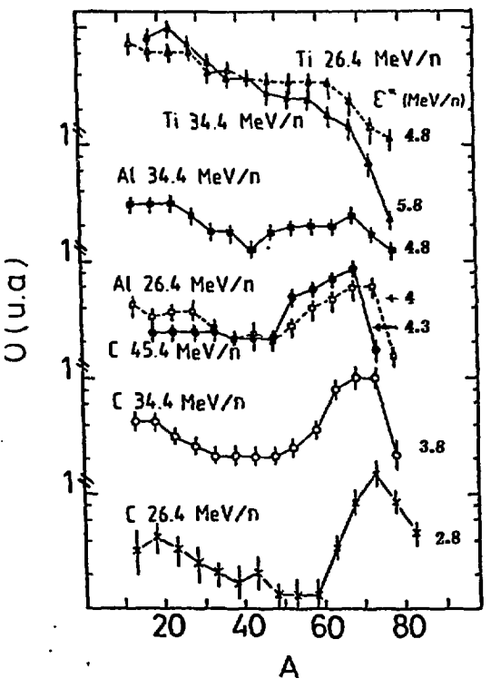

Fig. 2 : Final mass distributions for the deexcitation of the source of complex fragments. Normalization is arbitrary. We have indicated the excitation energies obtained with the kinematical analysis (figure 1)

References

1) V.E. Viola, B. B. Back, K.L. Wolf, T.C. Awes, C.K. Gelbke and H. Breuer, Phys. Rev. **C26** (1982) 178.
2) J. Wilczynski, K. Siwek-Wilczynska, J. Van Driel, S. Gonggrijp, D.C.J.M. Hageman, R.V.F. Janssens, J. Lukasiak, R.H. Siemssen and S.Y. Van der Werf, Nucl. Phys. **A373** (1982) 109.
3) S. Levit and P. Bonche, Nucl. Phys. **A437** (1985) 426.

Publications

- Physics Letters **154B** (1985) 259.
- XXIII International Winter Meeting on Nuclear Physics (Bormio, Italy - January 1985)
- J.M. Pascaud - Thesis - Bordeaux (1985)
- Physical Review **C35** (1987) 190.
- XXV International Winter Meeting on Nuclear Physics (Bormio, Italy - January 1987).
- B. Faure - Thesis - Orsay (1987).
- International Workshop on Gross Porperties of Nuclei and Nuclear Excitations (Hirschegg, Austria, January 1988).
- XXVI International Winter Meeting on Nuclear Physics (Bormio, Italy - January 1988).
- Winter Workshop on Nuclear Dynamics V (Sun Valley, Idaho - February 1988).
- Third International conference nucleus-nucleus collisions, contributed papers (Saint-Malo, France, June 1988).

HEAVY RESIDUE SPECTRA AND LINEAR MOMENTUM TRANSFER IN INTERMEDIATE ENERGY NUCLEUS - GOLD COLLISIONS

K. Aleklett[a], J.O. Liljenzin[b], W. Loveland[c], M. de Saint-Simon[d], G.T. Seaborg[e], and L. Sihver[a].

[a] University of Uppsala, Studsvik, S-611 82 Nykoping, Sweden
[b] University of Oslo, Oslo, Norway
[c] Oregon State University, Corvallis, OR 97331, USA
[d] Laboratoire Rene Bernas, Orsay, France
[e] Lawrence Berkeley Laboratory, Berkeley, CA 94720, USA

I. Motivation

The production of heavy residues is an important reaction channel in intermediate energy nucleus-nucleus collisions [1,2]. The heavy residue production cross section exceeds the fission cross section for Ar-Au reactions at projectile energies exceeding ~25 MeV/nucleon and is important at all intermediate energies (Figure 1). Thus an understanding of the mechanism(s) involved in heavy residue production is essential for understanding the majority of intermediate energy nucleus-nucleus collisions. Accordingly, we are engaged in a broad survey program of single-particle inclusive measurements of heavy residue production using radiochemical techniques.

The use of radiochemical techniques to study heavy residues is dictated by the extremely low residue energies. For example, in the reaction of 43 MeV/nucleon ^{86}Kr with ^{197}Au, the mean residue energies ranged from 15 keV/nucleon (A=189) to 300 keV/nucleon (A=135) (Fig. 2). This finding has important consequences for measurements of heavy residue properties by non-radiochemical techniques. A time-of-flight spectrometer with a typical low velocity cutoff of 0.5 cm/ns will miss 40% of residues with A=155 and

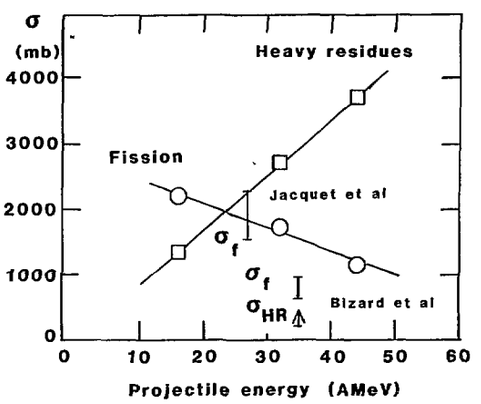

Figure 1. The dependence of the fission cross section (open circles) and the heavy residue formation cross section (open squares) on projectile energy for the interaction of Ar with Au[2].

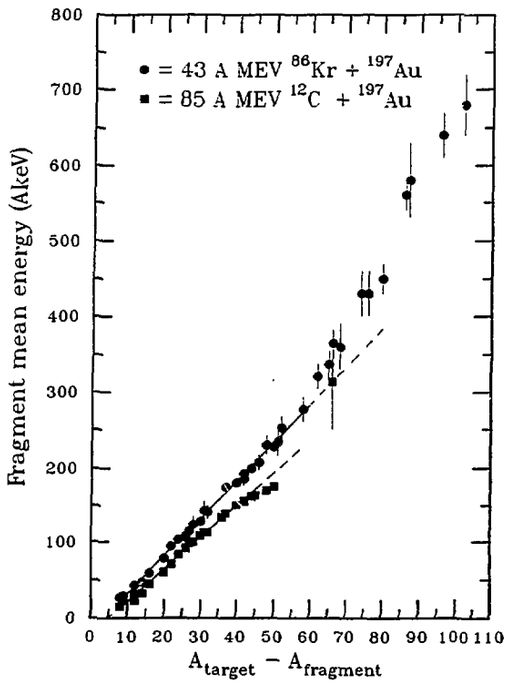

Figure 2. Mean heavy residue energies as a function of the difference between the residue mass number and the target mass number. The 85 A MeV C + Au data points are from reference 1.

100% of the residues with A>180, A demonstration of this effect is in the measurements of the heavy residue yields in the reaction of 35 MeV/nucleon ^{40}Ar with ^{197}Au where a radiochemical measurement [2] gave a residue production cross section of 2790 mb while a time-of-flight measurement gave a lower limit of 315 mb [3].

II. Results and Discussion

We have measured the heavy residue differential range distribution for the interaction of 43 MeV/nucleon ^{86}Kr with ^{197}Au as a function of residue Z and A in an attempt to characterize the linear momentum transfer. The range distributions were converted to energy spectra using known range-energy relationships. The deduced heavy residue longitudinal momenta (the linear momentum transfers) are shown in Figure 3 along with similar data for the interaction of 85 MeV/nucleon ^{12}C with ^{197}Au. The maximum fractional linear momentum transfer (FLMT) for the carbon induced reaction agrees with previous measurements, but the FLMT for the krypton induced reaction is very low

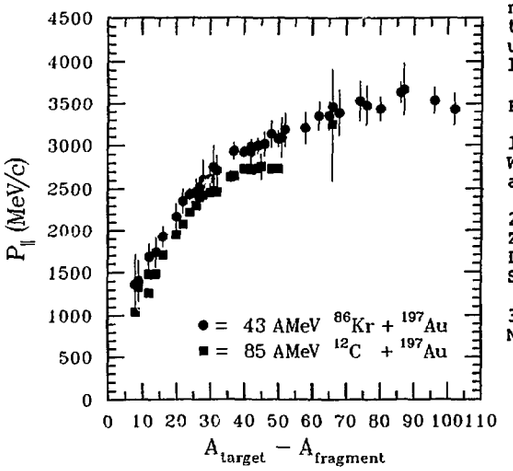

Figure 3. Deduced absolute values of the longitudinal momentum transfer as a function of the mass loss of the target nucleus (the excitation energy of the target like fragments).

(~40 MeV/c per projectile nucleon) and well below that expected from one-body dissipation (Figure 4). The striking similarity between the dependence of longitudinal momenta upon ΔA (and their magnitudes) for the two disparate reactions may be a consequence of the kinematics of momentum transfer in nucleon-nucleon collisions and the occurrence of incomplete fusion/massive transfer mechanisms.

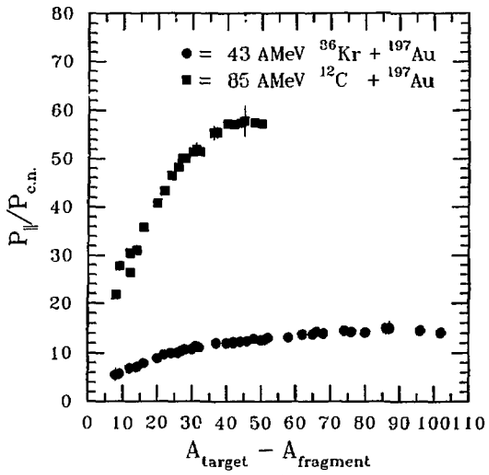

Figure 4. Deduced heavy residue fractional linear momentum transfer as a function of the mass loss of the target nucleus (the excitation energy of the target like fragments).

References.

1. K. Aleklett, M. Johansson, L. Sihver, W. Loveland, H. Groening, P.L. McGaughey, and G.T. Seaborg; Nucl.Phys.A (accepted)

2. K. Aleklett, W. Loveland, L. Sihver, Z. Xu, C. Casey, D.J. Morrissey, J.O. Liljenzin, M. de Saint-Simon and G.T. Seaborg; Phys.Rev.C (submitted).

3. G. Bizard, et al; Nucl.Phys. A456(1986)173.

REACTION MECHANISM EVOLUTION FROM 37 TO 50MeV/NUCLEON FOR THE SYSTEM $^{20}Ne + {}^{60}Ni$

F.Andreozzi*, A.Brondi*, A.D'Onofrio*, G.LaRana*, R.Moro*, E.Perillo*, M.Romano*, F.Terrasi*, R.Dayras+, B.Delaunay+, J.Delaunay+, H.Dumont+, F.Gady+, J.Gomez del Campo**, M.G.StLaurent++, S.Cavallaro***, L.Sperduto***, J.F.Bruandet+++
*Dipartimento di Scienze Fisiche and INFN-Sezione di Napoli- 80125 Napoli Italy;
+DPHN/BE CEN Saclay-91191 Gif/Yvette Cedex France;
**ORNL Oak Ridge,TN 37830 USA; ++GANIL BP 5027 Caen Cedex France;
***Dipartimento di Fisica and INFN Sezione di Catania-95129 Catania Italy;
+++Institut des Sciences Nucleaires-38044 Grenoble Cedex France

1.MOTIVATION

The evolution of reaction mechanisms in heavy-ion collisions for intermediate mass systems as a function of relevant parameters of the entrance channel (mass asymmetry, incident energy etc.) has been the object of extensive experimental and theoretical investigations over the past decade. In particular, limitations to the complete fusion have been experimentally proved down to 4MeV/nucleon and different limitation regimes found, with increasing incident energy. These limitations have been interpreted as due to the nuclear potential acting between projectile and target or to the location of a statistical yrast line of the intermediate system, besides other dynamical properties of the interaction, like prompt or preequilibrium particle emission. The influence of the mass asymmetry in the entrance channel on the onset of different regimes of limitations has also been explored[1].

With the aim of pursuing this kind of investigations we have undertaken the study of the system $^{20}Ne+{}^{60}Ni$ at Ganil energies, where a transition from the above mean field description to an interpretation in terms of interactions between two sets of quasi-free nucleons is expected.

2.EXPERIMENTAL RESULTS

Measurements have been performed at three incident energies, just above the Fermi energy: 37.1[1],44 and 50MeV/nucleon. Beam intensities ranging from 4 to 10pna and enriched selfsupporting ^{60}Ni targets of thicknesses from .5 to 5 mg/cm^2 were used. Charged particles of Z from 1 to 10 and γ-rays were detected. For the former ones telescopes made-up of Si solid state detectors and NaI scintillators were employed. For the latter ones Hyper-Pure Ge detectors of average efficiency of 24% and energy resolution of 1.8keV at 1.33MeV were used. In the experiment at 50MeV/nucleon the detection of γ-rays was accomplished by a special detector consisting of three Ge crystals arranged in the same cryostat in a three-stage telescope-like mount, the first stage being a planar detector 13mm thick. Coincidences between charged particles detected at different angles and discrete γ-rays were also recorded. Off-line γ-ray radioactivity spectra were collected by means of stack foil methods. More details about the experimental arrangements can be found in [2,3,4]

Discrete lines in singles γ-ray spectra were mainly produced by the deexcitation of low-lying levels of target-like nuclei with masses below the target mass. The intensities of ground-state transitions were used to deduce mass distributions of target-like nuclei. As an example the mass distribution measured at 50MeV/nucleon is shown in fig.1 (full dots with error bars).

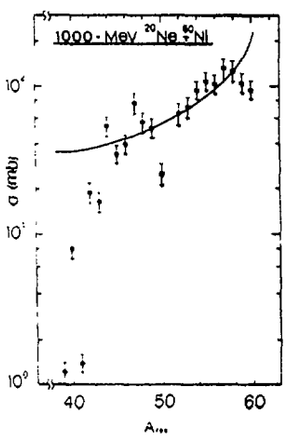

Fig.1-Measured mass distribution of target-like residues (full dots) compared to a modified geometrical model calculation (full line)

Radioactivity spectra from targets of different thicknesses and from Aluminum foils placed in front and on the back of the targets (stack foil arrangement) were used to measure production cross sections of radioactive residues. The percentage of cross section in Ni targets with respect to the total (target+absorbers) depends upon the component parallel to the beam axis of the residue velocity: the

[1]The run for this energy was carried out using the SARA facility in Grenoble

greater the percentage, the lower the velocity. For the 50MeV/nucleon run we used a target 1 mg/cm^2 thick and Aluminum foils of 15 μm and 99.99% purity; the corresponding results are summarized in fig.2 (full dots with error bars). As it can be seen, residues with lighter masses are faster compared to residues with heavier masses.

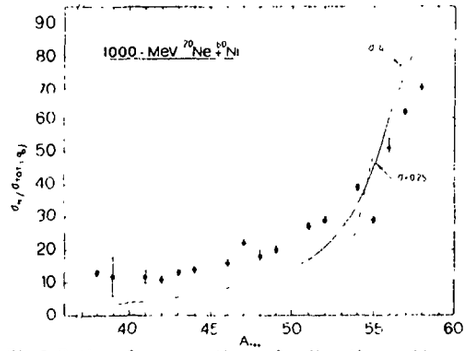

Fig.2-Ratios of cross sections of radioactive residues stopped in the target to corresponding total cross sections

3.MODIFIED GEOMETRICAL MODEL COMPARISON WITH DATA

First attempts to reproduce data at intermediate energies were done using pure geometrical models of a participant-spectator type, which had been successfull in describing data at relativistic energies [5]. Then more refined models, in the same geometrical framework, appeared to take into account mean field effects still present at intermediate energies. These more refined models smoothed the rigid scheme of the relativistic participant-spectator picture, depicting the exit channels as two cold projectile- and target-like spectators and a very hot "fireball" made-up of participant nucleons in the whole range of impact parameters, allowing different landscapes for more central collisions. The model of ref.4 evaluates one- and two-body energy dissipation in the framework of a Fermi-gas description of the colliding nuclei. One of the main features of the model is its capability to predict the value of the impact parameter for which the transition between massive transfer and three-body processes takes place, as well as the dependence of the latter upon the incident energy for a given system. Due to the geometrical basis of the model, one can establish a correlation between impact parameters and target-like residue masses[3], so that the ability of the model to reproduce target-like mass distributions is a significant test of its reliability. As a matter of fact fig.1 shows the kind of agreement between calculated and experimental mass distributions found at 50MeV/nucleon. Good agreements were also found at 37.1 and 44MeV/nucleon[2,3]. For the latter energy, the dependence of charged particle multiplicity versus the heavy residue mass, deduced from particle-γ coincidences, shows a decrease with increasing residue mass, coherently with the energy dissipation processes included in the model [2].

An observable more closely related to the dynamics of the interaction (compared to mass distributions) is the linear momentum transfer and sharing among reaction products. The percentages reported in fig.2 reflect the linear momentum distributions of the target-like fragments. Since the model is of a semiclassical nature, it does not predict distributions for the velocities of target-like fragments, but only average values for each mass. Using these values and taking into account the finite thickness of the target, one gets the dashed curve of fig.2, that does not reproduce the data, especially for lower masses. To improve the agreement, the model has to be upgraded in such a way that it can predict dispersions in the calculated quantities. For example, assuming gaussian distributions for the dissipated energy having standard deviations σ=25% of the average values, a substantially better agreement is obtained, full line in fig.2 (see ref.[6] for more details).

4.CONCLUSION

Inclusive and exclusive measurements have been performed for the system ^{20}Ne+^{60}Ni at three incident energies, 37.1, 44 and 50MeV/nucleon. A model for the reaction mechanisms predicting an evolution depending on the impact parameter and incident energy was successfully employed in reproducing target-like mass distributions. The importance of including dispersions in the semiclassical model has been pointed out, in order to reproduce linear momentum distributions of target-like residues.

1)H.Dumont et al., NPA435(1985)347
2)A.D'Onofrio et al., Lett. Nuovo Cim.42(1985)347
3)A.D'Onofrio et al., Phys.Rev. C35(1987)1167
4)A.D'Onofrio et al., in press in Phys.Rev. C
5)S.Nagamiya et al.,Ann.Rev.N.P.S.34(1984)155
6)F.Andreozzi et al.,to be published

PREEQUILIBRIUM EMISSION AND INCOMPLETE FUSION IN THE $^{40}Ar + ^{13}C$, ^{24}Mg and ^{45}Sc REACTIONS AT 27.5 MeV/NUCLEON

J.P. COFFIN[a], A. FAHLI[a], P. FINTZ[a], M. GONIN[a], G. GUILLAUME[a], B. HEUSCH[a], F. JUNDT[a], A. MALKI[a], P. WAGNER[a], S. KOX[b], F. MERCHEZ[b] and J. MISTRETTA[b]

a) Centre de Recherches Nucléaires and Université Louis Pasteur, 67037 Strasbourg Cedex (France)

b) Institut des Sciences Nucléaires, 383026 Grenoble Cedex (France)

1. Motivation

Both preequilibrium emission and incomplete fusion in heavy ion collisions carry information about the early stage of the collision and the manner in which the system evolves towards thermalization and the formation of a highly excited compound nucleus. Such studies present, however, several experimental difficulties that can be partly overcome by studing fairly light systems for which the fusion-fission component is relatively small compared to that of fusion-evaporation and by using inverse kinematic reactions to separate, at backward angles, preequilibrium emission from that subsequent to the decay of the thermalized system.

In order to obtain more information about incomplete fusion and preequilibrium emission, we have studied at 27.5 MeV/nucleon the two inverse kinematic $^{40}Ar + ^{13}C$ and $^{40}Ar + ^{24}Mg$ reactions and the nearly symmetrical system $^{40}Ar + ^{45}Sc$.

2. Results and discussion

The experiments were performed by using a beam of ^{40}Ar ions of 1100 MeV. Evaporation residues (ER) were detected by means of a time of flight system. ER lighter than the projectile could be separated from the heavy fragments resulting from reaction mechanisms other than fusion.

The process of incomplete fusion was studied by analyzing velocity distributions. In Fig. 1 are reported the ratios R of the velocity of the compound nucleus formed in incomplete fusion ($V_{ER}/\cos\Theta$) and in complete fusion (V_{FMT}) as a function of the mass A_{ER} of the ER, for the three systems. The figure shows also the evolution of the full width at half maximum of the velocity distributions. The ratios R and the widths exhibit a linear dependence with A_{ER}. $R < 1$ for $^{40}Ar + ^{45}Sc$ and $R > 1$ for the inverse kinematic reaction $^{40}Ar + ^{24}Mg$: this implies

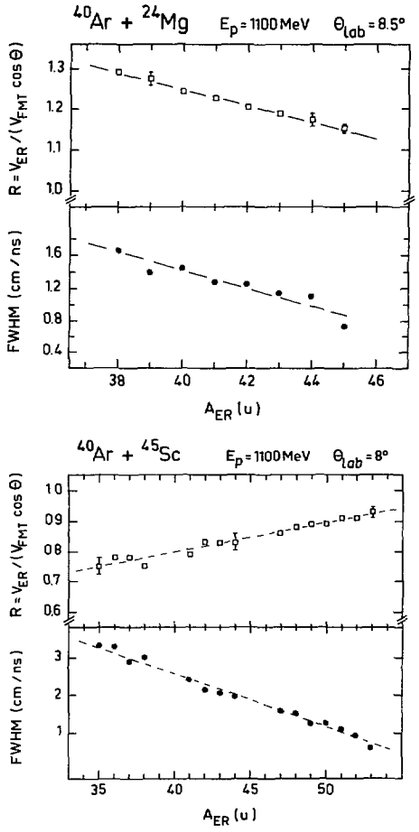

Fig. 1 :
Ratios R of the velocity of the CN formed in incomplete and complete fusion as a function of the mass of the ER and full width at half maximum of the ER invariant velocity distributions plotted versus A_{ER}.

that incomplete fusion is present in the two reactions, lighter is the ER more incomplete is the fusion and that the emission prior to fusion comes mostly from the lighter reactant.

We have analyzed the ratios R with a model based on linear momentum conservation to examine the pre-equilibrium emission (PE). Fig. 2 shows the ratio ρ of the PE velocity to that of the projectile and the multiplicity of PE with respect to A_{ER}. The dashed lines are to guide the eye. The histograms represent the relative experimental ER yields. The error bars indicate the variation on ρ within which the experimental A_{ER} are reproduced. Two PE regimes may exist, one can be described with the exciton model and a second is related to the Fermi-jet concept and corresponds essentially to the heavier ER. Coincidence measurements between particles with $V_{PE} > V_P$ and ER have been performed and analyzed in the context mentioned above.

Other interesting informations concerning excitation energies ε and temperatures T were obtained. For the $^{40}Ar + ^{45}Sc$ reaction, ε is nearly constant and close to 6.1 MeV (T = 7 MeV). The $^{40}Ar + ^{24}Mg$ system leads to lower values : ε = 3.5 MeV and T = 5 MeV.

In conclusion, the process of incomplete fusion has been studied : Detailed analysis of the velocity distributions has permitted to confirm the relevance of the relative velocity of the light reactant in the center of mass system as a parameter governing incomplete fusion. Two regimes of pre-equilibrium emission have been determined. The $^{40}Ar + ^{13}C$ reaction appears to be a special case as concerns the pre-equilibrium emission.

3. References

M. GONIN et al., XXVnd Int. Winter Meeting on Nuclear Physics, Bormio, Italy (1987)

J.P. COFFIN, VInd Adriatic Int. Conf. on Nuclear Physics, Dubrovnik, Yugoslavia (1987)

J.P. COFFIN, Workshop I N2 P3 – RIKEN, Shimoda, Japan (1987)

M. GONIN, Thesis, Université de Strasbourg, France (1987)

M. GONIN et al., Phys. Rev. C38 (1988) 135

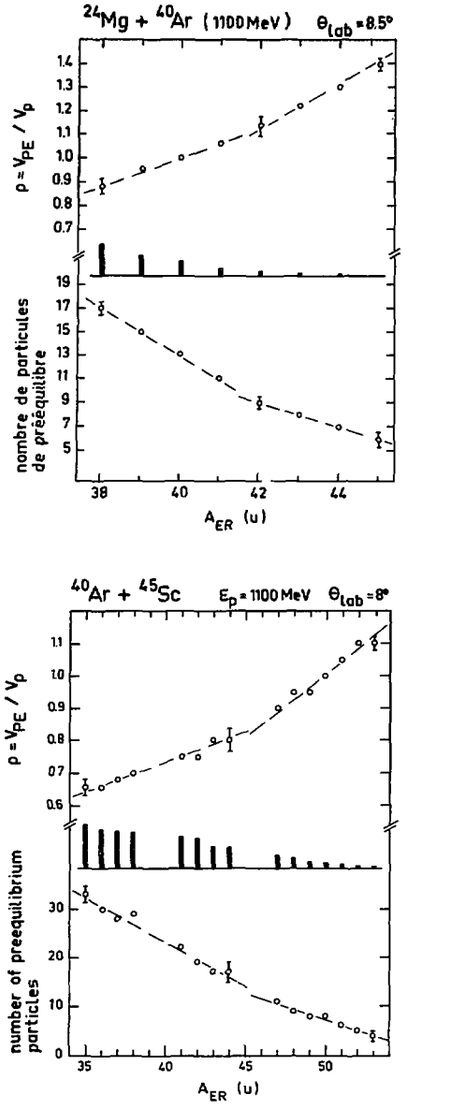

Fig. 2 :
The ratios ρ of the PE velocity (V_{PE}) to that of the projectile (V_P) and the number of PE nucleons (n_{PE}) are plotted as a function of A_{ER}. Note that, for the inverse kinematic case, the analysis has been done after conversion to direct kinematics.

TARGET RESIDUE CROSS SECTIONS AND RECOIL ENERGIES FROM THE REACTION OF 1760 MeV ^{40}Ar WITH MEDIUM AND HEAVY TARGETS

F. Hubert, R. Del Moral, J.P. Dufour, H. Emmermann, A. Fleury, C. Poinot, M.S. Pravikoff
CEN Bordeaux, IN2P3, Le Haut Vigneau, F-33170 Gradignan
H. Delagrange, GANIL, B.P. 5027, F-14021 Caen Cedex
A. Lleres, ISN-IN2P3, USMG, 53, Avenue des Martyres, F-38026 Grenoble Cedex

In the search for significant experimental facts revealing the true nature of the transition between the low and the high energy domain in heavy ion induced reactions, measured properties of heavy target residues are of prime interest. Since these residues lie relatively close to the target in the chart of nuclides, their degree of survival can be a clue to gain some knowledge of the violence of the reaction.

Deexcitation calculations of highly excited medium and heavy nuclei have shown that the final residues and whatever the A and Z of the initial excited nuclei are, always end-up in the same region (the so-called "residue corridor"). This region, remote from the stability valley is parallel to the line of β stability near the Γ_n/Γ_p=1 line (Γ_n and Γ_p being the particle decay widths for neutron and proton respectively). Then most of the independent yields for target residues are to be found for neutron deficient species with short half-lives. Rapid detection of these nuclei is then required. The method of electrostatic collection of nuclides we used makes possible on-line collection (in few milliseconds) of target residues on the surface of an alpha detector[1]. For rare earth nuclei an island of radioactive alpha decay exists for the N=84-85 neutron deficient isotones located in the residue corridor. The present investigation is devoted to the study of the formation of these isotones in several targets. Thus, in contrast to the usual experiments where different residues are observed for a given target, our results are obtained by detecting specific residues from various targets[2].

We have measured production cross sections (fig. 1) and mean recoil energies (fig. 2) of heavy residues (the rare-earth isotones N=84-85 which are α-emitters) formed in ^{40}Ar induced reactions at 1760 MeV with medium and heavy mass targets. The bell shape of the isotone yields is an indication of the origin of these isotones in the decay of highly excited precursors. The similarity of these data with those obtained in ^{12}C induced reactions (at 1 GeV) in comparable conditions confirms this interpretation. Significant production yields of trans-target isotopes have been measured. We are able, in the framwork of our analysis, to estimate the pattern of heavy residue production from an "average target".

A semi-quantitative analysis based on an incomplete fusion picture was used to try to classify our data. The experimental mass losses are reproduced, to first order, within this framework. For large mass lossed, the behavior of the deduced energy removed (per nucleon) during the decay process seems to indicate the evaporation of some heavy particles (^{4}He and heavier). Our data concern reactions where the mean fractional momentum transfer is rather small (30%). Such reactions can then be considered as peripherical reactions. Even if it is quite paradoxical at first sight, there can be a large amount of excitation energy in the primary fragments (E^* = 200-600 MeV).

It is far beyond the scope of this experimental study to go through exhaustive theoretical investigations. We have chosen to compare our data with, on one hand, the extended abrasion-ablation model of Dayras and, on the other hand, intranuclear calculations. As far as our results are concerned, there is no evidence of a transition from an abrasion-ablation behavior to an incomplete fusion picture. Comparison with intranuclear cascade calculations pinpoints the fact that n-n collisions only cannot lead to enough excitation energy in the precursors. So far these theoretical investigations have only been able to predict some qualitative aspects of the studied interactions ; but these data really stand as a meaningful test for more elaborate models.

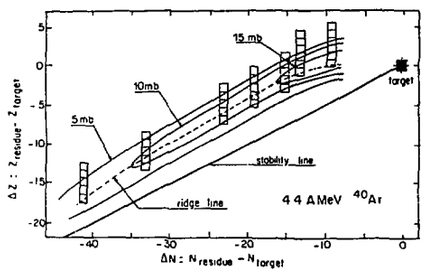

Fig. 1 : Deduced distribution of the residue cross sections in the (ΔN, ΔZ) plane. The dashed line gives the ridge line, i.e. the line for maximum yield. The open squares represent the location of the experimental measurements. The curves are the loci of the residues for a given value of the cross sections.

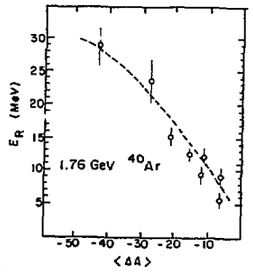

Fig. 2 : Experimental mean forward projected recoil energy E_R as a function of the mean nucleon loss (ΔA). The dashed line is drawn to guide the eye.

1 - J.P. Dufour et al., Nucl. Phys. A387 (1982) 157c
2 - F. Hubert et al., Nucl. Phys. A456 (1986) 535

LIGHT PARTICLES AND PROJECTILE-LIKE FRAGMENTS FROM THE $^{40}Ar + ^{12}C$ REACTION AT 44 MeV/NUCLEON

D. Heuer, R. Bertholet, C. Guet, M. Maurel, H. Nifenecker, Ch.Ristori, F.Schussler
CEN-G,DRF/SPh, F - Grenoble
J.P. Bondorf, O.B. Nielsen, N.B.I., DK-Copenhagen

Doubly differential spectra of light particles and projectile-like fragments were measured at laboratory angles in the range 3°-23° for the $^{40}Ar + ^{12}C$ reaction at 44 MeV/nucleon. The kinematical conditions of this reaction lead to a strong focussing of the reaction products in the forward direction and therefore to a good detection efficiency.

Production rates for heavy fragments (of charge around Z = 14), velocity distributions characterizing these fragments and also that characterizing the ^{4}He emission were consistently interpreted as resulting from the decay of a thermally equilibrated nucleus, initially made up by the transfer of an α -particle from ^{12}C to ^{40}Ar. Although depending upon a desexcitation model, an average excitation of about 3.6 MeV/nucleon of the compound system (^{44}Ca) is consistent with data. More details are found in ref.[1]. This experiment was among the first to identify the formation of highly excited nuclei and since then hot nuclei with higher temperature have been currently produced and observed.

1) D. Heuer et al., Phys.Lett.161B, 269 (1985)

STUDY OF PREEQUILIBRIUM IN INTERMEDIATE ENERGY HEAVY ION COLLISIONS

C. Cerruti*, J. Desbois**, R. Boisgard*, C. Ngô*, J. Natowitz*** and J. Nemeth****

*Laboratoire National Saturne, CEN Saclay, 91191 Gif sur Yvette Cédex, France
**Division de Physique Théorique+, Institut de Physique Nucléaire, 91406 Orsay Cédex, France
***Cyclotron Institute, Texas A&M University, College Station, TX 77843, USA
****Institute for Theoretical Physics, Eötvos University, Budapest, Hungary

To describe the first step of an heavy ion collision, we propose to use a preequilibrium model[1]. This approach will be, in principle, valid for very asymmetrical nuclear systems. Our aim is to calculate the number of emitted nucleons during the first stage of the collision, the linear momentum transferred from the projectile to the target and also the target excitation energy when the statistical equilibrium is reached. We proceed as follows.

At t=o, the volume of the target is filled with the total number of nucleons, namely $A_T + A_P$ (A_T and A_P are, respectively, the target and projectile masses). The added nucleons (A_P) are put on the energy states of the system corresponding to ε, the incident energy per nucleon (this corresponds to a "sudden hypothesis"). Following Harp and Miller[1], the nuclear system is described as a two components (protons and neutrons) Fermi gas which is entirely characterized by the occupation numbers of its single particle states. The evolution of these occupation numbers is governed by a set of Boltzmann-like master equations, the relaxation of the system being produced by nucleon-nucleon collisions and nucleon emission[2]. These equations are solved numerically and we stop when the initial peak corresponding to the projectile energy has completely vanished. This occurs at time $t_1 \approx 10^{-22}$ s. Therefore, it is reasonable to consider that, at time t_1, the preequilibrium phase is finished. The results concerning $N_e(t_1)$ (number of emitted nucleons) and $\varepsilon^*(t_1)$ (excitation energy per nucleon of the residual nuclear system) can be fitted by the following expressions[2]:

$$N_e(t_1) = 0{,}96 \cdot \mu^{5/4} \left[1 - \exp\left(-\frac{\varepsilon}{0{,}736\, A_T}\right) \right]$$

$$\varepsilon^*(t_1) = 6{,}8 \cdot A_T^{-1/3} \mu^{2/3} \left[1 - \exp\left(-\frac{\varepsilon}{350 \mu^{-1/3}}\right) \right]$$

where μ is the reduced mass of the system and ε the incident energy per nucleon. The quality of the fits can be seen in Figs. 1-2 where $N_e(t_1)$ and $\varepsilon^*(t_1)$ are displayed for three different systems (C, Ne, Ar+Au) as functions of ε and also of $E_{C.M.}$ (total center of mass energy).

At the end of the preequilibrium phase, the nuclear system is excited (presumably hot and compressed). We can study its subsequent evolution, using an hydrodynamical approach coupled to a percolation model (for details, see refs.[2-3]) and, also, the contribution of J. Nemeth et al. in this book). In this approach, the nucleus will exhibit monopolar oscillations ("breathing mode"). The percolation parameters, p and q, are, at each time, connected with the density and excitation energy of the nuclear system. Break-up will occur if the multifragmentation region (in the p-q plane) is reached. In Fig.3 we present the results for

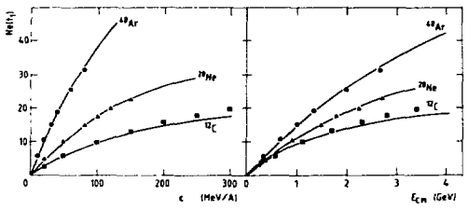

Fig. 1

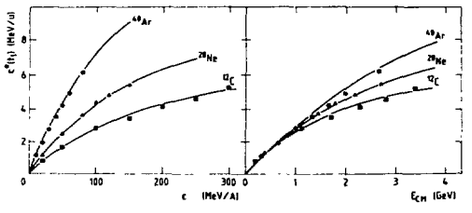

Fig. 2

a central Ar+Au collision at various bombarding energies (time t_2 corresponds to the end of the first half-period of oscillation). We see that the critical incident energy for multifragmentation is about 50 MeV/u for that system. In Fig.4, we show the critical regime for various systems (C, Ne, Ar+Au). Comparisons with the existing experimental data are rather encouraging.

In conclusion, we can say, in some sense, that we have built a complete scenario for a central heavy ion collision. So, we are able to study the influence of different parameters on the appearance of multifragmentation (essentially, the projectile and target sizes and the bombarding

+ Unité de Recherche des Universités Paris 11 et Paris 6 Associée au C.N.R.S.

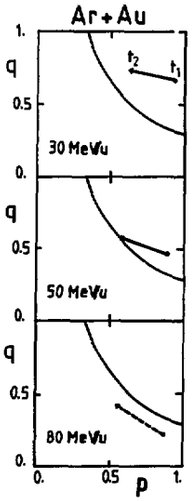

Fig.3

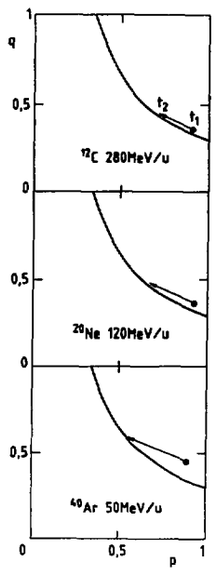

Fig.4

energy). We must say that, owing to the small size of a nuclear system, the transition from incomplete fusion to multifragmentation is rather smooth when the energy increases[4]. Recently, we have extended our model to non central collisions[4] and also to reactions involving very heavy ions[5]. However, we are aware that this approach is still schematic and sometimes very crude. We think that a lot of work remains to be done (concerning, in particular, preequilibrium and also the definition of the percolation parameters) in order to obtain a realistic description of an heavy ion collision.

1) G.D. Harp et al., Phys. Rev. C3 (1971) 1847
2) C. Cerruti et al., Nucl. Phys. A476 (1988) 74.
3) J. Nemeth et al., Z. Phys. A325 (1986) 347 ;
J. Desbois et al., Z. Phys. A328 (1987) 101.
4) C. Cerruti et al., to appear in Nucl. Phys. A.
5) O. Granier et al., Contribution to the XXVII Int. Winter Meeting on Nuclear Physics, Bormio (1989).

Study of light charged particles emitted in ^{40}Ar induced reactions at intermediate energies

G.Lanzanò, A. Pagano - INFN, Catania
R. Dayras, J. Barrette, B. Berthier, D.M.De Castro Rizzo, O. Cisse, R. Coniglione,
F. Gadi, R. Legrain, M.C. Mermaz, E.C. Pollacco - DPhN/BE, CEN Saclay
H. Delagrange, W. Mittig - GANIL, Caen
B. Heusch - CRN, Strasbourg

1. Motivation

The study of the evolution, with the incident projectile energy, of the reaction mechanism involved in peripheral interactions between heavy ions, has recently found a great opportunity with the delivery, at Ganil, of a variety of intermediate energy beams. In this aim we have accomplished a series of inclusive and coincidence experiments in which we have studied both the heavy products and the light charged particles (LCP) emerging from the reaction.

As the gross features deduced for the heavy fragments are treated elsewhere in this compilation[1], in the following we shall present some results on the LCP produced in reactions induced by an ^{40}Ar beam on an ^{27}Al target, at 44 and 60 MeV/n.

2. Experimental apparatus

The experiments were performed using 44 and 60 MeV/n ^{40}Ar beams delivered by the Ganil accelerator at Caen.

LCP were detected into telescopes, consisting each one of 2 ΔE (100 μm and 4000 μm thick) silicon detectors and a E (5 cm in diameter, 10 cm long) INa or BaF2 detector, in an angular range between 15° and 112.5°,in steps of 7.5°.

In a coincident experiment two of these telescopes were placed at -10° and + 25° with respect to the beam direction, while the coincident projectile-like fragments (PLF) were detected (mass and charged identified) in a five element silicon telescope, placed at +3.1° with respect to the beam direction.

3. Results and discussion

The LCP energy spectra, especially in the forward direction, are complex, suggesting that more than one emitting source is contributing. Fig 1 shows a typical energy spectrum for alpha-particles detected at 15° in the reaction ^{40}Ar +^{27}Al at 60 MeV/n;we notice in it a relatively low threshold (≈3Mev/nucleon) and a dip near 80 Mev, due to a dead layer in the second thick silicon detector of the telescope. We have analysed these spectra in terms of an abrasion-ablation model, that has already been successfull in explaining the gross features of the heavy remnants of the reaction[2]. In this model, LCP are produced during the ablation stage subsequent to the abrasion, so that three sources can be distinguished :

i) A high velocity source (HVS) associated with the primary PLF, characterised by a velocity near to that of the beam and a relatively low temperature
ii) An intermediate velocity source (IVS) , associated with the participant zone and characterised by a velocity intermediate between that one of the beam and that of the target,and by a high temperature
iii) A low velocity source (LVS), associated with the primary target-like fragments(TLF) and characterised by a low velocity and temperature.

We have described the LCP emission from each source by a Maxwell-Boltzmann distribution, including the effect of the Coulomb repulsion[3]).

As an example, table I shows the best set of parameters characterising the three sources, found by a fit procedure, for alphas and protons produced in the reaction ^{40}Ar +^{27}Al at 60 MeV/n. With this set of parameters we were able to reproduce remarkably well the experimental spectra throughout the explored angular range, from 15° to 112.5°. Fig 1. gives an example of the obtained results and, in particular, the relative contribution of the three sources to the spectrum. An interesting result of these calculations is shown in Fig. 2, where the relative contribution to the energy spectrum for each source is given as a function of the lab. angle for alpha particles. It is evident from this plot that an experimental signature of the participant zone can be obtained only in a limited angular range, depending on the type of particle. For instance, for alpha-particles the most suited angular range is located between 23° and 33°, where the ratio between the IES intensity and the total intensity reaches a maximum value of ≈ 0.70.

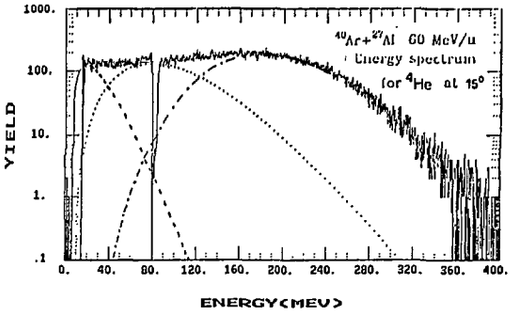

Fig 1

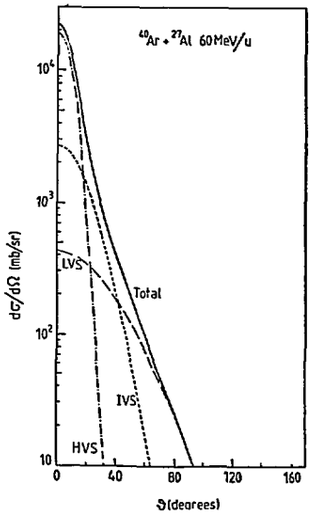

Fig. 2

TABLE I

SOURCE	v/c	T(Mev)	Ec(Mev)	Irel(mb)
		ALPHAS		
HES	0.31	6.9	4.0	2306.
IES	0.18	12.0	5.0	1538.
LES	0.06	7.5	3.0	1378.
		PROTONS		
HES	0.33	4.9	3.0	2206.
IES	0.16	14.5	4.0	2302.
LES	0.05	4.7	2.0	1497.

This result is confirmed by the coincidence experiment $^{40}Ar + ^{27}Al$ at 44 MeV/n, even if the correlations between PLF and LCP were performed at only two angles. We want to stress here only one aspect of the obtained results, referring the reader to ref.[4] for a more detailed presentation of the results.

Fig. 3 shows the dramatic change in the shape of the energy spectrum for alpha-particles detected respectively at -10° and + 25°, in coincidence with PLF detected at +3.1°. As compared to the spectrum at -10°, at +25° the high energy component has almost completely disappeared and the spectrum is now peaked at an energy corresponding to a velocity equal approximately to 60% of the beam velocity. Furthermore, the slope of the high energy side of the spectrum is much less steep than at -10°, indicating a higher temperature of the emitting source. This comparison suggests that the bulk of the emitted alpha- particles at -10° and +25° has its origin in two different sources, confirming the scenario of an abrasion ablation mechanism, as suggested by the inclusive experiments. The full line in Fig.

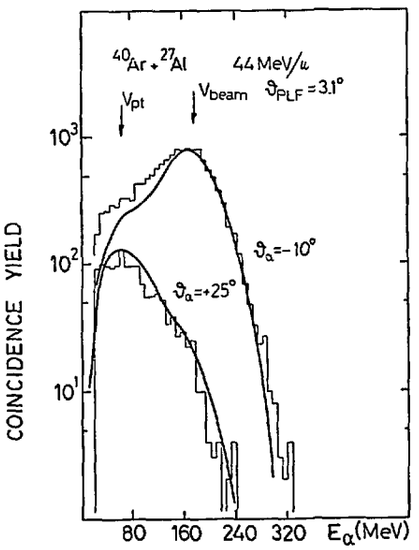

Fig. 3

3 represents just the result of a two sources calculation (the LES has been neglected), in which velocities and temperatures, as predicted by an extended Abrasion model[2], have been used as source parameters, see ref. [4].

A further confirmation that 25° is a suited angle to study the products originating from the participant zone, comes from the inspection of fig. 4, where the differential alpha-particle multiplicity, as measured at +25°, is reported as a function of the mass of the PLF detected ad +3.1°. If we make the reasonable assumption that the number of alphas emitted by the participant zone is proportional to its mass, then the differential alpha-particle multiplicity shown in Fig. 4 is nothing but the correlation between the PLF's mass and the mass of the participant zone. The full line in fig. 4 represents just this correlation as predicted by the abrasion model and calculated using the simple formula of ref.[5]

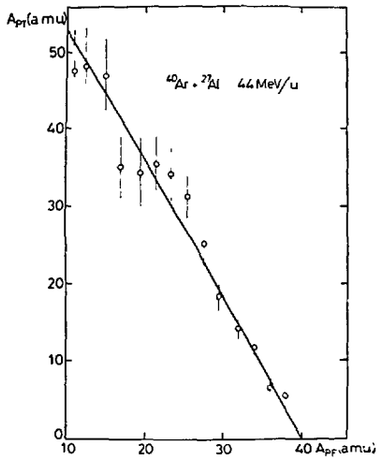

fig. 4

4. Conclusion

In conclusion, we have presented some features of light charged particles at intermediate energies. We have shown that the data can be successfully explained in terms of three thermalised sources, reflecting a scenario of a fast abrasion-ablation mechanism, in which two spectators (PLF and TLF) and a participant zone are created. We have also stressed the fact that only in a narrow angular range the intensity of the alpha-particles having the characteristics of an intermediate velocity source is predominant on the intensities relatives to the spectators. At the moment, however, due to the limited angular range explored in the coincident experiment, we cannot exclude that the IVS could result from the emission of fast, preequilibre particles, without formation of a participant zone. To better elucidate the reaction mechanism responsible of the observed LCP energy spectra and angular distribution, we have just undertaken a more complete coincident experiment, by looking, at several angles, at the spectra of LCP emitted in coincidence with a given fragment.

References

1) R.Dayras et al, this compilation
2) R.Dayras et al, Nucl.Phys.A460(1986)299-323 and R.Dayras et al, Phys.Rev.lett., in press
3) T.C. Awes et al,Phys.rev.C 25 (1982) 2361
4) G.Lanzanò et al. in Proc. of the XXIV Int. Winter Meeting on Nuclear Physics, Bormio (1986), pag. 183 - 191
5) G.Lanzanò et al, Nuovo Cimento Vol. 99A (1988) 839-856

EXPERIMENT N°50

LIGHT-PARTICLE CORRELATIONS : (I) SMALL RELATIVE MOMENTA CORRELATIONS

D. ARDOUIN[1]*, G BIZARD, H. DELAGRANGE, H. DOUBRE, C.K. GELBKE, C. GREGOIRE, A. KYANOWSKI, F. LEFEBVRES, W. LYNCH, M.MAIER, W. MITTIG, A PEGHAIRE, J PETER, J POCHODZALLA[2], J. QUEBERT, F. SAINT-LAURENT, B. TAMAIN, Y.P. VIYOGI[3], B. ZWIEGLINSKI.

Laboratoire National GANIL, BP. 5027, Caen Cedex, France.
National Superconducting Cyclotron Laboratory, Michigan State University, East-Lansing, MI 48824, USA.
Laboratoire de Physique Corpusculaire, Université de Caen 14032 Caen Cedex, France.
Centre d'Etudes Nucléaires de Bordeaux-Gradignan 33170 Gradignan, France

Most attempts to obtain experimental information about the temperature of highly excited systems in heavy-ion collisions were based on light-particle kinetic spectra analyses. Within a thermal model, the relative populations of particle-unstable states can be used to determine the temperature at the point where the particle leave the equilibrated system. We have measured these populations for the Ar + Au and O + Au reactions at E/A = 60 and 94 MeV respectively. Light-particles ($Z < 4$) were detected by a close-packed hexagonal array of $\Delta E - E$ telescopes positioned at laboratory angles of 30° and 45°. Energy calibrations of the NaI E detectors were established for all particles using momentum selected reactions products[1]. In addition, coincident charged particles, detected in the NAUTILUS Plastic Wall (θ=3-30°), were used as a multiplicity filter in the case of the Ar + Au reaction. The correlation function R(q)is defined by $\sigma_{12}(p_1,p_2)=\sigma_1(p_1).\sigma_2(p_2)$ [1+R(q)] where q is the two-particle relative momentum.

The population of different highly excited particle-unstable states in ^{8}Be, ^{7}Li, ^{6}Li, ^{5}Li and ^{4}He has indicated[2)3)] an emission temperature T=4-5 MeV (Fig.1) whereas lower temperatures were deduced from low-lying states. A quantitative comparison must address the question of sequential feeding. The inclusion of sequential feeding within the Quantum statistical model made it possible to describe the measured populations by a thermal distribution with a common temperature T=5.5 MeV. These results are much lower than the kinetic slopes of inclusive spectra indicating possible distortions by collective or expansion motion of the system. Several interesting and puzzling features have been revealed by the very little sensitivity[4)] of these measured temperatures to the charged particle multiplicity at forward angles or the kinetic energy of the emitted clusters (between 10 and 50 MeV/A). A dynamical limitation to the deposited thermal energy has been proposed[5)]. This is corroborated by Landau-Vlasov calculations where a limitation of excitation energy is found to result from a competition between preequilibrium emission following expansion and monopole mode excitation on one hand and thermalisation on the other hand.

Because of their sensitivity to final-state interactions, the correlation-function is known to contain information about the space-time extension of the emitting system. Another goal of the present experiment was based on this determination using different coincidences pairs : (p,p), (d,d), (t,t), (p,α) and (d,α). The space-time extent of the source was found to depend on the particle species and to decrease with the kinetic energies of the particle pairs. This is an indication of a sequential freeze-out of different species at different stages of the reaction. The energy dependence could be caused by a collective radial expansion of the interaction zone or an earlier stage of emission for the more energetic particles. The comparison of the source space-extension as a function of the

multiplicity shows an increase by a factor of 2 over the investigated range : higher multiplicities, associated with lower impact parameters producing larger extension and smaller correlations. It is the first time that such an observation is made in the intermediate energy domain. This points to a large sensitivity of the collision time and the emitting zone spatial extension with the impact parameter.

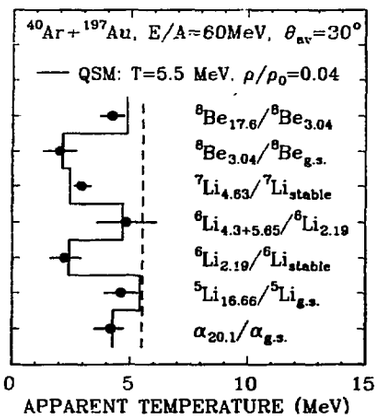

FIG. Apparent emission temperatures for ^{40}Ar induced reactions on ^{197}Au at $E/A=60$ MeV. The histogram shows the results of a quantum statistical calculation which includes the feeding by sequential decay; an initial temperature of $T=5.5$ MeV and a density of $\rho/\rho_0=0.04$ were assumed.

* Spokesman at the "Comités d'Expériences GANIL"

1) On leave from University of Nantes (France).

2) Present address : Inst. Kernphysik, Frankfurt (FRG).

3) On leave from VECC, Calcutta (India).

Publications relative to this work :

1) W. Mittig et al. Nouvelles de Ganil N° 7 (1984) 22.

2) J. Pochodzalla et al,
Phys. Rev. Lett. 55 (1985) 190 ;
Phys. Lett. 161B (1985) 256 ;
Phys. Lett. 161B (1985) 275 ;
Phys. Rev. C 35 (1987) 1695 ;
D. Ardouin et al, Nucl. Physics A 447 (1985) 585 c.

3) Z. Chen et al, Phys. Rev. C 36 (1987) 2297.
Phys. Lett. B 199 (1987) 171.

4) A. Kyanowski et al, Phys. Lett. B 181 (1986) 43.

5) F. Saint-Laurent et al, Phys. Lett. B 202 (1988) 190.

EXPERIMENT N°50

LIGHT-PARTICLE CORRELATIONS : (II) LARGE RELATIVE MOMENTA CORRELATIONS

D. ARDOUIN[1*], Z. BASRAK, G. BIZARD, H. DELAGRANGE, H. DOUBRE, C.K. GELBKE, C. GREGOIRE, A. KYANOWSKI, F. LEFEBVRES, W.G. LYNCH, M. MAIER, W. MITTIG, A. PEGHAIRE, J. PETER, J. POCHODZALLA[2], J. QUEBERT, F. SAINT-LAURENT, P. SCHUCK, B. TAMAIN, Y.P. VIYOGI[3], B. ZWIEGLINSKI

GANIL, BP 5027, 14032 Caen Cedex, France.
LPN Nantes, 2 rue de la Houssinière, 44072 Nantes Cedex 03, France.
ISN GRENOBLE, 53 avenue des Martyrs, 38026 Grenoble Cedex, France
LPC, Université de Caen, 14032 Caen Cedex, France.
CEN Bordeaux, 33170 Gradignan, France.
NSCL, Michigan State University, East-Lansing, MI 48824, USA.

A comparison of experiment and theory which can reveal the expected interplay between mean-field effects and two-body collisions is of great importance for the understanding of heavy-ion dynamics at energies around the Fermi energy. Light particle correlations at large relative momenta offer an opportunity to reveal mean-field effects via azimuthal and polar effects on the correlation-function.

We have measured such two-particle correlations for p,d,t,α species for the Ar + Au and Ar + Ti reactions at E/A = 60 MeV. Eleven ΔE - E telescopes were mounted at θ polar angles of 22°, 30°, 37°, 70°, 110°, 135° and 160° with possible variable relative azimuthal angle ($\Delta\Phi$) 0, 49°, 90°, 135° and 180° between them. For the Ar + Au reaction, the NAUTILUS Plastic-Wall covering $\Delta\theta$ = 3° - 30° was also used as a charged particle multiplicity filter.

The most salient feature is the strong energy dependence (Fig. 1) of the azimuthal $\Delta\Phi = \Phi_2 - \Phi_1$ distribution of the correlation function $\sigma_{12} / \sigma_1 \times \sigma_2$. An almost azimuthal isotropy has been observed at 60 MeV/A while a marked same-plane enhancement was established in previous studies at E/A = 25 MeV. (Fig. 1). We very satisfactorily can explain this behaviour by convoluting two singles emission probabilities $P(\theta, \Phi) = \sigma(\theta,\Phi)/ \sigma(\theta)$ with respect to the azimuthal angle Φ ; the distribution $P(\theta,\Phi)$ has been calculated from the Landau-Vlasov equation. According to the comparison of our data with these calculations, the increasing importance of the two-body collision rate with increasing energy, as opposed to mean-field effects is responsible for the above observations.

The importance of mean-field effects is found in the observation of collective motion felt by the participating nucleons. Such a signature was visible in the in-plane enhancement at E/A = 25 MeV (Fig.1). At E/A = 60 MeV, we have shown that the polar structure of the correlation function (Fig. 2) contains a fingerprint of the mean-field effect too. Indeed, the maxima observed around θ = 60° result from the favored deflection of participant nucleons by the mean-field of the two colliding nuclei towards negative angles. This effect is expected to offer also a target mass dependence : heavier targets giving less centrifugal ejecting forces as observed. Fig. 2 shows the observed dependence which is again well accounted for by Landau-Vlasov calculations including both mean-field and collisional effects. The spread of the maxima itself depends highly on the rate of two-body collisions. The position of the maxima, via mean-field dependence, is also expected to reflect the attractive or repulsive part of this mean-field. Our multiplicity selected data do show such a behaviour as smaller deflections seem to be associated with higher multiplicities or smaller impact parameters.

In summary the large angle two-particle correlations have been shown to contain one of the rare known fingerprint of the competitive role between nuclear mean-field and two-body collisions in nucleus-nucleus interactions.

* Spokesman at the "Comités d'Expériences GANIL"

1) On leave from University of Nantes (France).

2) Present address : Inst. Kernphysik, Frankfurt (FRG).

3) On leave from VECC, Calcutta (India).

Publications relative to this work :

D. ARDOUIN et al, Z Phys A 329 (1988) 505 and to be published

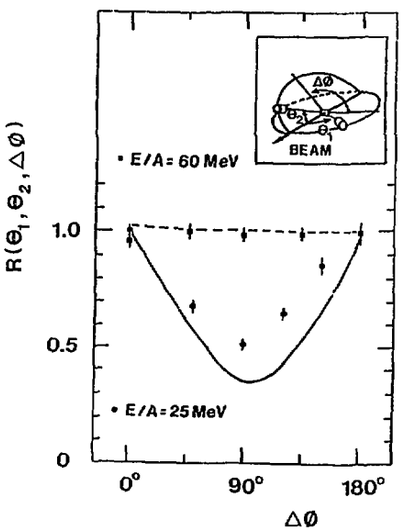

Fig 1

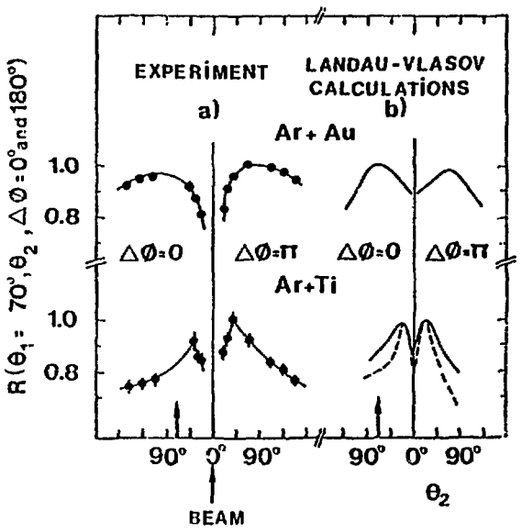

Fig 2

THE ROLE OF TIME IN THE DAMPING OF SOME FINAL STATE INTERACTIONS IN TWO-PARTICLE CORRELATIONS, P. Lautridou, R. Boisgard, J. Quebert Centre d'Etudes Nucleaires de Bordeaux-Gradignan, Le Haut-Vigneau 33170 Gradignan, France ; C. Lebrun, F. Guilbault, D. Goujdami, D. Durand, R. Tamisier, D. Ardouin, Laboratoire de Physique Nucleaire de Nantes, 2. Rue de la Houssiniere, 44072 Nantes, France ; A. Peghaire, F. Saint-Laurent, Laboratoire Ganil, 14021 Caen Cedex, France

The purpose of this study is to probe the specific range of time (10^{-20}-10^{-22}s) which governs particle emission from a highly excited (and possibly compressed) nucleus. We study in fact the emission of two particles for which a few resonances of given lifetimes can be used as probes in the final state. Thus, relative time emissions of the two particles can be studied since a prompt emission should tune in the resonance whereas induced time correlations (and relative time delay) should play a damping effect.

The method of two-particle correlations at small relative momenta is particularly well suited to study these modulation effects (for which other origins have been considered [1-3]). On the other hand, when the correlated pair concerns two like-particles, another effect due to Bose-Einstein or Fermi-Dirac statistics provides an interference pattern at small relative momenta which is also dependant on the lifetime of the source. These latter effects are in fact unambiguous in π-π correlations [4] ; To date, they have not been evidenced with heavier particles because of the prominant effects of final state interactions which often smear out the expected pattern.

In a recent study of such correlation functions in the backward hemisphere of ^{16}O + ^{197}Au at 94 MeV/A, we observed for the first time a progressive transition from the well known [5] final state interaction of two protons (^{2}He) to a typical shape that we assign to statistical interferometry. This is shown in Fig. 1, where a progressive damping (57 degrees) is observed to give rise to a typical new shape of the correlation function with complete disappearance of ^{2}He (135°).

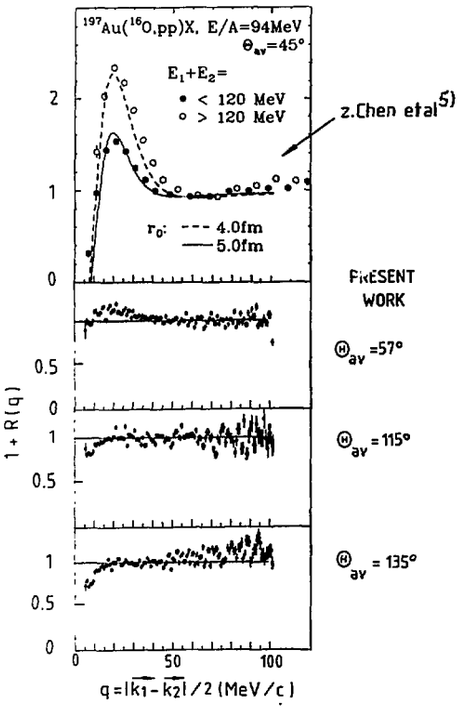

Fig. 1 :
p-p correlation functions measured at large scattering angles in ^{16}O + ^{197}Au at 94 MeV/A, we notice a disappearance of the final state interaction in the backward hemisphere.

This is also observed in another way in Fig. 2a) through the coincidence plot due to the only counters (CsI) which are set at 5 degrees from each other : whereas a clear ^{8}Be resonance is observed with α-α coincidences in Fig. 2b), a lack of data along the expected locus of the p-p coincidences in Fig. 2a) shows that the final state resonance is no longer formed.

In the same time, the singles proton spectra display a characteristic evaporation shape at backward angles which allows to conclude that we deal with a real stochastic emission of protons (evaporation and no final state interaction).

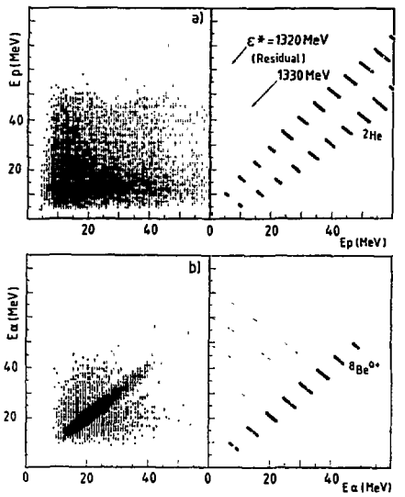

Fig. 2 :
Comparison between p-p and α-α coincidences at $\theta_{12} \simeq 5$ degrees. On the right are shown the expected final state interactions and the limits due to a residual system with a given excitation energy ε^*.

The new shape of the correlation function is then assigned to statistical interferometry because many data concerning other correlations like p-d or d-d show no influence of Coulomb distortions at such large angles.

For a uniform spherical source of radius Ru, decaying with lifetime τ, we get the following expression [6] :

$$1)\quad 1+\mathcal{R}(Q,q_{inv}) = 1-0.5\left[\frac{3\, j_1(Q\,Ru)}{Q\,Ru}\right]^2 \frac{1}{1+q_{inv}^2\,\tau^2}$$

With $\tau \neq 0$, the usual correlation function versus $q = Q/2$ has to be considered as a projection of a two-dimensional plot (Q, q_{inv}). It can be noticed that the limits of q_{inv} to be used in the integration are dependant on q as shown Fig. 3a).

The relevant projection of the plot (Fig. 3b) is then fitted with the following values :

$$\tau \geq 1.1\ 10\text{-}21\text{s} \ ;\ Ru = 6.5\ \text{fm}$$

The value of τ characterizes the average coherence time of emission in a stochastic process like proton evaporation.

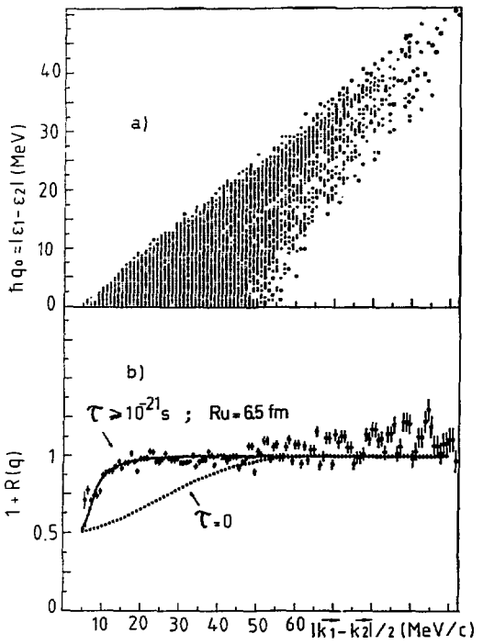

Fig. 3 :
The characteristic correlation function fitted after integration of expression 1) over the range of q_{inv} values. A lifetime of the order of 10^{-21}s is needed to account for the data with a reasonable value of Ru (6.5 fm).

Further studies on time effects are in progress in other kinds of collisions.

1) S. Koonin, Phys. Lett. 70B 43 (1977)
2) W.G. Lynch et al, Phys. Rev. Lett. 51, 1850 (1983)
3) D.H. Boal et al, Phys. Rev. Lett. 23, 2901 (1986)
4) T. Humanic et al, Z. Fur Physik 38, 79 (1988)
5) Z. Chen et al, Phys. Rev. C36, 2297 (1987)
6) G.I. Kopilov, M.I. Podgoretski, Sov. J. Nucl. Phys. 15, 219 (1972)

$^{40}Ar + {}^{68}Zn$ COLLISIONS : INCOMPLETE FUSION AND LIGHT PARTICLE EMISSION

J.P. COFFIN[a], A. FAHLI[a], P. FINTZ[a], G. GUILLAUME[a], B. HEUSCH[a], F. JUNDT[a], F. RAMI[a], P. WAGNER[a], A.J. COLE[b], S. KOX[b] and Y. SCHUTZ[c]

a) Centre de Recherches Nucléaires and Université Louis Pasteur, 67037 Strasbourg Cedex (France)

b) Institut des Sciences Nucléaires, 38026 Grenoble Cedex (France)

c) GANIL, B.P. 5027, 14021 Caen Cedex (France)

1. Motivation

With increasing projectile energy (~ 10 to 40 MeV/nucleon) in central collisions, incomplete fusion becomes preponderant with respect to complete fusion and the total fusion cross section is expected to decrease strongly. The aim of the present work was to gain some information about the incomplete fusion process and to contribute to a better understanding of the fall off of the fusion cross section.

The $^{40}Ar + {}^{68}Zn$ reaction has been investigated in a serie of experiments performed at 14.6, 19.6, 27.6 and 35 MeV/nucleon.

2. Results and discussion

The fusion-evaporation and fusion-fission components resulting from complete and incomplete fusion were identified and cross sections were measured for both components at all the energies. The velocity distributions of the evaporation residues were analyzed and the linear momentum transferred to the compound system deduced. The momentum transfer appears to depend on the asymmetry of the system and on the projectile mass when they are compared to other results. Fig. 1 shows the velocity of the evaporation residues, divided by the velocity of the compound nucleus formed by full momentum transfer, plotted against the relative velocity. The long-dashed curve represents theoretical predictions for the $^{40}Ar + {}^{68}Zn$ reaction and the short-dashed line corresponds to the Viola systematics. The mass, excitation energy and

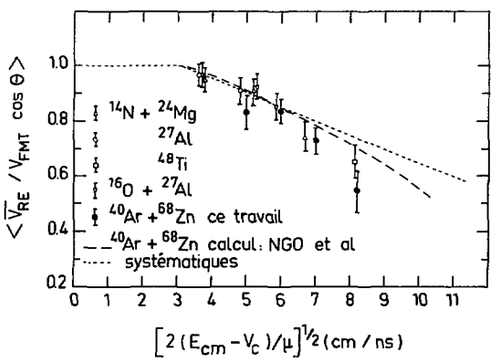

Fig. 1 :
Overall average velocity $\overline{V_{ER}}$ of the evaporation residues divided by V_{FMT} cosΘ plotted against the relative velocity.

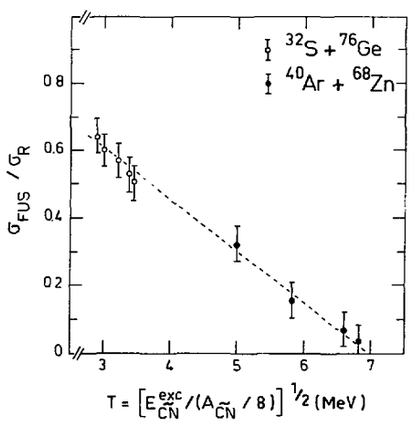

Fig. 2 :
Ratio of fusion to reaction cross sections plotted against the temperature of the reduced compound nuclei $\widetilde{CN}$.

temperature of the compound nuclei formed have been determined. Fig. 2 shows the ratio of fusion to reaction cross sections plotted against the temperature of the reduced compound nuclei. Fusion disappears slightly above 35 MeV/nucleon which corresponds to a compound nucleus excitation energy of 500 MeV (5.9 MeV/nucleon) and to a temperature of 6.8 MeV according to the simple parameterization $T = (E_{exc}/A_{CN}/8)^{1/2}$.

The nature of the falloff of the fusion cross section at higher energies remains an open question : although the reduced compound nucleus is highly excited, and may have reached the limit of stability, the large number of fast particles lost before fusion occurs may be responsible for this limitation.

The light charged particles emitted in the $^{40}Ar + ^{68}Zn$ reaction have been measured inclusively. The energy spectra were analysed in terms of preequilibrium emission, moving source and coalescence models. Moving source parameterization used in these calculations (Fig. 3) is in complete agreement with those deduced from heavy fragment analysis. At 14.6 and 19.6 MeV/nucleon, the data can be reproduced by assuming particle emission of statistical origin and from a sequential decay of the quasi projectile. At 35 MeV/nucleon a third source of intermediate rapidity is required. It can be correlated to the appearance of projectile fragmentation between 20 and 35 MeV/nucleon already observed in heavy fragment measurements. The emission of composite particles (d,t,α) raises the question of their production mechanism. Instead of being a preformed subset of nucleons they may result from the coalescence of nucleons. The coalescence model supposes that if a number A of nucleons has a relative momentum less than a given value p_o the nucleons form a composite particle. The coalescence radii of the thermalized volume related to p_o and extracted at 35 MeV/nucleon (~ 3 fm) may suggest the formation of a hot spot.

A complete coherence between the light particle data and those obtained separately from heavy fragment studies is obtained.

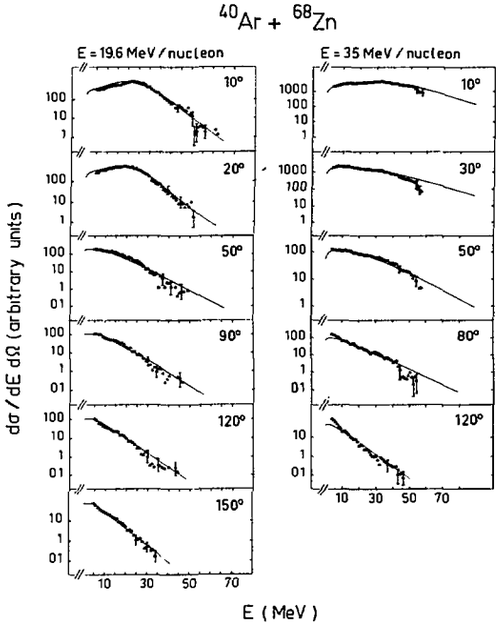

Fig. 3 :
Proton energy spectra measured at various angles and two incident energies. The solid curves correspond to the prediction of the moving source model.

3. References

G. GUILLAUME et al., Int. Conf. on Nucleus-Nucleus Collisions, Visby, Sweden (1985)

J.P. COFFIN et al., Symposium "Many Facets of Heavy-Ion Fusion Reactions", Argonne National Laboratory, U.S.A. (1986)

A.J. COLE et al., Workshop on hot Nuclei and Nuclear Disassembly, I.S.N. Grenoble, France (1986)

A. FAHLI et al., Phys. Rev. C34 (1986) 161

A. FAHLI, Thesis, Université de Strasbourg, France (1986)

A. FAHLI et al., Z. für Physik A326 (1987) 169

DENSITY FUNCTIONAL APPROACHES FOR THE DESCRIPTION OF COLD AND EXCITED NUCLEI *)

J. Bartel[1,a)], M. Brack[1)], C. Guet[2,b)], J. Meyer[3)], P. Quentin[4)], E. Strumberger[1,c)]

[1)] *Inst. f. Theor. Physik, Universität, D-8400 Regensburg*

[2)] *GANIL, B.P. 5027, F-14021 Caen*

[3)] *IPN, Univ. Lyon-I (and IN2P3), 43 bd du 11-11-1918, F-69622 Villeurbanne*

[4)] *Lab. Phys. Théor., Univ. Bordeaux-I (and CNRS), r. du Solarium, F-33170 Gradignan*

[a)] *permanent address: Phys. Théor., CRN, B.P. 20, F-67037 Strasbourg*

[b)] *permanent address: Service de Physique, DRF, CENG, F-38041 Grenoble*

[c)] *present address: Physik Department, TU München, D-8046 Garching*

*) *Work partially supported by the French-German exchange program 'PROCOPE'*

A systematic predictive description of nuclear properties either for cold systems (as exotic nuclei at low excitation energy) or for excited nuclei (as resulting from heavy ion collisions) is contingent upon the availability of microscopic calculations which should be both reliable and tractable. We report here on two contributions fitting in this broad framework which have been performed for a substantial part at GANIL. They use an effective interaction of the Skyrme type and the Hartree-Fock (HF) approximation, which together allow to express the total nuclear energy as a functional of the density matrix ρ.

One may furthermore simplify this functional, either by a suitable ansatz for the non-local part of ρ (cf. Sect. 1 below) or by performing a semiclassical approximation – which turns out to be exact at sufficiently high temperatures – in the extended Thomas-Fermi (ETF) approach (cf. Sect. 2 below).

1. Extended gaussian approximation for the density matrix [1]

A very simple parametrization for the nonlocality of ρ has been proposed as $\rho(\mathbf{R},\mathbf{s}) = \rho(\mathbf{R})(1-s^2/\alpha^2)exp[-s^2/(2\sigma^2)]$, where $\mathbf{R}$ and $\mathbf{s}$ are the center of mass and relative coordinates. In the above expression, α, σ are functionals of $\rho(\mathbf{R})$ which are chosen to yield the

correct local semiclassical kinetic energy density as well as the projector character of ρ in an integrated form.

The validity of this ansatz has been assessed in various nuclei for physical quantities sensitive to the non-local nature of the density matrix, such as the momentum distribution in the nucleus, the exchange energies for the Gogny and Coulomb forces and the two-body center of mass energy correction. In all cases, a very good overall agreement with exact (i.e. HF) results has been found. It had in most cases a better quality than previous approaches, such as the Slater or DME approximations. Obviously, the full relevance of the proposed phase-space distributions should be tested in dynamical calculations.

2. Liquid drop parameters for hot nuclei [2]

Highly excited nuclei at temperatures $T \gtrsim 3\ MeV$ exhibit no shell structure and can thus be ideally described by semiclassical methods, such as the ETF density variational method which has been widely employed for the selfconsistent description of average nuclear properties. For many practical applications, a droplet model type expansion of the nuclear free energy has been found useful and sufficient. The coefficients of this expansion have been determined selfconsistently from one of the most successful Skyrme forces (SkM*) as functions of the temperature T. They were further approximated by a low-temperature expansion quadratic in T and valid up to $T \simeq 4\ MeV$.

The application of these parameters in a very simple evaluation of the temperature dependent fission barriers of heavy nuclei has been shown to rather well reproduce the results of the more time-consuming variational ETF calculations.

The dependence of the infinite-nuclear-matter incompressibility on the temperature, which plays an important role in the equation of state, relevant e.g. in astrophysical supernovae calculations, was also discussed.

[1] J. Meyer, J. Bartel, M. Brack, P.Quentin, S. Aicher, Phys. Lett. **B 172** (1986) 122

[2] C. Guet, E. Strumberger, M. Brack, Phys. Lett. **B 205** (1988) 427

Static Properties of Hot Nuclei*

E. Suraud[1]

Institut des Sciences Nucléaires
53 Avenue des Martyrs, F-38026 Grenoble Cedex , France

1) Present address : GANIL, BP5027, F14021 Caen cedex, France

Heavy-ion collisions at intermediate energy (10-100 MeV/A) offer a very useful tool for investigating the properties of nuclei at finite temperature. Experimental evidences for the formation of such excited systems ($E^*/A \leq$ 2.5-3 MeV, $T \leq 5$ MeV) are now well established (see Ref [1] for a recent review). From a theoretical point of view the formation of hot nuclei has been studied within the framework of dynamical approaches [1,2], but their properties, once formed, may be described in a static picture, at least for a restricted amount of time [1,3]. One can then picture out the system as a hot nucleus in equilibrium with its own evaporated nucleons. The major difficulty is then to properly take into account the effects of evaporated nuclei.

An elegant solution to this problem was recently proposed by Bonche, Levit and Vautherin (BLV, [4]) in the framework of quantal Hartree-Fock (HF) calculations. These authors propose to isolate the "liquid" contribution by performing simultaneously two mean field calculations, one for the nucleus in equilibrium with its evaporated nucleons and one for the nucleon gas alone. These two "phases" are coupled by the Coulomb interaction which is calculated from the "liquid" proton density alone. However, these fully quantal calculations are very heavy, numerically speaking, in particular at high temperature. As shell effects are known to disappear at around T≈ 2-3 MeV [1] it is very interesting to develop semi-classical approximations [5] of the BLV formalism [6]. It turns out that these approximations allow to reproduce very accurately average quantal values while remaining much more tractable. A detailed study of these methods and a comparison with HF results is presented in Ref [6]. In the following we shall hence only focus on some physical applications.

*) Part of this work was done at the IPN, Orsay, France.

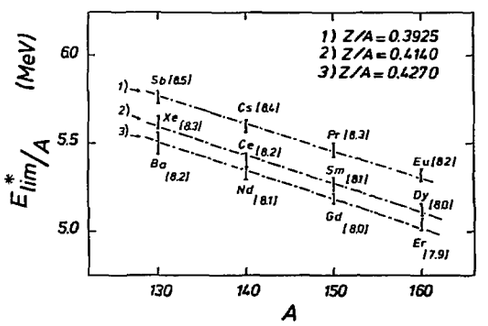

Figure 1
Limiting excitation energies of various nuclei in the A=130-160 mass region and along some Z/A lines. Also are indicated the corresponding limiting temperatures. The dashed-dotted line is only given for guiding the eye, presented results corresponding to actual microscopic calculations.

In the framework of BLV calculations hot nuclei exhibit a limiting temperature beyond which no solution to the coupled probem can be found ânymore [4]. One can show that this "instability" is due to the Coulomb interaction which overcome the nuclear stabilizing effect at high temperatures (T≈ 8 MeV). We have performed a systematic study of this phenomenon in the A= 150 mass region for which experimental data were avaiable [7]. Calculations have been done with the SKM Skyrme interaction and with various semi-classical approximations for the energy density functional [5]. Results are shown in Figure 1 were the limiting temperatures and excitation energies are plotted in this mass region. As suggested by schematic calculations [8] we find that the charge over mass ratio is a relevant parameter for the study of this limiting phenomenon.

The study of the temperature dependance of the level density parameter is also a subject of large interest [1] and we have hence used our

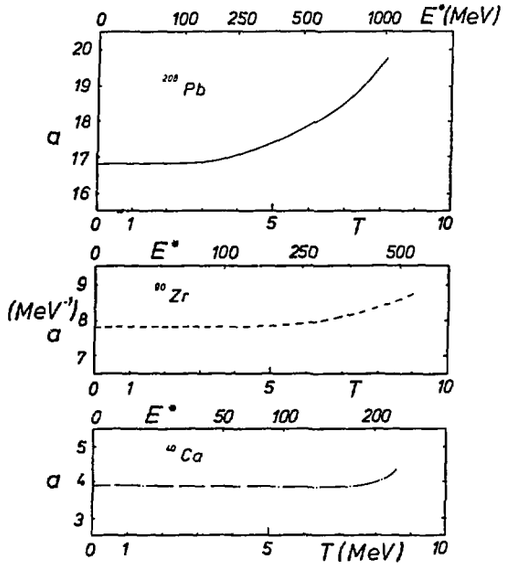

Figure 2
Temperature dependance of the mean field part of the level density parameter of 3 nuclei. The plotted quantity essentially reflects the temperature evolution of the single particle level density around the Fermi energy. Note that heavy nuclei are more sensitive to temperature than lighter ones with larger Z/A ratios.

semi-classical BLV approach to study its mean field part. In the lowest order semi-classical approximation the level density can be simply expressed in terms of integrals involving the single particle potentials associated to the two coexisting phases [9]. As can be seen in Figure 2, it turns out that up to about T≈ 4 MeV the effect of temperature is negligible so that, as a first approximation, zero temperature values (a≈A/8) can still be used, for example in estimating densities of states. In order to understand the possible effects on " a " at around T≈ 4 MeV one has however to include corrections beyond the mean field for which the temperature plays a more important role [10].

In this work we have investigated some static properties of hot nuclei in the framework of the semi-classical counterpart of the BLV subtraction procedure. We have found a very good agreement between the semi-classical values and the average quantal results. We have performed a detailed study of the limiting temperature of hot nuclei. The experimental study of this kind of situation remains an exciting subject, with the forthcoming possibility of accelerating heavy beams at moderate energies. Our study of the level density parameter has also shown the almost temperature independance of the mean field contribution in this quantity.

References

[1] E. Suraud, Ch, Grégoire and B. Tamain, to appear in Progress of Nucl. Part. Sci (1989)
[2] G.F. Bertsch and S. Das Gupta, Phys. Rep. **160** (1988) 189
[3] J. Treiner , Nucl. Phys. **A488** (1988) 279c
[4] P. Bonche, S. Levit and D. Vautherin, Nucl. Phys. **A427** (1984) 278 and Nucl. Phys. **A436** (1985) 265
[5] M. Brack, C. Guet and H.K. Hakansson, Phys. Rep. **163** (1985) 276
[6] E. Suraud, Nucl. Phys. **A462** (1987) 109
[7] B. Borderie and M.F. Rivet, Zeit. Phys. **A321** (1985) 703
[8] P. Bonche and S. Levit, Nucl. Phys. **A437** (1985) 426
[9] E. Suraud, P. Schuck and R.W. Hasse, Phys. Lett. **B164** (1985) 212
[10] R.W. Hasse and P. Schuck, Phys. Lett. **B179** (1986) 313

PROPERTIES OF HIGHLY EXCITED NUCLEI

P. BONCHE

Service de Physique Théorique, CEN Saclay, 91191 Gif-sur-Yvette Cedex, France

S. LEVIT

Department of Nuclear Physics, Weizmann Institute of Science, 76100 Rehovot, Israel

and

D. VAUTHERIN

Division de Physique Théorique, Institut de Physique Nucléaire[1]*, 91406 Orsay Cedex, France*

Received 24 October 1983
(Revised 20 March 1984)

Abstract: A prescription is proposed for calculating the contribution of unbound states in nuclear Hartree–Fock calculations at finite temperature. The method is based on the remark that a static Hartree–Fock calculation at finite temperature describes a hot nucleus in equilibrium with an external nucleon vapor. Properties of the hot nucleus including continuum effects are obtained by extracting the contribution of the external gas, which we calculate from a second Hartree–Fock calculation. We show that for a one-body potential this subtraction procedure yields standard formulae for partition functions in terms of phase shifts. Numerical calculations are performed in ^{56}Fe and ^{208}Pb. The resuls indicate that continuum contributions are large beyond temperatures of the order of 4 MeV. We also find the existence of a critical temperature, of the order of 10 MeV, beyond which solutions of the equations can no longer be found.

CONTRIBUTION AS SENT BY THE AUTHOR

Nuclear Physics A428 (1984) 95c-100c
North-Holland, Amsterdam

MEAN-FIELD DESCRIPTION OF NUCLEI AT HIGH TEMPERATURE

Paul BONCHE

Service de Physique Théorique, CEN SACLAY, 91191 Gif-sur-Yvette Cedex,France

Shimon LEVIT

Department of Nuclear Physics, Weizmann Institute of Sciences, 76100 Rehovot, Israël

Dominique VAUTHERIN

Institut de Physique Nucléaire, Division de Physique Théorique*, 91406 Orsay Cedex, France

We propose and discuss a prescription suitable to include the contribution of continuum states in mean-field calculations at high temperature.

CONTRIBUTION AS SENT BY THE AUTHOR

Nuclear Physics A436 (1985) 265–293

STATISTICAL PROPERTIES AND STABILITY OF HOT NUCLEI

P. BONCHE

Service de Physique Théorique, CEN, Saclay, 91191 Gif-sur-Yvette, Cedex, France

S. LEVIT

Department of Nuclear Physics, Weizmann Institute of Science, Rehovot 76100, Israel

and

D. VAUTHERIN

Institut de Physique Nucléaire, 91405 Orsay Cedex, France*

Received 6 June 1984
(Revised 6 September 1984)

Abstract: Results of temperature-dependent Hartree-Fock calculations for equilibrated hot nuclei are presented, extending to the highest temperatures at which the nuclei remain stable. A subtraction procedure developed earlier for isolating the properties of the nucleus from the nucleus+vapor system is applied. The temperature dependence of various quantities characterizing hot nuclei is investigated. The influence of different effective interactions in the Hartree-Fock equations is examined. Special attention is devoted to the study of the high-temperature stability limit of hot nuclei. This limit in nuclei with the Coulomb interaction artificially switched off (i.e. uncharged nuclei) is shown to correspond to the critical temperature of the liquid-gas phase transition expected on the basis of hot nuclear matter calculations. In realistic charged nuclei the Coulomb repulsion causes a nucleus to become electrostatically unstable and to fall apart at much lower temperatures than its uncharged partner. The approach to and the temperature of this Coulomb instability are very sensitive to the choice of the nuclear interaction. Studying this instability in compound nuclei with different charge-to-mass ratio provides a sensitive measure of the temperature dependence of the nuclear surface properties as well as of certain features of the nuclear equation of state.

CONTRIBUTION AS SENT BY THE AUTHOR

THOMAS–FERMI CALCULATIONS OF HOT DENSE MATTER

E. SURAUD and D. VAUTHERIN
Division de Physique Théorique [1], *Institut de Physique Nucléaire, 91406 Orsay Cedex, France*

Received 5 December 1983

We use the imaginary time-step method to perform fully variational Thomas–Fermi calculations at finite temperature. Results are given for hot nuclei and for the equation of state of the hot dense matter present in the late stages of stellar evolution. Transitions between various phases are calculated and a comparison with the results of Hartree–Fock calculations is given.

CONTRIBUTION AS SENT BY THE AUTHOR

EVOLUTION OF HOT COMPRESSED NUCLEI IN THE TIME-DEPENDENT HARTREE–FOCK APPROXIMATION ☆

D. VAUTHERIN [1]
Center for Theoretical Physics, Laboratory for Nuclear Science and Department of Physics, Massachusetts Institute of Technology, Cambridge, MA 02139, USA

J. TREINER and M. VÉNÉRONI
Division de Physique Théorique [2], Institut de Physique Nucléaire, F-91406 Orsay Cedex, France

Received 29 July 1986; revised manuscript received 12 March 1987

Spherical solutions of the TDHF equations are computed for initial conditions corresponding to hot nuclei under different compressions. Special care is devoted to the emission of particles and to the resulting separation between liquid and vapor phases.

CONTRIBUTION AS SENT BY THE AUTHOR

Nuclear Physics A422 (1984) 140–156

TEMPERATURE DEPENDENCE OF COLLECTIVE STATES IN THE RANDOM-PHASE APPROXIMATION

D. VAUTHERIN and N. VINH MAU

Division de Physique Théorique[1], *Institut de Physique Nucléaire, F-91406 Orsay Cedex, France*

Received 25 November 1983

Abstract: We investigate the temperature dependence of collective states in the framework of the random-phase approximation at finite temperature. We show that sum rules can be extended to collective energies at finite temperature. Numerical methods are developed to solve the RPA equations at finite temperature. Results are presented and discussed in the case of ^{40}Ca for isovector dipole and isoscalar octupole vibrations, using oscillator wave functions and a zero-range force. We show that the broadening of giant dipole resonances observed experimentally, appears as a natural consequence of the structure of the RPA equations. Comparison is made with the schematic model for which the temperature dependence of collective states can be worked out analytically.

CONTRIBUTION AS SENT BY THE AUTHOR

NUCLEAR PARTITION FUNCTIONS IN THE RANDOM PHASE APPROXIMATION AND THE TEMPERATURE DEPENDENCE OF COLLECTIVE STATES

D. VAUTHERIN and N. VINH MAU
Division de Physique Théorique[1], *Institut de Physique Nucléaire, F-91406 Orsay Cedex, France*

Received 16 September 1982

Green functions techniques at finite temperature are used to calculate nuclear partition functions in the random phase approximation. The theory is shown to yield corrections to the results of functional methods neglecting exchange terms. We discuss the special case of a schematic model for which the level density and the temperature dependence of collective states can be worked out explicitly.

CONTRIBUTION AS SENT BY THE AUTHOR

Nuclear Physics A458 (1986) 460-474
North-Holland, Amsterdam

EFFECT OF CORRELATIONS ON THE RELATION BETWEEN EXCITATION ENERGY AND TEMPERATURE

T. TROUDET. D. VAUTHERIN and N. VINH MAU

Division de Physique Théorique, Institut de Physique Nucléaire, F-91406 Orsay Cedex, France*

Received 18 November 1985
(Revised 15 May 1986)

Abstract: Formulae for the excitation energy of a nucleus as a function of its temperature are derived in the framework of the random phase approximation (RPA). Two methods are investigated. We first calculate the energy as the derivative of the grand potential obtained in random phase approximation. We also calculate the energy as the thermal average of the Hamiltonian operator using RPA Green functions at finite temperature. The two methods are compared by analyzing their content in terms of diagrams. We also discuss the effect of correlations on the relation between chemical potential and particle number.

CONTRIBUTION AS SENT BY THE AUTHOR

Windsurfing the Fermi Sea, Volume II
T.T.S. Kuo and J. Speth (editors),

THE LEVEL DENSITY PARAMETER OF A NUCLEUS IN THE SCHEMATIC MODEL*

D. VAUTHERIN†

Center for Theoretical Physics, Laboratory for Nuclear Science, and Department of Physics, Massachusetts Institute of Technology, Cambridge, Massachusetts 02139, U.S.A.

and

N. VINH MAU

Division de Physique Théorique,‡ Institute de Physique Nucléaire, F-91406, Orsay, Cedex, France

The level density parameter of a nucleus is calculated in the random phase approximation using the schematic model of Brown and Bolsterli. Using the known collective states in lead-208, we find that RPA correlations increase the level density parameter by 30% at low temperature. This increase disappears near $T = 4 - 5$ MeV in qualitative agreement with the recent measurements by Nebbia *et al.*

CONTRIBUTION AS SENT BY THE AUTHOR

INSTABILITIES IN AN EXPANDING FIREBALL

J. Cugnon
Université de Liège, Physique Nucléaire Théorique, Institut de Physique au Sart Tilman, B.5, B-4000 LIEGE 1, Belgium

The idea that the dynamical origin of the multifragmentation could be due to spontaneously growing instabilities, linked with the entrance of the system in the so-called spinodal zone was first proposed in ref. [1], and later discussed in ref. [2]. We recall here the basic ideas and list the remaining problems.

A piece of matter, heated and compressed, expands, due to the work of its bulk pressure. There are good reasons to believe that the system evolves along an isoentrope. If the initial entropy per baryon is lower than ~ 2 units, the system will be unstable under any density fluctuation when it enters the iscentropic spinodal zone (see ref. [1]). This is substantiated by the change in free energy induced by a density oscillation of amplitude a ($\delta\rho = a\, e^{i\vec{k}.\vec{r}}$) in nuclear matter. Fig. 1 illustrates this point.

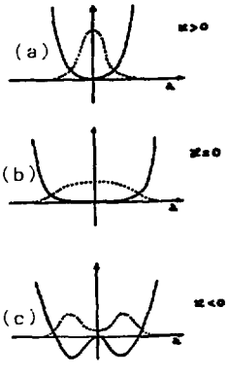

Fig. 1. Full curves : variation of the free energy necessary to create a fluctuation of amplitude a outside (a), inside (c) or at the boarder (b) of the isoentropic spinodal. Dotted curves : probability of observing a fluctuation in a canonical calculation.

Even though there is a large consensus on the relevance of this scenario for the dynamical origin of the fragmentation, many points are still to be clarified :

1. What are the importance of the finite size and surface effects ? Evaporation, i.e. the appearance of a gazeous phase at the surface more or less stabilizes the inner core[3].

2. Nuclear matter is a Fermi liquid. Perturbations do not propagate as in an ordinary fluid. Does this matter ? This question has been investigated in ref. [2], where it is shown that the stability of the matter is increased by this aspect.

3. How to describe the evolution of the instabilities ? How do they lead to the birth of clusters. Several lines of approach have been studied in condensed matter physics, especially the phase separation occuring after the quenching of a ferromagnet above the Curie point[4]. Transport theories, still at a phenomenological stage, have been devised[5], which describe the separation of ferromagnetic and diamagnetic domains. The nuclear case is more difficult because of surface tension and because of the expansion of the system.

4. It may be questioned whether the phase separation may take the form of bubble formation and growth. The strong nuclear surface tension as well as the surface thickness cooperate in such a way that only bubbles with large sizes can survive. This is shown by a study of bubble dynamics[6]. The critical radius may be as large as 4-5 fm. A similar conclusion is arrived at in a recent microscopic study of static bubble energy[7].

5. Is there some scaling law as in critical phenomena ? Experimentally, such laws seem to hold[8]. Apparently, the granular nature of nuclear matter do not play an important role.

In conclusion, according to this scenario, the onset of multifragmentation (energy, size,...) could depend upon the characteristics of the spinodal and of transport properties, but the mass yield may just depend upon a few critical exponents, which presumably do not depend much upon the equation of state.

1) J. Cugnon, Phys.Lett. 135B (1984) 374.
2) C.J. Pethick and D.G. Ravenhall, Nucl.Phys. A471 (1987) 19c.
3) N. Nemeth et al., Z.Phys. A323 (1986) 419.
4) J.W. Cahn and J.E. Hillard, J.Chem.Phys. 31 (1959) 688.
5) J.D. Gunton et al., Phase Transitions and Critical Phenomena, vol. 8, (1983) 1.
6) J. Cugnon, to be published.
7) H. Flocard et al., to be published.
8) X. Campi et al., Phys.Lett. 142B (1984) 8.

– B3 –
MULTI-FRAGMENT EMISSION

A SCHEMATIC HYDRODYNAMICAL AND PERCOLATION PICTURE FOR MULTIFRAGMENTATION OF EXCITED NUCLEI

J. Nemeth*, M. Barranco**, J. Desbois***, C. Ngô**** and R. Boisgard****

*Institute for Theoretical Physics, Eötvos University, Budapest, Hungary
** Departament de Fisica, Universitat de les Illes Balears, E-07071 Palma de Mallorca, Spain
*** Division de Physique Théorique+, Institut de Physique Nucléaire, 91406 Orsay Cédex, France
**** Laboratoire National Saturne, CEN Saclay, 91191 Gif sur Yvette Cédex, France.

Multifragmentation can occur in violent heavy ion collisions. In order to understand what conditions are required to reach this kind of break-up we propose the following simple model[1].

We start with an initial hot and compressed nucleus and assume that it remains spherical during its evolution (a rather drastic constraint, of course). The hot and compressed nucleus expands and this process is described by a time dependent Thomas Fermi model (TDTF)[2]. This expansion is assumed to be isentropic, which is probably a very good approximation in regards to cascade calculations performed for heavy ion collisions at higher bombarding energies[3]. The result of such a calculation is presented in Fig.1 where a ^{208}Pb nucleus is considered (Full line : initial density, dashed curve : density profile at t = 10^{-22}s ; E_c^* and E_T^* are, respectively, the initial compressional and thermal excitation energies).

At each stage of the expansion, the magnitude of the fluctuations of the mean field is evaluated using a 3-dimensional site-bond percolation model on a cubic lattice[4]. We recall that such a percolation is governed by two parameters :

- p, the fraction of occupied sites ;
- q, the probability that two neighbours occupied sites are linked.

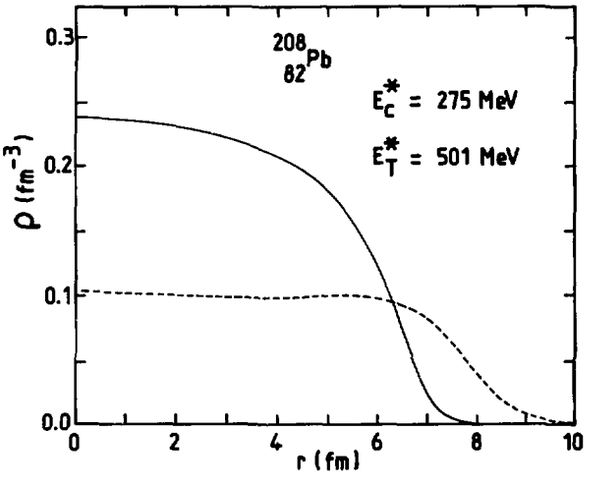

Fig.1

The connection between percolation and TDTF is made as follows :

$$p(t) = \frac{\langle \rho(t) \rangle}{\langle \rho_o \rangle} \quad \text{and} \quad q(t) = 1 - \frac{\varepsilon^*_T(t)}{B(t=o)}$$

where $\langle \rho(t) \rangle$ ($\langle \rho_o \rangle$) are the average densities at time t (t=o), B (t=o) is the binding energy per nucleon at time t=o and $\varepsilon^*_T(t)$ is the thermal excitation energy per nucleon at time t. So,

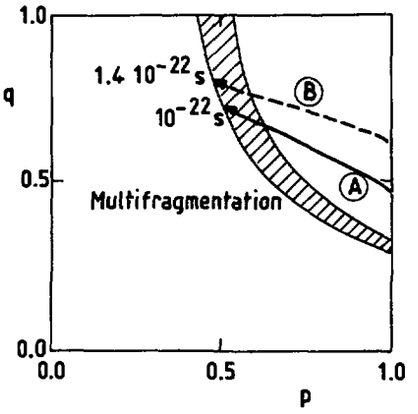

Fig.2

we can follow the dynamical evolution of the nucleus in p - q plane. The case of a ^{208}Pb nucleus is depicted in Fig.2 with two different sets of initial conditions :

A E_c^* = 102 MeV, E_T^* = 799 MeV
B E_c^* = 275 MeV, E_T^* = 501 MeV

As long as the fluctuations of the mean field remain small, the mean field approach used to describe the expansion process is perfectly suited. However, it can happen that this is no longer the case. Then, the nucleus breaks up into several pieces. Such a phenomenon is expected to occur for both cases in Fig.2 : the multifragmentation region is reached after the time indicated in the figure.

The most significant result of this model is that compressional energy turns out to be more efficient to break up nuclei than thermal energy. This is illustrated in Figs.3-4.

+ Unité de Recherche des Universités Paris 11 et Paris 6 Associée au C.N.R.S.

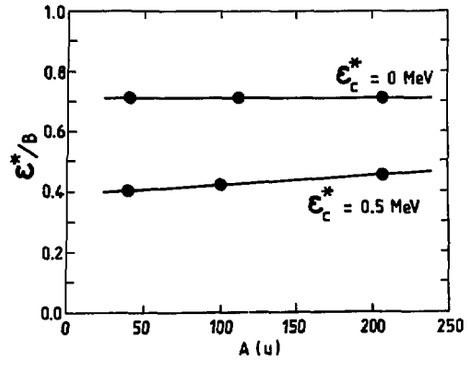

Fig.3

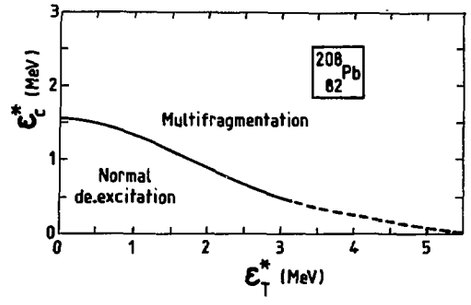

Fig.4

In Fig.3, we have plotted the quantity ε^*/B (ε^* : critical excitation energy per nucleon to undergo multifragmentation, B : binding energy per nucleon) as a function of the mass A of the initial nucleus. The two curves correspond to two different values ε_c^* of the initial compressional energy per nucleon. In Fig.4, we show the phase diagram of a ^{208}Pb nucleus in the plane $\varepsilon_c^* - \varepsilon_T^*$. We can see that a small amount of compressional energy greatly lowers the total excitation energy needed for the break-up.

This effect can be easily understood if one remembers that thermal excitation corresponds to desorganized energy while compression corresponds to coherent energy in the mode of instability.

To conclude, concerning our model, we want to say that a dynamical calculation, without any condition of spherical symmetry, is highly desirable. So, we expect that multifragmentation could occur dynamically, without recourse to percolation. Work in that direction is currently in progress.

1) J. Nemeth et al., Z. Phys. A325 (1986) 347 ; J. Desbois et al., Z. Phys. A328 (1987) 101.
2) J. Nemeth et al., Z. Phys. A323 (1986) 419.
3) G. Bertsch et al., Phys. Rev. C24 (1981) 2514.
4) J. Desbois, Nucl. Phys. A466 (1987) 724 ; X. Campi et al., Contribution to the XXIII Int. Winter Meeting on Nuclear Physics, Bormio (1985) p.497.

RESTRUCTURED AGGREGATION COUPLED TO LANDAU-VLASOV MODEL

S. Leray[1], C. Ngô[1], B. Remaud[2], F. Sébille[2] and M.E. Spina[1]

[1] Laboratoire National Saturne
[2] Université de Nantes

A central collision between two nuclei leads to the formation of a highly excited and compressed system. Before thermal equilibrium is reached, fast particles remove a large part of the available energy. When thermalization has been achieved the system is still hot and compressed, so it expands and cools down. If the expansion phase leads to a very low density situation the formation of clusters can be expected and thus multifragmentation can occur. Indeed, while a nuclear medium at normal density can be described by the mean field created by the whole set of the nucleons, at low density the distance between neighbouring nucleons can become larger than the range of nuclear forces. Thus, density fluctuations are important and some nucleons are close enough to each other to interact and therefore form clusters. Due to repulsive Coulomb force between the created clusters, the system disassembles. It is clear that in this case the mean field approximation is no longer valid and that calculations based on this approximation have to be stopped at the point where the fluctuations of the mean field become too large.

In the intermediate energy domain the model of Grégoire et al[1)] which uses the Landau-Vlasov (LV) equation has proved to be very successful in describing experimental data associated with one body observables. In order to study the possible disassembly of the system we couple the LV calculation, which describes the dynamical evolution of the system, to the restructured-aggregation model[2)] described elsewhere in this compilation[3)], which evaluates the fluctuations of the mean field. With this approach we know when the fluctuations of the mean field are too important to carry on the LV calculation. When this happens, we stop the LV calculation. The mass distribution of the fragments is obtained with the restructured-aggregation model and can be compared to the experimental one if we assume that the clusters are no longer modified as they separate.

This model was applied to the system $^{197}Au+^{197}Au$ at 200 MeV/u. In fig.1 we present the yield of clusters as a function of their mass at different time steps and at zero impact parameter. At 40 and 50 fm/c most of the nucleons aggregate into a big fragment. This

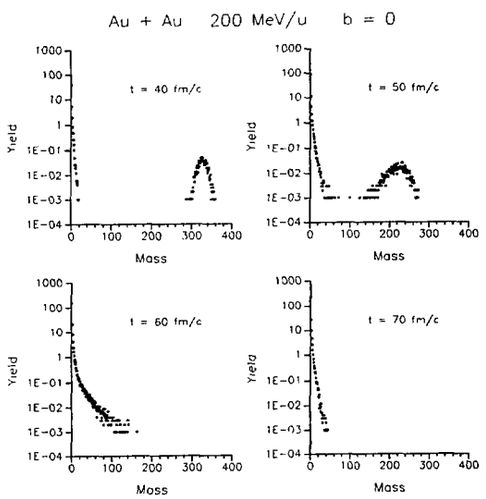

Fig.1. *Mass distribution of the fragments obtained at different time steps during the collision for the system Au + Au at 200 MeV/u*

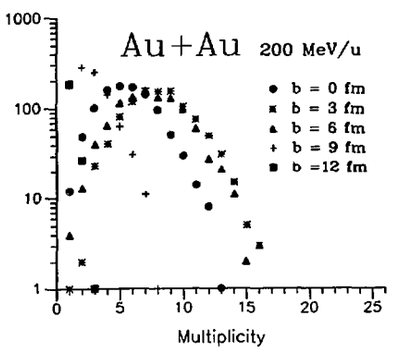

Fig.2. *Fragment multiplicity distribution as a function of impact parameter for the Au + Au system calculated at 60 fm/c.*

means that a mean field approximation is still valid and that we can carry on the LV calculation. On the other hand at 60 and 70 fm/c only small mass fragments are left indicating that the system has undergone multifragmentation. Several impact parameters were studied : for 0≤b≤6 fm the transition occurs around 55 fm/c in less than 10 fm/c, while at b=9 fm we do not reach a probability equal to one and the mass distribution shows that there is always a fragment of mass around 100 left, which would correspond to spectators in a participant-spectator picture. At b=12 fm the probability remains zero since the two nuclei reseparate without loosing there identity. In fact, multifragmentation arises when the density of the system has decreased down to around 0.4 times the initial value, the same as when studying the onset of multifragmentation in a single nucleus with variable density[3].

The system $^{197}Au+^{197}Au$ at 200 MeV/u was studied by Doss et al[4]. In this experiment intermediate mass fragments with 3≤Z≤10 were detected in the forward center of mass hemisphere and the centrality of the collision was evaluated through the total charged particle multiplicity. We can compare the experimental multiplicity distributions (fig.4 of ref.[4]) to our calculation. In our case the intermediate mass fragments have mass between 6 and 25. The distributions are taken at 60 fm/c when the system has undergone multifragmentation and are shown in Fig.2. The general trends of the data are rather well reproduced : for central collisions (0≤b≤6) the distributions are similar while their maximum is shifted towards lower multiplicity values when the collision becomes more and more peripheral. The mean value of the multiplicity is also rather well reproduced by our model.

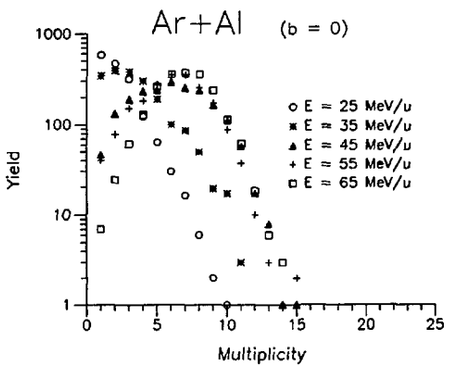

Fig.3. *Fragment multiplicity distribution obtained at different bombarding energies.*

Some experiments were performed at Ganil on the Ar+Al system at different bombarding energies[5,6] and it has been claimed that multifragmentation begins to appear between 25 and 36 MeV/u. We have applied our model to this system at 25, 35, 45, 55 and 65 MeV/u for zero impact parameter. We found that multifragmentation begins to be present at 35 MeV/u as observed experimentaly, but represents a significant part of the cross section only above 45 MeV/u. What is different from the Au+Au system is that the probability of multifragmentation is never 100 % in this range of energies (even at 65 MeV/u it reaches only 98 % at maximum). If we stop the LV calculation when the probability of multifragmentation is maximum we can construct multiplicity distributions for particles with mass between 2 and 20 as Fig.3 shows. It can be observed that there is a substantial difference between the 25, 35 MeV/u and the three other energies. As in fig.2 for the multiplicity distributions obtained for different impact parameters it seems that the shape of multiplicity distribution can be a probe for the occurrence of multifragmentation. Our results are in qualitative agreement with the ones of ref.[6] which show a difference in the multiplicity spectra between 25 and 36 MeV/u. This difference was attributed to the appearrance of multifragmentation. However, in our case, the difference is more significative between 35 and 45 MeV/u.

1) C.Ngô et al, Nucl. Phys. in press.
2) C.Grégoire et al, Nucl. Phys. **A436** (1985) 365.
3) S.Leray et al, this compilation.
4) K.G.R.Doss et al, Nucl. Phys. **A471** (1987) 241c.
5) G.Auger et al, Phys. Lett. **169B** (1986) 161.
6) G.M.Jin et al, 3rd Int. Conf. on Nucleus Nucleus Collisions, Saint-Malo (1988)

MULTIFRAGMENTATION AND RESTRUCTURED AGGREGATION

S. Leray[1], C. Ngô[1], H. Ngô[2] and M. E. Spina[1]

[1] Laboratoire National Saturne, [2] Physique théorique, IPN Orsay

We have developed a restructured aggregation model to study nuclear multifragmentation [1]. The aim of this approach is to try to evaluate the importance of the fluctuations of the mean field and thereby to find when the system becomes unstable with respect to multifragmentation. In this model each nucleon is supposed to be represented by a sharp sphere of radius r_0 = 1.03 fm. This value corresponds to about the range of the nuclear forces. For a given configuration of a system of mass A, one draws at random the position of the A nucleons and look if they overlap. Some of them do. In this case the overlapping nucleons are supposed to restructure in a single sphere of radius $R = 1.15\ A_c^{1/3}$, where A_c is the mass of the cluster. After a first iteration one is left with a distribution of clusters and nucleons. Some of these particles may still overlap due to the restructuration. If it is the case, one iterates again the aggregation process and the restructuration until no overlap exists anymore. In the end one is faced with two situations : either there is a percolation cluster or not. In the first case the fluctuations of the mean field are small while they are large in the second case which ends by multifragmentation. This process, done for a particular sampling of the nucleons, is repeated several times in order to generate an ensemble average and study average properties.

In order to illustrate the kind of result that one can obtain with a restructured aggregation model, let us present some results of ref. 1. Fig. 1 shows the mass distribution of the products obtained for a ^{208}Pb nucleus at different densities ρ :

- There are two components in the mass distribution for ρ=0.07 fm^{-3}: one, peaked around mass 200, corresponds to the percolation cluster. The other component, at smaller mass values, contains the nucleons and the light mass clusters. This mass distribution is typical of a situation in which the fluctuations of the mean field are small.
- For ρ = 0.04 fm^{-3} the shape of the mass distribution is completely different. The percolation cluster has disappeared and it remains a component containing light and medium mass fragments only. In this case, the fluctuations of the mean field are large and the system disassembles.
- The two other examples ρ = 0.06 fm^{-3} and ρ = 0.05 fm^{-3}, are in the transition region where one goes from percolation to multifragmentation.

Due to the small number of particles present in the system and to its finite size, a given event can lead to a percolation cluster or to multifragmentation with a probability which varies smoothly with the density of the system. For an infinite system the size of the percolation cluster is infinite. When it disappears the mass of the largest cluster drops suddenly. For nuclei, we do not have such an evolution but rather a continuous decrease of the size of the largest cluster. In order to estimate the influence of the finite size of the system it has been assumed that one has a percolation cluster if the size of the largest cluster is larger than half the initial mass of the system. Consequently, for a given event, the system undergoes multifragmentation only if the size of the largest cluster is smaller than half the

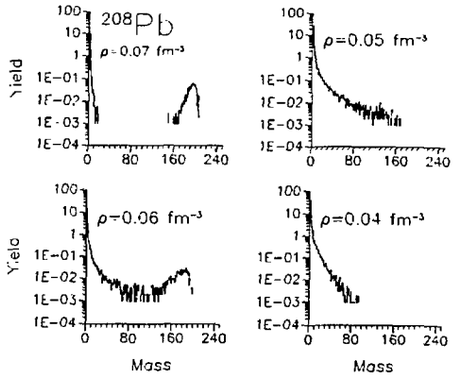

Fig. 1

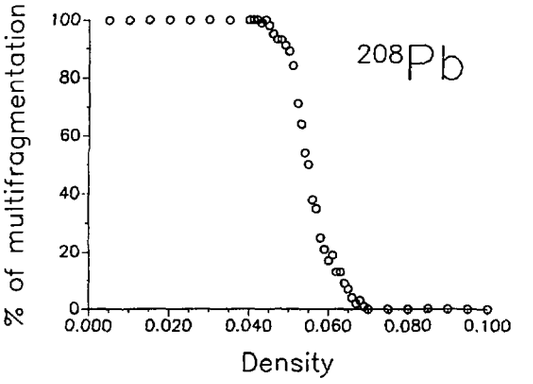

Fig. 2

initial mass of the system. This is arbitrary but one cannot avoid to introduce a convention (which of course could be chosen differently) due to the smoothness of the transition. The multifragmentation probability is deduced by averaging over many different events for each density. The results for the ^{208}Pb are shown in fig.2. Multifragmentation appears for density values between 0.06 and 0.07 fm^{-3} and the multifragmentation probability is equal to unity below ρ = 0.04 fm^{-3}. Similar results are obtained for the ^{40}Ca nucleus but the transition is smoother due to the smaller number of particles.

The smooth evolution due to the small number of particles contained in the system is illustrated also in fig.3 which shows the correlation between A_{max}, the mass of the largest cluster, and the density of the system. As we see, there is a continuous evolution of A_{max} as ρ decreases and the transition is not sharp.

It is interesting to perform a moment analysis as suggested by Campi [2]. For example the correlation between Log S_2 and Log S_3 (see ref.[2] for a definition of the moments) is related to the critical exponent τ entering into the inclusive mass distribution of the fragments. It is shown in fig 4 for an ensemble of multifragmentation events at different densities. This correlation is almost linear and, from the slope of the average behaviour of Log S_3 as a function of Log S_2, one finds τ = 2.2 which is very close to the value deduced from emulsion experiments (τ=2.2±0.1) [3].

[1] C.Ngô, H.Ngô, S.Leray and M.E.Spina, preprint
[2] X.Campi, J. Phys.A : Math. Gen. 19 (1986) 1917.
[3] C.J.Waddington and P.S.Freier, Phys. Rev. C31 (1985) 888.

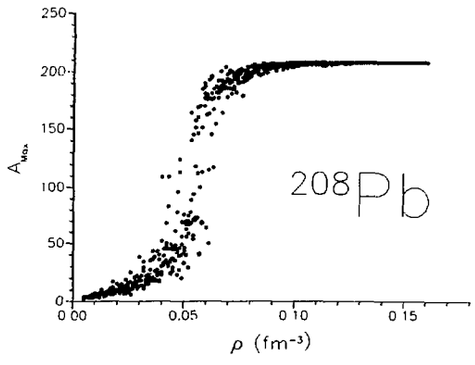

Fig.3

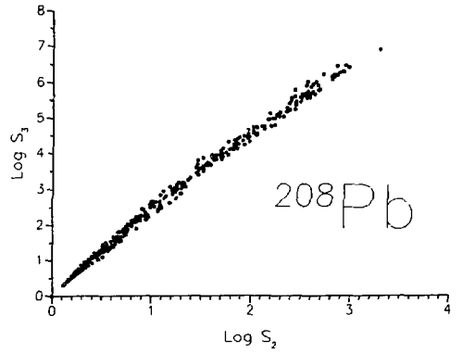

Fig.4

CONTRIBUTIONS TO THE DESCRIPTION AND UNDERSTANDING OF NUCLEAR FRAGMENTATION

J. RICHERT*, S.K. SAMADDAR**, P. WAGNER*

*Centre de Recherches Nucléaires et Université Louis Pasteur, Strasbourg, France
**Permanent address : Saha Institute of Nuclear Physics, Calcutta, India

The study of nuclear fragmentation is aimed to describe and explain how and why strongly excited nuclei can decay into many pieces. Experimental and theoretical investigations have lead to several questions most of which remain unsettled up to now. Among other points one may think about the dynamical time evolution of the multifragmentation which may develop sequentially or correspond to a violent quasi instantaneous process. This may depend on the energy regime, the details of the nature and range of the interactions among the constituents which are involved and the conditions under which the excited system is generated. Another point concerns the interesting question whether the multifragmentation regime sets in as more or less sharp transition governed by relevant physical quantities, the most evident being the degree of excitation of the system. We have tried to contribute to these problematics through two different investigations.

We considered the sequential decay of a strongly excited nucleus. This mechanism may be at work in heavy ion induced reactions at low GANIL energies. The model describes an evaporation process in which an initial excited nucleus decays by emitting particles and clusters of particles which, if they are excited, decay themselves into smaller pieces. As time flows the whole system expands in space due to the kinetic energies of particles and clusters and their mutual Coulomb repulsion. The yields of different fragments are obtained through a set of coupled master equations[1]). Resulting mass (fig. 1) and isotopic distributions for the reaction Ar on C at 27.5 MeV/A [2]) show quite a nice agreement with experimental results which are obtained under the assumption of preequilibrium particle emission followed by the decay of the remaining heavy system. In fig. 1 the bars indicate normalised measured mass yields. Unfortunately there exists no univoque identification of fragments with mass $A \leq 25$. In this calculation the system shows no critical behaviour with respect to the temperature when a percolation moment analysis[3]) is implemented. This is due to the too small yields of intermediate mass fragments obtained in the calculation. One would need at least the explicit measurement of the yields of fragments with mass $A \leq 25$ in order to state whether the present sequential decay picture is in trouble or not.

Percolation models are able to interpret qualitatively and quantitatively mass distributions generated through violent multifragmentation[4,5]). This interpretation involves the existence of a critical behaviour which is governed by pure space occupation characteristics of the system. It raises the question of the relevance of correlations between the onset of break up and internal features of the system. We investigated these points on a finite size Ising type model[6]). There one is able to show the connection between cluster multiplicities and the correlations generated by the two-body interaction acting between the spin constituents above, at, and below the critical temperature of the corresponding infinite system. The mass distributions are typically those expected in the percolation approach, the temperature being the relevant parameter. The quantitative effect of the spin interaction on the mass distribution has been investigated numerically on two and three dimensional models (fig. 2). Short (indicated by ①) and long range (indicated by ②) attractive interactions show marked differences at low excitation (see $T < 2.5$) and less discrepancy at high excitation (see T=5.0). The present analysis and the links of the models with the percolation approach raises the question of the existence or not of critical threshold for multifragmentation. This is definitely a point one would like the settle in the future in as much as other models seem to exhibit critical features[8]). In order to clarify the situation it would however be necessary to overcome the gap which exists between the present spin systems and actual nuclei (kinetic energy, density and Coulomb interaction effects, non equilibrium dynamics).

From the experimental side one faces the necessity to get more detailed information on mass and isotopic distributions. One knows now also from experience that these quantities may be rather insensitive to the details of the dynamical fragmentation process. Hence one would also definitely like to gather more exclusive information such as for example time and velocity correlation measurements between outcoming fragments in order to get closer to the problematics and the possible critical character of the process.

1) C. Barbagallo, J. Richert, P. Wagner, Z. Phys. A324 (1986) 97
2) J. Richert, P. Wagner, Z. Phys. A330 (1988) 283
3) X. Campi, J. Phys. A : Math. Gen. 19 (1986) L917
4) T. Biro, J. Knoll, J. Richert, Nucl. Phys. A459 (1986) 692
5) X. Campi, Contribution to the International Workshop on Nuclear Dynamics at Medium and High Energies, Bad Honnef, W. Germany, October 1988
6) S.K. Samaddar, J. Richert, to be published in Z. Phys. A

7) S.K. Samaddar, J. Richert, to be published in Phys. Lett. B
8) D.H.E. Gross, Yu-ming Zheng, H. Massmann, Phys. Lett. 200B (1988) 397

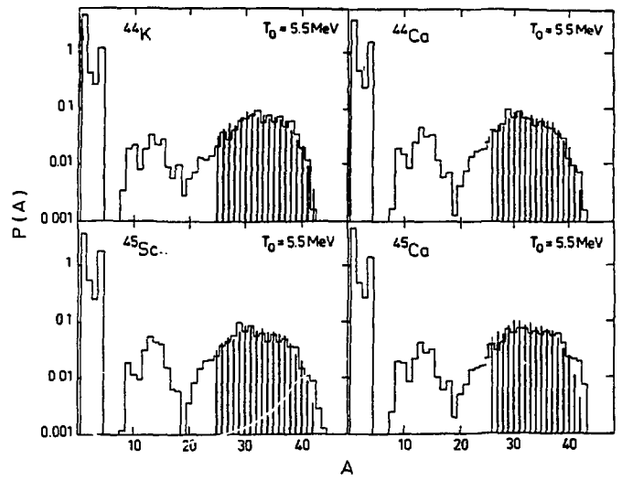

Fig. 1

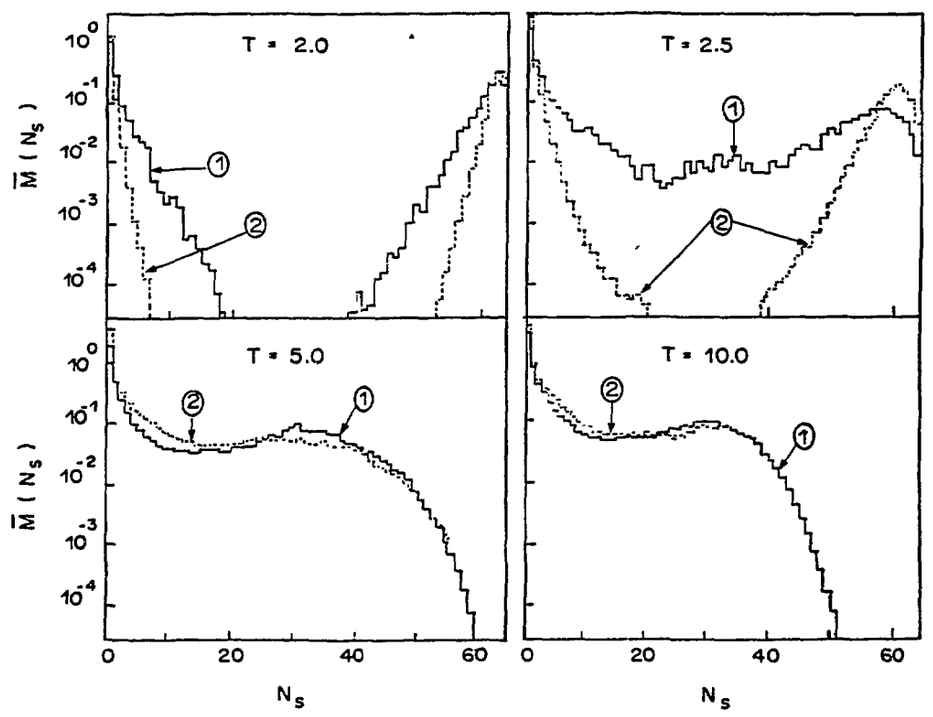

Fig. 2

Spinodal break up and the onset of multifragmentation

D. Cussol, Ch. Grégoire and E. Suraud*,[1]

GANIL, BP5027, F14021 Caen cedex, France

*) Institut des Sciences Nucléaires, 53 Avenue des Martyrs, F38026 Grenoble cedex, France

1) Present address : GANIL, BP5027, F14021 Caen cedex, France

Heavy-ion reactions provide a precious tool for investigating the nuclear matter Equation Of State (EOS). The onset of multifragmentation seems to be connected to the exploration of low density regions of the EOS by the excited nuclear system, as predicted by schematic models [1]. In order to study this effect in a more realistic way we have made an analysis in the framework of Landau-Vlasov simulations [2], which provide a dynamical microscopic description of one body observables. The complete description of final products, namely of the numerous produced fragments is hence beyond the scope of such an approach. The model however allows a reasonable description of the path towards the low density, unstable, spinodal region.

We have studied in detail two symmetric reactions (^{40} Ca + ^{40} Ca and ^{40} Ar + ^{50} Ti) at various beam energies. While at low energies the system fuses, it undergoes multifragmentation beyond E/A ≈ 40-50 MeV/A and vaporization at higher energies. In order to exhibit the spinodal region we extract from the total energy the kinetic collective component. The remaining energy corresponds to an intrinsic energy which represents an analogon of an EOS of the system when plotted as a function of the density (Figure 1). One can see on figure 1 that the actual explosion is connected to the crossing of the spinodal line corresponding to this EOS (between 40 and 60 MeV/A beam energies) [3,4].

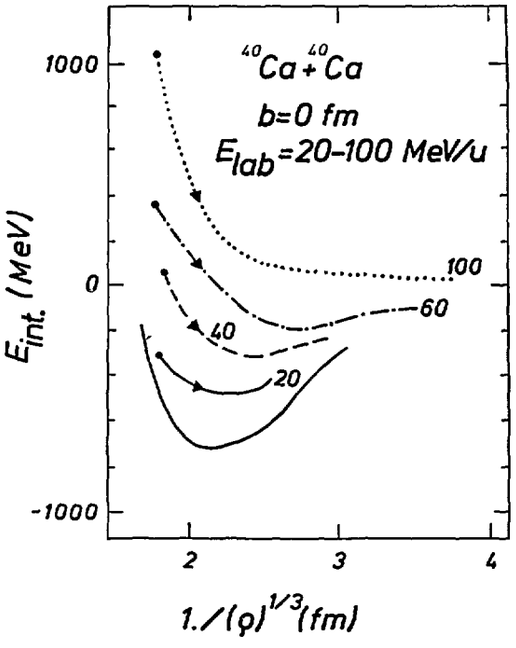

Figure 1
" Equation Of State " of the Ca + Ca reaction. The intrinsic energy E_{int} (in MeV) is plotted versus the average density for beam energies between 20 and 100 MeV/A, and in the case of central collisions.

In fact, as pointed out by Pethick and Ravenhall, crossing the spinodal line is a necessary but not sufficient condition for a system to explode [5]. The crucial quantity, for a given mode, is given by the integral I of the growing rate of instability over the time during which the system stays in the spinodal region. As the collective mode associated to the expansion of the system towards the spinodal region is dominantly of monopole nature [4] we have made an hydrodynamical monopole analysis of the motion. Introducing the corresponding collective mass allows to define the local monopole frequency associated to the evolution of the system. As soon as the system does enter the spinodal region this frequency becomes imaginary and one can estimate the transit time in the spinodal region. Values of the frequency versus time are plotted for the Ar + Ti system in Figure 2 and for two beam energies. At around 40 MeV/A one observes a rapid increase in the transit time, up to about 100 to 120 fm/c, which correponds to the actual explosion of the system.

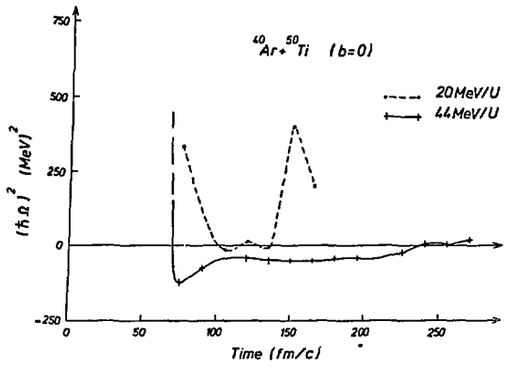

Figure 2
Time evolution of the square of the hydrodynamical monopole frequency for the Ar + Ti reaction at two beam energies (20 and 44 MeV/A). In the case at 44 MeV/A the systems stays more than 100 fm/c in the unstable region and does explode.

Moreover, rough estimates of I give results in very good agreement with the threshold obtained in a schematic analysis [5].

In order to go beyond schematic analysis of the explosion mechanism we have performed a microscopic estimate of the way an excited system may go into the unstable spinodal region. We have found that explosion is connected to entering the spinodal region. More precisely the system has to stay for about 100 to 120 fm/c in this region to let instabilities develop up to completely disrupt the nucleus. This is in good qualitative agreement with schematic studies.

References

[1] G.F. Bertsch and Ph. Siemens, Phys. Lett. **B126** (1983) 9
[2] Ch. Grégoire, B. Remaud, F. Sébille and L. Vinet, Nucl. Phys. **A465** (1987) 317
[3] E. Suraud, M. Pi, P. Schuck, B. Remaud, F. Sébille, Ch. Grégoire and F. Saint-Laurent, Preprint GANIL P88-04
[4] E. Suraud, D. Cussol, Ch. Grégoire, D. Boilley, M. Pi, P. Schuck, B. Remaud and F. Sébille, Nucl. Phys. A **495** (1989) 73c
[5] C.J. Pethick and D. G. Ravenhall, Nucl. Phys. **A471** (1987) 19c

INTERMEDIATE MASS FRAGMENTS PRODUCED AT LARGE ANGLE IN HEAVY ION REACTIONS

N.H. Papadakis[3], N.P. Vodinas[3], Y. Cassagnou[1], R. Dayras[1], R. Fonte[4], G. Imme[4], R. Legrain[1], A.D. Panagiotou[3], E.C. Pollacco[1], G. Raciti[4], L. Rodriguez[1], F. Saint-Laurent[2], M.G. Saint-Laurent[2], N. Saunier[1].

1. D.Ph.N/BE, C.E.N. Saclay, 91191 Gif-sur-Yvette Cedex, 2. GANIL, B.P. 5027, 14021 Caen Cedex,
3. University of Athens, Physics Department, Panepistimioupolis 15771 Athens,
4. I.N.F.N. and University of Catania, 57, Corso Italia I-95129 Catania.

The production of intermediate mass fragments ($5 \lesssim Z < 25$) at large angle ($15° < \theta < 127°$) was investigated as a function of incident energy and target mass in the reactions Ne + Ag and Ne + Au between 20 and 60 MeV/nucleon [1]. Looking for possible new processes such as the proposed "shattering of cold nuclear matter" [2] or "break up of a hot expanded participant zone into clusters" [3], a careful analysis of double differential cross sections was successful in unfolding the various sources of emission of every Z-separated fragment. In energy spectra, angular distributions and $V_{//}$-$V_{\perp}$ velocity plots, a contribution relevant to the well known low energy processes of evaporation and fission was separated on the ground of a discrimination between two sources, the velocities and temperatures of which are favourably defined in reactions using direct kinematics.

The evolution as a function of incident energy of the remaining "fragmentation component" is illustrated in Fig. 1. The two reactions exhibit

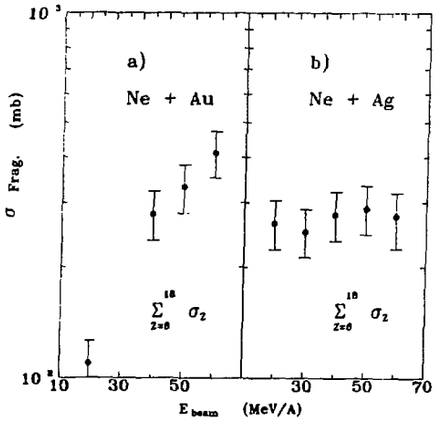

Fig. 1 : Yield of Intermediate Mass Fragments from 20 up to 60 MeV/nucleon.

trends in sharp contrast : Ne + Ag total fragment production is unchanging while that of Ne + Au grows as energy increases. The mass (charge) distribution of the fragments is an additionnal significant piece of information. It is usually well reproduced by a dependence on fragment mass A (charge Z) of the form $\sigma(Z) \propto Z^{-\tau}$. Values of τ , often found intermediate between 2 and 3, were considered at a time as a hint for a liquid-gas phase transition in nuclear matter[4]. Fig. 2 shows values of τ which are obtained for the two reactions considering the

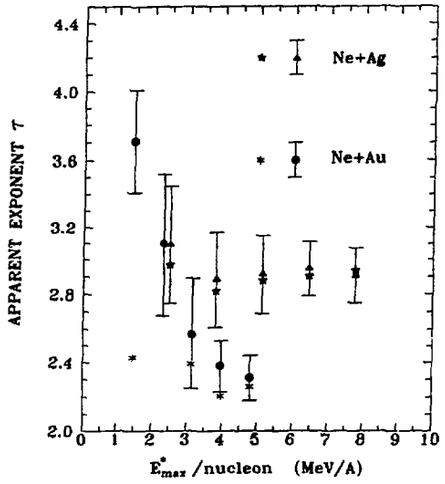

Fig.2 : Values of τ as a function of the maximum available energy.

whole set of data in comparison with the only so-called "fragmentation component" from which evaporation products, mostly for Ne + Ag, and fission fragments, for Ne + Au, have been eliminated. The energy dependence is expressed along the x-axis of Fig. 2 through the largest available energy per nucleon calculated as $E^*/A = \sqrt{8\, E_{CM}/A_{tot}}$ with A_{tot}= total number of nucleons.

Looking first at the unseparated data, the two reactions again show differences : for Ne + Ag (Δ), τ is rather constant while, for Ne + Au (.), one observes a steep decrease of τ at low energies, indicating that more heavy fragments are produced compared to light nuclei when more energy is brought in this system. If fragments from fission and evaporation are removed (*), values of τ for Ne + Au are obtained which are all but independent of energy as it is still the case for Ne + Ag. Furthermore, the values of τ for gold in the high energy limit are lower than those for silver, a trend in relation with the mass of the system according to theoretical predictions.

In summary, for the reaction Ne + Ag, from the steadfastness of its total cross section as well as the constancy of its charge distribution, the process of fragmentation, whatever it is, seems well established in the energy range investigated in this experiment. On the opposite, the rise of the cross section for gold along with the variation with energy of its τ values show that the same process, only spotted at the lower energies through a severe selection of the data against "relaxed" processes, is in its development as the incident energy increases.

The most interesting result of inclusive measurements, such as those just described, lies in the definition of a domain of angles, velocities and fragment masses for further investigations of a possible multifragmentation process (i.e. simultaneous emission of fragments in opposition to successive evaporation events). A first attempt along this line was recently made by measuring coincidences between intermediate mass fragments (IMF) and light particles (protons, deuterons, alphas) detected in a close-to-4π multidetector consisting in 150 scintillator counters. The dependence on the impact parameter of IMF production was investigated in this experiment, the data of which are presently being analysed [5].

Hoping for a more powerful detector in the future making possible the detection of both heavy and light nuclei in a 4π geometry, we expect a complete evidence of the "multifragmentation" process, understood as an extreme at a high excitation energy of both evaporation and fusion ; a glimpse of this process resulted from our previous experiments. We also expect a valuable insight into a mechanism inducing a small-sized system, such as a nucleus, to break into clusters when too much energy is brought in it.

References

1) N.H. Papadakis et al., to be published.
2) J. Aichelin and J. Hüfner, Phys. Lett. 136B, 15 (1984).
3) P.J. Siemens, Nature 305, 410 (1983).
4) J.E. Finn et al., Phys. Rev. Lett. 49, 1321(1982).
5) G. Bizard et al., C.R. Activité D.Ph.N., Note DP4N 89-1, Saclay.

Characterization of Multifragment Channels in 45 MeV/nucleon ^{84}Kr + ^{159}Tb Reaction

Z. Majka[1*], L.G. Sobotka[1], D.W. Stracener[1], D.G. Sarantites,[1] G. Auger[2], E. Plagnol[2], Y. Schutz[2], R. Dayras[3], J.P. Wieleczko[3], J. Barreto[4] and E. Norbeck[5]

[1]Department of Chemistry, Washington University, St. Louis, MO 63130
[2]GANIL, BP 5027, F14021 Caen Cedex, France
[3]CEN-Saclay, F91191, Gif-sur-Yvette Cedex, France
[4]Institut de Physique, Nucleare-BP01-91406-Orsay Cedex, France
[5]Department of Physics, University of Iowa, Iowa City, IA 52242

In this work we address the question of the multifragment production mechanism in the reaction of 45 MeV/nucleon ^{84}Kr + ^{159}Tb. The experiment was performed at the GANIL facility and the Dwarf Ball/Wall detection system was used. This detector array consists of 104 fast slow plastic-CsI elements with a total solid angle of 90% of 4π.

Two striking charcteristics of multi-intermediate mass fragment (IMF, $Z_{IMF} > 2$) exit channels were observed. These are: 1) high multiplicity of IMF's is correlated with large light-charged particle (LCP, $Z_{LCP} \leq 2$) multiplicity. 2) Events with large IMF multiplicity exhibit no planar character.

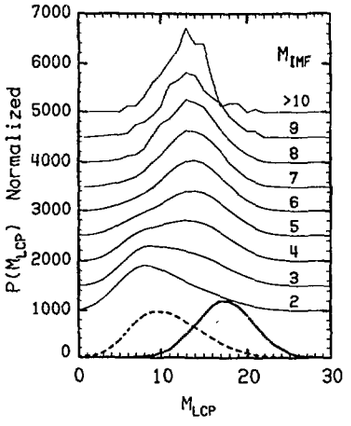

Figure 1. Normalized light charged particle (LCP) multiplicity distributions as a function of the number of intermediate mass fragments (IMF) are shown as thin solid lines. The LCP multiplicity distributions corresponding to values of the total detected charge $20 \leq Z_{Det} \leq 45$ and $Z_{Det} > 75$ are shown as dashed and thick solid lines, respectively. The curves are offset from the x axis for display.

The correlation between the multiplicity of the IMF's, M_{IMF}, and the LCP multiplicity, M_{LCP}, is shown in Fig. 1. One can see that the M_{LCP} distributions are composed of two parts. When only a few IMF's are detected the M_{LCP} distributions peak at rather low values < 8. As the number of detected IMFs is increased the M_{LCP} distributions become broader and extend to considerably higher values. For still larger M_{IMF} values, the M_{LCP} distributions regain a peaked form but with substantially greater mean value than for low M_{IMF} values. Also observed, but not shown in this report, is the trend that the total detected charge (Z_{Det}) increases with M_{IMF} (the Z_{Det} distributions extend up to 100% of the sum of the projectile and the target charge, Z_{Tot} = 101). Since the detection system is efficient for the detection of light ions but becomes more inefficient as the charge increases and the ion velocity decreases (due to absorbers), the events with low values of total detected charge must be associated with one or a few undetected massive heavy ions. This suggests that the component of the M_{LCP} distribution in coindence with only a few IMF's, which also tends to have a large deficit in the total detected charge, results from deep inelastic like or fusion events in which a massive residue survives but escapes detection. On the other hand, the component of the M_{LCP} distribution in coincidence with several IMF's is associated with well characterized ($Z_{Det} > 75$) nuclear explosions with no surviving very massive remnant. This is verified by the M_{LCP} distributions obtained by gating on regions of Z_{Det} values, see Fig. 1.

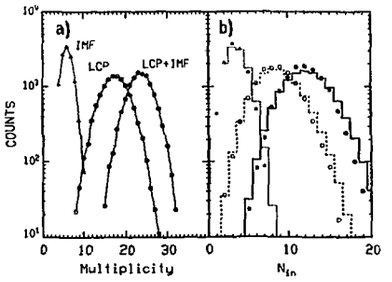

Figure 2. The multiplicity distributions of LCP's, IMF's and total, when the total detected charge is ≥ 75, are shown in part a). The symbols in part b) correspond to the number of ions, N_{in} which are within $\pm 45°$ of the plane defined by the beam and the ion with the largest charge. The histograms are the result of folding of the multiplicity distributions of part a) with binomial distributions with a chance probability of $p = 1/2$.

Our second observation is that these total explosion events show no planar quality. This is demonstrated in Fig. 2. Fig. 2a shows the multiplicity distributions for IMF's, LCP's and the total, for the events in which the total detected charge exceeds 75% of the Z_{Tot}. This selection, of almost complete event reconstruction, biases toward large M_{IMF} values. The event planarity is investigated by determining the number of ions, N_{in}, which are within 45° of the plane determined by the beam axis and the direction of the heaviest IMF of each event. These are shown as symbols in Fig. 2b. The mean values are close to 1/2 of those found in Fig. 2a suggesting a random distribution. This is verified by folding the multiplicity distributions in Fig. 2a with a binomial distribution with a chance probability $p = 1/2$. These folded distributions are displayed as histograms. The agreement is almost perfect indicating that these events exhibit no planar character.

*On leave from the Institute of Physics, Jagellonian University, PL30059, Krakow, Poland.

MULTIFRAGMENT PRODUCTION IN KRYPTON INDUCED COLLISIONS AT 43 MEV/u

R. Bougault, F. Delaunay, A. Genoux-Lubain, C. Le Brun, J.F. Lecolley, F. Lefebvres, M. Louvel
J.C. Steckmeyer - LPC, ISMRA, Université de Caen, France
J.C. Adloff, B. Bilwes, R. Bilwes, M. Glaser, G. Rudolf, F. Scheibling, L. Stuttgé - CRN, Strasbourg, France
J.L. Ferrero - Universitad di Valencia, Spain

Motivation

The main purpose of colliding heavy nuclei at energy far above the Coulomb barrier is to study the properties of nuclear matter in temperature and also density regions out of equilibrium. We then hope to learn about the nuclear matter equation of state and may be to see some new phenomena. To do that at GANIL energies, we chose to study the heavy fragment production, which is expected to be rather large in the Kr+Au, Ag, Th collisions at 44 MeV/u , due to either the collision mechanisms which may lead to the formation of several pieces of hot nuclear matter or the deexcitation stage. Indeed for very hot nuclei, the deexcitation through either a sequential emission of large fragments or a sudden process like multifragmentation has to be studied. Up to now, except for low statistics emulsion experiments, the multifragmentation is rather studied from inclusive experiment than from multifragment measurements. We used a set up covering with 30 cells, each one made of a parallel plate avalanche counter with localisation and of an ionisation chamber, 50 % of the solid angle between 3^o and 150^o with respect to the beam axis.
For each fragment we measured the velocity vector and get a Z identification, the threshold were at $Z = 8$ and $v = 3$ cm/ns for the 3^o-30^o angular range and at $Z = 10$ and $v = 0{,}5$ cm/ns for the 30^o-150^o angular range. The trigger was done on a number of detected fragments ($ND \geq 3$) requirement. In the forward direction ($3^o < \theta < 23^o$) the plastic wall was used to detect light charge particles with high velocity.

Results

Kr + Au 43 MeV/u	V_{beam}=9.1 cm/ns Z_{tot} = 115	Center of mass velocity=2.77 cm/ns Center of mass energy = 2.57 GeV			
Number of detected fragments	2	3	4	5	6
Normalized numbers of events	84%	14.5%	1.4%	0.1%	0.003%*
< Z >	25.5	22.7	18.5	16.6	15.5
< V > cm/ns	3.56	3.31	3.16	3.1	2.9

* (which represents 600 recorded events)

TABLE I

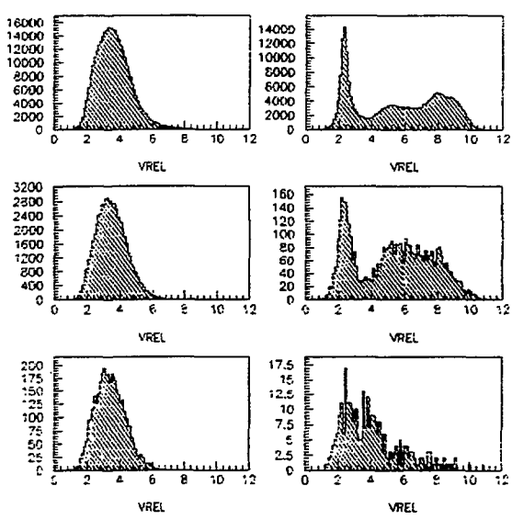

FIGURE I

The first raw observation is a large occurence of events with a high number of detected fragments ; the results are given on Table I without any correction for Gold and Silver targets.
The production rate for ND = 3 on Gold target overcomes without corrections 100 mb . The largest number of detected fragments, still significative, 5 for silver target and 6 for Gold target, exceed 4 , the number given by a double sequential fission which is known to be possible with so large nuclei. The velocity and Z mean values decrease as the fragment number ND increases.
To go further in the analysis we have to study event by event the correlations between the detected fragments to be able to separate various reaction mechanisms, to look for the sources and to study the deexcitation processes. The most relevant parameter is the relative velocity ($V_{rel} = |\vec{V}_i - \vec{V}_j|$) which is an invariant and depends strongly on the interactions between the fragments at the emission time. As the number of combinations of V_{rel} increases very quickly with ND (10 values for ND = 5) we will also use various moments of the V_{rel} distributions and specially the second one which allows to check the dispersion around the mean value. By this way we separate clearly the sequential mechanisms where the relative velocities are widely spread out according to their origin (several sources) from the more simultaneous one where the relative velocities are distributed around a single value. The results of such an analysis is displayed on the Figure I for the Kr+Au collisions at 44 MeV/u and for ND = 3,4,5 .

The sequential events on the right have two maxima one of them centered around 2.3 cm/ns which is the value found for fission events and for coulomb repulsion between two mid sized fragments. In the following, we will deal with the events displayed on the left where the relative velocities are distributed around the mean value 3 cm/ns higher than the coulomb repulsion and the same whatever the number of detected fragments. The mean properties of these events are given for the three systems under study in the Table II .

Target	ND	$<\Sigma Z>$	$<\Sigma P_{//}c>$	$<\Sigma P_{//}c> / <\Sigma Z>$	M_{LP}	$<Z_{LP}>$
		u.m.a.	GeV	GeV/u.m.a.		u.m.a.
Silver	3	38	9.8	255	2.9	2.4
$\Sigma Z = 83$	4	44	10.6	240	3.0	2.4
	3	52	8.0	154	2.7	2.3
Gold	4	63	9.6	154	2.6	2.2
$\Sigma Z = 115$	5	73	11.0	152	2.8	2.2
	3	56	8.2	146	2.5	2.3
Thorium	4	70	10.1	144	2.5	2.2
$\Sigma Z = 126$	5	80	11.1	140	2.4	2.1

TABLE II

$P_{//}c$ is the linear momentum of each fragment along the beam axis. The projectile linear momentum is 24,3 GeV/c . For each target whatever ND , a large fraction of the initial charge and linear momentum is missing. But for each target the parallel linear momentum divided by the detected charge remain constant. M_{LP} and $<Z_{LP}>$ are the mean multiplicity and the mean charge per light particle observed in the forward direction. They are the same whatever the target. All these results are a strong indications of a common process for each target and each number of detected fragment. To look for the source of the fragment we plot on Figure II iso contour lines of invariant cross section in the ($V_{//}$, $V_{\perp}$) plane for Kr + Au and ND = 5 . The fragments detected in the 30° - 150° angular range behave like if they originated from the same source. Their angular repartition given by the table associated to the picture shows that ≥ 3 fragments come from the same source with a velocity of 1 cm/ns . We are faced with events where 3 or 4 fragments are coming from the same source and have relative velocities centered around 3 cm/ns giving a strong indication of a multifragmentation process. In this case the whole system is not concerned and it is impossible to clearly identify a source in the forward direction.

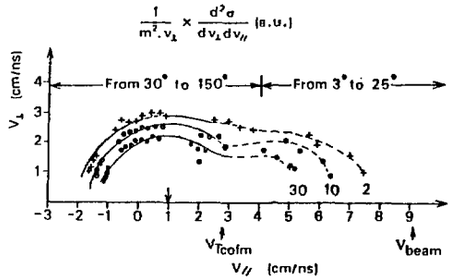

ANGULAR REPARTITION OF ND=5 EVENTS

(30°-150° angular range, 3°-25° angular range)

(5,0)	(4,1)	(3,2)	(2,3)	(1,4)	(0,5)
5.6%	42%	44%	8%	0.1%	0%

FIGURE II

Références

- D. Dalili et al - Zeitschrift für Physik A316 (1984) 371 .
- R. Bougault et al - NIM A259 (1987) 473 .
- G. Rudolf et al - Phys. Review Lett. 57 (1986) 2905 .
- R. Bougault et al - NPA 488c (1988) 255c .
- Etude expérimentale et analyse de l'émission des fragments corrélés dans la réaction Kr+Au à 35 et 44 MeV par nucléon ; A. Kamili - thèse de Doctorat es Sciences Physiques , ULP Strasbourg, 4 juillet 1986.
- Etude des mécanismes de réaction observés dans le système Kr+Au à 35 et 44 meV par nucléon J. Colin - thèse de l'Université de Caen, 5 juillet 1987.

ONSET OF MULTIFRAGMENTATION IN ^{40}Ar ON ^{27}Al CENTRAL COLLISIONS FROM 25 TO 85 MeV/u

K. Hagel[a,f], A. Péghaire[a], G.M. Jin[a,h], D. Cussol[a], H. Doubre[a], J. Péter[a,b], F. Saint-Laurent[a], G. Bizard[b], R. Brou[b], M. Louvel[b], J.P. Patry[b], R. Regimbart[b], J.C. Steckmeyer[b], B. Tamain[b], Y. Cassagnou[c], R. Legrain[c], C. Lebrun[d], E. Rosato[e], J. Natowitz[f], J.C. Jeong[i], S.M. Lee[i], Y. Nagashima[i], T. Nakagawa[i], M. Ogihara[i], J. Kasagi[j], T. Motobayashi[a,b,k]

[a] GANIL, F-14021 Caen-Cedex [b] LPC Université, F-14032 Caen-Cedex [c] CEN DPhN/BE, Saclay [d] LSN Nantes, F-44072 Nantes-Cedex 03 [E] Dipartimento di Scienze Fisiche, Univ. di Napoli (Italy) [f] Cyclotron Institute, Texas A&M Univ. USA [g] SUNY, Stony Brook U.S.A. [h] Inst. of Modern Physics, Lanzhou, China [i] Institute of Physics, Univ. of Tsukuba, Japan [j] Dept. of Physics, Inst. of Technology, Tokyo, Japan [k] University Rikkyo, Tokyo, Japan

For the system ^{40}Ar + ^{27}Al above 20 MeV/u, the production of fusion residues has been studied in an inclusive experiment [1]. It showed that the cross section of evaporation residues produced in central collisions vanishes between 32 and 36 MeV/u. The occurrence of multifragmentation is likely. For this system, we have made exclusive measurements of light charged particles and fragments, from 25 to 65 MeV/u by 10 MeV/u steps, and also at 85 MeV/u (with a poor statistics).

Since we are dealing with a system in reverse kinematics, almost all particles with non negligible velocities are found in the forward hemisphere. Then, the experimental set-up covered angles from 3.2 to 90° with two complementary multidetector systems : Mur [2] and Tonneau [3]. For each particle, one gets the velocity and the nuclear charge. This set-up has several limitations, taken into account in the analysis.

All events with a multiplicity greater than 1 in the 132detectors were recorded.

In parallel to the experiment, we have made extensive simulation calculations. Several hypothesis about the formation and decay of excited fusion nuclei have been used, at several impact parameter values. The resolution, threshold and geometry of the experimental set-up have been taken into account to see how they affect the observables : multiplicity, total momentum, eccentricity...

In the event-by-event analysis, the first step was to keep only those events where a sufficient information has been obtained. The criteria has been found to be the measured total parallel momentum value $P_{\|}$. The well detected events are kept for the next step of analysis. The simulation calculations show that all central collisions events belong to this group.

Since the largest excitation energies (in thermal or compressional forms are reached in central collisions, the next step was to separate central collisions events from intermediate impact parameter and peripheral collisions. For a better sorting, we must use the whole information obtained for each event. Such a complete information is contained in the sphericity tensor, which is determined by the mass, velocity and direction of all detected particles [4].

Figure 1 shows the distribution of events in a two-dimensional plot θ_{Q3} versus ϵ at 45 MeV/u. Similar plots have been obtained at other energies. The continuous evolution of reactions from peripheral to central collisions is reproduced in the continuous shape of the distribution. We cut it in 3 areas defined on the basis of simulation results. Area P corresponds to well detected "peripheral" collisions : their particles are focussed in the c.m. frame (large value of ϵ) at small angles. Fusion reactions not far from complete fusion are in areas C (for "central") or M, since their shape is close to a sphere, with the main axis randomly distributed between 0 and 90°. Reactions occuring at intermediate impact parameters belong to area M. (for "mixed").

An expected signature of multifragmentation is the production of several intermediate mass fragments (i.m.f). The measured probability to emitting 1,2... i.m.f. in central collisions is shown in figure 3 versus the incident energy. more) fragment We can calculate the average probability of emitting i.m.f. : it is the sum of the products νi.m.f. x probability to emit ν i.m.f. in figure 2. This average probability is close to 1 (slightly less than 1 at 25 MeV/u, and above 1 at higher energies), in agreement with the results of ref.[5]. Due to the detection velocity threshold, the measured proportions shown here are minimum values for $\nu i.m.f.$ >1, and maximum values for $\nu i.m.f. \leq$ 1The emission of more than 1 i.m.f. strongly increases between 25 and 36 MeV/u and more slowly above. These events can be attributed to a multifragmentation process. Its onset is located just where the evaporation residues cross section vanishes [1].

Another results exhibits a strong change in the decay process for central collisions : the distribution of the total measured charge.It is shown in figure 3 for energies from 25 to 65 MeV/u. A strong shift is seen between 25 to 36 MeV/u, both on the peak location and its width. Above 36 MeV/u, the width remains constant and the peak shifts slowly. At 25 MeV/u, the dominant process is sequential statistical de-excitation of the fusion nucleus, leaving a slow heavy residue [4] with a charge larger than ~13. This residue is undetected or its charge is taken to be 9 only ; hence, the total measured charge is low and never exceeds 22. At higher energies , the break-up in several lighter fragments allows to detect most fragments and correctly measure their charge ; hence, the total measured charge is much larger and even reaches the total charge of the system : 31 (note, however, that some events still have a low measured total charge, as at 25 MeV/u, which indicates a co-existence of both processes).

[1] G. Auger, E. Plagnol, D. Jouan, C. Guet, D. Heuer, M. Maurel, H. Nifenecker, C. Ristori, F. Schlusser, H. Doubre, C. Grégoire, Phys. Lett. 169B, 161 (1986).

[2] G. Bizard, A. Drouet, F. Lefebvres, J.P. Patry, B. Tamain, F. Guilbault, C. Lebrun, Nucl. Inst. Meth.

[3] A. Péghaire, B. Zwieglinski[g], E. Rosato[g], G.M. Jin[g], J. Kasagi[g], H. Doubre, J. Péter, Y. Cassagnou, R. Legrain, F. Guilbault, C. Lebrun, to be published.

[4] J. Cugnon, J. Knoll, C. Riedel, Y. Yariv Phys. Lett. 109B (1982) 167.

[5] E. Plagnol, L. Vinet, D.R. Bowman, Y.D. Chan, R.J. Charity, E. Chavez, S.B. Gazes, H. Han, W.L. Kehoe, M.A. MacMahan, L.G. Moretto, R.G. Stocktad, G.J. Wozniak, G. Auger, Report LBL-25742 (1988)

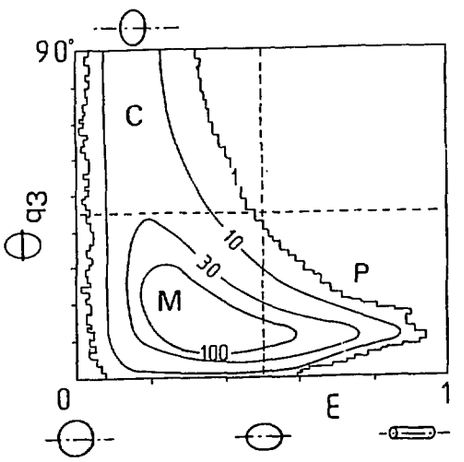

• Figure 1 : Distribution of events as a function of their eccentricity ϵ and the flow angle θQ_3.

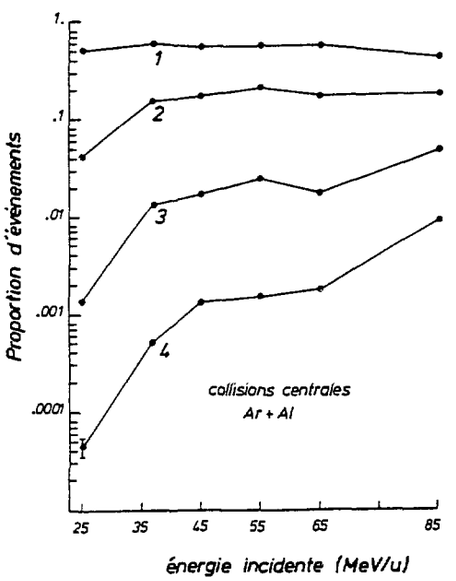

• Figure 2 : Excitation functions for the production of intermediate mass fragments in central collisions events.

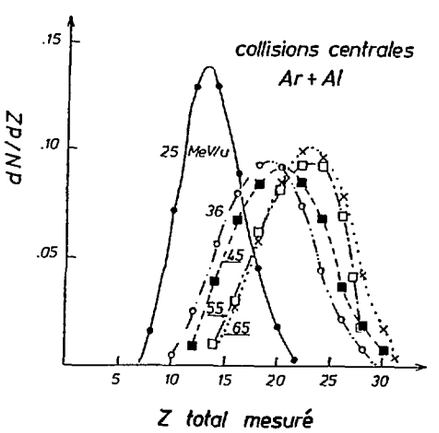

• Figure 3 : Normalized distributions of the total measured charge in central collision events, from 25 to 65 MeV/u.

Exp. E32 Event-by-Event Studies of ^{16}O Induced Reactions at GANIL Energies.

E32a Multifragmentation Studies in Nuclear Emulsions.

B Jakobsson, G Jönsson, L Karlsson, B Norén, K Söderström, Univ. of Lund, Sweden

E Monnand, F Schussler, ISN Grenoble.

These two experiments had the goal to study break up properties on an event-by-event basis of central heavy ion collisions over a variety of energies where critical behaviour of nuclear matter could be expected. By placing large enough stacks of nuclear emulsions of various sensitivity directly in vacuum we optimized the conditions to determine the collision energy the charge and energy of each fragment.

We select central collisions by a high total charged particle multiplicity (M) trigger. This parameter is not unambigous at low collision energies but we still believe it to be the best common trigger for central events. Fig 1 shows the projected image of a high multiplicity $^{36}Ar + ^{107}Ag$ collision at 32A MeV. By various kinds of ionization + range measurements[3] we are able to determine the charge (Z) of all fragments which leads to the conclusion that the event in Fig 1 is of multifragmentation type. This kind of measurements are right now in progress with the help of a recently developed CCD reading system for the ^{36}Ar collisions while it is finished with more conventional microscopic technique for ^{16}O collisions.

Fig 2 shows the complete Z-distribution for high multiplicity collisions at energies from 25A to 200A MeV. The transition from fusion-like collisions to multifragmentation-like, finally proceeding towards complete vaporization, is obvious. In order to understand the break-up properties we have considered several kinds of correlations between parameters which are supposed to give indications about a possible critical behaviour. One example of such correlations, namely γ_2-n, is shown in Fig 3 (γ_2 is the conditional second Z moment*) and n = $M/(Z_{beam} + Z_{target})$). The signal for a critical behaviour (the maximum in the curve) is hardly observed in the data which represents high multiplicity collisions between 15A - 210A MeV.

The type of questions which have been raised by our results is if this kind of complete 4π data, though it has low statistics, can select among models for heavy ion reactions.

Utilizing semi-automatic CCD measurement systems we hope to increase the statistics by a factor 5-10 and thereby to answer these questions better, in the Ar + Ag material.

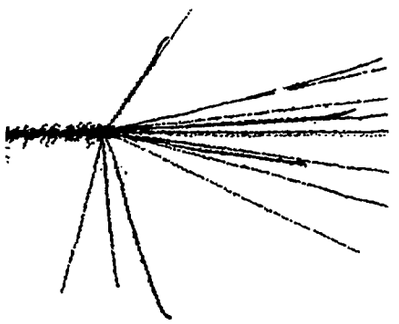

Fig 1. A photograph of an $^{36}Ar + ^{107}Ag$ collision at 32A MeV. The charges are identified as 5*1,3*2,2*3,5,6,2*8,10,13.

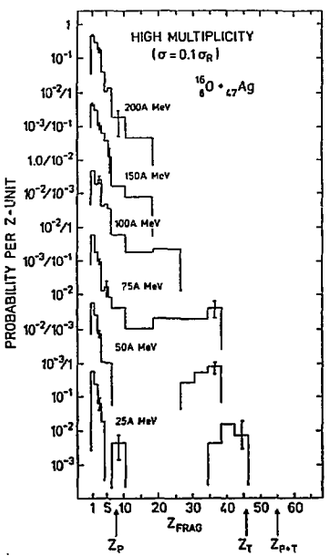

Fig 2. Charge distribution in high multiplicity (10%) O+Ag collisions.

*) X Campi, Phys Lett B208(1988)351.

Publications:

1. B Jakobsson, L Karlsson, V Kopljar, B Norén, K Söderström, E Monnand, H Nifenecker, F Schussler. Physica Scripta 38(1988)132.

2. L Karlsson et al., Proc. of the 3:rd Int Conf on Nucleus-Nucleus Collisions, St Malo, 1988.

3. B Jakobsson, G Jönsson, L Karlsson, V Kopljar, K Söderström, E Monnand, F Schussler, H Nifenecker, G Fai, K Sneppen, J P Bondorf, X Campi. Preprint from Univ of Lund, LUIP 8812(1988), submitted to Nuclear Physics.

4. B Jakobsson, L Karlsson, B Norén and A Oskarsson. Proc. of the Workshop on Intermediate and High Energy Heavy Ion Reactions, Krakow, 1987.

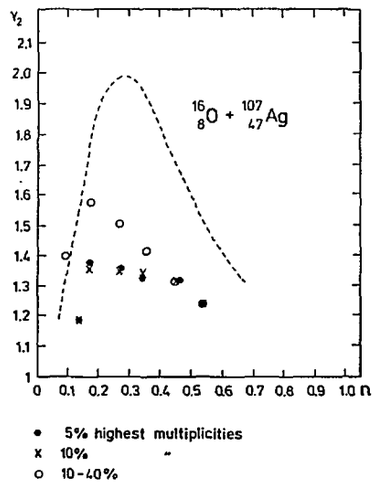

Fig 3. The conditional moment versus the multiplicity in high multiplicity (10%) and medium high multiplicity (10-40% highest M) collisions. The curve represents a 3-d perculation calculation.

— B4 —
PIONS AND PHOTONS

LINEAR MOMENTUM TRANSFER IN PION ACCOMPANIED ^{16}O INDUCED REACTION ON ^{232}Th AT 95 MeV PER NUCLEON

B. Erazmus, C. Guet, R. McGrath, M.G. St Laurent, Y. Schutz and J.L. Ciffre-Ganil, F-Caen

M. Bolorê, Y. Cassagnou, H. Dabrowski, M. Hisleur, J. Julien and R. Legrain, CEN-Saclay, DPhN, F-91191 Gif sur Yvette

C. Le Brun, J.F. Lecolley and M. Lowel, LPC, ISMRa, F-Caen

Positive pions and protons emitted at 90° were measured in coincidence with two fission fragments in the reaction ^{16}O+ ^{232}Th at 95 MeV/nucleon. The linear momentum transfer distribution has been determined from the folding angle between the fragments. The average momentum transfer is 2.5 Gev/c + 0.2 Gev/c for a pionic reaction. An analysis in terms of impact parameter distribution leads to the conclusion that subthreshold pion production requires a large overlap of projectile and target density profiles.

A detailed analysis of impact parameter distributions as predicted by different theoretical pion production models has been carried out by B. Erazmus in her thesis [1]. Although most models do indeed favour central collisions, the best agreement with the empirical impact parameter distribution is given by the statistical model [2] where it is assumed that the pion yield is governed by pure phase space considerations. The results of this experiment (described in detail in ref [3]) were soon confirmed by other methods ref.[4].

[1] B. Erazmus, thesis, Université de Caen, Ganil T 88 02 (1988)

[2] J. Knoll and R. Shyam, Nucl. Phys. A483, 711 (1988) and refs. therein

[3] B. Erazmus and al, Nucle. Phys. A481, 821 (1988)

[4] S. Aiello et al, Europhysics Lett.6, 25 (1988)

EXPERIMENTAL SEARCH FOR SUBTHRESHOLD COHERENT PION PRODUCTION

B.Erazmus, C.Guet, A.Gilibert, W.Mittig, Y.Schutz, A.C.Villari, GANIL, BP 5027,F-14021 CAEN CEDEX
W.Kühn, S.Riess,Universität Giessen, Giessen, W-Germany
H.Nifenecker, J.A.Pinston, CEN-G,DRF/SPh, F-38041 Grenoble Cédex
E.Grosse, R. Holzman, GSI Darmstadt, W-Germany
J.P. Vivien, CRN, F-Strasbourg
M. Soyeur CEN-Saclay, IRF-DPhG-SPhT- F 91191 Gif sur Yvette Cédex

It was been suggested that subthreshold pion production in peripheral heavy ion collisions could occur because of a coherent excitation of spin-isospin modes through the delta-hole channel in either projectile of target [1]. Theorgtical predictions for the production cross-section and pion spectral shapes have been worked out [2].

We have performed a first experiment to search for such a process. The reaction we looked for is :

$$^{12}C + ^{12}C \rightarrow ^{12}C\ (1^+,1;\ E^x = 15.1\ MeV) + \pi^o + X \quad (1)$$

at an incident energy of 95 MeV per nucleon. In a peripheral collision the projectile would undergo a Gamov-Teller transition ($\Delta S = \Delta T = 1$) to the well-known 15.1 MeV excited state which dominantly decays radiatively to the ground state (M1 transition). A part ($\sim$15 %) of the relative motion energy is transferred to the target to produce a neutral pion. A full identification of the process may be achieved by a coincidence measurement of the outgoing ejectile (^{12}C) the 15.1 MeV photon and the two high energy photons from the π^0 decay. In this preliminary experiment we restricted ourselves (for obvious reasons) to the following three-fold coincidence measurement :

- The slowed down ejectile was measured around $\theta = 0°$ by the SPEG spectrometer. Its kinetic energy was selected to be between E_b-140 MeV and E_b-270 MeV (E_b is the total beam energy).

- The 15.1 MeV photon was detected by a set of BaF_2 detectors covering a solid angle of 1.6 sr.

- Only one high energy photon (E > 30 MeV) was detected by the same set of BaF_2 detectors.

During a data taking time of about 20 hours, 9 events fullfilling the necessary conditions have been observed. Only an upper limit of the total cross-section is inferred by these data. We estimate that for this specific reaction (1) the total cross-section would be lower than 20 nbarn. A comparison to theoretical predictions is of course premature. However we firmly believe that a much improved and unambigous experiment is feasible by using a larger solid angle BaF_2 spectrometer (available in the near future) and getting more beam time.

1) G.E. Brown and P. Deutchman, Workshop on high resolution heavy ion physics at 100 MeV/N, Saclay 1987.

2) C. Guet, M. Soyeur, J. Bowlin and G.E. Brown. Nucl.Phys. (in print).

PION AND PROTON EMISSION IN NUCLEAR COLLISIONS INDUCED BY ^{16}O IONS OF 94 MeV/U

A. Badalá, R. Barbera, S. Aiello, A. Palmeri, G.S. Pappalardo and A. Schillaci — I.N.F.N, CATANE
G.Bizard, R.Bougault, D. Durand, A. Genoux-Lubain, J.L.Laville, F. Lefebvres, and J.P.Patry. — L P C, CAEN
G.M. Jin, E.Rosato — GANIL, CAEN

I - INTRODUCTION

The main interest of studying pion production in nuclear collisions stands in the fact that the pion is emitted by the interacting zone. So, it can provide a mean to test the role of collective effects in nuclear collisions. In such a purpose the first difficulty which is encountered is of course to disentangle the proper dynamics of pion creation among the various final state channels. A way to do that is to explore the final phase space configurations associated with pion and proton emission when that proton carries out a kinetic energy E_p which is at least equal to the pion rest mass. In order to establish such a comparison, we studied light charged fragments emission triggered either by a pion or by a high energy proton ("HEP", $E_p > 140$ MeV) in collisions induced by 94 MeV/u ^{16}O on Al, Ni and Au targets.

II - EXPERIMENTAL CONSIDERATIONS

Both charged pions and protons were detected using a range telescope in the energy domain between 25 and 75 MeV for pions ; and between 40 MeV and 160 MeV for protons. Charged fragments were observed with two large area multidetectors able to identify elements from Z = 1 to Z = 8 :the first one could work at forward angles between 1^o5 and 30^o over the whole azimuthal acceptance ; the second one at large angles between 30^o and 150^o over an azimuthal range of 180^o .Fragments velocities were measured by a time-of-flight technique.
This fragment emission was observed in the multidetectors both inclusively and triggered either by a pion or by a "HEP" detected at three angles : $\theta = 70^o$, 90^o and 120^o for every target.

III - GENERAL OVERVIEW OF THE DATA

Charged fragments multiplicities are shown in Fig.1 for inclusive ("INC") events, pion ("π") or proton ("HEP") triggered events, for reactions induced on the Al target. "π" multiplicities are rather similar to the "HEP" multiplicities but both differ nettely from the inclusive ("INC") ones. The increase of multiplicity when the fragments are correlated with a pion or a "HEP" accounts for a more central process in the latter case. Such a trend is confirmed by the fragment velocities. Fig.2 shows velocity spectra for Z > 2 elements (essentially Z = 6, 7, 8) emitted in collisions at forward angles close to the grazing one ($\theta_G = 3^o$) for the $^{16}O+^{197}Au$ system : the inclusive contribution peaks at a value close to the beam velocity, but the pion-coincident one does not exhibit such a quasi-elastic contribution. These features are observable whatever the target or trigger angle. Especially, we do not observe significantly any coincident event between a pion or a "HEP" and a projectile-like fragment (Z = 4 to 8) at angles close to the grazing ones corresponding to the three studied systems (^{16}O+Al, Ni, Au).
Such differences are also visible in Fig.3 presenting velocity spectra of Z = 2 particles for each triggering case : inclusive (3a), "HEP" (3b) and "π" (3c). Two components are clearly exbited : one is centered about the beam velocity and the other one at a lower velocity, corresponding to a possible emission by a slower source. Dashed lines in Fig.3 represent the two gaussian best fit to the velocity spectra, the continuous curves being the sum of these two contributions : in the "π" and "HEP" case (3b and 3c) , the hot source contribution is more pronounced than in the "INC" case (3a) which essentially arises from projectile fragmentation.

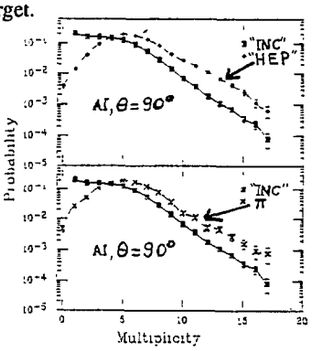

Figure 1

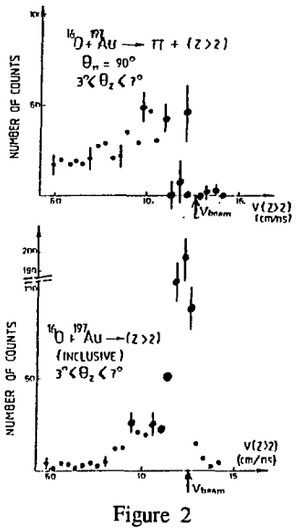

Figure 2

Such a two-component behaviour remains valid for α particles emitted between 3° and 30° and it evolves continuously from the dominance of the high velocity regime at small angles towards its complete cancellation at larger angles. Fig.4 shows azimuthal distributions of "HEP" triggered α-particles emitted at 4° (4a) and 21°.5 (4b) for "HEP"s detected at 70° (Fig.4a) and 90° (Fig.4b) respectively. In the former example, this azimuthal distribution has been separated according to the velocity partition of Fig. 3b : closed squares correspond to the high velocity (H.V.) component ; open squares to the low velocity (L.V.) one and diamonds indicate the total contribution.

Fig.4b shows (at a large polar angle) a strong asymmetric behaviour and a possible explanation of it could be the momentum balance effect of a given subsystem which recoils in the opposite direction of the detected "HEP" carrying out a large transverse momentum (more than 550 MeV/c). All these facts suggest that both proton and α-particle are emitted by a hot intermediate zone. The histogram in Fig.4b results from a calculation assuming a two-step process :

1) formation of a hot zone, the size of which is governed by the geometrical concepts of the fireball model ;
2) sequential decay which is described in the frame of the Weisskopf theory,

We can see on Fig.4b that this model - which works without any fitting parameter - reproduces the azimuthal distribution of the α-particles in shape and absolute magnitude at 21°5.

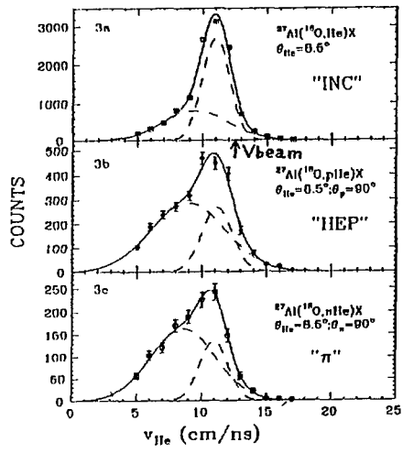

Figure 3

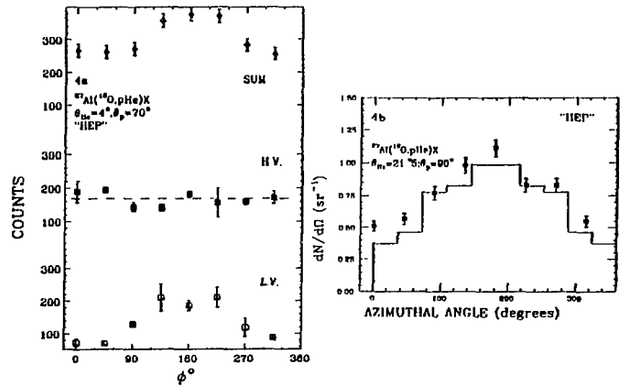

Figure 4

IV - DISCUSSION AND CONCLUSIONS

This calculation gives a good description of the azimuthal distributions of "HEP" triggered α-particles for θ_α angles larger than ~ 10°.

From these overall data, we can derive that pion emission, like high energy proton emission open the same final channels characterized by violent, partially damped collisions and is governed by simple phase-space constraints. The absence of quasi-elastic contribution in pion-coincident events seems to rule out any peripheral component in substhreshold pion production.

REFERENCES

1) Light fragment emission in heavy-ion reactions producing pions and protons in 16O+27Al collisions at 94 MeV/u. **Europhysics Letters 6** (1) (1988) p. 25 and XXV Int. Meeting on Nuclear Physics - Bormio (1987)

2) Semi exclusive pion production by heavy-ions at energy below 100 MeV/u .**Nuclear Physics** A482 (1988) p.511c-524c .

3) Subthreshold pion production in heavy ion collisions : peripheral or central interaction ?, III Int. Conf. on nucleus-nucleus collisions. SAINT-MALO (France).

4) **Thèse** : A. SCHILLACI, Dipartimento di Fisica dell'Universita di CATANIA (Italie).

LOW ENERGY CHARGED PION PRODUCTION IN ^{16}O+ X REACTIONS AT 93 MeV/u.

D. Lebrun [1], G. Perrin [1], P. de Saintignon [1], C. Le Brun [2],
J.F. Lecolley [2], J. Julien [3], R. Legrain [3].
1) ISN Grenoble; 2) LPC Caen; 3) DPhN Saclay; France.

1. Introduction.

In heavy ion reactions, very low momentum charged pions can be a tool to study the geometry of the collision. Those pions suffer a strong electromagnetic interaction which is very sensitive to the shape of nuclear charge distribution after the collision took place. In the frame of a positive distorting charge, Coulomb interaction affects mainly very low momentum particles, via a well known distortion phase space factor [1]. Effect results in an enhancement (depletion) of π^-(π^+) peaked at zero relative momentum. These distortions experimentally manifest as singularities in the pion distributions for p-values matching those of nuclear products. Such charged pion distributions were measured here at low transverse momenta (zero degrees), in reactions induced by a 93 MeV/u oxygen beam on various target:s: Li, C, Al, Ni, Ag, Au and Th.

2. Experiment.

To detect low energy subthreshold pions, the required main experimental features are: large solid angle (expected *low cross sections), high level particle rejection, efficient and* redundant particle identificationfor e, π, p...,compact system(to minimize inflight pion decay losses),variable momentum acceptance with adaptation to very low energy pions, few *percent momentum resolution, ability* to zero degrees detection, symmetric and simultaneous detection for π+ and π−, and operation under vacuum due to low energy pions and heavy ion beam. To fullfill these conditions a magnetic spectrometer (SPIC, Spectromètre à PIons Chargés) [2] was designed(fig. 1). It consists of a small circular dipole magnet ($\phi = 46$ cm), in the center of which is located the target. Each of the two symmetric detectors is made of two consecutive x-y multiwire proportionnal chambers allowing trajectory reconstruction,backed with three plastic scintillators. Detectors have no direct view of the target, eliminating rigid forward particles,but still have an appreciable solid angle for low rigidity particles. For one field B= 10 kG, the momentum acceptance was 45-120 MeV/c (T= 7-45 MeV) for particles emitted at $\theta = 0° \pm 15°$. Pions were identified via momentum, energy loss and time-of-flight combination usual techniques.

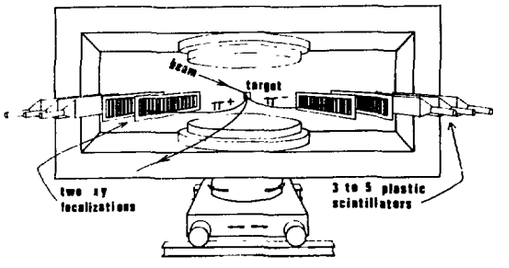

Fig. 1 Schematic view of the pion spectrometer.

3. π^-/π^+ distributions.

As an observable of nuclear collisions, the ratios of negative to positive pions have the advantage of beeing independent of experimental normalisations. Since, here, the detection was symmetric and simultaneous for both charge states, the momentum dependence of these ratios could be easily extracted. The momentum resolution permitted to

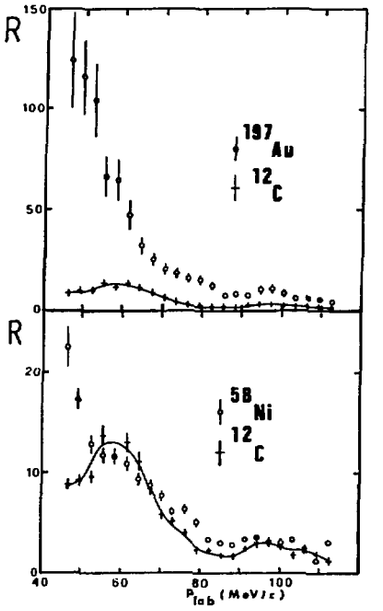

Fig. 2 Distribution of ratios π^-/π^+ in three systems.

clearly observe strong effects giving rise to very large values for these ratios. These values vary in different regions of p-space and depends on the colliding system. These effects are seen only for the lowest momenta; they disapear for higher momenta corresponding in the present study to pion with kinetic energy above 15 MeV. Focussed in this low energy domain, one observes a peak in the distribution of ratios in light mass systems.(fig.2) This peak is located at momentum corresponding to pions having the beam velocity. Similar effects were already observed in high energy nuclear collisions [3]. This was explained by Coulomb deflection from charged projectile fragments in the fragmentation region. But, as the mass of the system increases, this peak, while still present, is progressively shadowed by another phenomenon. The rise in the spectra is due to the increasing influence of, at least, one another nuclear charged fragment in the mid-rapidity region. A simple interpretation in term of Coulomb interaction allows to extract in each colliding system, the respective influence of these two contributions. Thus, charge and velocity of the distorting fragments in the pionic collision can be determined. In the mean time, the mid-rapidity charge presents an isotropic influence on ratios distributions, while in the fragmentation region the influence of projectile charged remnants stays peaked near zero degree [2].This indicates different behaviours of these charges located in different regions.

4. Pion yield.

In fact, when looked as a function of the size or charge of the mid-rapidity distorting fragment, the total charged pion yield exhibits a clean linear dependence (fig.3). This gives evidence that the mid-rapidity distorting charge behaves like the source of pions. Then the origin of these "subthreshold" pions is located in intermediate system whose charge and velocity govern the observed cross-sections. Among emitted pions, those travelling near beam velocity are further deflected by projectile remnants in the forward direction. At last, in the mid-rapidity moving source frame, pions present Boltzmann-like radiation spectra, with an apparent temperature around 8 MeV. This is well below the T value extracted from the slopes of neutral pions data in similar systems[4]. In our experiment these spectra present also a kind of saturation in T for system heavier than ^{27}Al. Here, this result seems to be in agreement with conclusions drawn from very different experiment (like particle correlations) in similar heavy ion reaction. In order to complete such studies, two other beam periods in 1988 were used studying the same colliding systems: first to look in the transverse momentum region, secund at zero degree but with 65 MeV per nucleon incident energy. Data reduction and analysis are still in progress.

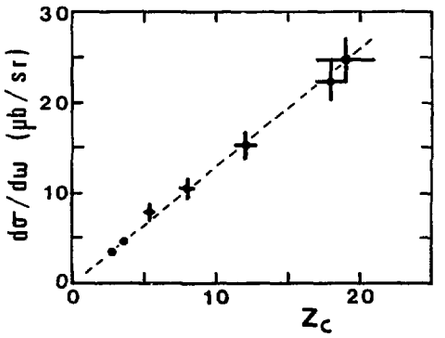

Fig. 3 Pion cross-sections versus mid-rapidity distorting charge Z_c

1) M. Gyulassy and S.K. Kauffmann, Nucl. Phys. A 362 (1981) 503.

2) D. Lebrun et al.. , Contribution to the third Int. Conf., Saint Malo, 1988, p. 158; Contribution to the Int. Winter Meeting on Nucl. Phys., Bormio,1989; and submitted for publication.

3) W. Benenson et al., Phys. Rev. Lett. 43 (1979) 683 and 44 (1980) 54.

4) P. Braun-Munzinger and J. Stachel, Ann. Rev. Nucl. Part. Sci. 37 (1987) 97.

" PION CONDENSATES " IN EXCITED STATES OF FINITE NUCLEI

R. Blümel and K. Dietrich*

Physikdepartment of the TUM, Garching, FRG

* Guest at the GANIL, August 1984 - March 1985

We investigated the following question : Given a symmetric nucleus (neutron nr N=proton nr Z) far from shell closure, is it possible that there exist low-lying excited states of such a nucleus with the following specific spin-isospin order : the angular momenta of the neutrons are pointing upward and the ones of the protons are pointing downward (or v. v.) in the topmost unfilled shells ?

This question was dealt with by many authors (see ref. 1 to 3 for references) for nuclear matter and very simplified models of a finite nucleus. The answer depends sensitively on the approximations and on the nuclear interactions used. Therefore, we performed a *selfconsistent* Hartree-Fock calculation based on Gogny's interaction complemented either by a coupling of the nucleons to a pion field[1,2]) or by an additional tensor interaction[3]). We studied only nuclei in the 2s-1d shell.

The 1st theory suffers from the drawback that the explicit coupling to the pion field introduces not only a (direct) tensor interaction but also an undesired additional interaction of the $\vec{\sigma}.\vec{\sigma}\ \vec{\tau}.\vec{\tau}$ character which is already taken care of in the Gogny interaction. In the 2nd mentioned model[3]), this double counting is avoided and, furthermore, the exchange contributions of the tensor force are not neglected.

The following results are obtained :

1) In the first-mentioned model[1,2]), a finite classical pion field (" pion condensate ") was never obtained as ground state of a nucleus.

2) It was, however, found for an oblate excited HF-state of the nucleus $^{32}_{16}S_{16}$, which mainly contained the isospins T=1 and T=2.

3) It was crucial for this result that the calculation was *self-consistent* (different sign of the quadrupole moment in the excited state and the ground state) and that the classical pion field contained *only odd components of the orbital angular momentum* ℓ, essentially only ℓ=1. This implies that the appearance of the finite classical pion field is *not* connected with parity breaking nucleonic orbitals !.

4) In the 2nd mentioned model[3]) we obtained qualitatively the same results, but the tendency to form a nucleonic spin-isospin order was less pronounced and only occurred for $^{32}_{16}S_{16}$ with a lower limit of the excitation energy of 5.8 MeV.

We note that the lowest $I^{\pi}=0^{+}$, T=1 and $I^{\pi}=0^{+}$, T=2 states of $^{32}_{16}S_{16}$ are measured at 7,536 MeV and 12,05 MeV, resp. Furthermore, very low-lying analog states of $I^{\pi}=0^{+}$, T=1 are obtained in $^{32}C\ell$ (E^{x}=0.537 MeV) and ^{32}P (E^{x}=0.513 MeV) and no such low-lying ones in the whole s-d shell. One may take this cautiously as an indication that the specific spin-isospin correlations we investigated may play a rôle in certain excited states of mid-shell s-d nuclei.

The only other favourable case (N=Z and far from shell closure) would be for N=Z isotopes of Cr and Ti. Unfortunately, very little is known experimentally on the spectra of these (unstable) nuclei.

1. R. Blümel, K. Dietrich, GANIL P.84-18
2. R. Blümel, K. Dietrich, Nucl. Phys. A454 (1986) 691
3. R. Blümel, K. Dietrich, Nucl. Phys. A471 (1987) 453

Hard Photons from Heavy Ion Collisions at 44 MeV/a

W. Kühn, Universität Gießen
(CRNS-GANIL-Gießen-GSI-Krakov Collaboration; E58/E58b)

The production of hard photons in heavy ion reactions has so far mainly been studied in inclusive experiments (for recent reviews, see [1,2]). The photon spectra exhibit three components: (i) an exponentially falling soft photon component arising from statistical γ-decay after particle evaporation, (ii) a hard photon component (slope parameter E_0) , (iii) a lorentzian-shaped excess yield in the Giant Dipole resonance region.
Both statistical emission from hot fragments as well as nucleon-nucleon bremsstrahlung have been identified as possible sources of such hard photons. The relative contribution of these two processes depends on the velocity in the nucleon-nucleon center-of-mass system and on the temperature of the fragments produced in the reaction. Above an incident energy of 30 MeV/a, nucleon-nucleon bremsstrahlung is the dominant process. This mechanism is of particular interest in that it constitutes a direct, undistorted probe of the phase space distribution in the collision zone [4].
At higher bombarding energies, the coexistence of different reaction mechanisms leads to severe ambiguities in the interpretation of such inclusive data. To improve this situation, we have performed two experiments where photon emission is studied in coincidence with particle detectors. In the first experiment, we have used a forward-angle charged particle hodoscope which allowed modest impact parameter selection. The second experiment was designed to focus on peripheral collisions with complete identification of the projectile-like fragment detected in the magnetic spectrometer SPEG. Both experiments investigated the reaction $^{40}Ar + ^{158}Gd$ at 44 MeV/a.

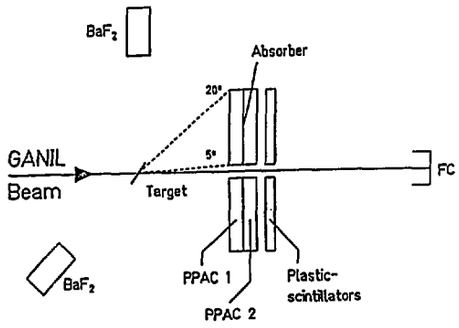

Figure 1: Experimental Setup (E58) [3]. Hard photons are detected with 7 BaF_2 detectors. Rough event characterization is performed by requiring different trigger conditions in the forward hodoscope.

The setup of the first experiment [3] is shown in fig 1.

Photons were detected with 7 BaF_2 detectors grouped in 2 blocks positioned at scattering angles of 90^0 and 145^0 , respectively. Event characterization was made by requiring a beam velocity heavy ion (peripheral) or a heavy slow fission-like fragment (central) in the forward hodoscope. Photon identification was made by time-of-flight with respect to the pulsed beam as well as exploiting the pulse shape discrimination properties of the BaF_2 detectors.

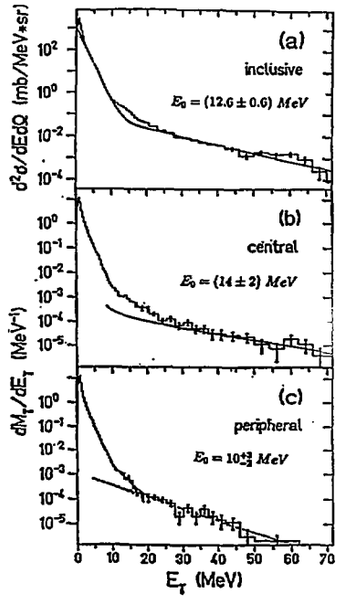

Figure 2: Photon spectra with different trigger conditions [3]

Fig.2 shows the inclusive photon spectrum (a) and the spectra obtained with the above conditions (b,c, respectively). Within the rough event characterization, no strong dependence of the slope parameter E_0 is observed. In contrast, the hard photon multiplicity ($E_\gamma > 30MeV$) increases by a factor of 2 when going from peripheral to central collisions.

The setup of the second experiment is shown in fig. 3. Photons were detected by means of 64 Bariumfluoride (BaF_2) detectors grouped in 4 blocks, positioned at laboratory angles between $\vartheta = 59°$ and $150°$ at 35 cm distance from the target.The projectile-like fragments (PLF) were detected with the magnetic spectrometer SPEG. This setup allows to study the hard photon component as a function of the PLF pa-

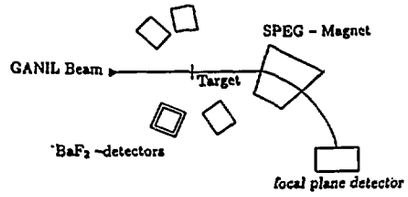

Figure 3: Experimental Setup (E58B). 64 BaF_2-detectors are employed to detect hard photons in coincidence with the PLF's in SPEG

rameters such as mass and total kinetic energy loss (TKEL).

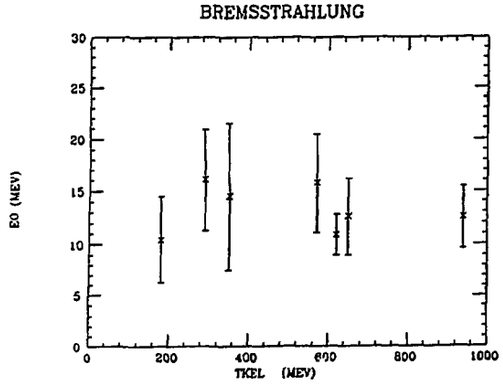

Figure 4: Slope Parameters for the hard photon component as a function of the PLF total kinetic energy loss

Fig.4 shows the slope parameter E_0 as a function of the total kinetic energy loss (TKEL) of the PLF's detected in SPEG. No strong dependence is observed indicating that the production mechanism is rather insensitive on impact parameter. In contrast, the observed multiplicity for γ-ray energies above 25 MeV increases for smaller PLF masses (fig.5). Smaller detected fragment masses are associated with larger energy losses and smaller impact parameters. The observed increase of the hard photon multiplicity could be interpreted as a geometry effect, yielding a larger number of p-n collisions for smaller impact parameters.

The analysis of this experiment is still in progress. From the theoretical point of view, existing VUU-codes are currently extended [5] to predict the fragment parameters, thus allowing a direct comparison to the experiment.

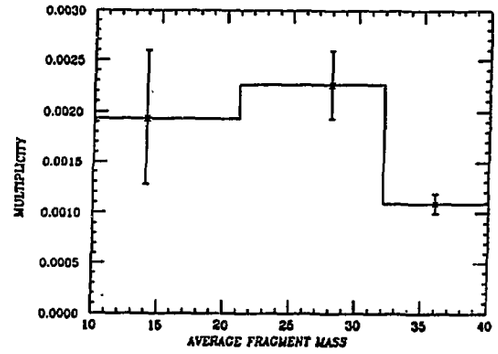

Figure 5: Hard Photon Multiplicity as a function of the PLF mass

References

[1] V. Metag Nucl.Phys. A488(1988)483c

[2] H. Nifenecker and J.A. Pinston, ISN Report 89.09, 1989

[3] R. Hingmann et al., Phys.Rev.Lett. 58(759)1987

[4] K. Niita et al., Nucl. Phys. A482(1988) 525c

[5] W. Cassing, U. Mosel, private conmunication

IMPACT PARAMETER DEPENDENCE OF HIGH ENERGY GAMMA-RAY PRODUCTION IN ARGON INDUCED REACTION AT 85 MeV/A

M. Kwato Njock, M. Maurel, E. Monnand, H. Nifenecker, P. Perrin, J.A. Pinston, F. Schussler
ISN and CEN.Grenoble
and
Y. Schutz, GANIL_Caen

The production of gamma rays with energies between 30 and 150 MeV has been studied both inclusively and exclusively using ^{36}Ar nuclei produced by the GANIL accelerator at 85 MeV/A.

- The inclusive production was studied for ^{12}C, ^{27}Al, ^{Nat}Cu, ^{Nat}Ag, ^{159}Tb, ^{197}Au targets in order to test the first collision scaling law found previously [1]. In all cases studied the source velocity was found to be close to the half beam velocity, thereby confirming previous results. The double differential cross section at 90° was found to be satisfactorily described by the expression:

$$\frac{d^2\sigma(\theta=90°, E_\gamma)}{dE_\gamma d\Omega} = \pi r_0^2 \frac{P_\gamma}{E_o} A_p \frac{5A_T^{2/3} \cdot A_p^{2/3}}{5} \left(\frac{Z_p N_T}{A_p A_T} + \frac{Z_T N_p}{A_p A_T}\right) e^{-\frac{E_\gamma}{E_o}}$$

where E_0 is the inverse slope of the exponential spectrum. $Z_{P(T)}$, $A_{p(T)}$, $N_{P(T)}$ are the charge, mass and neutron numbers of the smallest (largest) nucleus. The mass dependence can be deduced rigorously from the equal participant model after averaging over impact parameter [2]. Therefore the validity of the first collision model implies P_γ to be constant. Fig.1 shows that this is realized within 10%, with no systematic trend for the observed deviations.

- The exclusive experiment consisted in recording the gamma spectra in coincidence with a charged particle detector array (CPDA) of 24 detectors covering the angles between 5° and 13°. To optimize the efficiency of the CPDA we have chosen to study the system $^{36}Ar+^{27}Al$. It is found that the highest particle multiplicities correspond to the highest gamma intensities. Assuming the validity of the first collision model, and after normalization to the inclusive measurement, it was possible to assign an average number of n-p collisions, and thus an average impact parameter, b, to each of the gamma spectra conditionned by a given charged particle multiplicity. A variation of the inverse slope, E_0, of the spectra was correlated with the impact parameter as seen on Fig.2 where E_0 is plotted as a function of an overlap distance R_1+R_2-b. Also shown on Fig.2 are the results of the inclusive experiment where the average impact parameter was computed from a geometrical model of the reaction . The shape of the $E_0(b)$ correlation is interpreted as due to the spatial dependance of the Fermi momentum distribution of the nucleus.

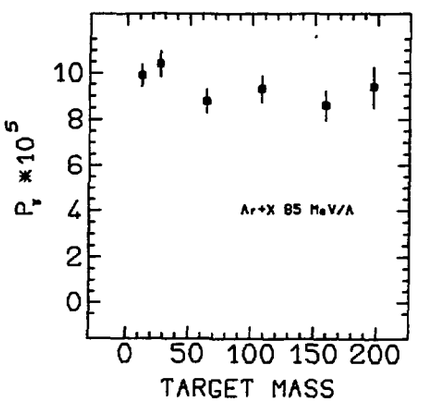

Fig. 1 - Probability of photon emission in a single n-p collision versus the target mass.

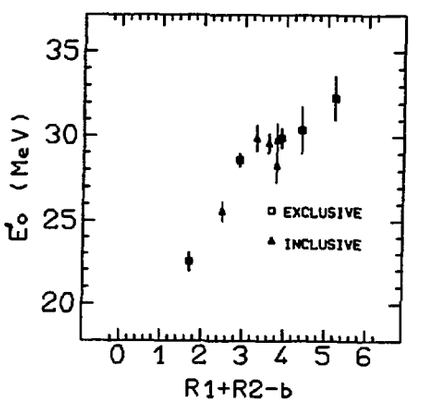

Fig. 2 - Inverse slope parameter versus the overlap distance.

The results of this experiment are reported in ref. [3,4].

1) R. Bertholet et al., Nucl. Phys. A474 (1987) 541
2) H. Nifenecker and J. P. Bondorf, Nucl. Phys. A442 (1985) 478
3) M Kwato Njock et al., Nucl. Phys. A488 (1988) 503C
4) M. Kwato Njock et al., Nucl. Phys. A489 (1988) 368

HIGH ENERGY GAMMA-RAY PRODUCTION FROM 44 MeV/A ^{86}Kr BOMBARDMENT ON NUCLEI

R. Bertholet, M. Kwato Njock, M. Maurel, E. Monnand, H. Nifenecker, P. Perrin, J. A. Pinston,
F.Schussler, CEN-Grenoble
D. Barneoud, ISN-Grenoble
C. Guet and Y. Schutz, GANIL-Caen

We report the results from an inclusive measurement of gamma rays with energies E_γ >20 MeV, produced in $^{86}Kr+^{12}C$,Ag and ^{197}Au at 44 MeV/A. In the experiments two identical detectors were used; one was placed at the fixed angle θ=90° and the other was used to explore scattering angles between 40° and 160°. Each detector consisted of one active BaF_2 converter (60X40X10 mm^3) and 3 plastic scintillators (2mm NE102) used to identify the electrons and positrons of the shower and a large volume NaI(Tl) scintillator (15 cm diameter and 20 cm length). The detection system was completed by a veto plastic scintillator to eliminate the charged particles entering the detector and a time-of flight measurement between the BaF2 detector and the radio frequency to eliminate the neutrons.

Fig. 1 shows the γ-energy spectra observed at three different laboratory angles for the Kr+Au reaction. It is apparent that the spectra have an exponential shape and their relative hardness increases as the angle decreases. This behaviour is characteristic of a photon emission from a moving source. The best fit parameters displayed in Table 1 were determined from a least squares fit to the data. It was assumed that the differential cross section in the γ-source rest frame writes:

$$\left(\frac{d^2\sigma}{dE_\gamma\, d\Omega}\right)_{c.m.} = K(1-\alpha+\alpha\sin^2\theta_{c.m.})\, e^{-E_{\gamma\, c.m.}/E_0},$$

and then the same quantity in the Lab. writes:

$$\left(\frac{d^2\sigma}{dE_\gamma\, d\Omega}\right) = \frac{K}{X}\left(1-\alpha+\frac{\alpha\sin^2\theta_{Lab}}{X^2}\right) e^{-XE_{\gamma Lab}/E_0},$$

with $X=(1-\beta\cos\theta_{Lab})\,(1-\beta^2)^{-1/2}$

In these equations the angular dependence is an isotropic term, plus a dipole term. Since the source velocity, β, the inverse slope parameter, E_0, and the relative amplitude of the E1, α, do not show any significant changes for the 3 targets, the mean values of these 3 parameters were deduced. They are reported in table 1 and they characterize the γ-ray emission for Kr induced reaction at 44 MeV/A incident energy.

The results obtained for the Kr induced reactions at 44 MeV/A are characteristic of those obtained at beam energies between 20 and 60 MeV/A. In summary a close inspection of the angular distribution data shows that :

- he velocity of the γ-source for symmetric and asymmetric systems is close to that of the nucleon nucleon c.m.
- in the source c.m. the angular distribution is mainly isotropic. However a small anisotropic component of E1 character has been also evidenced. The amplitude, α, of the E1 component increases with beam energy and takes the values α=0,25 and 40% respectively at 30 (ref.1), 44 and 60 MeV/A (ref.2).

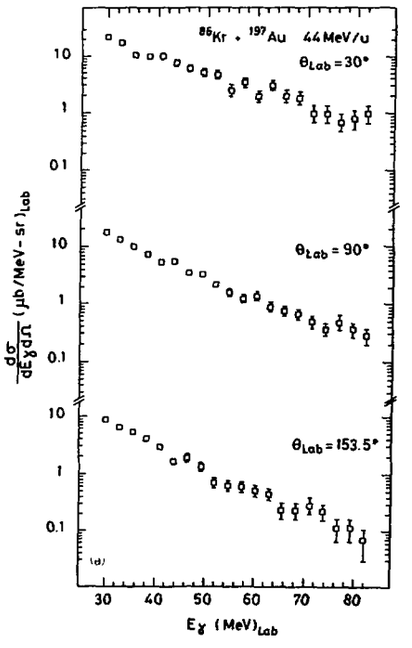

Fig. 1

Energy spectra of high energy photons for ^{86}Kr +^{197}Au at 44 MeV/A

– C –
DEVELOPMENTS

A number of theoretical studies of incoherent photon production by nucleon-nucleon collisions have been reported. The dynamic of the reaction have been treated within various models, using the Boltzmann-Uehling-Uhlenbeck equation [3], the Boltzmann master equation [4] or a transport model [5]. In these models a semi classical approximation was used for the neutron-proton bremsstrahlung elementary process. These three models are in good agreement with the Kr data. The Kr data are reported in ref.[6,7].

1) M. Kwato Njock et al., Phys. Lett. B175 (1986) 125
2) E. Grosse et al., Europhys. Lett. 2 (1986) 9
3) K. Niita et al., Texas A & M Symp. on Hot Nuclei (Dec. 1987)
4).B.A. Remington and M. Blann, Phys. Rev. C35 (1987) 1720
5) J. Randrup, Nucl Phys. A490 (1988) 418
6) R. Bertholet, Nucl Phys. A474 (1987) 541
7) R. Bertholet, J. de Phys. 47, C4 (1986) C4-201

Target	K (μb/MeV·sr)	E_0 (MeV)	α	β
C_{Nat}	30.9 ± 5.4	11.6 ± 0.5	0.31 ± 0.15	0.170 ± 0.013
Ag_{Nat}	165 ± 18	12.5 ± 0.3	0.16 ± 0.09	0.179 ± 0.010
^{197}Au	198 ± 14	12.1 ± 0.2	0.24 ± 0.06	0.143 ± 0.006
mean values		12.1 ± 0.5	0.24 ± 0.06	0.164 ± 0.015

Table 1

Least squares fit parameters calculated withe eq.(1) of the text.

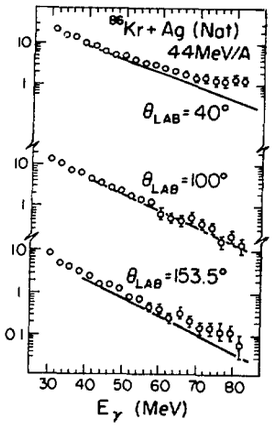

Fig.2

Comparison of experimental differential cross section of Kr+Ag reaction with calculations of ref. [5]

PROJECTILE FRAGMENTS ISOTOPIC SEPARATION :

APPLICATION TO THE LISE SPECTROMETER AT GANIL

J.P. Dufour, R. Del Moral, H. Emmermann, F. Hubert, A. Fleury, D. Jean, C. Poinot, M.S. Pravikoff
CEN Bordeaux, IN2P3, Le Haut Vigneau, F-33170 Gradignan
H. Delagrange, GANIL, B.P. 5027, F-14021 Caen Cedex
K.-H. Schmidt, GSI, D-6100 Darmstadt

The high intensity beams delivered by the GANIL facility at energies around 60 MeV/u allow the observation of many exotic light nuclei formed by projectile fragmentation. The spectrometer LISE at GANIL was designed to provide for the separation of the rare species from the close to stability isotopes which are orders of magnitude more produced. An important step was to combine the magnetic rigidity selection with a momentum loss in a solid material located in the intermediate focal plane of the two dipoles (the PFIS method). The very detailed characteristics of the LISE spectrometer and of the PFIS method can be found in refs. 1 and 2.

The study of a given nucleus requires the tuning of four parameters : the target thickness, the degrader thickness, the dipole 1 magnetic rigidity ($B\rho_1$) and the dipole 2 magnetic rigidity ($B\rho_2$).

The selection by the first dipole would allow a strict A/Z separation if the velocity of all the produced fragments was constant and if the target was thin. Even at intermediate energies (40-100 MeV/u), the reaction mechanism preserves the beam velocity rather well in average but a significant distribution width is observed which causes a band $A/Z \pm \Delta(A/Z)$ of nuclei to be simultaneously transmitted as shown in fig. 1. In addition the target also induces a spread since the fragments formed in the first or the last matter layers do not exit the target with identical velocities. The target thickness needs to be optimized to fill the $\Delta p/p$ acceptance of the spectrometer. The calculation of the optimum target must be made for each tuning according to the A, Z of the fragment and the opening of the slits defining the momentum acceptance.

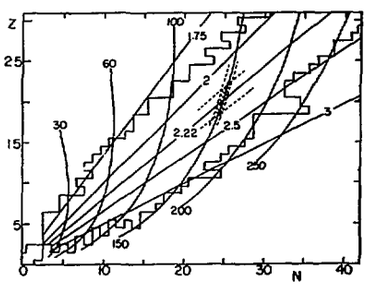

Fig. 1 : The selection operated by the degrader is shown here by a band in the N,Z plane. The lightly hatched area represents a typical selected domain which often includes only one isotope, while in less favorable cases two or three are included.

The second selection is independent of the reaction mechanism. All the ions entering the degrader are slowed down differently according to their A, Z and also their velocity. The $B\rho_2$ tuning can be analytically expressed as a function of $B\rho_1$, A, Z and d the degrader's thickness. The ions selected at the same $B\rho_2$ are those having the same ranges R_1 (A, Z, $B\rho_1$) at the exit of the first dipole. This point illustrates for example the fact that the method can separate the A and A + 1 isotopes having the same Z and dE/dx but different ranges. The ions not discriminated by the second selection are thus those having the same $Z^{1.5}/A^{2.5}$ ratios as shown in fig. 1.

In order the preserve the achromatism of the line the degrader must have a shape given by a formula independent of $B\rho_1$, $B\rho_2$, A and Z. This property is very useful since it allows the use of a unique degrader for several tunings on different ions. The only reasons to change the degrader are the mass and charge resolutions of the second selection. In practice this just implied that in one experiment with a ^{40}Ar beam at 60 MeV/n, a set of three aluminium degraders (600μ, 900μ, 1200μ) allowed to select a variety of ions ranging from ^{16}C to ^{40}S. The achieved resolution is shown in fig. 1 by a curved band crossing the $A/Z \pm \Delta(A/Z)$ band. The width of this second selection band can be estimated along a constant-Z cut, yielding a $(A/\Delta A)_d$ resolution. It must be noted that this momentum-loss resolution is very different from the usual momentum resolution of a magnet since it bears on ions all having the same initial magnetic rigidity $B\rho_1$. For degrader thicknesses going to zero, the $(A/\Delta A)_d$ also goes to zero and the width of the selection 2 in fig. 1 increases to infinity. In the case of LISE tuned on ^{37}P, the measured $(A/\Delta A)_d$ resolution reached 100 and was obtained from the ratio of the ^{37}P image diameter to the measured interval between the ^{37}P and ^{36}P images in the exit focal plane.

1 - J.P. Dufour et al., Nucl. Inst. Meth. A248 (1986) 267
2 - R. Anne et al., Nucl. Inst. Meth. A257 (1987) 215

PRODUCTION OF RADIOACTIVE SECONDARY BEAMS

R.BIMBOT, F.CLAPIER, S.DELLA-NEGRA, B.KUBICA,
Institut de Physique Nucléaire, F-91406 Orsay
R.ANNE, H.DELAGRANGE, Y.SCHUTZ, G.A.N.I.L., Caen
P.AGUER, G.BASTIN, C.S.N.S.M. Orsay
G.ARDISSON, A.HACHEM, Université de Nice
J.CHAPMAN, J.LISLE, University of Manchester (GB)
Y.GONO, K.HATANAKA, RIKEN, Japon
F.HUBERT, C.E.N. Bordeaux-Gradignan

1. Introduction

Among the recent developments concerning Nuclear Physics, one of the most promising seems to be the production of radioactive heavy ion beams. An experimental program centered on this objective was undertaken at GANIL in 1984. Secondary beams have been produced by projectile fragmentation or transfer reactions using incident ^{40}Ar and ^{18}O ions and light production targets.

2. Experimental technique

The experimental method implies the use of the magnetic spectrometer LISE for selecting the isotopes to be transmitted.

This spectrometer is composed of two dipoles, ten quadrupoles and one sextupole . The radioactive nuclei emitted around zero degree are separated from the primary beam, transported over 18 meters, and focused at the achromatic focal point F.Multiwire chambers, are used to visualize the beam profiles in several points. They are efficient in a broad range of intensities (10^3 to 10^8 particle per second). A solid state detector telescope is used to analyse the isotopic composition of the secondary beam.

3. Results

By interaction of the primary beam with the production target, a variety of secondary beams are produced. Among them, a given beam is selected by proper adjustment of the spectrometer magnetic rigidity $B\rho$. Various characteristics (beam profile, isotopic composition, intensity) of the secondary beam have been measured.

The beam profiles in F show a relatively good focusing, the beam spot being generally smaller than a 15 mm diameter circle.

The isotopic compositions of secondary beams are determined from ΔE-E (or ΔE-time of flight) bidimensional plots. The isotopes are clearly separated, as shown in Fig. 1. By varying the magnetic field in the spectrometer, a modification of the isotopic composition is observed. Thus, the spectrometer can be tuned up to achieve maximum production of a given beam.

The influence of target nature, target thickness and incident energy on the production rates have been studied.

The characteristics of several secondary beams are summarized in Table 1.

Production Mode	Secondary Beam			
	Nature	Energy* (MeV/u)	I/Io	I (pps)
44 MeV/u ^{40}Ar	^{39}Ar	35	3.10^{-4}	10^8
+	^{39}Cl	34	10^{-4}	3.10^7
99 mg/cm^2 Be	^{38}S	36	6.10^{-6}	2.10^6
45 MeV/u ^{18}O	$^{14}C, ^{17}N$	39	10^{-5}	10^7
+	^{16}C	38	$\simeq 5.10^{-7}$	5.10^5
187 mg/cm^2 Be	^{14}B	39	5.10^{-9}	5.10^3
65 MeV/u ^{18}O	$^{14}C, ^{17}N$	46	10^{-4}	10^8
+	^{16}C	52	2.10^{-6}	2.10^6
567 mg/cm^2 Be	^{14}B	47	2.10^{-8}	2.10^4

* $\Delta E/E = \pm 3.4$ %

Table 1

Note that intensities in the range 10^6 - 10^7 pps are obtained for neutron rich nuclei three-four mass units away from stability. These intensities are low, but nevertheless usable for inducing nuclear reactions.

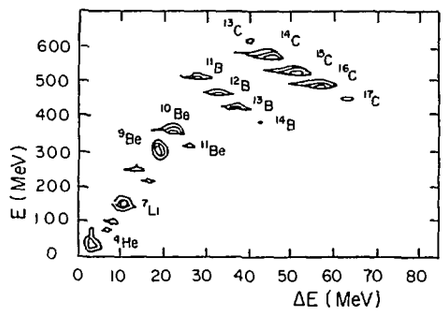

Fig. 1 : Bidimensional plot showing the isotopic composition of a secondary beam obtained in the following conditions : 65 MeV/u ^{18}O + 1036 mg/cm^2 Be. $B\rho$ = 2.248 Tm, $\Delta B\rho/B\rho$ = ± 0.22 %.

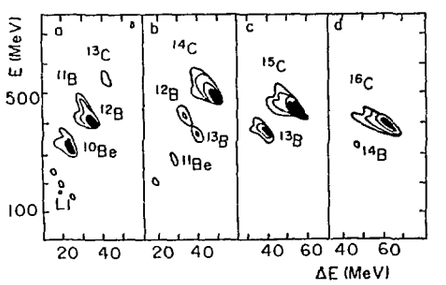

Fig. 2 : Isotopic composition of the beams obtained by purification of the beam analysed in Fig. 1 $\Delta B\rho/B\rho$ = ±2.7%. a. B2 = 1.077, b. B2 = 1.069, c. B2 = 1.057, d. B2 = 1.043.

An efficient purification of the secondary beam can be performed by using a degrader placed between the two dipoles. In order to preserve, at first order, the spectrometer achromatism, a wedge degrader must be used. Then the second dipole acts as a dispersive element. By setting properly its magnetic field (B2), one can achieve a spectacular purification of the secondary beam, leading, in the best case to the transmission of only one isotope (Fig. 2).

Secondary beams produced by this technique have already been used for Nuclear Physics experiments (spin alignment in fragmentation reactions, measurement of total reaction cross sections).

References

1. Production of Secondary Radioactive Beams from 44 MeV/u Ar Projectiles, R.Bimbot, S.Della-Negra, P.Aguer, G.Bastin, R.Anne, H.Delagrange and F.Hubert, Z. Phys. A322 (1985) 443.

2. Heavy Ion Secondary Beams, R.Bimbot, S.Della-Negra, M.Manasijevic, P.Aguer, G.Bastin, R.Anne, H.Delagrange, Y.Schutz, F.Hubert, Y.Gono and K.Hatanaka, Int. Conf. on Heavy Ion Nuclear Collisions in the Fermi Energy Domain, Caen (May 1986), J. Phys. C4 (1986) 241.

3. Nuclear Physics with Exotic Heavy Ion Beams, R.Bimbot, proc. 6th Adriatic Int. Conf. Nucl. Physics. Frontiers of Heavy Ion Physics, Dubrovnik (june 1987), 161.

4. Radioactive Heavy Ion Secondary Beams, R.Bimbot, Proc. RIKEN-IN2P3 Symposium, Shimoda (oct. 1987), 48, and Report IPNO-DRE-87-35 (1987).

5. Production of 400 MeV/u Radioactive Ion Beams for Therapy Purposes, R.Bimbot, Proc. EULIMA Workshop on the Potential Value of Light Ion Beam Therapy and Report IPNO-DRE-88-37.

A TELESCOPIC-MODE USE OF THE LISE SPECTROMETER FOR THE STUDY OF VERY FORWARD ANGULAR DISTRIBUTIONS

Ch. O. Bacri, P. Roussel, R. Anne*, M. Bernas, Y. Blumenfeld, F. Clapier,
H. Gauvin, J. Hérault, J.C. Jacmart, A. Latimier, F. Lelong,
F. Pougheon, J.L. Sida, C. Stéphan, T. Suomijarvi
Institut de Physique Nucléaire, 91406 Orsay Cédex, France

With the acceleration of heavy ions of increasingly large masses and high energies, a dominant part of the reaction products are found in a more and more reduced forward angular region [1].

The semi-classical grazing angle θ_{gr}^{lab} gives an evaluation of this angular range whereas the inverse of the grazing angular momentum ℓ_g gives a rough idea of the minimum size of any angular structure (oscillations..) which may result from an ondulatory behaviour in the collision. In turn this minimum size is related to the required experimental angular accuracy.

Projectile	^{16}O				^{84}Kr			
Target	^{12}C		^{197}Au		^{12}C		^{197}Au	
Energy (MeV/A)	25	80	25	80	25	80	25	80
θ_{gr}^{lab}(mr)	28,5	8,7	237	68	18	5,4	165	48
$1/\ell_{gr}^{lab}$(mr)	9,5	5,1	6,0	3,0	1,4	0,7	0,9	0,5

Table 1 : Grazing angle θ_{gr} and minimum angular size $1/\ell_{gr}$ (ℓ_{gr} grazing angular momentum) given in the laboratory for different H.I. collisions at GANIL.

At GANIL (table I) these figures may become rather small. It leads to specific experimental problems, even with the use of magnetic spectrometers when observations are performed both at 0° and close to the magnetic rigidity of the beam in one of its charge state [1,2,3].

Usually, the target and the focal-plane detector are linked by a point to point focusing (shifted focusing, sometimes used to accomodate finite emittance or kinematical factors, does not alter this basic mode) and angular measurements require ray-tracing techniques. Angular sorting is only achievable (though approximately) by the use of the magnet entrance slits or/and a beam catcher (Faraday cup). But they cannot any longer be used when they have to be set at very small angles and that they are submitted to a strong bombardment of scattered particles from the target and hence become prohibitive sources of doubly scattered fragments. Angular and energy straggling of the beam in the target, ghost beams, and elastic scattering on light target contaminants bring other limitations to very-forward measurements.

Drastic improvements as regards all these limitations are expected with a zero-dispersion double spectrometer used in a telescopic mode (the target and the detector are linked by a parallel to point focusing) [4]. This arrangement (fig. 1) allows (i) double Bρ and θ sorting, the latter being performed on events already selected by tuning Bρ (no strong double scattering) (ii) direct angular measurement from a position in the detector plane (iii) all other measurements (Bρ, ΔE, E, TOF...) on doubly-sorted events.

This arrangement has been set up on the spectrometer LISE [1]. The following limitations were found. Firstly, the angular dispersion R_{26} could not be given high enough a value for an accurate Bρ measurement, hence, the information on the energy had to come either from the Bρ sorting itself between the two dipoles or from a solid state telescope. Secondly, the angular aperture which was expected around ± 30 mr was found from ± 28 mr with a low efficiency down to ± 20 mr full efficiency. Within this limitations fo-

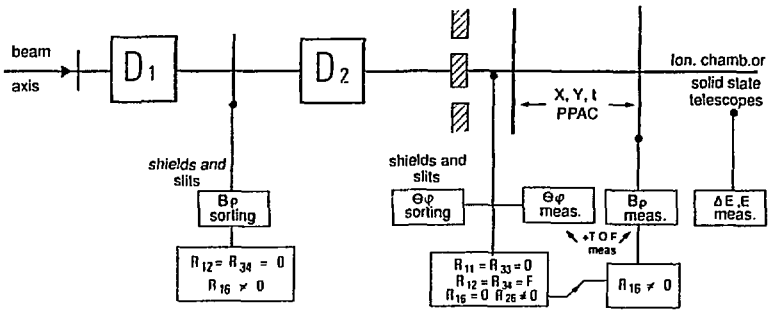

Fig. 1 : scheme of the experiment. D_1 and D_2 are the two dipoles (quadrupoles are not drawn)

*Ganil, Caen

cal lengths between 1.7 and 10 meters (R_{12} and R_{34} from 0.17 to 1.0 cm/mr) could be obtained and the 1.7 value most often used (fig. 2).

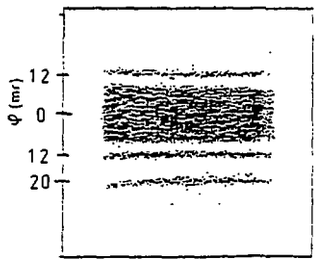

Fig. 2 : angular calibration in the detector plane (the Y non-dispersive plane is shown)

In the bombardment of *C*, *Al*, *Ni* and *Au* targets with a 44 MeV/A ^{40}Ar beam (50 to 200 nAe), angular distributions of the produced fragments at and around 0° have been measured for magnetic rigidities between 0.75 and 1.20 of that of the beam ($B\rho_0$).

A particular attention was paid to measurements close to the beam. With the gold target one could operate at 0° and as close as 2.3 °/oo of $B\rho_0$ while keeping good ion identification. Finally, by shelding the very central angular region of the beam ($\sim \pm$ 3 mr), the counting rate was decreased by more than one order of magnitude and identification still improved (fig. 3).

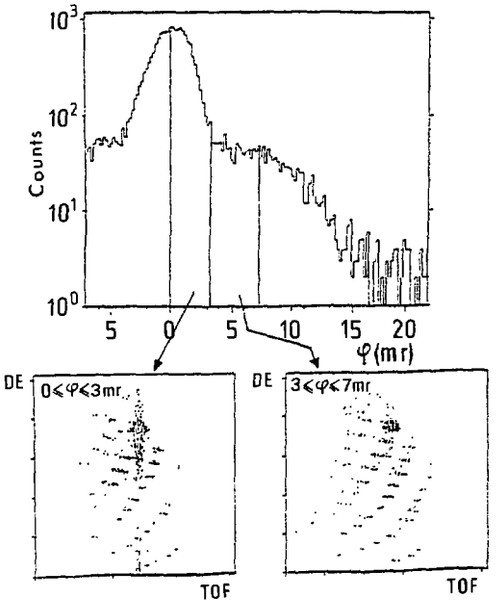

Fig. 3 : results in the study of the collision ^{40}Ar 44 MeV/A on the ^{197}Au target at 0°. The angular distribution is obtained with the indicated time of flight window. The two (partial) $\Delta E \otimes$ TOF plots are obtained for the indicated angular windows.

The results are being analysed, a sample of them is given here. Fig. 4 shows angular distributions with *Ni* target, at 0.9681 $< B\rho/B\rho_0 <$ 0.9754. We can see different behaviour (forward-peaked no-forward-peaked) of ^{40}Ar (dashed lines) and ^{38}Cl (dotted lines).

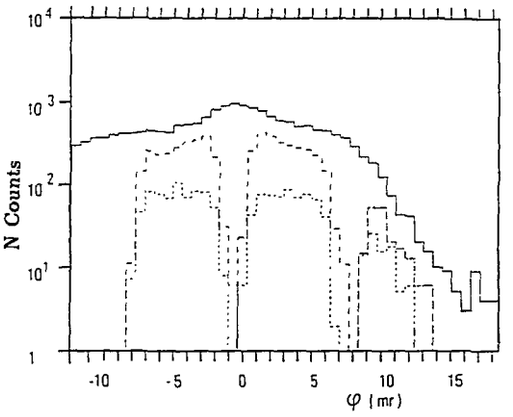

Fig. 4 : a sample of angular distribution. The continuous line is obtained with a window only on the time of flight while the full identification which requires ΔE is shopped by the granular structure of the solid state telescope.

A technical study is under process in order to increase the LISE angular acceptance in this telescopic mode which we have shown to be very efficient for these forward measurements.

References

[1] Ch. O. Bacri, thèse de l'Université Paris VII, Orsay, 1989

[2] E. Quiniou, thèse de 3e cycle, Orsay, 1985, IPNO-T-85-02
A.C. Mueller and al., Z. Phys. A 330 (1988) 63

[3] T. Suomijarvi and al, Phys. Rev. C 36 (1987) 2691

[4] P. Roussel, GEPL/05/83/58/AE/E, Orsay, 1983

DA7 "A Test of Detectors for Recoiling Fragments"

L Lavergne and L Stab, IPN, Orsay.
H-Å Gustafsson, B Jakobsson, A Kristiansson, A Oskarsson and M Westenius, Univ. of Lund, Sweden.
A J Kordyasz, Univ. of Warsaw, Poland.
K Aleklett and L Westerberg, Univ. of Uppsala, Sweden.

Though this was essentially a test of thin ion implanted Si detectors in a realistic experimental environment some results on fragmentation in 94A MeV ^{16}O induced reactions were obtained.

We placed three ΔE-E Si telescopes in the time-of-flight chamber in line D1. The E detectors were "standard" 300 μm epitaxial boron implanted detectors while the 10 μm transmission detectors were of planar type where the thinning has been made with electrochemical technique[1]. The 10 μm detectors were mounted with their junction sides facing each other and the rear side of the ΔE detector facing the target, thereby protecting against the strong electron flux. This mounting makes the energy cut-off fall from 0.9A MeV for ^{6}Li to 1.4A MeV for e.g. ^{14}N while the upper energy limit, set by the E detector thickness is 40 MeV. Fig 1, below shows the typical charge resolution ($\Delta Z=0.25\pm0.05$ units).

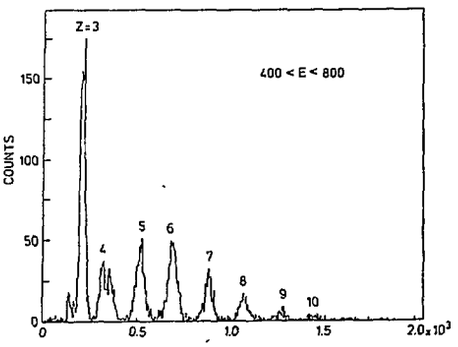

Fig 1. Charge resolution from projected ΔE-E correlations in the energy bin 2A - 3A MeV.

After corrections for the loss of particle instable isotopes we obtained the yield of $3 \leq Z \leq 12$ fragments with $1.1A \leq E \leq 6A$ MeV for $^{16}O + ^{27}Al$ and $^{16}O + ^{44}Ti$ reactions at 94A MeV. The yields at various angles for the former reaction is shown in Fig 2. Thus we observe a very high cross-section in a phase-space region which is not connected to true target fragmentation. An isotropic component - represented by the 180° yield in Fig 2 - may be the remnant of such a component and it has therefore been subtracted from the yields at 10°,30°,60° and 90° to obtain the second component. We stress that for $^{16}O + ^{44}Ti$ we find similar results for the yield in the $3 \leq Z \leq 18$ region. The question raised by our data is whether the high yields of medium heavy fragments could be explained by simple many-nucleon transfer processes or not. So far we have been able to exclude the simplest few-nucleon transfer reactions including also the knock-on mechanism and we are at present confronting our data with more complete dynamical models (e.g. VUU) possibly coupled to statistical multifragmentation processes.

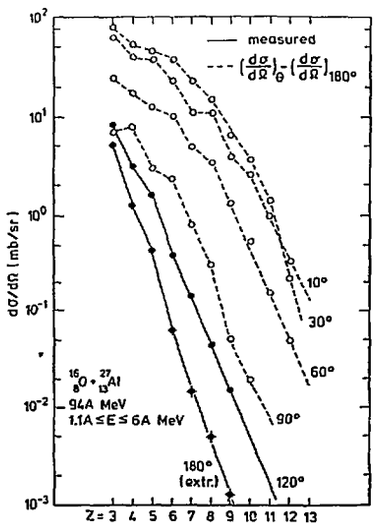

Fig 2. $d\sigma/d\Omega$ for $3 \leq Z \leq 12$ fragments in 94A MeV $^{16}O + ^{27}Al$ reactions.

Publications:

1) L Lavergne-Gosselin et al., Nucl. Instr. and Methods in press.

2) H-Å Gustafsson et al., Lund Internal Report LUIP 8901(1989)

INTERACTIONS OF 20-100 MeV/u HEAVY IONS WITH SOLID AND GASEOUS MEDIA : STOPPING POWERS, CHARGE DISTRIBUTIONS, ENERGY LOSS STRAGGLING AND ANGULAR STRAGGLING

R.BIMBOT, H.GAUVIN, J.HERAULT, B.KUBICA
Institut de Physique Nucléaire, F-91406 - Orsay Cedex
R.ANNE, G.A.N.I.L., B.P. 5027, F-14021 Caen Cedex
G.BASTIN, C.S.N.S.M., B.P.N° 1, F-91406 Orsay Cedex
F.HUBERT, C.E.N.B.G., Le Haut Vigneau, F-33170 Gradignan

1. Motivation

A study of heavy particle penetration through matter has been carried out at the GANIL facility to cover a domain of ions and energies for which no experimental information existed.

This experimental study made it possible to measure several essential parameters, namely :

- stopping powers,
- charge distributions,
- energy loss straggling,
- angular straggling.

The heavy ions which have been concerned were : $^{16-17}O$, ^{40}Ar, ^{40}Ca, $^{84-86}Kr$, ^{100}Mo, $^{129-132}Xe$ in the energy domain available for each of them at GANIL (20 to 100 MeV/u). This energy range is of great interest because it corresponds to a simplification of the slowing down process when the projectile tends to be totally stripped and the relativistic effects are still minor.

Solid and gaseous media have been used as targets in order to follow at high energy the gas-solid effect which had been observed at low energy.

All these experiments have been performed using the LISE magnetic spectrometer. Experimental details and results are given in references 1 to 9.

2. Stopping powers (ref. 1-2-7-8)

Stopping power data have been compared with calculations assuming fully stripped ions. This scaling law is derived from a relation in which the heavy ion stopping power S_{HI} is calculated from the $^4He^{++}$ one (S_{He}) at the same velocity, taking into account the ion effective charge γ :

$$S_{HI}/\gamma^2 Z_1^2 = S_{He}/\gamma_{He}^2 Z_{He}^2$$

(Z_1 atomic number of the incident ion, $\gamma_{He} = 1$, $Z_{He} = 2$). For fully stripped ions $\gamma = 1$ and the relation reduces to $S_{HI} = S_{He}\, Z_1^2/4$. S_{HI} is easily calculated with known values of S_{He} (Ziegler).

Two conclusions can be made :

- This scaling law leads to a fair agreement for projectiles which are effectively fully stripped at the target exit.
- By comparing results from solid and gaseous media with the same projectiles at the same energies, we observe a vanishing of the solid-gas effect when the projectile is totally stripped. This indicates that the solid-gas effect is really linked to the ion charge state.

From the very large set of experimental values of stopping power S a new parametrization for the effective charge γ has been deduced and an improved semi-empirical procedure to compute S values has been established (ref. 9). New tabulations of ranges and stopping powers of heavy ions in solid media will be published in the near future.

3. Charge distributions (ref. 1-2-7)

Charge distributions have been obtained for all the projectiles which have been used especially in Be, Al and Au degraders. For Kr ions in the energy range 4-50 MeV/u a semi-empirical expression has been obtained to predict the value of the mean charge state $\bar{Q}$. Some characteristics of the emission of

Auger electrons by ions exiting the targets have been emphasized.

4. Energy loss straggling (ref.4-5-9)

Experiments have been performed with solid and gaseous targets to eliminate possible discrepancies introduced by target inhomogeneities.

In the GANIL velocity regime the energy loss straggling comes from the statistical nature of the slowing down process by electronic collisions and by statistical fluctuations of the ion charge.

The energy loss straggling measurements have shown that the calculated collision straggling (Bohr's theory or Titeica formulation) cannot explain by itself the experimental values even when the projectile is totally stripped. For partially stripped ions, the charge exchange effect seems to account for most of the straggling. Calculations in some cases where only two charge states are present show a good agreement with experiment.

5. Angular straggling (ref. 3-5)

An original experimental method using the LISE spectrometer has been developed for measuring angular distributions of heavy ions exiting solid and gaseous targets in the energy range 20-90 MeV/u.

The results have been compared to multiple scattering theories based on classical or quantum mechanical calculations. Using the "reduced" Meyer parameters ($\tilde{\alpha}_{1,2}$ and τ - see ref. 3) the "universal" scaling law given by Sigmund et al has been extended over five orders of magnitude according to the expression $\tilde{\alpha}_{1,2} = 1.00\ \tau^{0.55}$ (see figure).

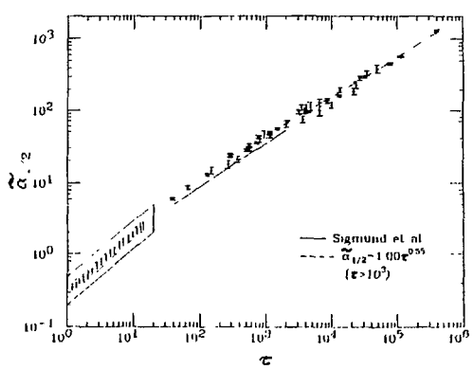

References

1. Stopping powers of solids for ^{40}Ar and ^{40}Ca ions at intermediate energies (20-80 MeV/u),
R.Bimbot, H.Gauvin, I.Orliange, R.Anne, G.Bastin, F.Hubert, Nucl. Instr. and Meth. B17 (1986) 1.

2. Stopping powers of solids for ^{16}O ions at intermediate energies (20-95 MeV/u),
H.Gauvin, R.Bimbot, J.Hérault, R.Anne, G.Bastin, F.Hubert, Nucl. Instr. and Meth. B28 (1987) 191.

3. Multiple angular scattering of heavy ions ($^{16-17}$O, ^{40}Ar, ^{86}Kr and ^{100}Mo) at intermediate energies (20-90 MeV/u),
R.Anne, J.Hérault, R.Bimbot, H.Gauvin, G.Bastin, F.Hubert, Nucl. Instr. and Meth. B34 (1988) 295.

4. Interaction of 20-100 MeV/u heavy ions with cold matter,
J.Hérault, R.Bimbot, H.Gauvin, R.Anne, G.Bastin and F.Hubert, 4th Int. Workshop "Atomic Physics for Ion Driven Fusion", Orsay, 20-24 june 1988, J. Phys. C7 (1988) 33.

5. Etude expérimentale du ralentissement d'ions lourds de 20 à 100 MeV par nucléons dans la matière,
J.Hérault, Thesis, Toulouse (1988), Orsay Report IPNO-DRE-88-25 (1988).

6. Semi-empirical formula for heavy ion stopping powers in solids in the intermediate energy range,
F.Hubert, R.Bimbot, H.Gauvin, Nucl. Instr. and Meth. (in press). Bordeaux-Gradignan Report CENBG-88-36 (1988).

7. Stopping powers of solids for $^{84-86}$Kr, ^{100}Mo and $^{129-132}$Xe ions at intermediate energies (20-45 MeV/u). Charge state distributions at the equilibrium,
H.Gauvin, R.Bimbot, J.Hérault, B.Kubica R.Anne, G.Bastin and F.Hubert, Orsay Report IPNO-DRE-89-03 (1989).

8. Stopping powers of gaseous media for ^{17}O, ^{40}Ar, ^{86}Kr and ^{132}Xe ions at intermediate energies (25-85 MeV/u),
J.Hérault, R.Bimbot, H.Gauvin, B.Kubica R.Anne, G.Bastin and F.Hubert, to be published.

9. Energy loss straggling of heavy ions (^{16}O, ^{40}Ar, ^{40}Ca, $^{84-86}$Kr, ^{100}O, ^{132}Xe) in solid and gaseous media at intermediate energies (20-100 MeV/u),
J.Hérault, R.Bimbot, H.Gauvin, R.Anne, G.Bastin and F.Hubert, to be published.

SEMI-EMPIRICAL FORMULA FOR HEAVY ION STOPPING POWERS IN SOLID IN THE INTERMEDIATE ENERGY RANGE

F. Hubert, C.E.N. Bordeaux, IN2P3, Le Haut Vigneau, F-33170 GRADIGNAN
R. Bimbot et H. Gauvin, IPN Orsay, B.P. n° 1, F-91405 ORSAY

Stopping-powers and ranges have played a crucial role in many aspects of the heavy-ion physics. Requirements in Nuclear Physics, Atomic and Solide State Physics, aerospace projects, ionizing radiation effects on matter have fostered many revisions and new calculations on the subject. Due to the complexity of atomic structures all these calculations have to adopt some approximations in order to simplify the calculations and/or to rely on a semi-phenomenological treatment. Then they must be justified by experimental data when available.

In the 2-10 MeV/A energy range the comparison between experimental stopping powers and calculations such as those tabulated by Northcliffe and Schilling[1] or the more recently published curves of Ziegler[2] have shown significant discrepancies, particularly for light stopping media and heavy projectiles. In this energy domain the best agreement is generally obtained with the tables of Hubert et al.[3]. With the GANIL, the energy domain from 20 to 100MeV/A has become accessible for heavy ions. This made it possible to measure stopping powers in this energy range and an extensive study has been performed using the GANIL spectrometer LISE. In the 20-80MeV/A energy range, the tabulations of Hubert et al are in reasonable agreement with most of the data, but overestimate the stopping powers essentially in light stopping media. In this case a better agreement is obtained with the values from Ziegler.

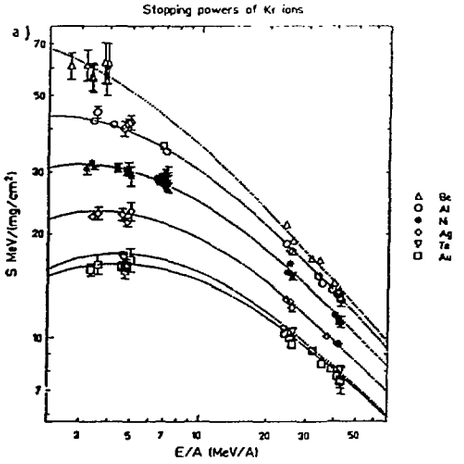

It appeared then that it was worth reconsidering the prospects for a semi-empirical calculation of heavy ion stopping in the light of the considerable body of heavy ion data now available in the energy range from 3 to 80MeV/A.

The generalization of heavy ion stopping powers was made using the Bethe equation : the stopping power $S_{1,2}$ of a given medium (2) for a given ion (1) is calculated from that of this medium for α particles at the same velocity (same E/A value) denoted $S_{\alpha,2}$ using the following equation :

$$[1] \qquad S_{1,2} = (S_{\alpha,2}/4) \cdot (\gamma_{1,2} Z_1)^2$$

The effective charge parameter γ cannot be easily deduced from basic principles. We then used eq.[1] to calculate γ values from the available experimental stopping powers. Thus, a set of about 600 effective charge parameters have been calculated.

The analysis of these data has clearly pointed out the necessity of taking into account the variation of γ with the stopping medium. The following formulae have been derived for the calculation of heavy ion effective charges in solids which are suitable for the intermediate energy region.

$$\gamma = 1 - x_1 \exp(-x_2 (E/A)^{x_3} Z_1^{-x_4})$$

with $x_1 = D + 1.658 \exp[-0.05170 Z_1]$
$D = 1.1764 + 0.2319 \exp(-0.0043022 Z_2)$
$x_2 = 8.144 + 0.09876 \ln Z_2$
$x_3 = 0.3140 + 0.01072 \ln Z_2$
$x_4 = 0.5218 + 0.02521 \ln Z_2$

Fig. 1 gives examples of the agreement observed in most of the case.

Fig. 1 : Comparison of experimental stopping powers with the results of calculations presented in the text (dotted lines).

1) L.C. Northcliffe and R.F. Schilling, Nucl. Data Tables A7 (1970)233
2) J.F. Ziegler, Handbook of stopping cross sections for energetic ions in all elements (Pergamon, New York, 1980).
3) F. Hubert, A. Fleury, R. Bimbot and D. Gardes, Ann. Phys. (France) vol 5S (1980) 1.
4) F. Hubert, R. Bimbot, H. Gauvin, accepted for publication in NIM B

AUTHOR INDEX

AUTHOR INDEX

LABORATORY INDEX

BELGIUM

Service de Physique Théorique
Univ. Libre de Bruxelles (ULB)
Campus de la Plaine C.P. 225
Bd. du Triomphe
B-1050 BRUXELLES

Inst. de Phys. au Sart-Tilman
Service de Phys. Théor. et Math.
Univ. de Liège
Bât B5
B-4000 LIEGE 1

BRAZIL

Inst. de Fisica (IFUSP)
Univ. de São Paulo
Caixa Postal 20516
01498 SAO PAULO SP
Brazil

CANADA

Foster Radiation Laboratory
Me Gill Univ.
MONTREAL PQ, Canada, H3A 2B2

CHINA

Inst. of Modern Physics
Acad. Sinica
P.O. Box 31
57 Nanchang Road
LANZHOU (Gansu)
China

DENMARK

Niels Bohr Inst.
Univ. of Copenhagen
Blegdamsvej 17
DK -2100 KOBENHAVN

FRANCE

Grand Accélérateur National d'Ions Lourds (GANIL)
BP 5027
F-14021 CAEN Cédex

Centre de Recherche Interdisciplaire
avec les Ions lourds (CIRIL)
BP 5133
14040 CAEN Cédex

Laboratoire de Physique Corpusculaire
Boulevard du Maréchal Juin
14032 CAEN Cédex

Laboratoire National Saturne (LNS)
Centre d'Etudes Nucléaires de Saclay (CEN)
F-91191 GIF sur YVETTE Cédex

Service de Physique Nucléaire (DPhN)
Centre d'Etudes Nucléaires de Saclay (CEN)
F-91191 GIF sur YVETTE

Laboratoire de Physique Théorique
Univ. de Bordeaux 1
Rue du Solarium
F-33170 GRADIGNAN

Centre d'Etudes Nucléaires (CEN)
Univ. de Bordeaux 1
Le Haut Vigneau
F-33170 GRADIGNAN

Centre d'Etudes Nucléaires (CEN)
DRF/PhN
BP 85 X
F-38041 GRENOBLE Cédex

Inst. des Sciences Nucléaires (ISN)
Univ. de Grenoble
Avenue des Martyrs 53
F-38026 GRENOBLE Cédex

Laboratoire de Physique Nucléaire
Fac. de Sciences et de Techniques
Univ. de Nantes
2, rue de la Houssinière
F-44072 NANTES Cédex 03

Ireste
La Chanterie
Université de Nantes
F-44087 NANTES Cédex 03

Laboratoire René Bernas
F-91405 ORSAY

Inst. de Physique Nucléaire (IPN)
Univ. de Paris-Sud (Paris XI)
B.P. 1
F-91406 ORSAY Cédex

Centre de Spectrométrie Nucléaire et
de Spectrométrie de Masse (CSNSM)
Bât. 104-108
F-91504 ORSAY

Centre de Recherches Nucléaires (CRN)
B.P. 20 CRO
F-67037 STRASBOURG Cédex

Inst. de Physique Nucléaire (IPN)
Univ. Claude Bernard Lyon 1
43, bd du 11 Novembre 1918
F-69622 VILLEURBANNE Cédex

GREECE

Physics Depat.
Univ. of Athens
Panepistimioupoli-Kouponia
GR-157 71 ATHINAI

HUNGARY

Inst. for Theoretical Physics
Eötvös Lorand Univ.
Puskin utca 5-7
HH-1088 BUDAPEST

INDIA

Saha Inst. of Nuclear Physics
92 Acharya Prafulla Chandra Road
CALCUTTA 700 009

ISRAEL

Weissmann Institute of Science
Nuclear Physics Dept.
P.O. Box 26
76 100 REHOVOT
Israël

ITALY

Dept. di Fisica
Univ. di Catania
Corso Italia 57
I-95129 CATANIA

Dept. di Fisica dell' Universita (INFN)
Ist. di Sci. Fis. Aldo Pontremolo
Univ. Degli Studi di Milano
Via Celoria, 16
I-20133 MILANO

Ins. Naz. di Fisica Nucleare (INFN)
Mostra d'Oltremare, Pad 20
I-80125 NAPOLI

JAPAN

Inst. of. Physics
Univ. of Tsukuba
IBARAKI 305

Dept. of Physics
Tokyo Inst. of Technology
2-12-1 Oh-Okayama
Meguro-Ku
TOKYO 152

Inst. of Physical and Chemical Research (Riken)
2-1 Hirosawa
Wako-Shi
SAITAMA 351-01

Dept. of Physics
Rikkyo Univ.
Nishi-Ikebukuro
Toshima-ku
TOKYO 171

Dept. of Physics
Tokyo Inst. of Technology
2-12-1 Oh-okayama
Meguro-ku
TOKYO 152

NORWAY

Dept. of Physics
Univ. of Oslo
P.O. Box 1048
Blindern
N-0316 OSLO 3

POLAND

Univ. of Warsaw
ul. HOZA 69
Pl.00681 WARSZAWA
Poland

R.F.A.

Hahn-Meitner-Institut (HMI)
Berlin GmbH
Glienicker Str. 100
D-1000 BERLIN 39

Ges. f. Schwerionenforschung mbH (GSI)
Postfach 110 552
Planckstr. 1
D-6200 DARMSTADT 11

Inst. f. Kernphysik
Tech. Hochschule
Schlossgartenstr. 9
D-6100 DARMSTADT

Physics Dept. T30
Tech. Univ. München
James-Franck-Strasse
D-8046 GARCHING BEI MUNCHEN

Inst. f. Physik
Univ. Göttigen
Bunsenstrasse 9
D-3400 GOTTINGEN

Physikalisches Inst.
Univ. Heidelberg
Philosophenweg 12
D-6900 HEIDELBERG

Inst. f. Physik
Johannes-Gutenberg-Univ.
Postfach 39 80
D-6500 MAINZ

Inst. f. Thor. Phys.
Univ. Regensburg
Postfach 397
Universitätsstrasse 31
D-8400 REGENSBURG

ROMANIA

Inst. for Physics and Nuclear Energy (INPE)
P.O. Box MG-6
R-76900 BUCURESTI-MAGURELE

SPAIN

Dept. de l'Estructura i Constitucats de la Materia
Fac. de Fisica
Univ. de Barcelona
Diagonal 64
E-08028 BARCELONA

Dept. de Fisica
Univ. de les Illes Baléares
E-07071 PALMA DE MALLORCA

SWEDEN

Dept. of PHYSICS
Univ. of Lund
Sölvegatan 14A
S-223 62 LUND

Univ. of Uppsala
P.O. Box 533
S-751 21 UPPSALA

UNITED KINGDOM

Daresbury Lab.
Daresbury
WARRINGTON WA4 4AD

U.R.S.S.

Laboratory of Nuclear Reactions
Joint Inst. for Nuclear Rescarch (JINR)
Dubna, Head Post Office
P.O. Box 79
101 000 Moskva
DUBNA
URSS

U.S.A.

Lawrence Berkeley (LBL)
1 cyclotron Road
BERKELEY CA 94720
U.S.A.

Center for Theoritical Physics
Massachusetts Inst. of Technology (MIT)
CAMBRIDGE MA 02139
U.S.A.

Cyclotron Institute
Texas A and M Univ.
COLLEGE STATION TX 77843
U.S.A.

Dept. of Physics
Oregon State Univ.
CORVALLIS OR 97331
U.S.A.

Dept. of Physics
Univ. of Iowa
IOWA CITY IA 52242
U.S.A.

Physics Division
Oak Ridge National Lab. (ORNL)
P.O. Box 2008
OAK RIDGE TN 37831-6369
U.S.A.

Dept. of Chemistry
Washington Univ.
Campus Box 1105
1 Brookings Dr
ST LOUIS MO 63130-4899
U.S.A.

Dept. of Physics
State Univ. of New York (SUNY)
STONY BROOK NY 11794-3800
U.S.A.

YUGOSLAVIA

Dept. of Theor. Physics
Boris Kidric Inst. Vinca (BKI)
P.O. Box 522
YU-11001 BEOGRAD

II
PUBLICATION LIST

1983-1984

ISOTOPIC DISTRIBUTIONS OF PROJECTILE-LIKE FRAGMENTS IN 44 MeV/u ^{40}Ar INDUCED REACTIONS
GUERREAU D., BORREL V., JACQUET D., GALIN J., GATTY B., TARRAGO X.
IPN - ORSAY
PHYS. LETT. B131 (1983) 293.

PERIPHERAL Ar INDUCED REACTIONS AT 44 MeV/u - SIMILARITIES AND DEVIATIONS WITH RESPECT TO A HIGH ENERGY FRAGMENTATION PROCESS
BORREL V., GUERREAU D., GALIN J., GATTY B., JACQUET D., TARRAGO X.
IPN - ORSAY
Z. FUR PHYSIK A314 (1983) 191.

ELASTIC SCATTERING OF ^{40}Ar ON ^{60}Ni, ^{120}Sn AND ^{208}Pb AT 44 MeV/u
ALAMANOS N., AUGER F., BARRETTE J., BERTHIER B., FERNANDEZ B., GASTEBOIS J., PAPINEAU L., DOUBRE H., MITTIG W.
CEN - SACLAY, GANIL - CAEN
PHYS. LETT. B137 (1984) 37.

EXPERIMENTAL EVIDENCE OF HIGHLY ENERGY RELAXED PRODUCTS IN THE 35 MeV/u ^{84}Kr + ^{197}Au REACTION
DALILI D., LHENORET P., LUCAS R., MAZUR C., NGO C., RIBRAG M., SUOMIJARVI T., TOMASI E., BOISHU B., GENOUX LUBIN A., LEBRUN C., LECOLLEY J.F., LEFEBVRES F., LOUVEL M., REGIMBART R., ADLOFF J.C., KAMILI A., RUDOLF G., SCHEIBLING F.
CEN - SACLAY, LPC - CAEN, CRN - STRASBOURG
Z. FUR PHYSIK A316 (1984) 371

FEW NUCLEON TRANSFER VERSUS FRAGMENTATION IN THE PRODUCTION OF PROJECTILE-LIKE FRAGMENTS IN THE ^{40}Ar + ^{68}Zn REACTION AT 27.6 MeV/NUCLEON
RAMI F., COFFIN J.P., GUILLAUME G., HEUSCH B., WAGNER P., FAHLI A., FINTZ P.
CRN - STRASBOURG
Z. FUR PHYSIK A318 (1984) 239

HEAVY PRODUCTS FROM VIOLENT COLLISIONS IN THE ^{40}Ar + ^{nat}Ag SYSTEM AT 27 MeV/u
BORDERIE B., RIVET M.F., CABOT C., FABRIS D., GARDES D., GAUVIN H., HANAPPE F., PETER J.
IPN - ORSAY, UNIV. LIBRE DE BRUXELLES, GANIL - CAEN
Z. FUR PHYSIK A316 (1984) 243

INVESTIGATION OF THE ^{40}Ar + ^{197}Au, ^{238}U SYSTEMS AT 44 MeV/u
LERAY S., NEBBIA G., GREGOIRE C., LA RANA G., LHENORET P., MAZUR C., NGO N., RIBRAG M., TOMASI E., CHIODELLI S., CHARVET J.L., LEBRUN C.
CEN - SACLAY, IPN - LYON, CEN - BRUYERES-LE-CHATEL, LPC - CAEN
NUCL. PHYS. A425 (1984) 345

HIGH MOMENTUM AND ENERGY TRANSFER INDUCED BY 1760 MeV ^{40}Ar ON ^{197}Au AND ^{232}Th TARGETS
POLLACO E.C., CONJEAUD M., HARAR S., VOLANT C., CASSAGNOU Y., DAYRAS R., LEGRAIN R., NGUYEN M.S., OESCHLER H., SAINT-LAURENT F.
CEN - SACLAY, TECHNISCHE HOCHSCHULE - DARMSTADT, GANIL - CAEN
PHYS. LETT. B146 (1984) 29

INCOMPLETE LINEAR MOMENTUM TRANSFER IN NUCLEAR REACTIONS : AN INTERPLAY BETWEEN ONE-BODY AND TWO-BODY DISSIPATION
GREGOIRE C., SCHEUTER F.
GANIL - CAEN
PHYS. LETT. B146 (1984) 21

REACHING THE CAPACITY OF A COMPOSITE NUCLEUS FOR ENERGY AND SPIN CONTAINMENT

JACQUET D., DUEK E., ALEXANDER J.M., BORDERIE B., GALIN J., GARDES D., GUERREAU D., LEFORT M., MONNET M., RIVET M.F., TARRAGO X.
IPN - ORSAY

PHYS. REV. LETT. 53 (1984) 2226

FISSION-FRAGMENT KINETIC-ENERGY DISTRIBUTIONS FROM A TWO-DIMENSIONAL FOKKER-PLANCK EQUATION

SCHEUTER F., GREGOIRE C., HOFMANN H., NIX J.R.
GANIL - CAEN, PHYS. DEPT. - MUNICH, LANL - LOS ALAMOS

PHYS. LETT. B149 (1984) 303

LIGHT FRAGMENTS PRODUCED IN ^{40}Ar + ^{nat}Ag REACTIONS AT 27 MeV/u

BORDERIE B., RIVET M.F., CABOT C., FABRIS D., GARDES D., GAUVIN H., HANAPPE F., PETER J.
IPN - ORSAY, UNIV. LIBRE DE BRUXELLES, GANIL - CAEN

Z. FUR PHYSIK A318 (1984) 315

SUBTHRESHOLD PRODUCTION OF NEUTRAL PIONS WITH Ar IONS OF 44 MeV/u

HECKWOLF H., GROSSE E., DABROWSKI H., KLEPPER O., MICHEL C., MULLER W.F.J., NOLL H., BRENDEL C., ROSCH W., JULIEN J., PAPPALARDO G.S., BIZARD G., LAVILLE J.L., MUELLER A.C., PETER J.
GSI - DARMSTADT, GSI AND UNIV. OF FRANKFURT, TH - DARMSTADT, CEN - SACLAY, LPC - CAEN, GANIL - CAEN

Z. FUR PHYSIK A315 (1984) 243

1985

NUCLEUS-NUCLEUS POTENTIAL INSIDE THE STRONG-ABSORPTION RADIUS FROM ^{16}O + ^{12}C ELASTIC SCATTERING AT 94 MeV/u
ROUSSEL P., ALAMANOS N., AUGER F., BARRETTE J., BERTHIER B., FERNANDEZ B., PAPINEAU L., DOUBRE H., MITTIG W.
CEN - SACLAY, GANIL - CAEN
PHYSICAL REVIEW LETTERS 54 (1985) 1779

SOME OPTICAL-MODEL ANALYSES OF THE ELASTIC SCATTERING OF ^{40}Ar AT 1760 MeV
EL-AZAB FARID M., SATCHLER G.R.
ASSIUT UNIV. (EGYPT), OAK RIDGE (USA)
NUCLEAR PHYSICS A441 (1985) 157

DIRECT SURFACE TRANSFER REACTIONS INDUCED BY A 1102 MeV ^{40}Ar BEAM ON ^{68}Zn TARGET NUCLEUS
MERMAZ M.C., RAMI F., COFFIN J.P., GUILLAUME G., HEUSCH B., WAGNER P., FAHLI A., FINTZ P.
CEN - SACLAY, CRN - STRASBOURG
PHYSICAL REVIEW C31 (1985) 1972

DIRECT SURFACE-TRANSFER REACTION TO THE CONTINUUM STATES INDUCED BY A 1760 MeV ^{40}Ar BEAM ON ^{27}Al AND ^{nat}Ti TARGET NUCLEI
MERMAZ M.C., DAYRAS R., BARRETTE J., BERTHIER B., DE CASTRO RIZZO D.M., CISSE O., LEGRAIN R., PAGANO A., POLLACCO E., DELAGRANGE H., MITTIG W., HEUSCH B., LANZANO G., PALMERI A.
CEN - SACLAY, GANIL - CAEN, CRN - STRASBOURG, INFN - CATANIA
NUCLEAR PHYSICS A441 (1985) 129

TRANSFER OF NUCLEONS AT HIGH RELATIVE VELOCITIES
VON OERTZEN W.
ISN - GRENOBLE, GANIL - CAEN
PHYSICS LETTERS 151B (1985) 95

INVESTIGATION OF THE Kr + Au SYSTEM AT 22 MeV/u
DALILI D., BERLANGER M., LERAY S., LUCAS R., MAZUR C., NGO C., RIBRAG N., SUOMIJARVI T., CERRUTI C., CHIODELLI S., DEMEYER A., GUINET D., GENOUX LUBIN A., LEBRUN C., LECOLLEY J.F., LEFEBVRES F., LOUVEL M.
CEN - SACLAY, IPN - LYON, LPC - CAEN
Z. FUR PHYSIK A320 (1985) 349

STUDY OF THE ^{40}Ar + ^{68}Zn REACTION AT 27.6 MeV/NUCLEON
RAMI F., COFFIN J.P., GUILLAUME G., HEUSCH B., WAGNER P., FAHLI A., FINTZ P.
CRN - STRASBOURG
NUCLEAR PHYSICS A444 (1985) 325

SEMI-CLASSICAL PHASE SPACE APPROACH FOR THE CHARGE EQUILIBRATION FLUCTUATIONS IN HEAVY ION REACTIONS
DI TORO M., GREGOIRE C.
GANIL - CAEN
Z. FUR PHYSIK A320 (1985) 321

HIGH ENERGY FRAGMENTS PRODUCED IN THE ^{84}Kr + ^{93}Nb REACTION AT 34.5 MeV/u
CHARVET J.L., JOLY S., MORJEAN M., PATIN Y., PRANAL Y., SINOPOLI L., UZUREAU J.L., BILLEREY R., CHAMBON B., CHBIHI A., CHEVARIER A., CHEVARIER N., DRAIN D., PASTOR C., STERN M., PEGHAIRE A.
CEN - BRUYERES-LE-CHATEL, IPN - LYON, GANIL - CAEN
Z. FUR PHYSIK A321 (1985) 701

NUCLEAR FRAGMENTATION PROCESSES IN THE ^{20} Ne + ^{27} Al SYSTEM AT 30 MeV/A
MORJEAN M., CHARVET J.L., UZUREAU J.L., PATIN Y., PEGHAIRE A., PRANAL Y., SINOPOLI L., BILLEREY A., CHEVARIER A., CHEVARIER N., DEMEYER A., STERN M., LA RANA G., LERAY S., LUCAS R., MAZUR C., NEBBIA G., NGO C., RIBRAG M.
CEN - BRUYERES-LE-CHATEL, IPN - LYON, CEN - SACLAY
NUCL. PHYS. A438 (1985) 547.

PRODUCTION AND IDENTIFICATION OF NEW NEUTRON-RICH FRAGMENTS FROM 33 MeV/u ^{86} Kr BEAM IN THE 18 $\leqslant$ Z $\leqslant$ 27 REGION
GUILLEMAUD-MUELLER D., MUELLER A.C., GUERREAU D., ANNE R., DETRAZ C., POUGHEON F., BERNAS M., GALIN J., JACMART J.C., LANGEVIN M., NAULIN F., QUINIOU E., DETRAZ C.
GANIL - CAEN, IPN - ORSAY
Z. FUR PHYSIK A322 (1985) 415

PRODUCTION OF NEUTRON-RICH NUCLEI AT THE LIMITS OF PARTICLES STABILITY BY FRAGMENTATION OF 44 MeV/u ^{40} Ar PROJECTILES
LANGEVIN M., QUINIOU E., BERNAS M., GALIN J., JACMART J.C., NAULIN F., POUGHEON F., ANNE R., DETRAZ C., GUERREAU D., GUILLEMAUD-MUELLER D., MUELLER A.C.
IPN - ORSAY, GANIL - CAEN
PHYSICS LETTERS B150 (1985) 71

PRODUCTION OF SECONDARY RADIOACTIVE BEAMS FROM 44 MeV/U Ar PROJECTILES
BIMBOT R., DELLA NEGRA S., AUGER P., BASTIN G., ANNE R., DELAGRANGE H., HUBERT F.
IPN - ORSAY, CSNSM - ORSAY, GANIL - CAEN, CEN/BG - GRADIGNAN
Z. FUR PHYSIK A322 (1985) 443

APPROACH TO THE LIMITS FOR MASSIVE ENERGY AND SPIN DEPOSITION INTO A COMPOSITE NUCLEUS
JACQUET D., GALIN J., BORDERIE B., GARDES D., GUERREAU D., LEFORT M., MONNET F., RIVET M.F., TARRAGO X., DUEK E., ALEXANDER John M.
IPN - ORSAY, DEPT. OF CHEMISTRY - STONY BROOK
PHYS. REV. C32 (1985) 1594

STUDY OF THE ^{40} Ar + ^{68} Zn REACTION AT 27.6 MeV/NUCLEON
RAMI F., COFFIN J.P., GUILLAUME G., HEUSCH B., WAGNER P., FAHLI A., FINTZ P.
CRN - STRASBOURG
NUCL. PHYS. A444 (1985) 325

CENTRAL COLLISIONS IN THE ARGON INDUCED FISSION OF THORIUM IN THE TRANSITION ENERGY REGIME
CONJEAUD M., HARAR S., MOSTEFAI M., POLLACCO E.C., VOLANT C., CASSAGNOU Y., DAYRAS R., LEGRAIN R., OESCHLER H., SAINT-LAURENT F.
CEN - SACLAY, TECHNISCHE HOCHSCHULE - DARMSTADT, GANIL - CAEN
PHYS. LETT. B159 (1985) 244

INVESTIGATION OF LINEAR MOMENTUM TRANSFER ON THE 35 MeV/u Ar + U SYSTEM
LERAY S., GRANIER O., NGO C., TOMASI E., CERRUTI C., L'HENORET P., LUCAS R., MAZUR C., RIBRAG M., CHARVET J.L., HUMEAU C., LOCHARD J.P., MORJEAN M., PATIN Y., SINOPOLI L., UZUREAU J., GUINET D., VAGNERON L., PEGHAIRE A.
CEN - SACLAY, CEN - BRUYERES-LE-CHATEL, IPN - LYON, GANIL - CAEN
Z. FUR PHYSIK A320 (1985) 533

LIGHT PARTICLES AND PROJECTILE LIKE FRAGMENTS FROM ^{40} Ar + ^{12} C REACTION AT 44 MeV/NUCLEON
HEUER D., BERTHOLET R., GUET C., MAUREL M., NIFENECKER H., RISTORI Ch., SCHUSSLER F., BONDORF J.P., NIELSEN O.B.
CEN - GRENOBLE, NBI - COPENHAGEN
PHYSICS LETTERS B161 (1985) 269

OBSERVATION OF COMPOSITE NUCLEI AT VERY HIGH TEMPERATURES
AUGER G., JOUAN D., PLAGNOL E., POUGHEON F., NAULIN F., DOUBRE H., GREGOIRE C.
IPN - ORSAY, GANIL - CAEN
Z. FUR PHYSIK A321 (1985) 243

VANISHING OF THE FUSION-LIKE PROCESS IN HEAVY-ION COLLISIONS
BORDERIE B., RIVET M.F.
IPN - ORSAY
Z. FUR PHYSIK A321 (1985) 703

^{124} Sn TARGET RESIDUES IN THE INTERACTION OF HEAVY IONS AT INTERMEDIATE ENERGIES
BLACHOT J., CRANCON J., DE GONCOURT B., GIZON A., LLERES A.
CEN - GRENOBLE, ISN - GRENOBLE
Z. FUR PHYSIK A321 (1985) 645

HEAVY FRAGMENTS EMISSION IN THE ^{84} Kr ON ^{12} C REACTION AT 35 MeV/NUCLEON
MITTIG W., CUNSOLO A., FOTI A., WIELECZKO J.P., AUGER F., BERTHIER B., PASCAUD J.M., QUEBERT J., PLAGNOL E.
GANIL - CAEN, CEN - SACLAY, CEN - BORDEAUX-GRADIGNAN, IPN - ORSAY
PHYS. LETT. B154 (1985) 259

EMISSION TEMPERATURES IN INTERMEDIATE ENERGY NUCLEAR COLLISIONS FROM THE RELATIVE POPULATIONS OF WIDELY SEPARATED STATES IN ^{5} Li AND ^{8} Be
POCHODZALLA J., FRIEDMAN W.A., GELBKE C.K., LYNCH W.G., MAIER M., ARDOUIN D., DELAGRANGE H., DOUBRE H., GREGOIRE C., KYANOWSKI A., MITTIG W., PEGHAIRE A., PETER J., SAINT-LAURENT F., VIYOGI Y.P., ZWIEGLINSKI B., BIZARD G., LEFEBVRES F., TAM QUEBERT J.
NSCL - MICHIGAN STATE UNIVERSITY, GANIL - CAEN, LPC - CAEN, CEN - BORDEAUX-GRADIGNAN
PHYS. LETT. B161 (1985) 275

NUCLEAR TEMPERATURES AND THE POPULATION OF PARTICLE-UNSTABLE STATES OF ^{6} Li IN ^{40} Ar-INDUCED REACTIONS ON ^{197} Au AT E/A = 60 MeV
POCHODZALLA J., FRIEDMAN W.A., GELBKE C.K., LYNCH W.G., MAIER M., ARDOUIN D., DELAGRANGE H., DOUBRE H., GREGOIRE C., KYANOWSKI A., MITTIG W., PEGHAIRE A., PETER J., SAINT-LAURENT F., VIYOGI J.P., ZWIEGLINSKI B., BIZARD G., LEFEBVRES F., TAMAIN B., QUEBERT J.
NSCL - MICHIGAN STATE UNIVERSITY, GANIL - CAEN, LPC - CAEN, CEN - BORDEAUX-GRADIGNAN
PHYS. REV. LETT. 55 (1985) 177

REACTION MECHANISM STUDY FOR THE SYSTEM : ^{20} Ne + ^{60} Ni AT 44 MeV/A
D'ONOFRIO A., DUMONT H., DELAUNAY B., DELAUNAY J., BRONDI A., MORO M., ROMANO M., TERRASI F., CAVALLARO S., SPERDUTO L., SAINT-LAURENT M.G.
CEN - SACLAY, INFN - NAPOLI, INFN - CATANIA, GANIL - CAEN
LETTERE AL NUOVO CIMENTO 42 (1985) 347

SEMICLASSICAL APPROACHES TO PROTON EMISSION IN INTERMEDIATE-ENERGY HEAVY-ION REACTIONS
GREGOIRE C., SCHEUTER F., REMAUD B., SEBILLE F.
GANIL - CAEN, IPN - NANTES
NUCL. PHYS. A436 (1985) 365

THREE-PARTICLE EFFECTS OBSERVED IN TWO-PARTICLE CORRELATION MEASUREMENTS
POCHODZALLA J., FRIEDMAN W.A., GELBKE C.K., LYNCH W.G., MAIER M., ARDOUIN D., DELAGRANGE H., DOUBRE H., GREGOIRE C., KYANOWSKI A., MITTIG W., PEGHAIRE A., PETER J., SAINT-LAURENT F., VIYOGI Y.P., ZWIEGLINSKI B., BIZARD G., LEFEBVRES F., TAMAIN B., QUEBERT J.
MSU - EAST LANSING, GANIL - CAEN, LPC - CAEN, CEN - BORDEAUX-GRADIGNAN
PHYS. LETT. B161 (1985) 256

NUCLEAR COLLISIONS AT INTERMEDIATE ENERGIES : ACHIEVEMENTS AND PROSPECTS OF GANIL

DETRAZ C.
GANIL - CAEN

NATURE 315 (1985) 6017

1986

CONTRIBUTION OF DECAY PRODUCTS OF TRANSFER REACTIONS TO HEAVY-ION INELASTIC AND TRANSFER SPECTRA
BLUMENFELD Y., ROYNETTE J.C., CHOMAZ Ph., FRASCARIA N., GARRON J.P., JACMART J.C.
IPN - ORSAY
NUCLEAR PHYSICS A445 (1985) 151

ONE-NUCLEON TRANSFER REACTIONS TO DISCRETE LEVELS INDUCED BY A 793 MeV ^{16}O BEAM ON A ^{208}Pb TARGET
BERTHIER B., BARRETTE J., GASTEBOIS J., GILLIBERT A., LUCAS R., MATUSZEK J., MERMAZ M.C., MICZAIKA A., VAN RENTERGHEM E., SUOMIJARVI S., BOUCENNA A., DISDIER D., GORODETZKY P., KRAUS L., LINCK I., LOTT B., RAUCH V., REBMEISTER R., SCHEIBLING F., SCHULZ N., SENS J.C., GRUNBERG C., MITTIG W.
CEN - SACLAY, CRN - STRASBOURG, GANIL - CAEN
PHYSICS LETTERS B182 (1986) 15

ANGULAR EVOLUTION OF PERIPHERAL HEAVY ION REACTIONS AT INTERMEDIATE ENERGIES
BLUMENFELD Y., CHOMAZ Ph., FRASCARIA N., GARRON J.P., JACMART J.C., ROYNETTE J.C., ARDOUIN D., MITTIG W.
IPN - ORSAY, GANIL - CAEN
NUCLEAR PHYSICS A455 (1986) 357

FRAGMENTATION AND/OR TRANSFER REACTIONS IN THE 35 MeV/u Ar + Ag SYSTEM
BIZARD G., BROU R., DROUET A., HARASSE J.M., LAVILLE J.L., PATRY J.P., PLOYARD G., STECKMEYER J.C., TAMAIN B., DOUBRE H., PETER J., GUILBAULT F., LEBRUN C., OUBAHADOU A., HANAPPE F.
LPC - CAEN, GANIL - CAEN, IPN - NANTES, FNRS AND UNIV. LIBRE DE BRUXELLES
PHYSICS LETTERS B172 (1986) 301

NUCLEAR CALEFACTION
NGO C., DALILI D., LUCAS R., CERRUTI C., LERAY S., MAZUR C., RIBRAG M., SUOMIJARVI T., BERLANGER M., CHIODELLI S., DEMEYER A., GUINET D.
CEN - SACLAY, IPN - LYON
PROGRESS IN PARTICLE AND NUCL. PHYS. 15 (1986) 171

PROJECTILE LIKE FRAGMENT PRODUCTION IN Ar INDUCED REACTIONS AROUND THE FERMI ENERGY : I. EXPERIMENTALS RESULTS - COMPETING MECHANISMS
BORREL V., GATTY B., GUERREAU D., GALIN J., JACQUET D.
IPN - ORSAY, GANIL - CAEN
Z. FUR PHYSIK A324 (1986) 205

PROJECTILE LIKE FRAGMENT PRODUCTION IN Ar INDUCED REACTIONS AROUND THE FERMI ENERGY : II. DIRECT SURFACE TRANSFER REACTIONS
MERMAZ M.C., BORREL V., GALIN J., GATTY B., JACQUET D., GUERREAU D.
CEN - SACLAY, IPN - ORSAY, GANIL - CAEN
Z. FUR PHYSIK A324 (1986) 217

CORRELATED SOURCES OF HEAVY FRAGMENTS IN THE Kr + Au REACTION AT 35 AND 44 MeV/u
RUDOLF G., ADLOFF J.C., KAMILI A., SCHEIBLING F., BOISHU B., GENOUX-LUBAIN A., LE BRUN C., LECOLLEY J.F., LEFEBVRES F., LOUVEL M., REGIMBART R., GRANIER O., LERAY S., LUCAS R., MAZUR C., NGO C., RIBRAG M., TOMASI E.
CRN - STRASBOURG, LPC - CAEN, CEN - SACLAY
PHYS. REV. LETT. 57 (1986) 2905

PERIPHERAL INTERACTIONS FOR 44 MeV/u ^{40}Ar ON ^{27}Al AND ^{nat}Ti TARGETS
DAYRAS R., PAGANO A., BARRETTE J., BERTHIER B., CASTRO RIZZO D.M., CHAVEZ E., CISSE O., LEGRAIN R., MERMAZ M.C., POLLACO E.C., DELAGRANGE H., MITTIG W., HEUSCH B., CONIGLIONE R., LANZANO G., PALMERI A.
CEN - SACLAY, GANIL - CAEN, CRN - STRASBOURG, INFN - CATANIA
NUCLEAR PHYSICS A460 (1986) 299

BETA DECAY OF ^{17} C, ^{19} N, ^{22} O, ^{24} F, ^{26} Ne, ^{32} Al, ^{34} Al, $^{35-36}$ Si, $^{36-37-38}$ P, ^{40} S

DUFOUR J.P., DEL MORAL R., FLEURY A., HUBERT F., JEAN D., PRAVIKOFF M.S., DELAGRANGE H., GEISSEL H., SCHMIDT K.H.
CEN - BORDEAUX-GRADIGNAN, GANIL - CAEN, GSI - DARMSTADT
Z. FUR PHYSIK A324 (1986) 487

FIRST OBSERVATION OF THE EXOTIC NUCLEUS ^{22} C

POUGHEON F., QUINIOU E., BERNAS M., JACMART J.C., HOATH S.D., GUILLEMAUD-MUELLER D., SAINT-LAURENT M.G., ANNE R., BAZIN D., GUERREAU D., MUELLER A.C., DETRAZ C.
IPN - ORSAY, GANIL - CAEN
EUROPHYSICS LETT. 2 (1986) 505

MAPPING OF THE PROTON DRIP-LINE UP TO Z = 20 : OBSERVATION OF THE Tz = _ 5/2 SERIES ^{23} Si, ^{27} S, ^{31} Ar AND ^{35} Ca

LANGEVIN M., BERNAS M., GALIN J., JACMART J.C., NAULIN F., POUGHEON F., QUINIOU E., MUELLER A.C., GUILLEMAUD-MUELLER D., SAINT-LAURENT M.G., ANNE R., GUERREAU D., DETRAZ C., HOATH S.D.
IPN - ORSAY, GANIL - CAEN, UNIV. OF BIRMINGHAM
NUCL. PHYS. A455 (1986) 149

MASS MEASUREMENT OF LIGHT NEUTRON-RICH FRAGMENTATION PRODUCTS

GILLIBERT A., BIANCHI L., FERNANDEZ B., GASTEBOIS J., CUNSOLO A., FOTI A., GREGOIRE C., MITTIG W., PEGHAIRE A., SCHUTZ Y., STEPHAN C.
CEN - SACLAY, INFN - CATANIA, GANIL - CAEN, IPN - ORSAY
PHYSICS LETT. B176 (1986) 317

PROJECTILE FRAGMENTS ISOTOPIC SEPARATION : APPLICATION TO THE LISE SPECTROMETER AT GANIL

DUFOUR J.P., DEL MORAL R., EMMERMANN H., HUBERT F., JEAN D., POINOT C., PRAVIKOFF M.S., FLEURY A., DELAGRANGE H., SCHMIDT K.H.
CEN/BG - GRADIGNAN, GANIL - CAEN, GSI - DARMSTADT
NIM A248 (1986) 267

A SEMI-EXCLUSIVE STUDY OF HEAVY-RESIDUE PRODUCTION IN THE ^{40} Ar + Ag REACTION AT 35 MeV/u INCIDENT ENERGY

BIZARD G., BROU R., DROUET A., HARASSE J.M., LAVILLE J.L., PATRY J.P., PLOYART G., STECKMEYER J.C., TAMAIN B., DOUBRE H., PETER J., GUILBAULT F., LEBRUN C., OUBAHADOU A., HANAPPE F.
LPC - CAEN, GANIL - CAEN, IPN - NANTES, FNRS AND UNIV. LIBRE DE BRUXELLES
Z. FUR PHYSIK A323 (1986) 459

REACTION MECHANISMS IN THE ^{40} Ar + ^{197} Au COLLISIONS AT 35 MeV/NUCLEON

BIZARD G., BROU R., DROUET A., HARASSE J.M., LAVILLE J.L., PATRY J.P., PLOYARD G., STECKMEYER J.C., TAMAIN B., HANAPPE F., GUILBAULT F., LEBRUN C., OUBAHADOU A., DOUBRE H., PETER J.
LPC - CAEN, FNRS AND UNIV. LIBRE DE BRUXELLES, LNS - NANTES, GANIL - CAEN
NUCL. PHYS. A456 (1986) 173

CONTRIBUTION OF DECAY PRODUCTS OF TRANSFER REACTIONS TO HEAVY-ION INELASTIC AND TRANSFER SPECTRA

BLUMENFELD Y., ROYNETTE J.C., CHOMAZ Ph., FRASCARIA N., CARRON J.P., JACMART J.C., CHOMAZ Ph.
IPN - ORSAY
NUCL. PHYS. A445 (1985) 151

DEEXCITATION OF NUCLEI FORMED NEAR THE INSTABILITY TEMPERATURE

RIVET M.F., BORDERIE B., GAUVIN H., GARDES D., CABOT C., HANAPPE F., PETER J.
IPN - ORSAY, FNRS AND UNIV. LIBRE DE BRUXELLES, GANIL - CAEN
PHYS. REV. C34 (1986) 1282

INCOMPLETE FUSION IN THE ^{40} Ar + ^{68} Zn REACTION : TRENDS AND LIMITS
FAHLI A., COFFIN J.P., GUILLAUME G., HEUSCH B., JUNDT F., RAMI F., WAGNER P., FINTZ P., COLE A.J., KOX S., SCHUTZ Y.
CRN - STRASBOURG, ISN - GRENOBLE, GANIL - CAEN
PHYS. REV. C34 (1986) 161

INVESTIGATION OF THE ^{84} Kr + ^{92,98} Mo, ^{nat} Ag AND ^{197} Au SYSTEMS AT 22 MeV/u
DALILI D., LUCAS R., NGO C., CERRUTI C., LERAY S., MAZUR C., RIBRAG M., SUOMIJARVI T., BERLANGER M., CHIODELLI S., DEMEYER A., GUINET D.
CEN - SACLAY, IPN - LYON
NUCL. PHYS. A454 (1986) 163

LIMITS OF THE OBSERVATION OF FUSION-LIKE PRODUCTS IN THE ^{40} Ar + ^{27} Al SYSTEM
AUGER G., PLAGNOL E., JOUAN D., GUET C., HEUER D., MAUREL M., NIFENECKER H., RISTORI C., SCHUSSLER F., DOUBRE H., GREGOIRE C.
IPN - ORSAY, CEN - GRENOBLE, GANIL - CAEN
PHYS. LETT. B169 (1986) 161

TARGET RESIDUE CROSS SECTIONS AND RECOIL ENERGIES FROM THE REACTION OF 1760 MeV 40 Ar WITH MEDIUM AND HEAVY TARGETS
HUBERT F., DEL MORAL R., DUFOUR J.P., EMMERMANN E., FLEURY A., POINOT C., PRAVILOFF M.S., DELAGRANGE H., LLERES A.
CEN - BORDEAUX-GRADIGNAN, GANIL - CAEN, ISN - GRENOBLE
NUCL. PHYS. A456 (1986) 535

MULTIPLICITY DEPENDENT LIGHT PARTICLE CORRELATIONS IN ^{40} Ar ^{197} Au REACTION AT E/A = 60 MeV
KYANOWSKI A., SAINT-LAURENT F., ARDOUIN D., DELAGRANGE H., DOUBRE H., GREGOIRE C., MITTIG W., PEGHAIRE A., PETER J., VIYOGI Y.P., ZWIEGLINSKI B., QUEBERT J., BIZARD G., LEFEBVRES F., TAMAIN B., POCHODZALLA J., GELBKE C.K., LYNCH W., MAIER M.
GANIL - CAEN, CEN - BORDEAUX-GRADIGNAN, LPC - CAEN, MSU - EAST-LANSING
PHYS. LETT. B181 (1986) 43

NEW DEVELOPMENTS OF THE GANIL CONTROL SYSTEM
LECORCHE E. AND THE GANIL CONTROL GROUP
GANIL - CAEN
NIM A247 (1986) 37

STOPPING POWERS OF SOLIDS FOR ^{40} Ar AND ^{40} Ca IONS AT INTERMEDIATE ENERGIES (20-80 MeV/u)
BIMBOT R., GAUVIN H., ORLIANGE I., ANNE R., BASTIN G., HUBERT F.
IPN - ORSAY, GANIL - CAEN, CSNSM - ORSAY, CEN - BORDEAUX-GRADIGNAN
NIM B17 (1986) 1

DYNAMICAL DECAY OF NUCLEI AT HIGH TEMPERATURE : COMPETITION BETWEEN PARTICLE EMISSION AND FISSION DECAY
DELAGRANGE H., GREGOIRE C., SCHEUTER F., ABE Y.
GANIL - CAEN, KYOTO UNIV. - KYOTO
Z. FUR PHYSIK A323(1986) 437

DYNAMICAL MODEL OF NUCLEAR FISSION WITH SHELL EFFECTS
BONASERA A.
GANIL - CAEN
PHYS. REV. C34 (1986) 740

THE FUSION PROCESS IN LANDAU-VLASOV DYNAMICS
REMAUD B., SEBILLE F., GREGOIRE C., VINET L.
IPN - NANTES, GANIL - CAEN
PHYS. LETT. B180 (1986) 198

1987

^{16} O + ^{28} Si ELASTIC SCATTERING AT E L = 94 MeV/NUCLEON
ROUSSEL P., BARRETTE J., AUGER F., BERTHIER B., FERNANDEZ B., GASTEBOIS J., GILLIBERT A., PAPINEAU L., MITTIG W., DISDIER D., LOTT B., RAUCH V., SCHEIBLING F., STEPHAN C., TASSAN-GOT L.
CEN - SACLAY, GANIL - CAEN, CRN - STRASBOURG, IPN - ORSAY
PHYS. LETT. B185 (1987) 29

ONE-NUCLEON STRIPPING REACTIONS TO DISCRETE LEVELS INDUCED BY A 793 MeV ^{16} O BEAM ON A ^{208}Pb TARGET
MERMAZ M.C.,BERTHIER B.,BARRETTE J.,GASTEBOIS J.,GILLIBERT A.,LUCAS R.,MATUSZEK J., MICZAIKA A.,VAN RENTERGHEM E.,SUOMIJARVI T.,BOUCENNA A.,DISDIER D.,GORODETZKY P., KRAUS L.,LINCK I.,LOTT B.,RAUCH V.,REBMEISTER R.,SCHEIBLING F.,SCHULZ N., SENS J.C.,GRUNBERG C.,MITTIG W.
CEN,SACLAY - CRN,STRASBOURG - GANIL,CAEN
Z PHYS A326 (1987) 353

HIGH EXCITATION INELASTIC SCATTERING INDUCED BY INTERMEDIATE ENERGY ^{40} Ar BEAMS
FRASCARIA N., BLUMENFELD Y., CHOMAZ Ph., GARRON J.P., JACMART J.C., ROYNETTE J.C., SUOMIJARVI T., MITTIG W.
IPN ORSAY, GANIL CAEN
NUCLEAR PHYSICS A474 (1987) 253

BINARY BREAK-UP OF A HIGH-VELOCITY HOT SOURCE FORMED IN THE ^{84} Kr + ^{93} Nb REACTION AT 34.5 MeV/u
CHARVET J.L., DUCHENE G., JOLY S., MAGNAGO C., MORJEAN M., PATIN Y., PRANAL Y., SINOPOLI L., UZUREAU J.L., BILLEREY R., CHAMBON B., CHBIHI A., CHEVARIER A., CHEVARIER N., DRAIN D., PASTOR C., STERN M., PEGHAIRE A.
CEN, BRUYERES-LE-CHATEL - IPN, LYON - GANIL, CAEN
PHYS. LETT. B189 (1987) 388

FORWARD ANGLE MEASUREMENTS OF 60 MeV/NUCLEON ^{40} Ar PERIPHERAL INTERACTIONS ON 208 Pb
SUOMIJARVI T., BEAUMEL D., BLUMENFELD Y., FRASCARIA N., GARRON J.P., JACMART J.C., ROYNETTE J.C., CHOMAZ Ph., BARRETTE J., BERTHIER B., FERNANDEZ B., GASTEBOIS J., MITTIG W.
IPN ORSAY, CEN SACLAY, GANIL CAEN
PHYSICAL REVIEW C36 (1987) 2691

ORIGIN OF PROJECTILE-LIKE FRAGMENTS FROM ^{40} Ar + ^{68} Zn COLLISIONS BETWEEN 15 AND 35 MeV/NUCLEON : DIRECT TRANSFER OF NUCLEONS AND PROJECTILE FRAGMENTATION
RAMI F., FAHLI A., COFFIN J.P., GUILLAUME G., HEUSCH B., JUNDT F., WAGNER P., FINTZ P., KOX S., SCHUTZ Y., MERMAZ M.C.
CRN, STRASBOURG - ISN, GRENOBLE - GANIL, CAEN - CEN, SACLAY
Z. PHYS. A327 (1987) 207

PERIPHERAL COLLISIONS IN THE ^{84}Kr +^{92,98}Mo,^{nat}Ag AND ^{197}Au REACTIONS AT 22 MeV/U
LUCAS R.,NGO C.,SUOMIJARVI T.,BERLANGER M.,CERRUTI C.,CHIODELLI S.,DALILI D., DEMEYER A.,GUINET D.,LERAY S.,MAZUR C.,RIBRAG M.
CEN,SACLAY
NUCL PHYS A 464(1987)172

BETA-DELAYED PROTON DECAY OF THE Tz = - 5/2 ISOTOPE ^{31} Ar
BORREL V., JACMART J.C., POUGHEON F., RICHARD A., ANNE R., BAZIN D., DELAGRANGE H., DETRAZ C., GUILLEMAUD-MUELLER D., MUELLER A.C., ROECKL E., SAINT-LAURENT M.G., DUFOUR J.P., HUBERT F., PRAVIKOFF M.S.
IPN - ORSAY, GANIL - CAEN, CEN BORDEAUX-GRADIGNAN
NUCLEAR PHYSICS A473 (1987) 331

DIRECT OBSERVATION OF NEW PROTON RICH NUCLEI IN THE REGION $23 \leqslant Z \leqslant 29$ USING A 55 A. MeV 58 NI BEAM

POUGHEON F., JACMART J.C., QUINIOU E., ANNE R., BAZIN D., BORREL V., GALIN J., GUERREAU D., GUILLEMAUD-MUELLER D., MUELLER A.C., ROECKL E., SAINT-LAURENT M.G., DETRAZ C.

IPN, ORSAY - GANIL, CAEN

Z. PHYS. A327 (1987) 17

MEASUREMENT OF TOTAL REACTION CROSS SECTIONS OF EXOTIC NEUTRON-RICH NUCLEI

MITTIG W., CHOUVEL J.M., ZHAN WEN LONG, BIANCHI L., CUNSOLO A., FERNANDEZ B., FOTI A., GASTEBOIS J., GILLIBERT A., GREGOIRE C., SCHUTZ Y., STEPHAN C.

GANIL - CAEN , CEN - SACLAY , DIPARTIMENTO DI FISICA NUCLEARE - CATANIA , IPN - ORSAY , INSTITUTE OF MODERN PHYSICS - LANZHOU

PHYSICAL REVIEW LETTERS 59 (1987) 1889

NEW MASS MEASUREMENTS FAR FROM STABILITY

GILLIBERT A.,MITTIG W.,BIANCHI L.,CUNSOLO A.,FERNANDEZ B.,FOTI A.,GASTEBOIS J., GREGOIRE C.,SCHUTZ Y.,STEPHAN C.

GANIL,CAEN - CEN,SACLAY - INFN,CATANIA - IPN,ORSAY

PHYS LETT B192 (1987) 39

OBSERVATION OF A BOUND Tz = -3 NUCLEUS: ^{22}Si

SAINT-LAURENT M.G.,DUFOUR J.P.,ANNE R.,BAZIN D.,BORREL V.,DELAGRANGE H.,DETRAZ C., GUILLEMAUD-MUELLER D.,HUBERT F.,JACMART J.C.,MUELLER A.C.,POUGHEON F.,PRAVIKOFF M.S., ROECKL E.

GANIL,CAEN - CEN,BORDEAUX - IPN,ORSAY

PHYS REV LETT 59 (1987) 33

FORMATION AND DECAY OF HOT NUCLEI

VOLANT C.,CONJEAUD M.,HARAR S.,MOSTEFAI M.,POLLACO E.C.,CASSAGNOU Y.,DAYRAS R., LEGRAIN R.,KLOTZ-ENGMANN G.,OESCHLER H.

CEN,SACLAY- TECHNISHE HOCHSCHULE,DARMSTADT

PHYS. LETT. B195 (1987) 22

GAMMA RAYS FROM PERIPHERAL AND CENTRAL COLLISIONS IN THE REACTION ^{40}Ar + ^{158}Gd AT 44 MeV/NUCLEON

HINGMANN R., KUHN W., METAG V., MUHLHANS R., NOVOTNY R., RUCKELSHAUSEN A., CASSING W., EMLING H., KULESSA R., WOLLERSHEIM H.J., HAAS B., VIVIEN J.P., BOULLAY A., DELAGRANGE H., DOUBRE H., GREGOIRE C., SCHUTZ Y.

GIESSEN UNIV. - GIESSEN, GSI - DARMSTADT, - CRN - STRASBOURG,- GANIL - CAEN

PHYS. REV. LETT. 58 (1987) 759

HIGH ENERGY GAMMA-RAY PRODUCTION FROM 44 MeV/A ^{86} Kr BOMBARDMENT ON NUCLEI

BERTHOLET R., KWATO NJOCK M., MAUREL M., MONNAND E., NIFENECKER H., PERRIN P., PINSTON J.A., SCHUSSLER F., BARNEOUD D., GUET C., SCHUTZ Y.

CEN - GRENOBLE, ISN - GRENOBLE, GANIL - CAEN

NUCLEAR PHYSICS A474 (1987) 541

PRODUCTION AND DECAY OF HIGHLY EXCITED NUCLEAR SYSTEMS FORMED IN ^{84} Kr + ^{12} C AND ^{27} Al COLLISIONS AT 35 MeV/NUCLEON

AUGER F., BERTHIER B., CUNSOLO A., FOTI A., MITTIG W., PASCAUD J.M., PLAGNOL E., QUEBERT J., WIELECZKO J.P.

CEN - SACLAY, INFN - CATANIA, GANIL - CAEN, CEN - BORDEAUX, IPN - ORSAY

PHYS. REV. C35 (1987) 190

LIGHT CHARGED PARTICLE EMISSION IN ^{40}Ar INDUCED REACTIONS ON ^{68}Zn AT 14.6,19.6 AND 35 MeV/NUCLEON

FAHLI A.,COFFIN J.P.GUILLAUME G.,HEUSCH B.,JUNDT F.,RAMI F.,WAGNER P.,FINTZ P., COLE A.J.,KOX S.,SCHUTZ Y.,CINDRO N.

CRN - STRASBOURG - ISN - GRENOBLE, GANIL - CAEN, RUDJER BOSKOVIC INST. - ZAGREB

Z.PHYS A326 (1987) 169

INCLUSIVE TWO-PARTICLE CORRELATIONS FOR ^{16}O-INDUCED REACTIONS ON ^{197}Au AT E/A = 94 MeV

CHEN Z., GELBKE C.K., GONG W.G., KIM Y.D., LYNCH W.G., MAIER M.R., POCHODZALLA J., TSANG M.B., SAINT-LAURENT F., ARDOUIN D., DELAGRANGE H., DOUBRE H., KASAGI J., KYANOWSKI A., PEGHAIRE A., PETER J., ROSATO E., BIZARD G., LEFEBVRES F., TAMAIN B., QUEBERT J., VIYOGI Y.P.

MSU - EAST LANSING, GANIL - CAEN, CEN - BORDEAUX-GRADIGNAN, VARIABLE ENERGY CYCLOTRON CENTRE - CALCUTTA

PHYSICAL REVIEW C36, (1987) 2297

POPULATION OF PARTICLE UNBOUND STATES FOR THE REACTION ^{16}O + Au AT E/A = 94 MeV

CHEN Z., GELBKE C.K., GONG W.G., KIM Y.D., LYNCH W.G., MAIER M.R., POCHODZALLA J., TSANG M.B., SAINT-LAURENT F., ARDOUIN D., DELAGRANGE H., DOUBRE H., KASAGI J., KYANOWSKI A., PEGHAIRE A., PETER J., ROSATO E., BIZARD G., LEFEBVRES F., TAMAIN B., QUEBERT J., VIYOGI Y.P.

NSCL MSU - EAST LANSING, GANIL - CAEN, LPC - CAEN, CEN - BORDEAUX-GRADIGNAN, VARIABLE ENERGY CYCLOTRON CENTRE - CALCUTTA

PHYSICS LETTERS B199 (1987) 171

TWO-PARTICLE CORRELATIONS AT SMALL RELATIVE MOMENTA FOR ^{40}Ar-INDUCED REACTIONS ON ^{197}Au AT E/A = 60 MeV

POCHODZALLA J., GELBKE C.K., LYNCH W.G., MAIER M., ARDOUIN D., DELAGRANGE H., DOUBRE H., GREGOIRE C., KYANOWSKI A., MITTIG W., PEGHAIRE A., PETER J., SAINT-LAURENT F., ZWIEGLINSKI B., BIZARD G., LEFEBVRES F., TAMAIN B., QUEBERT J., VIYOGI Y.P., FRIEDMAN W.A., BOAL D.H.

NSCL, EAST LANSING - GANIL, CAEN - LPC, CAEN - CEN, BORDEAUX - WISCONSIN UNIV., MADISON - SIMON FRASER UNIV., BURNABY

PHYS. REV. C35 (1987) 1695

SUBTHRESHOLD PION PRODUCTION AND STATISTICAL MULTIFRAGMENTATION IN NUCLEUS-NUCLEUS COLLISIONS

BARZ H.W., BONDORF J.P., GUET C., LOPEZ J., SCHULZ H.

NIELS BOHR INST. - COPENHAGEN, CENTRAL INST. OF NUCL. RESEARCH - DRESDEN, GANIL - CAEN

EUROPHYS. LETT. 4 (1987) 997

ACHROMATIC SPECTROMETER LISE AT GANIL

ANNE R., BAZIN D., MUELLER A.C., JACMART J.C., LANGEVIN M.

GANIL, CAEN - IPN, ORSAY

NIM A257 (1987) 215

"DELF" A LARGE SOLID ANGLE DETECTION SYSTEM FOR HEAVY FRAGMENTS

BOUGAULT R.,DUCHON J.,GAUTIER J.M.,GENOUX-LUBAIN A.,LE BRUN C.,LECOLLEY J.F., LEFEBVRES F.,LOUVEL M.,MOSRIN P.,REGIMBART R.

LPC - CAEN

NIM A259 (1987) 473

STOPPING POWERS OF SOLIDS FOR ^{16}O IONS AT INTERMEDIATE ENERGIES (20-95 MeV/u)

GAUVIN H., BIMBOT R., HERAULT J., ANNE R., BASTIN G., HUBERT F.

IPN - ORSAY, GANIL - CAEN, CSNSM - ORSAY, CEN - BORDEAUX-GRADIGNAN

NIM B28 (1987) 191.

A STUDY OF THE DISINTEGRATION OF HIGHLY EXCITED NUCLEI WITH VLASOV-UEHLING-UHLENBECK EQUATION

VINET L.,GREGOIRE C.,SCHUCK P.,REMAUD B.,SEBILLE F.,

GANIL - CAEN, IPN - NANTES

NUCL. PHYS. A468 (1987) 321.

DISSIPATIVE EFFECTS IN PROJECTILE FRAGMENTATION

BONASERA A., di TORO M., GREGOIRE C.

GANIL - CAEN, INFN - CATANIA

NUCL. PHYS. A463 (1987) 653.

PERIPHERAL REACTIONS AT INTERMEDIATE ENERGIES IN LANDAU-VLASOV DYNAMICS
GREGOIRE C., REMAUD B., SEBILLE F., VINET L.
GANIL - CAEN - IRSTE - NANTES
PHYS. LETT. B186 (1987) 14.

SEMI-CLASSICAL DYNAMICS OF HEAVY ION REACTIONS
GREGOIRE C., REMAUD B., SEBILLE F., VINET L., RAFFRAY Y.
GANIL - CAEN, IPN - NANTES
NUCL. PHYS. A465 (1987) 317.

1988

^{16} O ELASTIC SCATTERING AT Elab = 94 MeV/NUCLEON
ROUSSEL-CHOMAZ P., ALAMANOS N., AUGER F., BARRETTE J., BERTHIER B., FERNANDEZ B., PAPINEAU L., DOUBRE H., MITTIG W.
CEN - SACLAY, GANIL - CAEN
NUCLEAR PHYSICS A477 (1988) 345

HIGH SPIN LEVELS POPULATED IN MULTINUCLEON-TRANSFER REACTIONS WITH ^{48}O MeV ^{12} C
KRAUS L., BOUCENNA A., LINCK I., LOTT B., REBMEISTER R., SCHULZ N., SENS J.C., MERMAZ M.C., BERTHIER B., LUCAS R., GASTEBOIS J., GILLIBERT A., MICZAIKA A., TOMASI-GUSTAFSSON E., GRUNBERG C.
CRN - STRASBOURG, CEN - SACLAY, GANIL - CAEN
PHYSICAL REVIEW C37, 6 (1988) 2529

ONE-NUCLEON STRIPPING REACTIONS TO DISCRETE LEVELS INDUCED BY A ^{48}O MeV ^{12} C BEAM ON A ^{208} Pb TARGET
MERMAZ M.C., TOMASI-GUSTAFSSON E., BERTHIER B., LUCAS R., GASTEBOIS J., GILLIBERT A., MICZAIKA A., BOUCENNA A., KRAUS L., LINCK I., LOTT B., REBMEISTER R., SCHULZ N., SENS J.C., GRUNBERG C.
CEN SACLAY, CRN STRASBOURG, GANIL CAEN
PHYSICAL REVIEW C37, 5 (1988) 1942

APPROACHING PERIPHERAL COLLISIONS IN THE REACTION Ar + Au AT 27.2 MeV/U BY THE ASSOCIATED NEUTRON MULTIPLICITIES
MORJEAN M., FREHAUT J., GUERREAU D., CHARVET J.L., DUCHENE G., DOUBRE H., GALIN J., INGOLD G., JACQUET D., JAHNKE U., JIANG D.X., LOTT B., MAGNAGO C., PATIN Y., POUTHAS J., PRANAL Y., UZUREAU J.L.
CEN BRUYERES-LE-CHATEL - GANIL CAEN - HMI BERLIN - IPN ORSAY
PHYSICS LETTERS B203, 3 (1988) 215

MULTIPLE ANGULAR SCATTERING OF HEAVY IONS (^{16,17} O, ^{40} Ar, ^{86} Kr AND ^{100} Mo) AT INTERMEDIATE ENERGIES (20-90 MeV/u)
ANNE R., HERAULT J., BIMBOT R., GAUVIN H., BASTIN G., HUBERT F.
GANIL - CAEN, IPN - ORSAY, CSNCM - ORSAY, CEN - BORDEAUX-GRADIGNAN
NIM B34 (1988) 295

STUDY OF THE ^{129} Xe + ^{nat} Ag, ^{197} Au SYSTEMS AT 23.7 AND 27 MeV/u
GRANIER O., CERRUTI C., LERAY S., L'HENORET P., LUCAS R., MAZUR C., NATOWITZ J., NGO C., RIBRAG M., TOMASI E., IMME G., RACITI G., SPINELLA G., ALBINSKI L., GOBBI A., HERMANN N., HILDENBRAND K.D., OLMI A.
CEN SACLAY - INFN CATANIA - GSI DARMSTADT - INFN FIRENZE
NUCLEAR PHYSICS A481 (1988) 109

DEEPLY INELASTIC COLLISIONS AS A SOURCE OF INTERMEDIATE MASS FRAGMENTS AT E/A = 27 MeV
BORDERIE B., MONTOYA M., RIVET M.F., JOUAN D., CABOT C., FUCHS H., GARDES D., GAUVIN H., JACQUET D., MONNET F., HANAPPE F.
IPN - ORSAY, FNRS AND UNIV. LIBRE DE BRUXELLES
PHYSICS LETTERS B205, 1 (1988) 26

BETA DELAYED MULTI-NEUTRON RADIOACTIVITY OF ^{17} B, ^{14} Be, ^{19} C
DUFOUR J.P., DEL MORAL R., HUBERT F., JEAN D., PRAVIKOFF M.S., FLEURY A., MUELLER A.C., SCHMIDT K.H., SUMMERER K., HANELT E., FREHAUT J., BEAU M., GIRAUDET G.
CEN - BORDEAUX GRADIGNAN, GANIL - CAEN, GSI - DARMSTADT, TECHNISCHEN HOCHSCHULE - DARMSTADT, CEN - BRUYERES LE CHATEL
PHYSICS LETTERS B206, 2 (1988) 195

BETA-DELAYED NEUTRON EMISSION OF ^{15} B, ^{18} C, ^{19,20} N, ^{34,35} Al AND ^{39} P
MUELLER A.C., BAZIN D., SCHMIDT-OTT W.D., ANNE R., GUERREAU D., GUILLEMAUD-MUELLER D., SAINT-LAURENT M.G., BORREL V., JACMART J.C., POUGHEON F., RICHARD A.
GANIL - CAEN, IPN - ORSAY
Z. PHYS. A330 (1988) 63

EVIDENCE FOR PERSISTING MEAN FIELD EFFECTS AT E/A = 60 MeV FROM PARTICLE-PARTICLE CORRELATION MEASUREMENTS AND THEORETICAL INVESTIGATIONS WITH THE LANDAU VLASOV EQUATION

ARDOUIN D., BASRAK Z., SCHUCK P., PEGHAIRE A., DELAGRANGE H., DOUBRE H., GREGOIRE C., KYANOWSKI A., MITTIG W., PETER J., SAINT-LAURENT F., ZWIEGLINSKI B., VIYOGI Y.P., GELBKE C.K., LYNCH W.G., MAIER M., POCHODZALLA J., QUEBERT J., BIZARD G. , LEFEBVRES F., TAMAIN B.

NANTES UNIV.- NANTES, ISN - GRENOBLE, VECC - CALCUTTA, NSCL - EAST LANSING, CEN BORDEAUX - GRADIGNAN, LPC - CAEN

Z. PHYS. A329 (1988) 505

POSSIBLE DYNAMICAL LIMITATIONS TO EXCITATION ENERGY STORAGE IN NUCLEI

SAINT-LAURENT F., KYANOWSKI A., ARDOUIN D., DELAGRANGE H., DOUBRE H., GREGOIRE C., MITTIG W., PEGHAIRE A., PETER J., BIZARD G., LEFEBVRES F., TAMAIN B., QUEBERT J., VIYOGI Y.P., POCHODZALLA J., GELBKE C.K., LYNCH W., MAIER M.

GANIL - CAEN, LPC CAEN UNIV. - CAEN, CENB - GRADIGNAN, VARIABLE ENERGY CYCLOTRON CENTRE - CALCUTTA, NSCL MICHIGAN STATE UNIV. - EAST LANSING

PHYSICS LETTERS B202 (1988) 190

NEUTRON ENERGY DISTRIBUTIONS IN THE DYNAMICAL COMPETITION BETWEEN EVAPORATION AND FISSION

GREGOIRE C., DELAGRANGE H., POMORSKI K., DIETRICH K.

GANIL CAEN - TUM GARCHING

Z. PHYS. A329 (1988) 497

PREEQUILIBRIUM EMISSION AND INCOMPLETE FUSION OF LOW AND MEDIUM MASS HEAVY ION SYSTEMS

GONIN M., COFFIN J.P., GUILLAUME G., JUNDT F., WAGNER P., FINTZ P., HEUSCH B., MALKI A., FAHLI A., KOX S., MERCHEZ F., MISTRETTA J.

CRN - STRASBOURG, ISN - GRENOBLE

PHYS. REV. C38, 1 (1988) 135

HIGH ENERGY GAMMA-RAY PRODUCTION IN HEAVY ION REACTIONS

KWATO NJOCK M., MAUREL M., MONNAND E., NIFENECKER H., PINSTON J.A., SCHUSSLER F., BARNEOUD D., SCHUTZ Y.

CEN - GRENOBLE, ISN - GRENOBLE, GANIL - CAEN

NUCLEAR PHYSICS A482 (1988) 489c

LIGHT-FRAGMENT EMISSION IN HEAVY-ION REACTIONS PRODUCING PIONS AND PROTONS IN ^{16}O + ^{27}Al COLLISIONS AT 94 MeV/NUCLEON

AIELLO S., BADALA A., BARBERA R., LO NIGRO S., NICOTRA D., PALMERI A., PAPPALARDO G.S., BIZARD G., BOUGAULT R., DURAND D., GENOUX-LUBAIN A., LAVILLE J.L., LEFEBVRES F.

INFN CATANIA - LPC ISMRA CAEN

EUROPHYSICS LETTERS 6, 1 (1988) 25

LINEAR MOMENTUM TRANSFER IN PION ACCOMPANIED ^{16}O INDUCED REACTION ON ^{232}Th AT 95 MeV PER NUCLEON

ERAZMUS B., GUET C., McGRATH R., SAINT-LAURENT M.G., SCHUTZ Y., BOLORE M., CASSAGNOU Y., DABROWSKI H., HISLEUR M., JULIEN J., LEGRAIN R., LE BRUN C., LECOLLEY J.F., LOUVEL M.

GANIL - CAEN, CEN - SACLAY, LPC ISMRA - CAEN

NUCL. PHYS. A481 (1988) 821

DISPERSIONS IN SEMICLASSICAL DYNAMICS

ZIELINSKA-PFABE M., GREGOIRE C.

SMITH COLLEGE - NORTHAMPTON, GANIL - CAEN

PHYSICAL REVIEW C37, 6 (1988) 2594

FLUCTUATIONS OF SINGLE-PARTICLE DENSITY IN NUCLEAR COLLISIONS

AYIK S., GREGOIRE C.

TENNESSEE TECHNOLOGICAL UNIVERSITY - COOKEVILLE, GANIL - CAEN

PHYS. LETT. B212 (1988) 269

LIQUID DROP PARAMETERS FOR HOT NUCLEI

GUET C., STRUMBERGER E., BRACK M.
GANIL - CAEN, REGENSBURG UNIV. - REGENSBURG

PHYSICS LETTERS B205, 4 (1988) 427

1989

TRANSFER REACTIONS AND SEQUENTIAL DECAYS OF THE PROJECTILE-LIKE FRAGMENTS IN THE 60 MeV/NUCLEON ^{40}Ar + ^{nat}Ag, ^{197}Au REACTIONS

STECKMEYER J.C., BIZARD G., BROU R., EUDES P., LAVILLE J.L., NATOWITZ J.B., PATRY J.P., TAMAIN B., THIPHAGNE A., DOUBRE H., PEGHAIRE A., PETER J., ROSATO E., ADLOFF J.C., KAMILI A., RUDOLF G., SCHEIBLING F., GUILBAULT F., LEBRUN C., HANAPPE F.

LPC - CAEN, GANIL - CAEN, CRN - STRASBOURG, LSN - NANTES, FONDS NATIONAL DE LA RECHERCHE SCIENTIFIQUE - BRUXELLES

NUCL. PHYS. A500 (1989) 372.

EXCITATION OF GIANT RESONANCES IN ^{20}Ne + ^{90}Zr AND ^{208}Pb INELASTIC SCATTERING AT 40 MeV/u

SUOMIJARVI T., BEAUMEL D., BLUMENFELD Y., CHOMAZ Ph., FRASCARIA N., GARRON J.P., JACMART J.C., ROYNETTE J.C., BARRETTE J., BERTHIER B., FERNANDEZ B., GASTEBOIS J., ROUSSEL-CHOMAZ P., MITTIG W., KRAUS L., LINCK I.

IPN - ORSAY, CEN - SACLAY, GANIL - CAEN, CRN - STRASBOURG

NUCLEAR.PHYSICS A491 (1989) 314

HEAVY ION CHARGE EXCHANGE REACTIONS TO PROBE THE GIANT ELECTRIC ISOVECTOR MODES IN NUCLEI

BERAT C., BUENERD M., CHAUVIN J., HOSTACHY J.Y., LEBRUN D., MARTIN P., BARRETTE J., BERTHIER B., FERNANDEZ B., MICZAIKA A., MITTIG W., STILIARIS E., VON OERTZEN W., LENSKE H., WOLTER H.H.

ISN - GRENOBLE, CEN - SACLAY, GANIL - CAEN, HMI - BERLIN, UNIVERSITY OF MUNICH - MUNICH

PHYSICS LETTERS B218, 3 (1989) 299

DYNAMICAL ASPECTS OF VIOLENT COLLISIONS IN Ar + Ag REACTIONS AT E/A = 27 MeV

RIVET M.F., BORDERIE B., GREGOIRE C., JOUAN D., REMAUD B.

IPN - ORSAY, GANIL - CAEN, LPN/UA - NANTES

PHYS. LETT. B215 (1988) 55

BETA DECAY OF ^{22}O

HUBERT F., DUFOUR J.P., DEL MORAL R., FLEURY A., JEAN D., PRAVIKOFF M.S., DELAGRANGE H., GEISSEL H., SCHMIDT K.H., HANELT E.

CEN - BORDEAUX-GRADIGNAN, GANIL - CAEN, GSI - DARMSTADT, INST. FUR KERNPHYSIK - DARMSTADT

Z. PHYS. A333 (1989) 237.

OBSERVATION OF NEW NEUTRON RICH NUCLEI ^{29}F, ^{35,36}Mg, ^{38,39}Al, ^{40,41}Si, ^{43,44}P, $^{45-47}$S, $^{46-49}$Cl, AND $^{49-51}$Ar FROM THE INTERACTIONS OF 55 MeV/u ^{48}Ca + Ta

GUILLEMAUD-MUELLER D., PENIONZHKEVICH Yu.E., ANNE R., ARTUKH A.G., BAZIN D., BORREL V., DETRAZ C., GUERREAU D., GVOZDEV B.A., JACMART J.C., JIANG D.X., KALININ A.M., KAMANIN V.V., KUTNER V.B., LEWITOWICZ M., LUKYANOV S.M., MUELLER A.C., HOAI CHAU N., POUGHEON F., RICHARD A., SAINT-LAURENT M.G., SCHMIDT-OTT W.D.

GANIL - CAEN, JINR - DUBNA, IPN - ORSAY, GOTTINGEN UNIV. - GOTTINGEN

Z. PHYS. A332 (1989) 193.

SATURATION OF THE THERMAL ENERGY DEPOSITED IN Au AND Th NUCLEI BY Ar PROJECTILES BETWEEN 27 AND 77 MeV/u

JIANG D.X., DOUBRE H., GALIN J., GUERREAU D., PIASECKI E., POUTHAS J., SOKOLOB A., CRAMER B., INGOLD G., JAHNKE U., SCHWINN E., CHARVET J.L., FREHAUT J., LOTT B., MAGNAGO C., MORJEAN M., PATIN Y., PRANAL Y., UZUREAU J.L., GATTY B., JACQUET D.

GANIL - CAEN, HMI - BERLIN, CEN - BRUYERES-LE-CHATEL, IPN - ORSAY

NUCL. PHYS. A503 (1989) 560.

CORRELATIONS BETWEEN PROJECTILELIKE AND TARGETLIKE FRAGMENTS IN THE REACTION ^{27} Al + 44-MeV/NUCLEON ^{40} Ar

DAYRAS R., CONIGLIONE R., BARRETTE J., BERTHIER B., de CASTRO RIZZO D.M., CISSE O., GADI F., LEGRAIN R., MERMAZ M.C., DELAGRANGE H., MITTIG W., HEUSCH B., LANZANO G., PAGANO A.

CEN - SACLAY, GANIL - CAEN, CRN - STRASBOURG, ISTITUTO NAZIONALE DI FISICA NUCLEARE - CATANIA

PHYS. REV. LETT. 62 (1989) 1017.

INCOMPLETE FUSION IN NUCLEUS-NUCLEUS CENTRAL COLLISIONS. STUDY OF ^{40} Ar ON ^{27} Al FROM 25 TO 85 MeV/u

HAGEL K., PEGHAIRE A., JIN G.M., CUSSOL D., DOUBRE H., PETER J., SAINT-LAURENT F., BIZARD G., BROU R., LOUVEL M., PATRY J.P., REGIMBART R., STECKMEYER J.C., TAMAIN B., CASSAGNOU Y., LEGRAIN R., LEBRUN C., ROSATO E., MACGRATH R., JEONG S.C., LEE S.M., NAGASHIMA Y., NAKAGAWA T., OGIHARA M., KASAGI J., MOTOBAYASHI T.

GANIL-CAEN, TEXAS A&M UNIV.-COLLEGE STATION, LPC-CAEN, CEN-SACLAY, LPN-NANTES, DIPARTIMENTO DI SCIENZE FISICHE-NAPLES, SUNY-STONY BROOK, TSUKUBA UNIV.-IBARAKI-KEN, TOKYO INST.TECH.-TOKYO, RIKKYO UNIV.-TOKYO, INST.MOD.PHYS.-LANZHOU

PHYS. LETT. B229 (1989) 20.

TOTAL CROSS SECTIONS OF REACTIONS INDUCED BY NEUTRON-RICH LIGHT NUCLEI

SAINT-LAURENT M.G., ANNE R., BAZIN D., GUILLEMAUD-MUELLER D., JAHNKE U., JIN GEN MING, MUELLER A.C., BRUANDET J.F., GLASSER F., KOX S., LIATARD E., TSAN UNG CHAN, COSTA G.J., HEITZ C., EL-MASRI Y., HANAPPE F., BIMBOT R., ARNOLD E., NEUGART R.

GANIL - CAEN, ISN - GRENOBLE, CRN - STRASBOURG, FONDS NAT. RECH.SCI. - BRUXELLES AND UCL/ULB - LOUVAIN-LA-NEUVE, IPN - ORSAY, MAINZ UNIV. - MAINZ

Z. PHYS. A332 (1989) 457.

HEAVY ION COLLISION GEOMETRY AT 93 MeV/u FROM PI-/PI+ MEASUREMENT

LEBRUN D., CHAUVIN J., REBREYEND D., PERRIN G., DE SAINTIGNON P., MARTIN P., BUENERD M., LE BRUN C., LECOLLEY J.F., CASSAGNOU Y., JULIEN J., LEGRAIN R.

ISN - GRENOBLE, LPC - CAEN, DPHN/CEN SACLAY - GIF SUR YVETTE

PHYS. LETT. B223 (1989) 139.

IMPACT PARAMETER DEPENDENCE OF HIGH-ENERGY GAMMA-RAY PRODUCTION IN ARGON INDUCED REACTION AT 85 MeV/NUCLEON

KWATO NJOCK M., MAUREL M., MONNAND E., NIFENECKER H., PERRIN P., PINSTON J.A., SCHUSSLER F., SCHUTZ Y.

CEN - GRENOBLE, ISN - GRENOBLE, GANIL - CAEN

NUCL. PHYS. A489 (1988) 368

A NE213 LIQUID SCINTILLATOR, NEUTRON DETECTOR DESIGNED FOR LIFETIME MEASUREMENTS OF VERY NEUTRON-RICH NUCLEI

BAZIN D., MUELLER A.C., SCHMIDT-OTT W.D.

GANIL - CAEN, UNIVERSITAT GOTTINGEN -- GOTTINGEN

NIM A281 (1989) 117.

A TEST OF NEW POSITION SENSITIVE DETECTORS FOR SPEG

VILLARI A.C.C., MITTIG W., BLUMENFELD Y., GILLIBERT A., GANGNANT P., GARREAU L.

INST. DE FISICA DA UNIV. DE SAO PAULO - SAO PAULO, GANIL - CAEN, IPN - ORSAY, CEN SACLAY - GIF SUR YVETTE

NIM A281 (1989) 240.

SEMI-EMPIRICAL FORMULAE FOR HEAVY ION STOPPING POWERS IN SOLIDS IN THE INTERMEDIATE ENERGY RANGE

HUBERT F., BIMBOT R., GAUVIN H.

CEN - BORDEAUX-GRADIGNAN, IPN - ORSAY

NIM B36 (1989) 357.

COMPRESSIONAL EFFECTS IN HEAVY ION COLLISIONS. SPINODAL DECOMPOSITION AND THERMAL ENERGY SATURATION
SURAUD E., PI M., SCHUCK P., REMAUD B., SEBILLE F., GREGOIRE C., SAINT-LAURENT F.
ISN - GRENOBLE, LPN - NANTES, GANIL - CAEN
PHYSICS LETTERS B229 (1989) 359.

DETERMINATION OF NUCLEAR PROPERTIES BELOW NORMAL DENSITY FROM THE MULTIFRAGMENTATION PATTERN
SNEPPEN K., CUSSOL D., GREGOIRE C.
NIELS BOHR INST. - COPENHAGEN, GANIL - CAEN
PHYS. LETT. B220 (1989) 342.

NUCLEAR DYNAMICS WITH THE (FINITE-RANGE) GOGNY FORCE : FLOW EFFECTS
SEBILLE F., ROYER G., GREGOIRE C., REMAUD B., SCHUCK P.
LSN - NANTES, GANIL - CAEN, IRESTE - NANTES, ISN - GRENOBLE
NUCL. PHYS. A501 (1989) 137.

III
SCIENTIFIC ACTIVITIES AT GANIL

COLLOQUE GANIL

(GIENS - Var)

I – REACTIONS DE TRANSFERT ET FRAGMENTATION AUX ENERGIES INTERMEDIAIRES.
(20-25 MAI 1984)

II – COLLISIONS CENTRALES
(19-24 MAI 1985)

III – NOYAUX EXOTIQUES
(20-23 MAI 1986)

IV – L'EXCITATION DE MODES ELEMENTAIRES DANS LES NOYAUX PAR DES COLLISIONS D'IONS LOURDS AUX ENERGIES INTERMEDIAIRES.
(11-15 MAI 1987)

V – LES INTERACTIONS MATIERE-IONS LOURDS DE GRANDE VITESSE : EFFET DE LA DENSITE DE DEPOT D'ENERGIE INELASTIQUE.
(17-20 MAI 1988)

VI – LA PHYSIQUE AVEC LES MULTIDETECTEURS : PERSPECTIVES
(22-26 MAI 1989)

– I –

"Réactions de transfert et fragmentation aux énergies intermédiaires".

- Diffusion élastique et inélastique d'ions lourds aux énergies intermédiaires.
  Aspect expérimental : *M. Buenerd.*
  Aspect théorique : *C. Marty.*

- Etude de la disparition des effets de Pauli dans le potentiel optique en fonction de l'énergie. *P. Schuck.*

- Réactions directes aux énergies intermédiaires. *A. Nagarajan.*

- Some ideas and facts on the evolution of direct processes up to 80 MeV/u. *W. von Oertzen.*

- Expériences sur SPEG aux énergies intermédiaires. *W. Mittig.*

- Evolution des réactions à 2 corps et structure nucléaire. *L. Kraus.*

- Avantages comparés des ions légers et lourds pour l'étude des résonances géantes. *B. Bonin.*

- Structures et résonances géantes dans les réactions par ions lourds. *J.-C. Roynette.*

- Nuclear structure studies in grazing heavy ion collisions. *G. Pollarolo.*

- Calculs microscopiques de l'excitation de résonances géantes dans les réactions par ions lourds. *D. Vautherin.*

- Modèle théorique pour la réaction Ca + Ca. *K. Dietrich.*

- Résonances géantes et excitation de multiphonons. *Ph. Chomaz.*

- Résonances géantes à température finie. *N. Vinh Mau.*

- Fragmentation du projectile : l'avant GANIL. *R. Legrain.*

- Pourquoi étudier la multifragmentation aux énergies GANIL ? *X. Campi.*

- Caractère transitoire de mécanismes de réaction observés dans des collisions $^{27}Al + ^{63}Cu$ à 13 MeV/nucléon. *J.-L. Laville.*

- Réactions périphériques induites par un faisceau de ^{40}Ar à 44 MeV/u. Friction et fragmentation ? *R. Dayras.*

- Fragments du projectile : distributions isotopiques et taux de production. *V. Borrel.*

- Transfert de quelques nucléons et fragmentation du projectile aux énergies intermédiaires. *Y. Blumenfeld.*

- Quelques aspects des mécanismes de la réaction $^{40}Ar + ^{68}Zn$ à 27 MeV/u. *G. Guillaume.*

- Fragmentation et instabilité thermodynamique. *J. Cugnon.*

- Fragments légers émis à grand angle dans la réaction $^{40}Ar + ^{197}Au$ à 44 MeV/u. Fragmentation ou condensation. *Y. Cassagnou.*

- Liquid-gas phase transitions in nuclear systems. *A. Panagiotou.*

• Fragmentation de systèmes nucléaires chauds. *D. Heuer.*

• Hodoscope de particules légères à GANIL. Technologie et applications. *B. Tamain.*

• Fragmentation of target nuclei at 84 MeV/u. Is this an indication of a phase transition. *U. Lynen.*

• Production de fragments légers de basse énergie dans la réaction $^{20}Ne + {}^{27}Al$ à 30 MeV/u. *M. Morjean.*

• Etude des mécanismes d'interaction entre 20 et 100 MeV/u par la mesure des résidus de la cible. *F. Hubert.*

• Formation and decay of localized excitations in nuclei. *C. K. Gelbke.*

• Effets collectifs et individuels aux énergies intermédiaires. *C. Grégoire.*

De courts exposés sur de très récents résultats ont, par ailleurs, été présentés par *N. Alamanos, A. Gamp, A. Demeyer et J. Blachot.*

– II –

Collisions centrales

• Fission along the mass asymmetry coordinate. An experimental evaluation of the conditional saddle masses and of the Businaro Gallone point. *L. Moretto.*

• Emission statistique de fragments lourds à haute température. *W. Mittig.*

• Noyaux à très haute énergie d'excitation par nucléon. *E. Plagnol.*

• Linear and angular momentum transfer at 8.5 to 35 MeV/u. *J. Natowitz.*

• Résidus lourds produits dans les réactions Ar + Ag et Ar + Ho à 27MeV/u. *M.-F. Rivet.*

• Etude de la fusion complète et incomplète à partir des résidus de la cible. *J. Crançon.*

• Fusion incomplète et transferts de moments dans les interactions du ^{12}C avec des cibles de masses moyennes et lourdes. *M. Pravikoff.*

• La systématique des moments linéaires obtenus par la méthode des reculs des noyaux radioactifs. *J. Jastrzebski.*

• Effets respectifs du champ moyen et des collisions individuelles aux énergies GANIL : approches théoriques et signatures expérimentales ? *B. Remaud.*

• Transfert d'impulsion et d'énergie dans les régions de champ moyen et d'intéraction nucléon-nucléon. *S. Harar.*

• Particules chargées rapides et transfert incomplet d'impulsion. *Y. Patin.*

• Dynamics of energy thermalisation. *E. Pollacco.*

• Les particules légères, sondes de collisions entre noyaux aux énergies comprises entre 10 et 100 MeV/u. *J. Galin.*

• Transfert incomplet d'impulsion dans les réactions Ar + Au, U à 20, 35. 44 MeV/u. *S. Leray.*

• Etude des interactions du Krypton sur des noyaux lourds à 35 MeV/u. *C. Le Brun.*

- Formation et désexcitation de noyaux chauds produits au cours de la réaction ^{40}Ar + ^{238}U à 1080 MeV. *D. Jacquet.*

- Stabilité des noyaux chauds. *P. Bonche.*

- Calculs semi-classiques de noyaux chauds. *E. Suraud.*

- Le modèle E.T.F. à température finie. *M. Brack.*

- Multifragmentation de noyaux lourds. *N. Carjan.*

- Le paramètre de densité de niveau en fonction de la température avec inclusion de corrélations dynamiques. *P. Schuck.*

- Des barrières de fission en fonction de la température - Une approche de goutte liquide chaude. *J. Bartel.*

- Corrélations de particules légères émises dans les collisions Ar + Au, Ti à 60 MeV/u. *D. Ardouin.*

- Interplay between light particle evaporation and fission like reactions around 10 MeV/u. *J. Alexander.*

- Désexcitation du noyau composé par fission et émission de particules : expérience et théorie. Cas de ^{158}Er. *P. Grange.*

- Compétition entre l'émission de particules légères et la fission à haute température. *H. Delagrange.*

- Calcul de Hauser-Feshbach pour l'émission de fragments lourds. *J. Gomez del Campo.*

- Collisions centrales dans la réaction ^{40}Ar + ^{68}Zn entre 14 et 27 MeV/u. *F. Rami.*

- Evolution du processus de fusion entre 7 et 38 MeV/n pour le système ^{14}N + ^{27}Al. *D. Guinet.*

- Fusion complète et incomplète dans le système Ar + Ag et Ar + Au à 35 MeV/u. *C. Lebrun.*

- Dispersions en masse et en moment dans les réactions par ions lourds. *H. Flocard.*

- Evolution avec la température des barrières de fission. *Ph. Quentin.*

- Désexcitation de noyaux chauds. *H. Nifenecker.*

- Neutron multiplicity as a measure for energy dissipation and momentum transfer. *U. Jahnke.*

- Fusion ? Excitation ? Changements de phase ? Quelles questions ? Quelles réponses ? *M. Lefort.*

– III –

Noyaux exotiques.

- Etude de noyaux exotiques par la méthode du champ moyen. *P.-H. Heenen.*
- LISE : un dispositif expérimental pour la production et l'identification de noyaux exotiques. *D. Bazin.*
- Identification en ligne de noyaux légers riches en neutrons. *E. Quiniou.*
- Calculs H.F. triaxiaux de noyaux légers riches en neutrons. *F. Naulin.*
- Mesure de masse de noyaux exotiques avec SPEG. *A. Gillibert.*
- Description microscopique des excitations collectives, des degrés de libertés de particules et de leur couplage. *Ph. Quentin.*
- Approche théorique de noyaux pair-pair lourds. *M. Meyer.*
- The renormalisation of the axial-vector strength in nuclei : experiments on superallowed beta decay. *P.-G. Hansen.*
- Properties of new beta-delayed proton emitters in the lanthanide region. *J.-M. Nitschke.*
- Quelques aspects de la prévision des propriétés nucléaires loin de la stabilité par la méthode de Hartree-Fock. *F. Tondeur.*
- Production de noyaux exotiques dans le modèle de la percolation. *X. Campi.*
- Séparation isotopique à LISE - Application aux noyaux légers riches en neutrons. *J.P. Dufour.*
- Production et étude de noyaux très riches en neutrons dans la "fission froide" des isotopes de l'uranium. *C. Signarbieux.*
- Faisceaux secondaires d'ions lourds. *R. Bimbot.*
- Les exotiques côté machine : aujourd'hui, demain et après-demain. *A. Chabert.*
- Spectroscopie laser pour des isotopes voisins de Z = 50. *G. Huber.*
- Moments and radii of exotic nuclei by laser spectroscopy in the rare-earth region. *R. Neugart.*
- Nuclear structure studies of proton rich and neutron rich nuclei at the GSI on line mass separator. *E. Roeckl.*
- Production de noyaux exotiques et mesures de masses dans les réactions par ions lourds. *Y. Penionzhkevich.*
- Energy sharing in deeply inelastic reactions. *H. Körner.*
- Quelques réflexions sur les développements de la physique des noyaux exotiques au GANIL. *C. Detraz.*

– IV –

"L'excitation de modes élémentaires dans les noyaux par des collisions d'ions lourds aux énergies intermédiaires".

- Le rôle du pion en physique nucléaire. *J. Delorme.*
- Excitations nucléaires avec un ordre spécifique dans l'espace spin-isospin. *K. Dietrich.*
- Production de pions sous le seuil : phénomène(s) incohérent(s) et/ou cohérent(s). *B.-E. Erazmus.*
- Emission de pions chargés en coincidence avec des fragments légers. *J.-L. Laville.*
- Subthreshold pion production with a heavy beam and multiplicity filter. *W. Benenson.*
- Detection de γ Techniques et résultats. *E. Grosse.*
- Production de photons de haute énergie dans les collisions noyau-noyau aux énergies intermédiaires. *M. Kwato Njock.*
- Rayonnement γ émis dans les collisions d'ions lourds aux énergies intermédiaires. *N. Alamanos.*
- Rayonnement électromagnétique dans les collisions d'ions lourds aux énergies GANIL - Etude théorique. *C. Grégoire.*
- Nuclear excitations at finite temperature. *F. Bortignon.*
- Effets collectifs à 15 et 24 MeV/u. Emission gamma provenant de la décroissance de résonances géantes bâties sur des états excités. *J.-J. Gaardhoje.*
- Giant resonances in hot rotating nuclei. *P. Ring.*
- Damping of rotational motion. *M. Dossing.*
- Calcul semi-classique de résonances géantes à température finie. *M. Brack.*
- Résonances géantes à température finie. *E. Suraud.*
- Collisions périphériques : distinction entre transfert et fragmentation par mesure des énergies déposées dans le noyau-cible pour des collisions Ar + U. *J. Galin.*
- Contribution du mécanisme de transfert évaporation aux spectres d'ions lourds. *Y. Blumenfeld.*
- Delta excitation with charge exchange reactions. *C. Gaarde.*
- Réactions d'échange de charge. *M. Buenerd.*
- Charge exchange reactions at 30 MeV/u. *H.-G. Bohlen.*
- Excitation des résonances géantes par réactions d'échange de charge à GANIL. Les premiers résultats. *C. Berat.*
- La résonance E1dans les réactions d'échange de charge $^{12}C + {}^{12}C$, $^{40\text{-}44}Ca$, ^{90}Zr à E_{lab} = 840 MeV. *A. Miczaika.*

- Etats à une particule et fonction de réponse du noyau en réaction de transfert aux énergies intermédiaires. *S. Gales.*

- Réactions de transfert direct de 1,2 et 3 nucléons induites par faisceaux de ^{16}O et ^{12}C à énergie incidente élevée. *M. Mermaz.*

– V –

"Les interactions matière-ions lourds de grande vitesse : effet de la densité de dépôt d'énergie inélastique".

- Revue des différents processus de dépôt d'énergie lors du passage d'ions dans la matière. *A. L'Hoir.*

- Interaction ion-atome. *A. Salin.*

- Aspects collectifs du dépôt d'énergie dans les solides. *N. Cue.*

- Ions de recul multichargés de faible énergie produits par impact d'ions lourds sur cible gazeuse. *J.-P. Grandin.*

- Interférence entre excitation élémentaire du réseau (processus de capture) et excitation électronique collective en collisions d'ions Kr^{36+} de haute vitesse avec des cibles solides minces. *K. Wohrer.*

- Pouvoirs d'arrêt, straggling en énergie et straggling angulaire aux énergies GANIL. *R. Bimbot.*

- Etude de la collection de charges dans les semi-conducteurs lors de l'irradiation par ions lourds (funneling). *Y. Patin.*

- Redistribution spatiale de l'énergie déposée. *S. Bouffard.*

- Interaction d'électrons accélérés avec la matière condensée : expériences et modèles. *J. Delaire.*

- Ondes de choc engendrées par irradiations laser de grande puissance. *R. Fabbro.*

- Echelles de temps, interactions électro-phonons, pointe thermique. *J.-A. Davies.*

- Observation de la réponse transitoire d'un film mince de Nb supraconducteur à l'impact d'un ion lourd. *E. Paumier.*

- Désorption et pulvérisation par les ions lourds de haute énergie. *S. Della Negra.*

- La conversion d'une excitation électronique en défauts ponctuels. *L. Zuppiroli.*

- Défauts ponctuels induits dans les cristaux ioniques par forts dépôts d'énergie inélastique. *A. Perez.*

- Relations entre les propriétés conductrices induites par bombardement avec des ions lourds dans le polyimide et les conditions d'irradiation. *J. Davenas.*

- Transitions de phase et formation de composés métastables sous irradiation. *G. Martin.*

- Contribution des effets de freinage électronique à la création de défauts dans des métaux (fer) et des alliages métalliques. *A. Dunlop.*

- Amorphisation sous irradiation d'ions lourds : parallèle avec les irradiations laser rapide. *F. Studer et M. Toulemonde.*

- Modifications structurales induites dans quelques ferrites magnétiques : étude par microscopie électronique et spectroscopie Mossbauer. *D. Groult.*
- Mélange par faisceaux d'ions. *J. Grihle.*
- Trace dans les isolants. *J.-P. Duraud.*
- Effet de l'irradiatioon sur la viscosité des verres. *A. Barbu.*
- Modification de la structure électronique du quartz sous bombardement d'ions de haute énergie. *F. Jollet.*
- Rôle du (dE/dx) électronique sur le dopage du Hg, Cd, Te par implantation. *C. Blanchard.*
- Spectroscopie d'émission et d'absorption résolue à l'échelle des femto-secondes. *A. Antonetti.*

– VI –

La physique avec les multidétecteurs : perspectives (22-26 mai 1989)

- Noyaux chauds : production, désexcitation, température limite. *D. Guerreau.*
- Decay of hot nuclear systems formed in dissipative collisions. *K.-D. Hildenbrand.*
- Formation et désexcitation de noyaux chauds. *K. Dietrich.*
- Que devient la fission lorsqu'elle n'existe plus ? *M. Louvel.*
- Noyaux chauds : émission de fragments complexes et transfert de moment linéaire. *E.C. Pollacco.*
- Intermediate mass fragment and energetic particle emission from equilibrated sources. *M. Di Toro.*
- Quelques résultats obtenus avec des émulsions nucléaires. *F. Schussler.*
- La résonance géante dipolaire : une sonde de la collectivité et de la forme des noyaux chauds. *N. Alamanos.*
- Quelles signatures pour une transition de phase ? *Ph. Chomaz.*
- Emission de photons lors des collisions périphériques ^{40} Ar + ^{158} Gd at 44 Mev/u. *W. Kuhn.*
- Description du multidétecteur PACHA - Analyse des résultats et description des méthodes de simulation utilisées. *J.A. Scarpaci.*
- New results with the MSU 4π array. *G. Westfall.*
- Sur les détecteurs 4π et les analyses des données aux énergies relativistes. *D. L'Hote.*
- Présentation du projet INDRA : la physique et les choix techniques retenus. *E. Plagnol.*

- Réaction dans le domaine de l'énergie de Fermi : persistance des collisions fortement relaxées, fragmentation dissipative et une solution non thermique du dilemme des températures. *H. Fuchs.*
- Sur les observables dans la fragmentations. *X. Campi.*
- Multifragmentation et propriétés de la matière nucléaire. *J. Cugnon.*
- Multifragmentation - Revue expérimentale et résultats récents pour des systèmes lourds. *J.F. Lecolley.*
- Multifragmentation du système Ar + Al de 25 Mev/u à 85 Mev/u. *D. Cussol.*
- Corrélations entre fragments à 44 MeV/u. *L. Stugge.*
- Caractéristiques globales de la multifragmentation dans les systèmes $^{20}Ne + Ag$ et $^{20}Ne + Au$ à 60 MeV/u. *C. Volant.*
- Using streamer chambers for intermediate energy heavy ions. *J. Sullivan.*
- Transition entre la fission et la multifragmentation. *H. Oeschler.*
- Vous avez dit multifragmentation ? *E. Surraud.*
- Etude dynamique des modes d'instabilité du noyau. *B. Remaud.*
- Corrélations et formation d'amas dans les systèmes de spins finis excités : une contribution à l'étude de la fragmentation. *J. Richert.*
- Production of intermediate mass fragments - the onset of multifragmentation. *U. Lynen.*
- Multifragmentation dans le cadre d'un modèle d'agrégation restructurée. *S. Leray.*
- A BaF_2 crystal ball to study heavy ion collisions. *E. Migneco.*
- EMRIC : un détecteur pour la mesure des corrélations entre 7 et 200 Mev/u. *S. Kox.*
- Interférométrie de particules avec multidétecteur à ICs. *P. Lautridou.*
- Qu'apportent les multidétecteurs de particules chargées dans les mesures de corrélation entre particules légères ? *F. Saint-Laurent.*
- Complex fragment emission from Nb + Au reactions at 50 to 100 MeV/u. *N. Namboodiri.*
- Le multidétecteur 4π Amphora. *A. Giorni.*
- Calorimètrie neutronique appliquée à l'étude des collisions dissipatives. *M. Morjean.*
- Eden, un outil pour étudier des structures de grande énergie. *A. Van der Woude*

Achevé d'imprimé
sur les presses de Drakkar Conseil
Décembre 1989
Dépôt légal 4e trimestre 1989

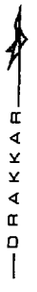

GANIL

GRAND ACCELERATEUR NATIONAL D'IONS LOURDS
BP 5027 — 14021 CAEN CEDEX FRANCE — TEL. : 31 45 46 47
TELEX 170 533 F — FAX 31 45 46 65